AFFTC-TIM-11-07

F-16D PACER CALIBRATION TECHNIQUES (SPEED PACER)

TOMOYUKI D. ONO
Captain, USAF
Project Manager and Engineer

DARYL G. CORNEILLE
Major, USAF
Project Pilot

A F F T C

JULY 2012

TECHNICAL INFORMATION MEMORANDUM

Approved for public release; distribution is unlimited.

AIR FORCE FLIGHT TEST CENTER
EDWARDS AIR FORCE BASE, CALIFORNIA
AIR FORCE MATERIEL COMMAND
UNITED STATES AIR FORCE

This technical information memorandum (AFFTC-TIM-11-07, *F-16D Pacer Calibration Techniques, SPEED PACER*) was submitted under job order number MT11A100 by the Commandant, USAF Test Pilot School, Edwards AFB, California 93524-6485.

Foreign announcement and dissemination by the Defense Technical Information Center are not authorized because of technology restrictions of the U.S. Export Control Acts as implemented by AFI 16-201, *Air Force Foreign Disclosure and Technology Transfer Program.*

Prepared by:

TOMOYUKI D. ONO, Capt, USAF
Program Manager and Flight Test Engineer

DARYL G. CORNEILLE, Maj, USAF
Project Pilot

TODD T. PATTERSON, Capt, USAF
Project Pilot

TIMOTHY J. STEVENS, Maj, USAF
Project Pilot

RYAN P. LEMAIRE, Capt, USAF
Project Engineer

FRANCOIS MEIGNIEN, Maj, DGA
Project Engineer

This report has been reviewed and is approved for publication.

RUSSELL E. ERB, NH-III, DAF
Performance Branch Master Instructor
USAF Test Pilot School

MARY E. McNEELY, NH-III, DAF
Test Management Master Instructor
USAF Test Pilot School

DAVID L. VANHOY, NH-IV, DAF
Technical Director
USAF Test Pilot School

LAWRENCE M. HOFFMAN, Colonel, USAF
Commandant, USAF Test Pilot School

NOV 6 2012

REPORT DOCUMENTATION PAGE

Form Approved
OMB No. 0704-0188

Public reporting burden for this collection of information is estimated to average 1 hour per response, including the time for reviewing instructions, searching existing data sources, gathering and maintaining the data needed, and completing and reviewing this collection of information. Send comments regarding this burden estimate or any other aspect of this collection of information, including suggestions for reducing this burden to Department of Defense, Washington Headquarters Services, Directorate for Information Operations and Reports (0704-0188), 1215 Jefferson Davis Highway, Suite 1204, Arlington, VA 22202-4302. Respondents should be aware that notwithstanding any other provision of law, no person shall be subject to any penalty for failing to comply with a collection of information if it does not display a currently valid OMB control number. **PLEASE DO NOT RETURN YOUR FORM TO THE ABOVE ADDRESS.**

1. REPORT DATE	2. REPORT TYPE	3. DATES COVERED *(From – To)*
XX-07-2012	Technical Information Memorandum	7 through 16 September 2011

4. TITLE AND SUBTITLE

F-16D Pacer Calibration Techniques (SPEED PACER)

5a. CONTRACT NUMBER

5b. GRANT NUMBER

6. AUTHOR(S)
Tomoyuki D. Ono, Captain, USAF, Program Manager and Flight Test Engineer
Daryl G. Corneille, Major, USAF, Project Pilot
Todd T. Patterson, Captain, USAF, Project Pilot
Timothy J. Stevens, Major, USA, Project Pilot
Ryan P. Lemaire, Captain, USAF, Project Engineer
Francois Meignien, Major, DGA, Project Engineer

5c. PROGRAM ELEMENT NUMBER

5d. PROJECT NUMBER

5e. TASK NUMBER

5f. WORK UNIT NUMBER

7. PERFORMING ORGANIZATION NAME(S) AND ADDRESS(ES)
Air Force Flight Test Center, 412th Test Wing
USAF Test Pilot School
220 South Wolfe Ave
Edwards AFB, CA 93524-6485

8. PERFORMING ORGANIZATION REPORT NUMBER

AFFTC-TIM-11-07

9. SPONSORING / MONITORING AGENCY NAME(S) AND ADDRESS(ES)
773 TS/ENFB
Attn: Mr Reagan Woolf
307 E Popson Ave
Edwards AFB CA 93524-6485

10. SPONSOR/MONITOR'S ACRONYM(S)

11. SPONSOR/MONITOR'S REPORT NUMBER(S)

12. DISTRIBUTION / AVAILABILITY STATEMENT
Approved for public release; distribution is unlimited.

13. SUPPLEMENTARY NOTES
CA: Air Force Flight Test Center Edwards AFB, CA CC:012100 Print in **Color**

14. ABSTRACT

This technical information memorandum documents the results of the investigation of various techniques and data analysis methods to calibrate the AFFTC F-16D pacer aircraft. Testing was requested by the Flight Systems Integration Test Squadron, 773 TS/ENF. The responsible test organization was the 412th Test Wing, located at the AFFTC, Edwards AFB, California. The test execution organization was the USAF Test Pilot School, Edwards AFB. Testing was conducted by the Speed Pacer Test Management (TMP) team at Edwards AFB from 7 through 16 September 2011 and testing consisted of nine sorties (17.4 flight hours). The overall test objective was to compare the calibration techniques and data analysis methods for the pacer aircraft. The test aircraft was modified with an additional flight test total temperature probe mounted on the left wingtip to compare calibrations at both locations. Additionally, a new atmospheric truth source method was used, which included data from multiple balloons released from different points to map atmospheric variations. Test methodology focused on comparing the possible combinations of truth source data, calibration flight test techniques, data reduction methods, and calibrated sources for both temperature and position corrections. All test objectives were met.

15. SUBJECT TERMS
F-16D aircraft, pacer, air data system, level acceleration, level deceleration, cloverleaf, stabilized cruise, Orbis, Boomer Turn, rawinsonde, Atmospheric Analysis pass, self survey, trailing cone, position correction

16. SECURITY CLASSIFICATION OF:			17. LIMITATION OF ABSTRACT	18. NUMBER OF PAGES	19a. NAME OF RESPONSIBLE PERSON
a. REPORT	b. ABSTRACT	c. THIS PAGE			412 TENG/EN (Ms. Lorrie Miller)
Unclassified	Unclassified	Unclassified	Same as Report	150	19b. TELEPHONE NUMBER *(include area code)* (661) 277-8615

This page was intentionally left blank.

EXECUTIVE SUMMARY

This technical information memorandum documents the results of the investigation of the various techniques and data analysis methods to calibrate the Air Force Flight Test Center (AFFTC) F-16D pacer aircraft. Testing was requested by the Flight Systems Integration Test Squadron, 773 TS/ENF, Edwards AFB, California. The responsible test organization was the 412th Test Wing, AFFTC, Edwards AFB. The test execution organization was the USAF Test Pilot School, Edwards AFB. Testing was conducted by the Speed Pacer Test Management Project team. Testing was performed at Edwards AFB from 7 through 16 September 2011, and consisted of one system check flight and eight test flights totaling nine sorties (17.4 flight hours). The overall test objective was to compare the calibration techniques and data analysis methods for the pacer aircraft. Overall, the cone and the noseboom could be calibrated with the same level of uncertainty. The cone and the noseboom calibrations were a function of altitude.

The 773 TS/ENF requested testing to compare the different pacer calibration techniques and truth sources available to determine the most accurate methods while balancing cost and efficiency. The calibrations were executed at 2,300, 10,000, and 30,000 feet, and throughout the range of subsonic airspeeds from an airspeed corresponding to 11 degrees angle-of-attack through 0.93 Mach number. Pacer calibrations used the F-16D production temperature probe in the past, but previous testing showed the temperature reading from the production probe might be affected by engine inlet airflow, reducing the accuracy of the result. Therefore, a total temperature probe was installed on a LAU-129 and placed on the wingtip for temperature calibration. New analysis techniques and new flight test techniques (FTTs) were compared to the existing techniques previously used for pacer calibrations. Test methodology focused on comparing the possible combinations of truth source data, calibration flight techniques, data reduction methods, and calibrated sources for both temperature and static source error corrections.

The test aircraft was the AFFTC pacer Block 40 F-16D aircraft, USAF S/N 87-0391. This production aircraft was modified with specialized pacer instrumentation, including a trailing cone. The only new modification for this test program was a flight test total temperature probe mounted on a LAU-129 on aircraft station one (left wingtip). The specialized pacer instrumentation modifications increased the accuracy of the air data system calibration for the pacer mission and were not production representative.

The results showed that the new flight test temperature probe mounted on the LAU-129 provided a more linear calibration. The production probe standard error was larger for all cases than the wing-tip probe. Hysteresis in the level acceleration and deceleration results was a big factor in the larger standard errors for the production probe. The repeatability of the two probes was also evaluated and showed that gross weight changes (for level acceleration and deceleration) or sortie dates (tower flyby) did not affect the calibration results.

The level acceleration and deceleration FTTs gave similar results as the cruise and tower flyby FTTs for both temperature and static source error correction. The level acceleration and deceleration was found to be the most efficient and cost effective of all calibration techniques. The speed calibration techniques, which included the cloverleaf, Orbis, and Boomer Turn methods, gave static source error correction with much larger scatter than other techniques. For truth sources, the two balloon atmospheric data, the Atmospheric Analysis and the Self-Survey analysis did not significantly improve the results over the one balloon data.

This page was intentionally left blank.

TABLE OF CONTENTS

This page was intentionally left blank.

INTRODUCTION

GENERAL

This technical information memorandum documents the results of the investigation of the various techniques and data analysis methods to calibrate the AFFTC F-16D pacer aircraft. Testing was requested by the Flight Systems Integration Test Squadron, 773 TS/ENF, Edwards AFB, California. The responsible test organization is the 412th Test Wing, AFFTC, Edwards AFB. The test execution organization was the USAF Test Pilot School, Edwards AFB. Testing was conducted by the Speed Pacer Test Management Project (TMP) team. Testing was performed at Edwards AFB from 7 through 16 September 2011. Testing consisted of one system check flight and eight test flights totaling nine sorties (17.4 flight hours).

BACKGROUND

Pacer aircraft have been used as the truth source for air data system calibrations throughout much of AFFTC's history. The pacer method involved flying the test aircraft in formation with a calibrated pacer aircraft. The airspeed and altitude readings on the test aircraft were compared with the calibrated pacer readings to determine the static source error corrections. Another use of pacer aircraft was for Reduced Vertical Separation Minima (RVSM) certification missions. When higher-than-normal accuracy pacer missions were required, such as for RVSM, the trailing cone could be installed and used as the truth source when requested by the customer.

In order to use an aircraft as a pacer aircraft, the static source error corrections of the aircraft's static source and the recovery factor of its total air temperature probe had to be determined. Historically, a variety of calibration methods have been used to determine the static source error corrections across a wide range of altitudes and airspeeds. Tower flybys (TFBs) have been used to determine corrections at low altitudes for a wide variety of subsonic airspeeds and have been flown with the trailing cone attached. Cruise points have been used to determine corrections for medium to high altitudes at a variety of subsonic airspeeds. Level accelerations and decelerations have been used to determine corrections at medium to high altitudes for subsonic airspeeds with the trailing cone and supersonic airspeeds without the trailing cone. Global Positioning System (GPS) Cloverleaf calibration technique maneuvers have been used to determine corrections at medium to high altitudes for a wide range of subsonic airspeeds and have been flown with or without the trailing cone. Attempts to increase the accuracy and efficiency of the calibration have also led to an additional flight method with two analysis techniques. This flight test technique was the 360-degree turn, either associated with the Orbis data reduction method developed by a Flight Test Engineer (FTE) from the Honda Aircraft Company as described in *Orbis Matching, Precision Pitot Static-Statics Calibration* (reference 1) or with the Boomer Turn data reduction method developed by a FTE from the USAF Test Pilot School detailed in *Statistical Pitot-Static Calibration Technique Using Turns and Self-Survey Method* (reference 2). When the static source error corrections have been calculated in the past, the total source error corrections have been assumed to be zero; this assumption was used again for this test.

A recurring calibration of the pacer aircraft was required to maintain the pacer's accuracy. These calibrations were performed annually or as required to support customers. The most current calibration test plan, AFFTC-TP-10-74, *AFFTC F-16D Pacer Calibration Plan* (reference 3) written by the 773 TS/ENF, was being used for recurring aircraft calibrations using traditional proven methods. The recurring calibration requirements would become costly if accomplished inefficiently. This test compared the different techniques and truth sources available to produce the most resource effective calibration.

TEST ITEM DESCRIPTION

The system under test was the modified Pitot-static systems and the total temperature probes on the AFFTC pacer Block 40 F-16D aircraft, USAF S/N 87-0391 with an F110-GE-100B engine powering the aircraft. The pacer aircraft featured a special air data system that included five precision pressure transducers, a flight test total temperature probe, and a data acquisition and display system. The pacer aircraft used a flight test Yaw Angle-of-Attack Pitot Static (YAPS) noseboom as the source of total pressure, static pressure, angle-of-attack, and angle-of-sideslip. This noseboom included a Lockheed Martin boom (P/N 16IH001) and a Rosemount Pitot-static tube (P/N 855EJ). The static pressure was also obtained from the trailing cone system. The data acquisition system (DAS) along with the production and pacer air data systems are discussed in detail in appendix B.

The aircraft was flown with two 370-gallon external fuel tanks on wing stations four and six for the eight data flights and with a single 300-gallon centerline tank for the first systems check flight. An Advanced Range Data System (ARDS) (AN/ARQ-52-V17) was attached on station nine (right wingtip). The ARDS pod on the wingtip was assumed to have negligible effect on the aircraft's Pitot-static system. A GPS-Aided Inertial Navigation Reference-Lite (G-Lite) Differential Global Positioning System (DGPS) was installed in the aircraft to provide time-space-position information (TSPI). See appendix B for a detailed description of these systems.

A non-retractable trailing cone system was installed on the aircraft as an independent static pressure source. The system consisted of an anchor fixture, a pressure transducer, Nylaflow® pressure tubing reinforced with a steel cable, a heat-resistant Kevlar® fire sleeve, a stainless steel static pressure sensing sleeve, and a 10 inch diameter drag cone. The system was attached to the aft tip of the vertical stabilizer in the location of the radar threat warning system, which was removed to accommodate the trailing cone system anchor fixture (figure B12). A Paroscientific 0 to 15 pounds per square inch (0 to 30.54 inches of mercury) absolute pressure transducer, which was installed inside the anchor fixture and attached to the pressure tubing, measured the static pressure from the static pressure sleeve.

A Goodrich Model 102 total temperature sensor was mounted on the bottom surface of a Launcher Armament Unit (LAU)-129 attached to wingtip station one, with its opening facing forward. Figure 1 shows the mounting of the probe on the LAU-129. Additional wiring was installed to connect the new temperature probe to the DAS. The production F-16D total temperature probe remained connected. See Temporary-2 Modification Number M07B391D, *Pacer Wingtip Total Air Temperature Probe Interface* (reference 4) for further details.

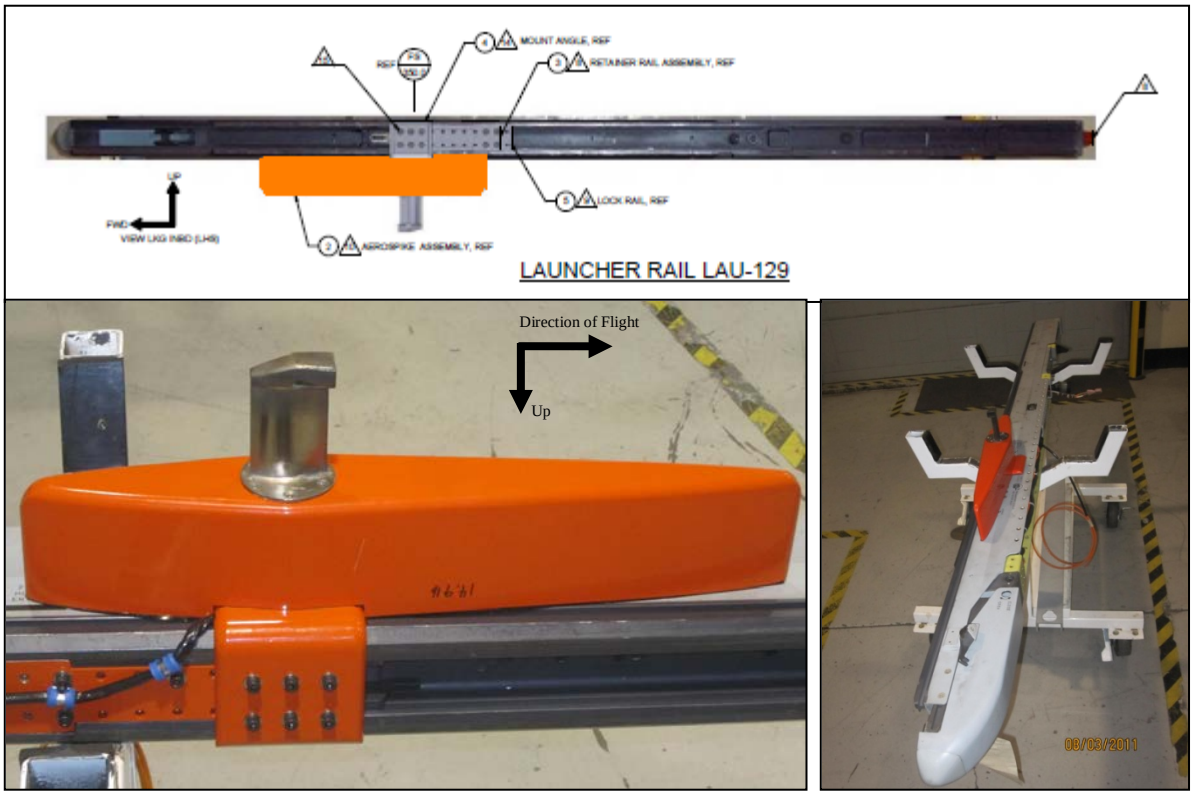

Figure 1 Wingtip Total Temperature Probe

Operational procedures for the pacer air data system and the trailing cone system are presented in F-16 C/D Support Fleet, *Modification Flight Manual Change 5* (reference 5).

TEST OBJECTIVES

The overall objective was to compare calibration techniques and data analysis methods for the pacer aircraft. The specific objectives were:

1. Compare the calibration of the total temperature probe mounted on a LAU-129 missile rail to the production temperature probe.

2. Compare the total temperature probe calibration techniques and data analysis methods for the pacer aircraft.

3. Compare the static source error correction calibration techniques and data analysis methods for the pacer aircraft.

All test objectives were met.

This page was intentionally left blank.

TEST AND EVALUATION

OVERALL TEST RESULTS

The two total temperature probes were compared and results showed that the wing-tip temperature probe resulted in a more linear fit than the production probe. The standard error of the linear fit was smaller for the wing-tip temperature probe than the production probe and the mean squared error between the temperature recovery correction model and the test data was smaller for the wing-tip temperature probe. Calibration methods were compared and showed the level acceleration and deceleration (LAD) was the least expensive and time-consuming method and produced the smallest standard errors at each altitude. Tower flyby method had the highest recovery factor uncertainties while the one balloon temperature truth source had smaller uncertainties at 10,000 feet than the two balloons but higher at 30,000 feet for cruise and level acceleration and deceleration methods.

The static source error correction was determined for each combination of FTT, truth source and system to be calibrated. The noseboom and the cone could be calibrated with the same level of precision. The calibration for both the noseboom and the cone was a function of altitude. The LAD method was found to give a similar result as the cruise points. Using one or two balloons did not change the results significantly. Using the tower flyby technique gave similar results as using the cruise technique with one balloon as a truth source, at the tower flyby altitude. Both the Atmospheric Analysis and the Self-Survey analysis gave unsatisfactory results, as the model that was created by these analyses was either mathematically or physically incorrect. The speed calibration techniques, which included the cloverleaf, the Orbis, and the Boomer Turn methods, gave static source error correction with a much larger scatter than the altitude techniques (tower flyby, cruise, and LAD).

The FTT truth source combination with the least cost was the level acceleration and deceleration combined with the one balloon rawinsonde. Furthermore, it received a “simple and quick” data reduction efficiency rating and a level 2 Bedford workload rating (appendix E). The highest total cost was the cloverleaf and Atmospheric Analysis combination.

Overall, the level acceleration and deceleration technique with one balloon as the truth source was the least expensive and time consuming, was the easiest to analyze, and gave results with acceptable uncertainty, both for static pressure and total temperature calibrations.

Test Methods and Conditions:

To determine the total temperature and static source error corrections, two profiles were flown. The first profile included tower flyby data points and the second profile up-and-away data points. On each profile, the calibration techniques were flown with all truth source data collected simultaneously. The flight test data were then analyzed using combinations of different calibrated systems, calibration techniques, and truth sources. The combinations applicable to each test objective are detailed in the Test Results section.

Calibrated Systems.

The four systems tested were the wingtip mounted total temperature probe, the F-16D production temperature probe, the flight test YAPS noseboom, and the trailing cone system. The YAPS noseboom included two Pitot-static systems, designated as “system one” and “system two”. Complete descriptions of these systems can be found in appendix B.

Calibration Techniques.

All calibration techniques were flown at both 10,000 feet pressure altitude (PA) and 30,000 feet PA, with the exception of tower flyby, which was flown at 100 feet AGL. All techniques were flown throughout the range of subsonic airspeeds from an airspeed corresponding to 11 degrees AoA, through 0.93 Mach number.

Tower Flyby

The tower flyby technique provided low altitude test data for both temperature and static source calibrations. By stabilizing at a specific Mach number, the temperature and static pressure measured by the calibrated systems could be compared to truth source data for ambient temperature, pressure altitude, and aircraft height above the flyby tower. Detailed data reduction methods used for tower flyby data are discussed in appendix D.

The profile was flown in accordance with the approved tower flyby circuit detailed in AFI 11-1, *Flying Operations, Air Operations* (reference 6). The test aircraft flew down the tower flyby line marked on the Edwards AFB lakebed. The test pilot stabilized at approximately 100 feet AGL at the target indicated airspeed. When the aircraft passed the tower, the aircrew marked an event on the aircraft's DAS and the flyby tower crew simultaneously recorded the truth source data. The data collected at the tower are discussed in the Truth Sources section. The passes were considered valid if airspeed was held within 2 KCAS, as indicated in the cockpit and aircraft vertical speed was held to approximately 0 for 5 seconds before passing abeam the flyby tower.

Level Acceleration and Deceleration

The LAD technique provided data for both temperature and static error calibrations at both 10,000 and 30,000 feet pressure altitude (PA). This technique enabled collection of data through the entire test airspeed range at one altitude in a single maneuver. Both the acceleration and deceleration were flown through the full range of airspeeds to take into account any hysteresis or lag in the calibrated systems by approaching each airspeed from both above and below.

The technique was flown by stabilizing at the target altitude and starting airspeed for at least 10 seconds. The pilot then adjusted power to accelerate or decelerate at 2 to 5 KCAS per second. All level accelerations began at the airspeed corresponding to 11 degrees AoA and ended at 0.93 Mach number. All level decelerations began at 0.93 Mach number and ended at the airspeed corresponding to 11 degrees AoA. The runs were considered valid if altitude was held within 100 feet PA of the starting altitude, and if the acceleration or deceleration rate was below 5 KCAS per second.

To remain between the two rawinsonde balloons, which were used as one of the truth sources, a turn was performed after the level acceleration and before starting the level deceleration. The level decelerations were flown on a reciprocal heading over the same airspace as the level acceleration. Figure 2 shows the start points and flight path flown for this technique. The LAD was flown using the Rawinsonde balloons release coordinates as starting and ending points.

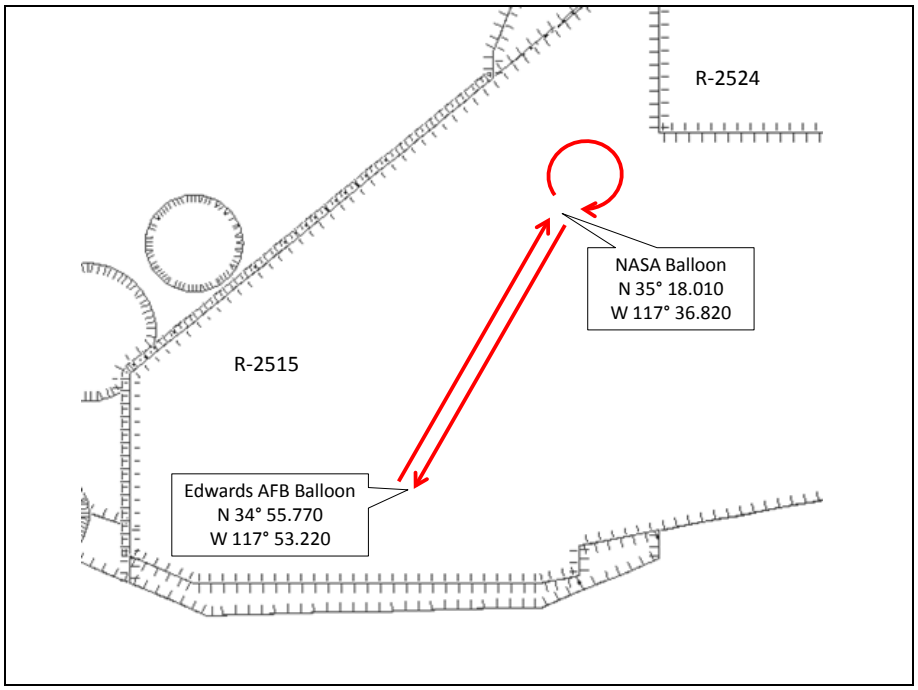

Figure 2 Level Acceleration, Deceleration, and Atmospheric Analysis Waypoints

GPS Cloverleaf

The GPS cloverleaf technique provided data for static error calibrations at both 10,000 and 30,000 feet PA. This technique used the difference between the Pitot-static based true airspeed and the GPS/INS based true airspeed that was calculated using ground velocity vectors and wind vectors to determine the static source error correction. Wind vectors were found by flying the Cloverleaf maneuver with a DGPS, as explained in appendix D. An assumption for this technique was that the wind vectors and ambient air temperature were constant throughout the maneuver, thus requiring that the three passes be flown over the same airspace and within a short time span.

Each GPS cloverleaf maneuver consisted of flying three passes on headings approximately 120 degrees apart, through the same point in the sky. Heading and airspeed were held constant during the three straight-and-level runs. The aircrew used a waypoint to ensure each leg was flown through the same point in the sky. The waypoint was displayed on the horizontal situational display and the aircraft was flown to it visually. The accuracy was sufficient using this method. Figure 3 shows a typical flight path used for the maneuver. All maneuvers were flown in the airspace between the two truth source balloons so that the data from each pass could also be used as cruise points. The three straight-and-level runs were stabilized on altitude and airspeed for a minimum of 10 seconds. Airspeed and altitude tolerances during the stabilized legs were ±2 KCAS and ±50 feet PA, respectively.

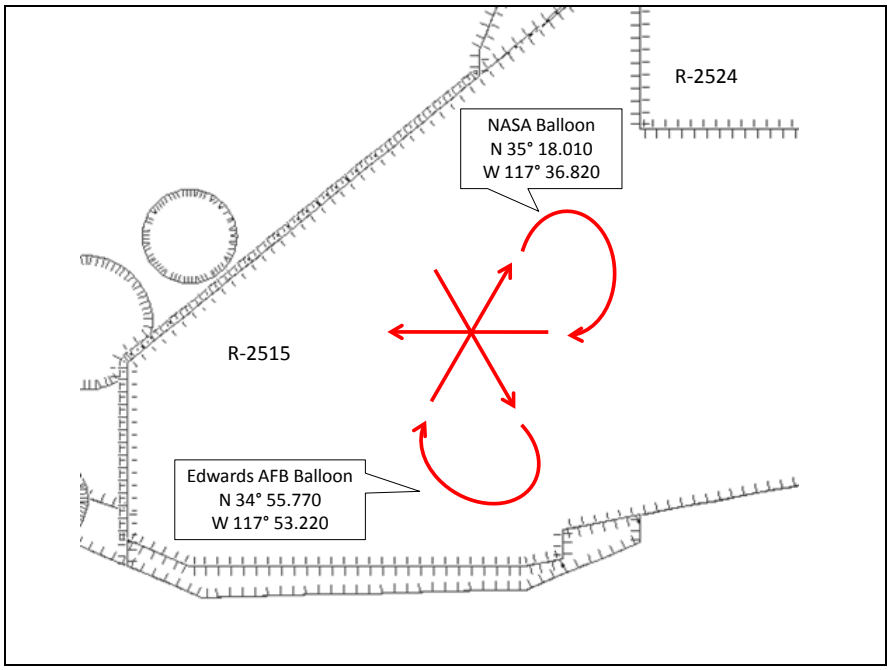

Figure 3 Nominal GPS Cloverleaf Maneuver Track

Stabilized Cruise

The stabilized cruise technique provided data for temperature and static pressure error calibrations at both 10,000 feet PA and 30,000 feet PA. The technique was flown by stabilizing at the target Mach number and altitude for 10 seconds before collecting data. This stabilization was intended to reduce any potential lag effects in the temperature and Pitot-static systems. The points were considered stabilized if airspeed and altitude were held within 2 KCAS and 50 feet. Since the GPS Cloverleaf maneuver required more than 10 seconds stabilized on altitude and airspeed, stabilized cruise points were also collected during the GPS cloverleaf maneuver. Rawinsonde balloons were used as temperature and static pressure truth sources and the Atmospheric Analysis passes were used as an additional static pressure truth source.

360-Degree Turns

The 360-degree turn technique provided data for static error calibrations at both 10,000 feet PA and 30,000 feet PA. This technique used the difference between the ground track determined from DGPS and the indicated ground track from instrument-corrected true airspeed and aircraft heading. Instrument-corrected true airspeed was calculated using the instrument-corrected static and total pressure, and total temperature. The wind vector could then be determined from the vector between the DGPS circle center and the indicated ground track circle center. The wind vector and ground speed were then used to find actual true airspeed, which could then be used to determine the static pressure error. The truth source data required for the 360-degree turns were GPS speed, heading, static and total pressure (instrument-corrected) and truth source total or ambient temperature. Details on the data reduction methods used are discussed in appendix D.

The 360-degree turn technique was flown by stabilizing on airspeed and altitude, and then flying a constant bank angle turn through a full 360 degrees. For turns at 11 degrees AoA, 20 degrees of bank was used. For all other airspeeds, 30 degrees of bank was used. Tolerances during the turns were ±2 degrees for bank angle, ±5 KCAS for airspeed, and ±100 feet for altitude.

Truth Sources.

Since the calibration techniques were analyzed using truth data from multiple sources, all applicable truth data were collected on each sortie.

Flyby Tower Sources

Aircraft height above the ground, temperature, and ambient pressure data were collected at the flyby tower for both sorties including tower flyby passes. Readings were taken as the aircraft passed abeam of the tower and were compared to the data collected on the aircraft.

The theodolite mounted in the flyby tower was used to determine the aircraft geometric height above the flyby tower as the aircraft passed. Using an eyepiece, the observer, taking the readings carefully, adjusted their eye position until the horizontal grid line marked as 'zero' was aligned with the far edge of the lakebed. As the aircraft passed abeam of the tower, the observer read the gridline where the aircraft crossed. The theodolite and eyepiece are shown in figure 4. Knowing the distance from the eyepiece to the theodolite, the distance from the eyepiece to the tower flyby line, and the distance between theodolite lines, geometry was used to determine the aircraft height above the flyby tower. All theodolite readings were taken using the point on the aircraft where the canopy met the aircraft spine behind the rear cockpit crewmember. The vertical distance from this point on the aircraft was translated to the locations of the pressure transducers using aircraft pitch angle, as described in appendix D.

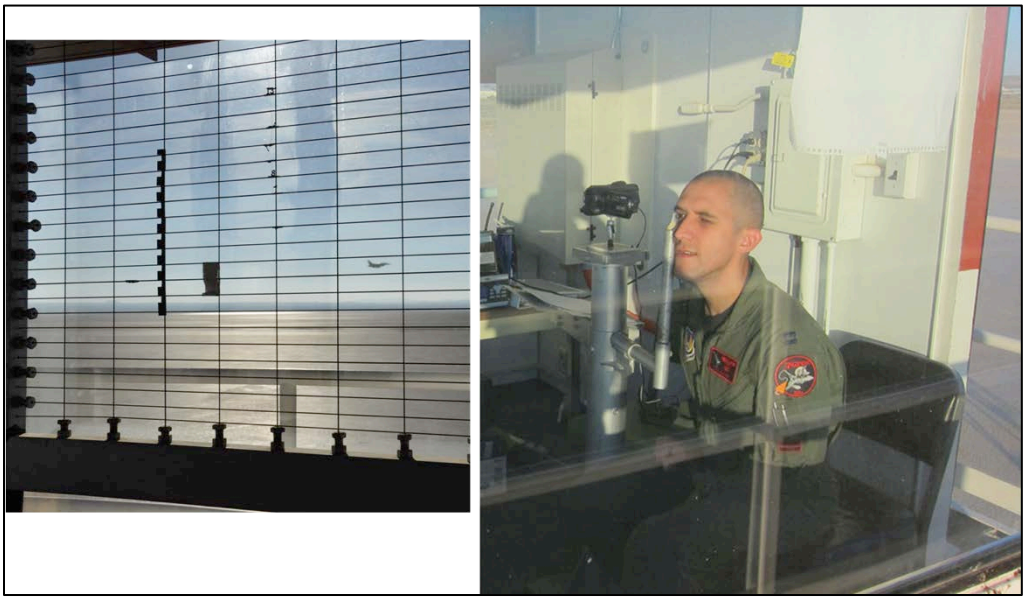

Figure 4 Tower Flyby Theodolite Setup

A Druck digital pressure gauge (Model DPI-145, S/N 14501855) was used to measure the ambient air pressure at the flyby tower. The gauge was placed inside the tower, but the door remained opened throughout the mission to ensure ambient pressure was measured. Four Omega Engineering HH40 series thermistor-type thermometers (S/Ns 073, 074, 103, and 012) were used to measure the ambient air temperature at the flyby tower. The thermometers were placed on the northwest corner of the flyby tower. Care was taken to ensure all sensing elements were in the shade. Two sensing elements were placed in front of the stand and the other two behind the stand (figure 5). The average of the four readings was used for all data reduction.

Figure 5 Flyby Tower Thermocouple Location

One Balloon and Multiple Balloon Atmospheric Data

On each sortie, two rawinsonde weather balloons were launched approximately 15 minutes prior to takeoff. Each balloon recorded temperature data along with GPS altitude and calculated pressure. The GPS altitude was then correlated with the test aircraft GPS altitude to determine the ambient pressure and ambient temperature at the aircraft's altitude.

Since each rawinsonde balloon provided truth source data at one point in the airspace, errors could be introduced with the calibration techniques being flown a distance away from where the truth source data were collected. The multiple balloon truth source attempted to reduce errors from flying a distance away from the balloons by bracketing the airspace to determine how pressure and temperature changed in the distance between the balloons. The temperature and static source calibrations were performed using both one balloon and multiple balloon atmospheric data to determine differences in the truth source data.

For each sortie, the rawinsonde balloon launched by the Edwards AFB Weather Section, 412 OSS/OSW, was released from the same location. The balloon launched by NASA Dryden was released from different points in the airspace depending on the sortie profile. For the two sorties, which included tower flyby test points, the NASA balloon was launched from the NASA ramp on Edwards AFB. The tower flyby launch locations are shown in figure 6. For all other sorties, the NASA balloon was launched from the northern portion of R-2515, as shown in figures 2 and 3. The rawinsonde balloons released by NASA and 412 OSS/OSW were identical.

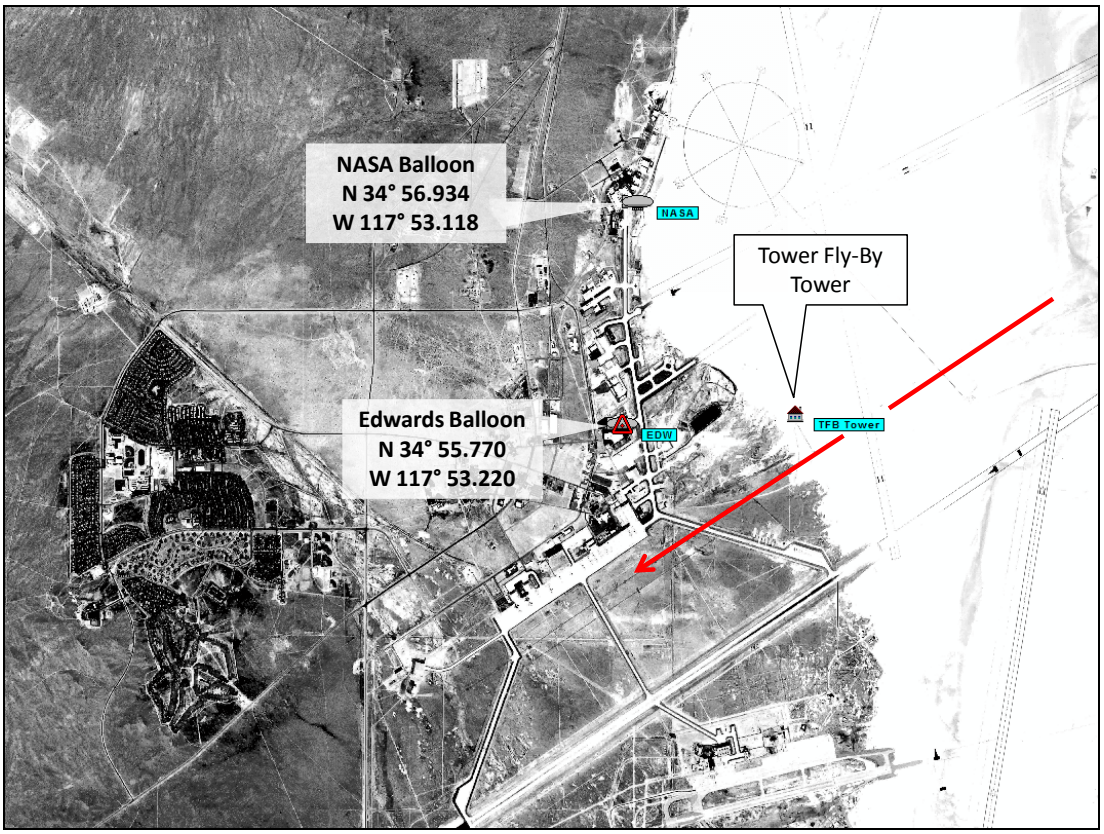

Figure 6 Weather Balloon Launch Location for Tower Flyby

Atmospheric Analysis and Self-Survey

The Atmospheric Analysis passes flight test technique led to two different truth sources: the Atmospheric Analysis, which required the Atmospheric Analysis passes in conjunction with a balloon, and the Self-Survey, which required the Atmospheric Analysis passes in conjunction with a previous calibration at one specific airspeed. This airspeed was 0.70 Mach number for this test.

Atmospheric Analysis passes were used to supplement the rawinsonde atmospheric data for time and distance away from where the weather balloons collected data. The maneuver consisted of four constant airspeed, altitude, and heading passes through the airspace planned for the calibration techniques. One pass was flown above and one pass was flown below the test altitude before flying the calibration techniques and the same two passes were repeated after completing the calibration techniques. For the 10,000 feet PA test points, the atmospheric passes were flown at 9,500 feet PA and 10,500 feet PA. For the 30,000 feet PA test points, the passes were flown at 29,500 feet PA and 30,500 feet PA. Each pass was flown at 0.70 Mach number, which was the Mach number at which the static source error correction was the best known from previous calibration tests. During each pass, DGPS altitude, static pressure, total pressure, and total temperature were recorded. Then, the DGPS altitude and ambient air pressure from one balloon were used to correct for the bias in the tested Pitot-static system at 0.70 Mach number. Since each sortie only included test points at either 10,000 feet PA or 30,000 feet PA, the Atmospheric Analysis passes were flown at the beginning of the sortie and again at the end of the sortie. Several 360-degree turns were also flown before and after the Atmospheric Analysis passes since these truth source data were not required for the turn technique.

The Self-Survey truth source was similar to the Atmospheric Analysis except that the bias was corrected using previous calibrations, instead of using the data from one balloon. For this specific test, data from the cruise points were used to correct the bias.

Each pass began at the coordinates for one of the rawinsonde balloon launch locations and ended at the coordinates for the other balloon launch location. The second pass was then flown on a reciprocal heading, again overflying the balloon launch coordinates. Since the maneuvers were flown near the weather balloons, the change in temperature and pressure was mapped for the airspace where the techniques were flown. By flying the Atmospheric Analysis passes before and after the calibration techniques, the change in temperature and pressure over time was also mapped.

TEST RESULTS, CONCLUSIONS, AND RECOMMENDATIONS

This section presents the results of the investigation of the various techniques and data analysis methods to calibrate the AFFTC F-16D pacer aircraft. This section will draw results, conclusions, and recommendations for the calibration of the total temperature probe, the static source error correction calibration, and the efficiency of these calibration techniques.

Temperature Probe Comparison:

The specific test objective was to compare the calibration of the total temperature probe mounted on a LAU-129 missile rail to the production temperature probe. The two probes were compared by determining the linearity of the calibration line fit and the repeatability of the calibration results.

Data Analysis Techniques.

Detailed data analysis techniques are described in the Total Air Temperature (TAT) Probe Recovery Factor and Temperature Correction section of appendix D. The position-corrected Mach number (M_c) for all total temperature calibration results was derived from the first static pressure transducer (System 1) of the YAPS boom transducer tray.

Test Results

Comparison of the two temperature probes consisted of model fit and repeatability. Model fit looked at the standard error of the first order fit of the recovery factor plots and the mean squared error (MSE) between the test data and the manufacturer provided temperature recovery correction model (see appendix D). Repeatability consisted of comparing the standard errors and MSE for different conditions.

Plots of the linear fits for the combinations of methods and truth sources are available in appendix C, figures C1 through C11. Each plot shows the recovery factor, the bias, and the standard error for that method and truth source combination. For comparison of the temperature probes, all test points with the same method, truth source, and altitude conditions were combined to produce the final values. Table 1 is the results comparing the two probes' standard error.

Table 1 Standard Error Comparison

Method	Truth Source	Standard Error (n/d)	
		Wing-Tip	Production
Tower Flyby	Flyby Tower	0.0191	0.0224
Tower Flyby	One Balloon	0.0245	0.0275
Tower Flyby	Two Balloon	0.0228	0.0244
Cruise – 10K Ft	One Balloon	0.0026	0.0116
Cruise – 10K Ft	Two Balloon	0.0028	0.0097
Cruise – 30K Ft	One Balloon	0.0062	0.0141
Cruise – 30K Ft	Two Balloon	0.0058	0.0149
Level Accel/Decel – 10K Ft	One Balloon	0.0037	0.0179
Level Accel/Dece l – 10K Ft	Two Balloon	0.0051	0.0181
Level Accel/Decel – 30K Ft	One Balloon	0.0094	0.0217
Level Accel/Decel – 30K Ft	Two Balloon	0.0089	0.0214

The results for all methods showed that the wing-tip probe standard error was smaller than the production probe standard error. The difference in the standard errors between the probes was smaller for the tower flyby method, but for cruise and LAD techniques the difference was an order of magnitude smaller. Also for the LAD method, the production probe displayed a hysteresis effect. The deviation from the model at medium Mach increased the standard error. The hysteresis effect was not as apparent in the wing-tip temperature probe but was present in most cases. Figure 7 is an example of the LAD method for both temperature probes. The production probe produced nonlinear results at higher Mach numbers that would increase the standard error no matter what method was used.

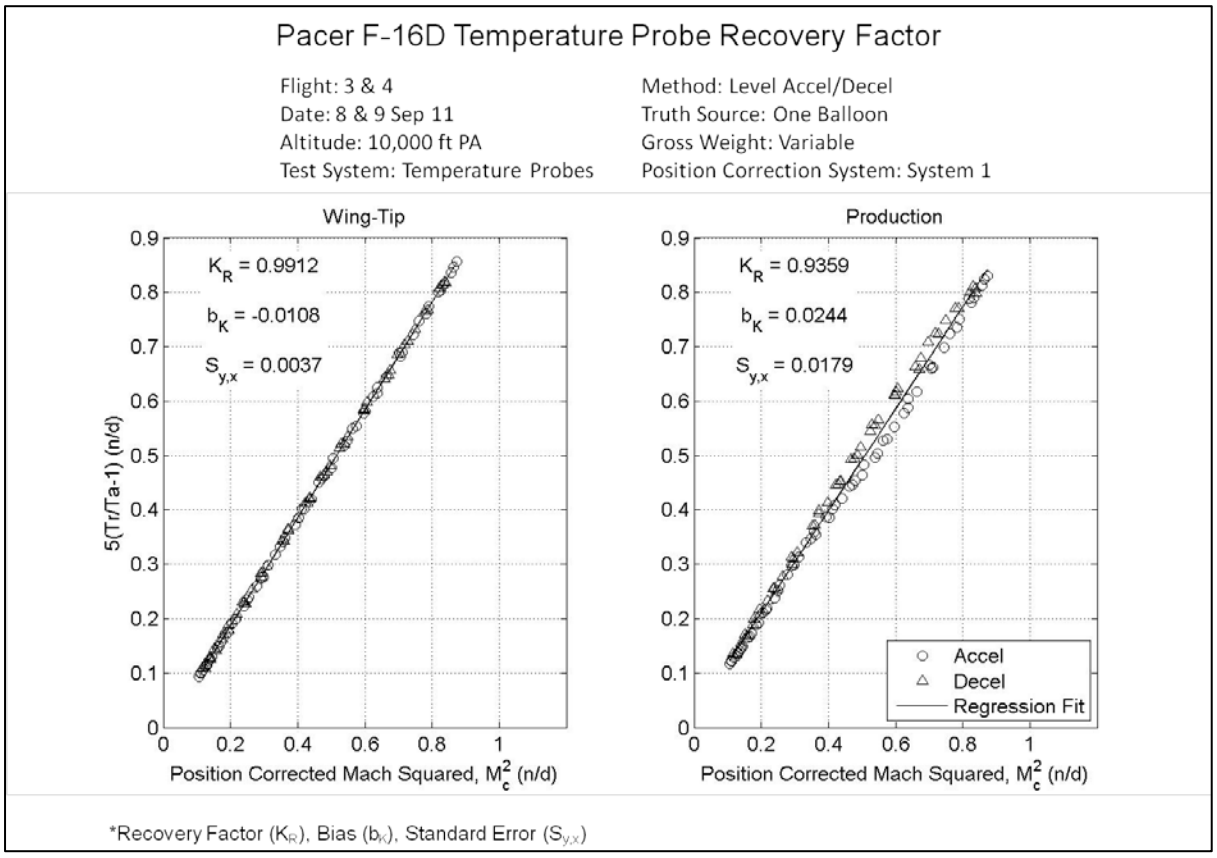

Figure 7 Example of Level Acceleration and Deceleration Result

The values of the recovery factors for the wing-tip probe ranged between 0.99 and 1.00 while for the production probe they ranged between 0.93 and 0.95. The bias for the wing-tip probe ranged from -0.03 to 0.02, bracketing zero and the production probe ranged from 0.02 to 0.04. There was no other discernable trend or pattern with the bias. A purely adiabatic temperature relationship occurs when the recovery factor equals one and the bias equals zero. The wing-tip probe was closer to the theoretical values for both recovery factor and bias than the production probe. A summary of the results is shown in table 2.

Table 2 Recovery Factor and Bias Comparison

Method	Truth Source	Recovery Factor (n/d)		Bias (n/d)	
		Wing-Tip	Production	Wing-Tip	Production
Tower Flyby	Flyby Tower	0.9857	0.9294	-0.0285	0.0066
Tower Flyby	One Balloon	0.9954	0.9338	0.0156	0.0536
Tower Flyby	Two Balloon	1.0010	0.9419	0.0092	0.0446
Cruise – 10K Ft	One Balloon	0.9936	0.9497	-0.0144	0.0221
Cruise – 10K Ft	Two Balloon	0.9921	0.9322	-0.0130	0.0220
Cruise – 30K Ft	One Balloon	0.9937	0.9550	-0.0043	0.0418
Cruise – 30K Ft	Two Balloon	0.9877	0.9492	-0.0029	0.0430
Level Accel/Decel - 10K Ft	One Balloon	0.9912	0.9359	-0.0108	0.0244
Level Accel/Decel - 10K Ft	Two Balloon	0.9908	0.9355	-0.0121	0.0231
Level Accel/Decel - 30K Ft	One Balloon	0.9900	0.9484	0.0008	0.0465
Level Accel/Decel - 30K Ft	Two Balloon	0.9921	0.9505	-0.0062	0.0394

Temperature recovery correction was the second calibration parameter that was analyzed. The recovery correction was calculated from the test data and was compared to the manufacturer provided model from Goodrich's Technical Report 5755, *Total Temperature Sensors* (reference 7). The test points were plotted against the model and a bias (b_η) was used that minimized the MSE (appendix D). Figures C26 through C36 show the results for each method and truth source combinations for each temperature probe. Table 3 shows the comparisons of the MSEs and the bias.

Table 3 Temperature Recovery Correction Summary

Method	Truth Source	Mean Square Error X100 (n/d)		Bias *100 (n/d)	
		Wing-Tip	Production	Wing-Tip	Production
Tower Flyby	Flyby Tower	0.0392	0.0721	-0.4994	-0.2725
Tower Flyby	One Balloon	0.0497	0.0805	0.3927	0.5816
Tower Flyby	Two Balloon	0.0430	0.0631	0.3161	0.4992
Cruise – 10K Ft	One Balloon	0.0024	0.0461	-0.1878	0.1945
Cruise – 10K Ft	Two Balloon	0.0015	0.0400	-0.1757	0.0741
Cruise – 30K Ft	One Balloon	0.0076	0.0508	0.0198	0.5252
Cruise – 30K Ft	Two Balloon	0.0069	0.0600	-0.0075	0.4999
Level Accel/Decel - 10K Ft	One Balloon	0.0060	0.1746	-0.1279	0.0829
Level Accel/Decel - 10K Ft	Two Balloon	0.0105	0.1770	-0.1542	0.0565
Level Accel/Decel - 30K Ft	One Balloon	0.0239	0.1437	0.0816	0.5292
Level Accel/Decel - 30K Ft	Two Balloon	0.0218	0.1374	-0.0271	0.4199

Overall the differences in MSE between the temperature probes showed that the wing-tip probe errors were smaller than the production probe errors. One interesting note is the shape of the plots of temperature recovery correction versus Mach number between the two probes. The wing-tip temperature probe test points were grouped fairly consistently with about the same amount of scatter from the model

at different Mach numbers. The production probe, however, consistently had a unique shape where at higher Mach numbers the deviation from the model was much greater than at lower Mach numbers. The higher MSE was attributed to these large scatters at the higher Mach numbers, especially for the LAD methods. Figure 8 is one example comparing the two test probes.

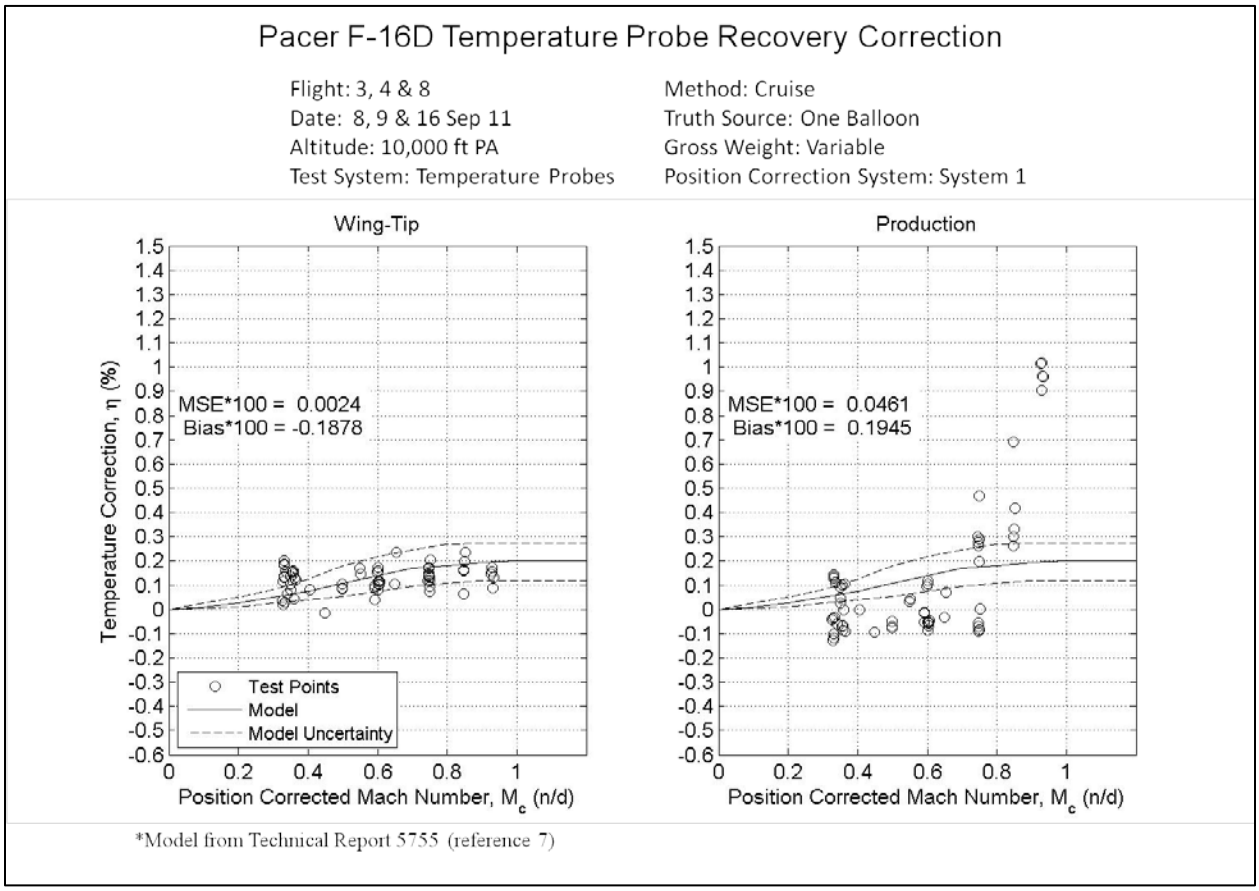

Figure 8 Example of Temperature Recovery Correction

How closely the test data resembles the model is key since the central air data computer (CADC) used a model provided by Goodrich (reference 9) and added a self-heating error bias to it to derive the temperatures from the production probe. In all methods and truth source combinations and for both temperature probes, the temperature recovery correction derived from the test points were scattered and did not follow the shape of the manufacturer provided model. For the wing-tip, the scatter at lower Mach numbers was about the same as at high Mach numbers, contrary to the model boundaries. Even then, the wing-tip probe produced data closer to the model than the production temperature probe. To make clear the consequences of this scatter, the resulting errors in total temperature were calculated. For the temperature recovery correction method, the model and the measured total temperature, T_r, were used to calculate the derived total temperature ($T_{t,derived}$) using the following equation, which was derived from the temperature recovery correction equation, D13, plus the bias, b_η, previously determined from the minimization:

$$T_{t,derived} = \frac{T_r}{1 - (\eta - b_\eta)}$$

The derived total temperature was subtracted from the theoretical total temperature based on the ambient temperature truth source and position-corrected Mach number. The production probe resulted in a wider range of error values than the wing-tip probe. The error from the results for one balloon cruise at 10,000 feet is shown in figure 9. Plots for other combinations can be found in figures C37 through C47.

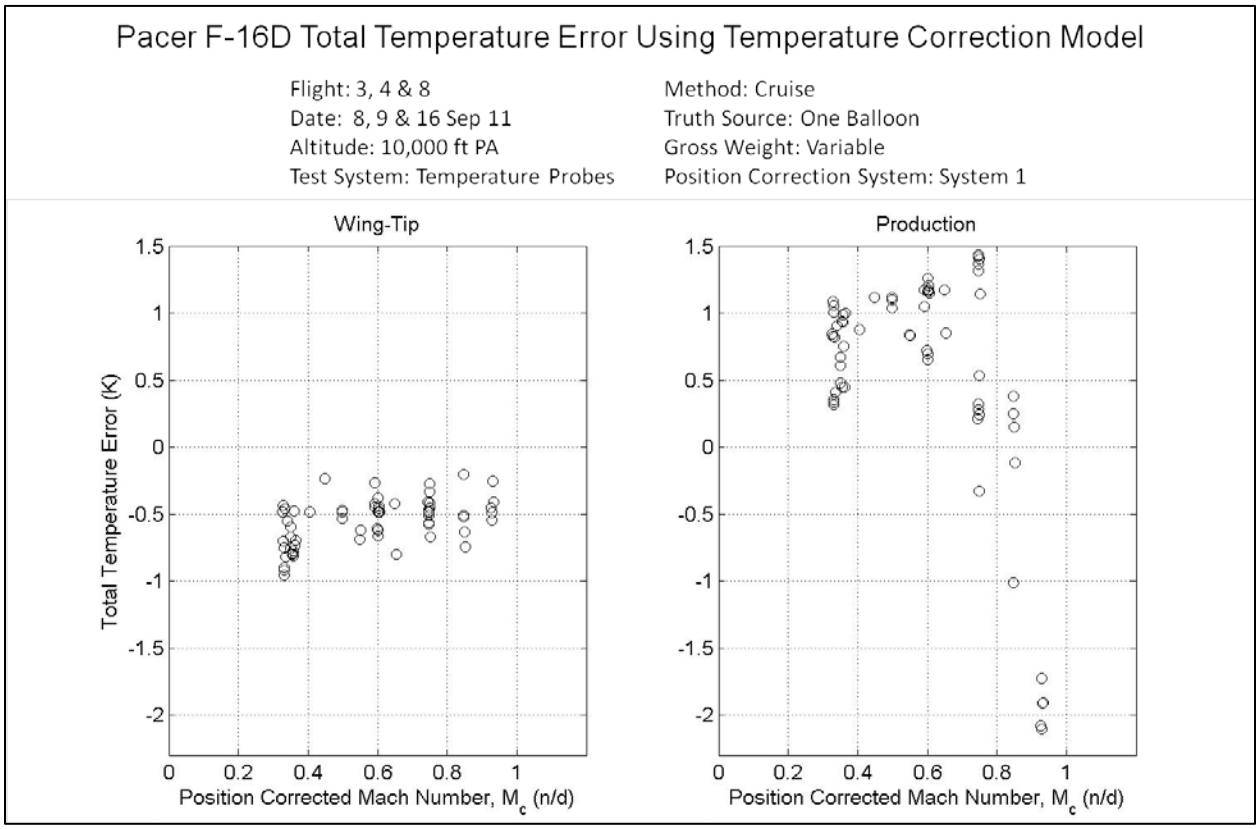

Figure 9 Total Temperature Error Comparison

From the total temperature error results, it was evident that the production probe had a larger error than the wing-tip probe. Also, despite the temperature correction results not matching the shape of the model, using the model to derive the total temperature allowed for the error to be within one degree Kelvin for the wing-tip probe. This result showed that for the wing-tip probe, the manufacturer's model could be used to derive the temperatures without needing recovery factors, but not for the production probe. The F-16D CADC used the model method for its production temperature probe to calculate the total temperature.

Repeatability was another consideration for comparing the two temperature probes. Repeatability consisted of looking at calibration data from different conditions and seeing if the change in conditions affected the results. The comparison was expressed in percent differences for recovery factor while the comparison for bias was expressed in actual difference due to the results spanning zero. First for the tower flyby, different sortie results were compared since it was most efficient to fly all the test points in one sortie. The second comparison was between LADs. The LADs were flown at different aircraft gross weights. Heavy gross weight was defined as the aircraft having over half of the usable fuel remaining and lightweight was defined as having less than half of the usable fuel remaining. Based on the aircraft empty weight in the test configuration and fuel available, heavyweight was defined as greater than 26,500 pounds gross weight and lightweight was defined as less than 26,500 pounds gross weight. All heavy runs were combined and all light runs were combined and results compared to determine

repeatability. Table 4 shows a summary of the results. Figures C12 through C25 show the plots of the results for each condition used for table 4.

Table 4 Repeatability Comparisons

Method	Truth Source	Difference Compared	Wing-Tip Differences		Production Differences	
			K_R (%)	b_K (n/d)	K_R (%)	b_K (n/d)
Tower Flyby	TFB	Flight 2 to Flight 6	-0.4	-0.020	-0.1	-0.021
Tower Flyby	1 Balloon	Flight 2 to Flight 6	2.6	0.024	3.8	0.019
Tower Flyby	2 Balloon	Flight 2 to Flight 6	3.2	0.018	3.7	0.016
Level Accel/Decel - 10K Ft	1 Balloon	Heavy to Light Gross Weight	-0.2	0.000	-0.6	0.001
Level Accel/Decel - 10K Ft	2 Balloon	Heavy to Light Gross Weight	-0.1	0.001	-0.5	0.002
Level Accel/Decel - 30K Ft	1 Balloon	Heavy to Light Gross Weight	0.4	-0.005	1.4	-0.011
Level Accel/Decel - 30K Ft	2 Balloon	Heavy to Light Gross Weight	0.4	-0.004	1.1	-0.010
See appendix D for percent difference equation						

The recovery factors were less than four percent different between the compared data for tower flyby and less than 0.5 percent for all other methods for the wing-tip probe and less than two percent for the production probe. The bias error differences did not have a discernable trend and ranged from -0.035 differences to 0.029 differences. The best repeatable combination for recovery factor and bias was the LADs at 10,000 feet. The differences in recovery factor between the tower flyby points with one or two balloons were greater than the LADs. This may be due to the fact that the balloon data were from one specific time of the day. During the course of the tower flyby, the temperature measured at the tower changed about five degrees Celsius on the first sortie (two hours of flying) and about two degrees Celsius on the second sortie (one hour of flying). The terrestrial heating that was not accounted for may have caused the greater differences. For the higher altitude points, time did not affect the temperature as it did near the ground.

Overall, the wing-tip temperature probe was more appropriate for the linear recovery factor model. First, the recovery factor value was closer to one, and second, the standard error was smaller than the production probe results. The use of the temperature correction model to derive total temperatures worked better with the wing-tip probe than the production probe, due to the smaller MSEs and a closer matching of the model shape. Repeatability was acceptable for both temperature probes, with the percent differences in recovery factor at less than four percent for every method. The bias did not show the same repeatability characteristics as the recovery factor nor did it show any discernable patterns.

Temperature Calibration Techniques:

The specific test objective was to compare the total temperature probe calibration techniques and data analysis methods for the pacer aircraft. The techniques were compared by looking at the resources required for each combination of calibration method and truth sources as well as the random uncertainties for each combination.

Data Analysis Techniques.

The procedure for comparison of resources required is described in detail in the Static Source Error Correction Calibration Techniques section. The same number of points as discussed in that section was used to determine the total cost for each maneuver and truth source combination.

For the uncertainty analysis, only the wing-tip temperature probe and the recovery factor calibration were used. The temperature correction method only required verification that the model used was acceptable, which was not practical in comparing the calibration methods and truth source combinations.

The uncertainty of the recovery factor and intercept was defined as the 95 percent confidence interval of each parameter generated by the MATLAB® 'regress.m' linear regression function. To ensure independence of each point for LAD data, data points every 10 seconds were used per previous Pacer test results described by J. Clark in *The Effects of Aircraft Acceleration and Deceleration on Static Source Error Corrections* (reference 8).

The uncertainties determined through the above method describe the random uncertainties from the method and truth source. It must be noted that there were also systematic uncertainties from measurement devices that were not taken into account. These uncertainties were not used as part of the results due to the values being unavailable.

The number of data points also affects the uncertainties. The number of points used for each method can be found in table C1. The uncertainty values were determined from using all the points available from flight test.

Test Results.

Comparison of temperature calibration techniques consisted of comparing the resources, logistics, and time required for each combination of methods and truth sources as well as the uncertainties of those combinations.

Supporting data for resources comparison are in the Static Pressure Position Correction Calibration Techniques section. For this analysis, the tower flyby method with one and two balloons truth sources were analyzed as cruise points. The results showed that the LADs were the cheapest and easiest to fly. The tower flyby and the cruise points were close in cost and data reduction workload.

In addition to comparing resources, random uncertainties for recovery factor and bias were calculated for each combination of methods and truth sources. Figure 10 shows the recovery factor and the upper and lower 95 percent confidence intervals in the form of error bars for each method and truth source combinations.

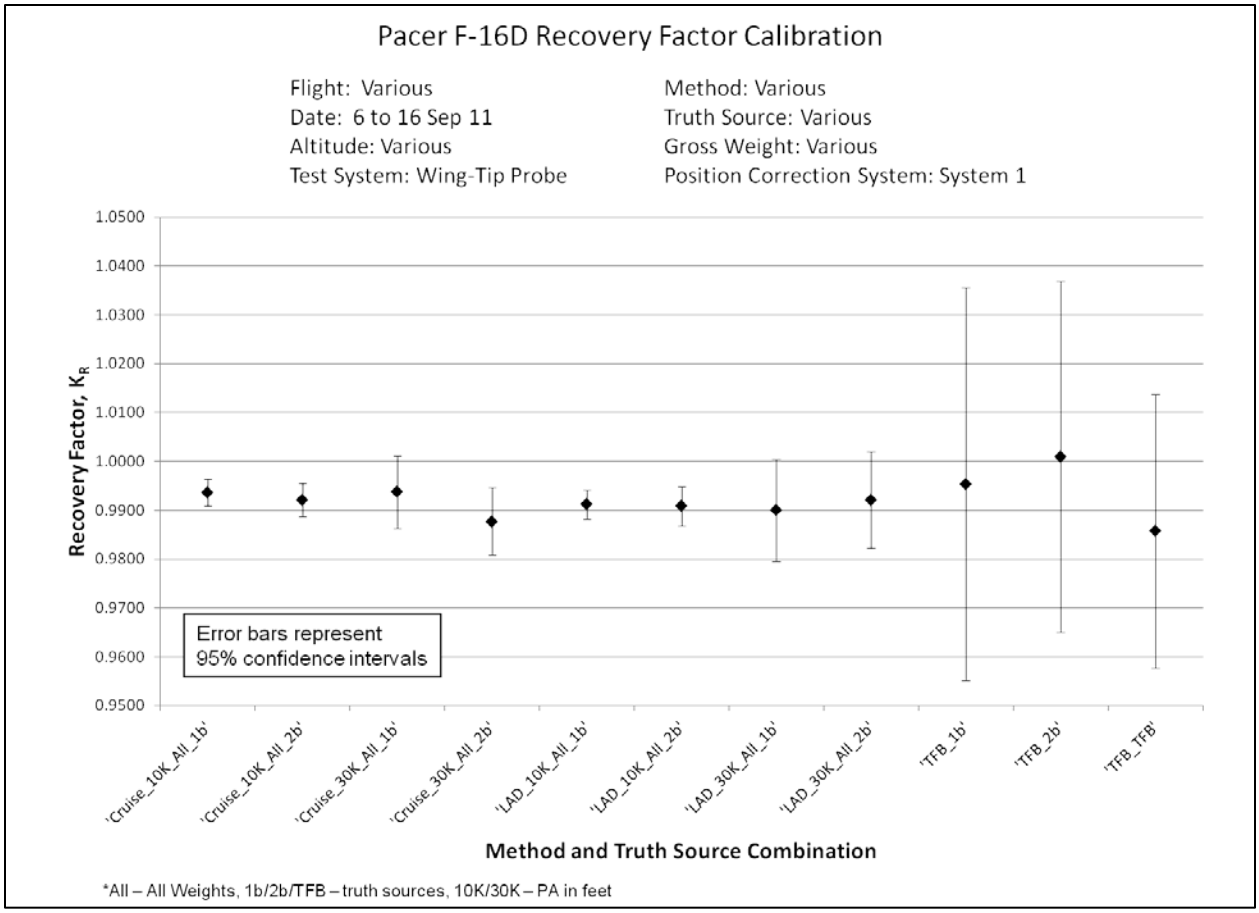

Figure 10 Recovery Factor Uncertainties

By looking at the random uncertainties, the tower flyby method with all three truth sources had the largest uncertainties. On the other hand, the cruise method at 10,000 feet had the least uncertainties followed by LAD at 10,000 feet and then the 30,000 feet methods and truth sources.

During the two days on which tower flyby testing was conducted, temperature inversions were noted from the balloon data due to terrestrial heating. The standard atmosphere assumes that temperature decreases as altitude increases. During the test time frame the temperature was increasing as altitude increased up until 3,280 feet MSL on flight 2 and 3,070 feet MSL for flight 6. For the flyby tower truth data, the corrected temperature assumed standard atmosphere. For the one balloon and two balloon truth sources, the data from one time (when the balloon was launched) were used. Uncertainties with the balloon truth data included the change in temperature with time. It was determined from the flyby tower truth source that within the 2 hours of flight 2, the temperature at the tower increased 5 degrees. This change was not reflected in the balloon data.

All combinations overlapped at a recovery factor value of about 0.99. This overlap signified that each combination of method and truth source produces the same recovery factor. This tells us that any combination can be used at any altitude to determine the recovery factor, but with some risk of assuming that they are the same when they are actually not (Type II or beta error).

Figure 11 shows the intercept biases and their associated uncertainties. The uncertainty results showed some scatter with non-overlapping differences between the 10,000 feet and the 30,000 feet points. This showed that there may have been a significant difference for the intercepts at different altitudes. The

uncertainties at 30,000 feet were greater than at 10,000 feet for all maneuvers, as it was with the uncertainties for the recovery factor. The 10,000 feet combinations had the smallest uncertainties. Tower flybys had the greatest uncertainties.

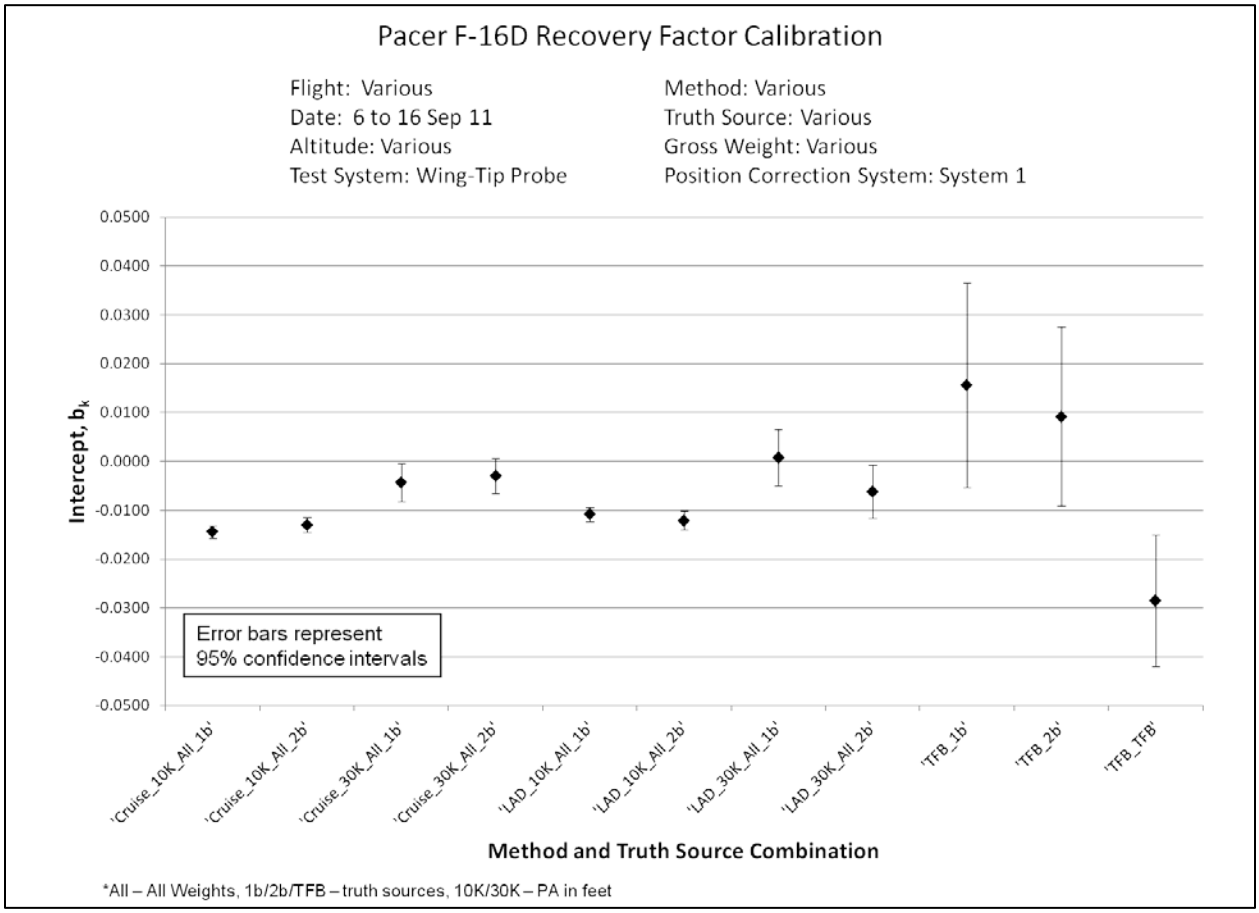

Figure 11 Recovery Factor Intercept Uncertainty

Overall the uncertainties for both the recovery factor and bias depended primarily on the altitude of the calibration with calibrations at 10,000 feet having the smallest uncertainties. The tower flyby method had the largest random uncertainties with flyby tower truth source being the smallest out of the three tower flyby truth sources. The cruise method had smaller uncertainties at each altitude compared to the LAD method. The one balloon truth source produced smaller uncertainties at 10,000 feet than two balloon truth source. At 30,000 feet, the two balloon truth source produced smaller uncertainties than the one balloon truth source. Table 5 shows the magnitude of the uncertainty interval for all method and truth source combinations.

Table 5 Summary of Uncertainty Intervals in Order of Magnitude for the Wing-Tip Probe

Method	Truth Source	Altitude (ft)	Slope Uncertainty Interval (+/-)	Intercept Uncertainty Interval (+/-)
Cruise	One Balloon	10,000	0.0027	0.0012
Level Accel/Decel	One Balloon	10,000	0.0030	0.0015
Cruise	Two Balloon	10,000	0.0033	0.0015
Level Accel/Decel	Two Balloon	10,000	0.0040	0.0020
Cruise	Two Balloon	30,000	0.0069	0.0036
Cruise	One Balloon	30,000	0.0074	0.0039
Level Accel/Decel	Two Balloon	30,000	0.0099	0.0054
Level Accel/Decel	One Balloon	30,000	0.0104	0.0057
Tower Flyby	Flyby Tower	2,300	0.0280	0.0135
Tower Flyby	Two Balloon	2,300	0.0359	0.0183
Tower Flyby	One Balloon	2,300	0.0403	0.0209

Static Source Error Correction Calibration Techniques:

The specific test objective was to compare the static pressure position correction calibration techniques and data analysis methods for the pacer aircraft. For all sorties, the various techniques were flown and truth source data were collected. The data were then analyzed using combinations of truth source, calibration technique, and calibrated systems. These combinations were then compared by determining the static pressure position correction, the repeatability of the results, and the resources, logistics, and time required.

Data Analysis Techniques.

All data reduction techniques are detailed in appendix D. Some of the techniques used during this project were not well known, even from groups involved with Pitot-statics calibrations, and are briefly described in the following paragraphs.

For this project, the ‘multiple balloon atmospheric model’ used two different balloons. Both pressure and pressure gradient at each of the balloons and at each altitude were used to model the atmosphere’s pressure as a polynomial function of latitude and longitude. Complete details are given in appendix D. This truth source was intended to reduce the maximum possible error for points not flown at the balloon’s position (compared to the one-balloon truth source).

The Self-Survey and Atmospheric Analysis truth sources were intended to use Atmospheric Analysis passes in order to correct for the variability of the atmosphere in time and position. For the Self-Survey truth source, the aircraft Pitot-static correction at a specific airspeed, obtained from previous calibrations, was used as the initial reference, whereas the Atmospheric Analysis truth source used a balloon as the initial reference. Complete details are provided in appendix D.

Uncertainty could not be obtained by calculation because of the complexity of the algorithm used to transform the measured data into the final result, and because of the very large number of inputs. Instead, it was noted that uncertainty (U) was the root mean square of the systematic and the random

uncertainties $U = \sqrt{(b^2 + s^2)}$. The systematic uncertainty could not easily be estimated, which was one of the reasons for conducting this test program. The random uncertainty could be determined by fairing a model through the data, then calculating the random uncertainty of the data from that model, using the following equation: $\sqrt{\sum(xi - xref)^2/(n * (n-1))}$, with (*xi – xref)* being the difference between the data and the model for each sample, and *n* the number of samples.

Test Results.

The static source error correction was determined for each combination of FTT, truth source, and system to be calibrated. Unless mentioned otherwise, all static source error corrections are presented as $\Delta P_{pc}/P_{sic}$, or static pressure correction divided by the instrument-corrected static pressure, and is non-dimensional.

Resources, Logistics, and Time Required

FTT Efficiency

Time and fuel required was hand recorded in-flight prior to setting up for each maneuver and after completion of the maneuver. For sequential maneuvers, the ending time and fuel from the previous maneuver was used as the starting time and fuel for the next maneuver. The production F-16D fuel totalizer was used for all fuel data. These data were compiled and analyzed to determine the operational efficiency of each of the calibration techniques for the range of subsonic airspeeds from an airspeed corresponding to 11 degrees AoA through 0.93 Mach number. Table 6 below displays the analysis and figure 12 displays the results.

Table 6 FTT Efficiency Analysis

FTT	LAD	TFB	Cruise	Turns	Cloverleaf
Avg Time/Event (min)	10.2	4.6	3.1	6.6	6.9
Avg Fuel/Event (lbs)	792	359	262	399	512
Events Required	2	16	24	24	24
Total Time (min)	20.3	74.4	75.6	158.0	165.8
Total Fuel (lbs)	1,583	5,744	6,288	9,566	12,278
Total F-16 Ops Cost	**$5,983**	**$21,903**	**$22,245**	**$46,491**	**$48,774**

Notes: 1. Events required are based on a calibration through the range of airspeed from 11AOA to 0.93M.
2. Abbreviations, acronyms, and symbols are defined in appendix F.

The analysis was divided into time and fuel requirements per event and then multiplied by the number of events required to calibrate the aircraft. The F-16 operational costs were determined from total time using a standard F-16 operational cost per flight hour of $17,655. Pacer customers do not always require the same level of uncertainty for their calibrations. Therefore, the number of events required to calibrate the aircraft could increase or decrease based on the required uncertainty of the customer. Also, all data presented applies to calibrating the F-16D pacer aircraft over an airspeed range from the airspeed corresponding to 11 degrees AoA through 0.93 Mach number. The total number of points to calibrate the aircraft, and therefore the total cost, would change if pacer customers require a smaller or larger range of calibrated airspeeds.

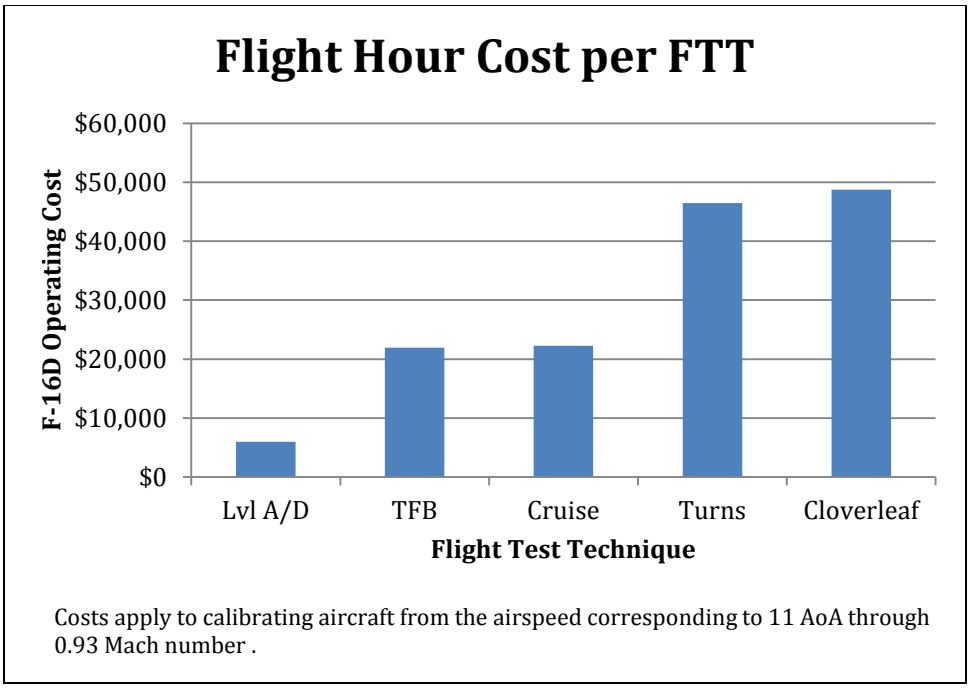

Figure 12 FTT Efficiency Results

Total time and the resulting F-16 operational cost were the most significant results to determine FTT efficiency, because they could be quantitatively compared to other results (figure 12). The LAD method was by far the most efficient, requiring only 20 minutes at a cost of $5,983. The remaining FTTs, in order of efficiency, were tower flyby, cruise, 360-degree turn, and cloverleaf.

FTT Pilot Workload

The pilot rated each of the five FTTs with respect to required workload using the Bedford workload scale (appendix F). These data were collected to compare further the calibration techniques and the ease of execution, while maintaining tolerances. Flight test techniques were typically executed using the F-16's autopilot, when appropriate. Although the Bedford workload ratings typically do not include a rating of levels, these were created for simplification of comparison. Levels are defined as follows: Level 1 – rating 1, 2, 3; Level 2 – rating 4, 5, 6; and Level 3 – rating 7, 8, and 9 (appendix E). The results are summarized in table 7.

Table 7 Pilot FTT Bedford Workload Ratings

Events	Pilot 1	Pilot 2	Pilot 3	**Level**
Cruise	2	3	3	**1**
Turns	3	4	4	**1/2**
LAD	4	5	5	**2**
Cloverleaf	5	6	4	**2**
Tower Flyby	*	7	6	**2/3**
* Pilot 1 did not perform any tower flyby events				

All the FTTs proved executable on test day conditions. Tower flyby was the only maneuver that received a rating of 7 (Level 3). The FTT with the lowest workload rating by all three pilots was cruise.

The remaining FTTs from lowest to highest workload ratings were: 360-degree turn; level acceleration/deceleration; cloverleaf; and tower flyby. Pilots commented that the combination of pattern procedures, lack of ability to use the autopilot, and ground proximity led to the higher TFB Bedford workload rating.

Data Reduction Efficiency

The Bedford scale did not apply to the evaluation of the workload inherent to the different data reduction techniques. Additionally, it was not relevant to measure just the time required to analyze one point, because it was almost impossible to ensure repeatability, with variables such as concentration, tiredness, and so on.

Instead, the team member that accomplished the most data reduction rated each technique with the following qualitative descriptors: simple or complex, and quick or long. Tables 8 and 9 summarize these ratings.

Table 8 Data Reduction Efficiency – Altitude Techniques

Truth Source/FTT	Cruise	Level Accel/Deccel	Tower Flyby
One balloon	Simple and quick	Simple and quick	N/A
Two balloons	Complex and quick	Complex and quick	N/A
Self-Survey	Complex and long	Complex and long	N/A
Atmospheric Analysis	Complex and long	Complex and long	N/A
Tower flyby	N/A	N/A	Simple and quick

Note: Abbreviations, acronyms, and symbols are defined in appendix F.

Table 9 Data Reduction Efficiency – Speed Techniques

Truth Source/FTT (data reduction technique)	Cloverleaf	360-degree turn (Boomer Turn)	360-degree turn (Orbis)
Calibrated wingtip temperature probe	Simple and long	Simple and quick	Simple and quick
One balloon	Simple and long	Simple and quick	Simple and quick

The data reduction involved several steps, regardless of the technique. The first step was to write the MATLAB® code used to process the raw data. Because it was a one-time required work and would not need to be repeated, it was not taken into account in this analysis. The second step was to prepare the raw data so that they could be processed by MATLAB®. This involved cutting the DAS excel file into pieces, one piece for each data point, formatting the balloon files, and preparing the m-file (or MATLAB® function) for each data point. To maintain traceability, it was decided that each data point would be reduced using a new m-file. The last step was to concatenate all the derived data, create the appropriate plots and calculate the standard deviations for each set of points. This last step was common to all techniques.

The cruise and LAD data reduction techniques were identical except for the size of the files involved, which did not change the complexity or the time required to run each data point. Using one balloon as a truth source was simple since it only involved using the balloon data as a look-up table. Using two balloons as a truth source increased the complexity. The mathematical model could sometimes lead to unreasonable values, which forced the analyst to then modify the code. For the Atmospheric Analysis, after creating the model for one flight, it was necessary to verify the validity of that model, which took more time. This was done by ensuring that the p-values for each variable was smaller than 0.05, indicating that there was a 95 percent or higher confidence that the variable was indeed statistically significant in the model. When the model was not correct, modification of the code was then necessary. This made the technique a complex and difficult one since true understanding of the code itself and of the underlying physics was required, and the technique could not be programmed to be a simple "click and obtain the data". This lack of simplicity was found to be objectionable if this technique must be employed on a regular basis but by different personnel each time. The same was true for the Self-Survey algorithm, which was very similar to that of the Atmospheric Analysis.

The tower flyby data were quick to reduce. It was only slightly longer than the one balloon cruise technique because the truth source data had to be collected from handheld data and then transcribed into an excel file.

The algorithm for the cloverleaf technique was longer to run than for the one balloon cruise technique because it involved processing three runs for each data point.

Finally, both turn algorithms (Orbis and Boomer Turn) were simple to use. Running the code was fast, similar to the one balloon cruise technique. Both algorithms had the advantage to provide visual feedback on the quality of the data by comparing the circles representing the north and east components of the different speeds during the turn (DGPS, true, and ground). The cloverleaf technique, although based on the same principle, did not provide such a good visual feedback.

Truth Source Cost

The cost of each of the five truth sources (one balloon rawinsonde, two balloon rawinsonde, Atmospheric Analysis, Self-Survey, and tower flyby) was documented. The costs involved in each of these techniques were unique. However, a dollar amount was calculated for each combining expendable resource, F-16 flying hour and manhour costs. The F-16 time requirements for the Atmospheric Analysis and Self-Survey were documented in the same manner as the five FTTs in the previous section. These costs were important because they involved separate maneuvers from the calibration FTTs and therefore, would add flight hours to accomplish. Other variables used in creation of the total costs are as follows: F-16 flying hour costs per hour were $17,655; labor costs were $56.57 per hour. Total costs are presented in table 10.

Table 10 Truth Source Costs

Truth Source	Expendable Resource Cost ($)	F-16 Hours	F-16 Operational Costs ($)	Man-Hours	Labor Costs ($)	Total ($)
One balloon rawinsonde	400	N/A	N/A	1	56	456
Two balloon rawinsonde	800	N/A	N/A	12	678	1,478
Self-Survey	N/A	0.84	14,830	N/A	N/A	14,830
Atmospheric Analysis	400	0.84	14,830	1	56	14,886
Tower Flyby	N/A	N/A	N/A	8	452	452

The majority of truth source costs were in expendable resources and manhours. The tower flyby cost was least because it required no expendable resources; however, the one balloon rawinsonde cost was approximately the same. The two balloon rawinsonde cost did not increase appreciably. The Self-Survey and Atmospheric Analysis costs increased significantly due to the F-16 flight hours required to accomplish this method.

Equipment Cost

The trailing cone system and wingtip total temperature probe required modification of the aircraft. These activities incurred manhour costs to modify and de-modify the aircraft and manhour costs during the test. The manhour costs are summarized in table 11. Furthermore, there were expendable resource costs. For example, the trailing cone was only serviceable for approximately three sorties, resulting in three cones being used for this test program for a cost of $4,500. Any sunk costs, such as initial production, which would not be required for future tests, were not included. These equipment costs were not compared to each other, as they accomplish separate tasks. These values were calculated so that the total cost of a truth source or technique could be accurately calculated.

Table 11 Equipment Costs

Equipment	Mod/Demod Man Hours	ManHours Per Flight	Total Flights	Total Man Hours	ManHour Cost*	Expendable Resources	Total Cost
Trailing Cone	40	13	8	144	$8,146	$4,500**	$12,646
Total Temperature Probe	20	0	8	20	$1,131	0	$1,131

* 2011 manhour costs were $56.57 per hour.
** Cost is for 3 trailing cones at $1,500 per cone.

Summary of Resources, Logistics, and Time

Calibration FTT costs and truth source costs did not stand alone. Each FTT required a truth source and therefore, there were 21 different combinations of FTT and truth sources. The only unique FTT and truth source was the tower flyby, which could not be combined with another truth source. Table 12 displays the combined cost of both FTT and truth source combinations. Furthermore, it includes the data reduction efficiency ratings and the FTT Bedford workload ratings (in levels) previously assigned. This table summarizes significant results in order to make a direct FTT and truth source comparison.

The FTT truth source combination with the least cost was the level acceleration and deceleration combined with the one balloon rawinsonde. This had a total cost of $6,440. Furthermore, it was rated with a simple and quick data reduction efficiency and a level two Bedford workload rating. Twenty more combinations are displayed with various costs, and efficiency/workload ratings. The most expensive combination was the cloverleaf and Atmospheric Analysis at $63,661.

Table 12 Summary of Resources, Logistics, and Time

			FTTs - in increasing order of difficulty →				
			Cruise	**Turns**	**Lvl A/D**	**Cloverleaf**	**TFB**
		Individual Costs	$22,245	$46,492	$5,983	$48,774	$21,904
Truth Sources - in increasing order of workload ↓	**1 balloon**	$457	$22,702 Simple & Quick | 1	$46,948 Simple & Quick | 1/2	$6,440 Simple & Quick | 2	$49,231 Simple & Quick | 2	N/A
	TFB	$453	N/A	N/A	N/A	N/A	$22,357 Simple & Quick | 2/3
	2 balloon	$1,479	$23,724 Complex & Quick | 1	$47,970 Complex & Quick | 1/2	$7,462 Complex & Quick | 2	$50,253 Complex & Quick | 2	N/A
	Self Survey	$14,830	$37,076 Complex & Long | 1	$61,322 Complex & Long | 1/2	$20,813 Complex & Long | 2	$63,605 Complex & Long | 2	N/A
	Atmospheric Analysis	$14,887	$37,132 Complex & Long | 1	$61,378 Complex & Long | 1/2	$20,870 Complex & Long | 2	$63,661 Complex & Long | 2	N/A

Notes: 1. Costs are based on a calibration through the range of airspeed from 11AOA to 0.93M.
2. Cloverleaf truth source is only necessary if a calibrated total temperature probe is not available.

Inner box legend:

Total Cost: FTT + Truth Source	
Data Reduction Efficiency	FTT Workload Rating

	Best / Level 1
	Medium / Level 2
	Worst / Level 3

Static Source Error Correction: Comparison of Different FTTs

Cruise Technique: Trailing Cone and Noseboom Calibrations

The noseboom had two sets of static ports (system 1 and system 2), linked to individual transducers, resulting in two individual systems. Both systems of the noseboom had a very similar static source error correction, with a difference of 0.00005, which corresponded to 1.3 feet at 10,000 feet PA. Only results for system one of the two noseboom systems are presented.

The cone's and the noseboom's static source error corrections were of similar magnitude, even though the shapes the error correction curves differed, as shown in figure 13. The cone error correction change with indicated Mach number was linear whereas for the noseboom, it was piecewise linear (two lines joining around 0.74M). This specific shape for the noseboom could have been caused by a balance between AoA and compressibility effect, but was not investigated. This shape was similar in previous calibrations accomplished by the 773 TS/ENF. The random uncertainties were also similar, with a value of 2.32×10^{-5} for the noseboom and 2.75×10^{-5} for the cone. As a reminder, all static source error corrections, and their random uncertainties, are dimensionless. The non-calibrated cone static pressure had a position error correction of the same magnitude than the non-calibrated noseboom. Yet, both the noseboom, which was a test noseboom and not production representative, and the cone presented small errors before calibration. Indeed, the maximum error was 0.002, which equated to about 50 feet at 10,000 feet PA. At 2,300 and 30,000 feet, the comparison of the noseboom and the cone error gave similar results, the main difference being a larger random uncertainty at 30,000 feet, and that the higher the altitude, the larger the altitude correction for a given static source error correction $\Delta P_{pc}/P_{sic}$. Corresponding values are given in table C3. Corresponding graphs are given in figures C48 and C49.

Both the cone and the noseboom could be calibrated for use as a reference in a pacer calibration.

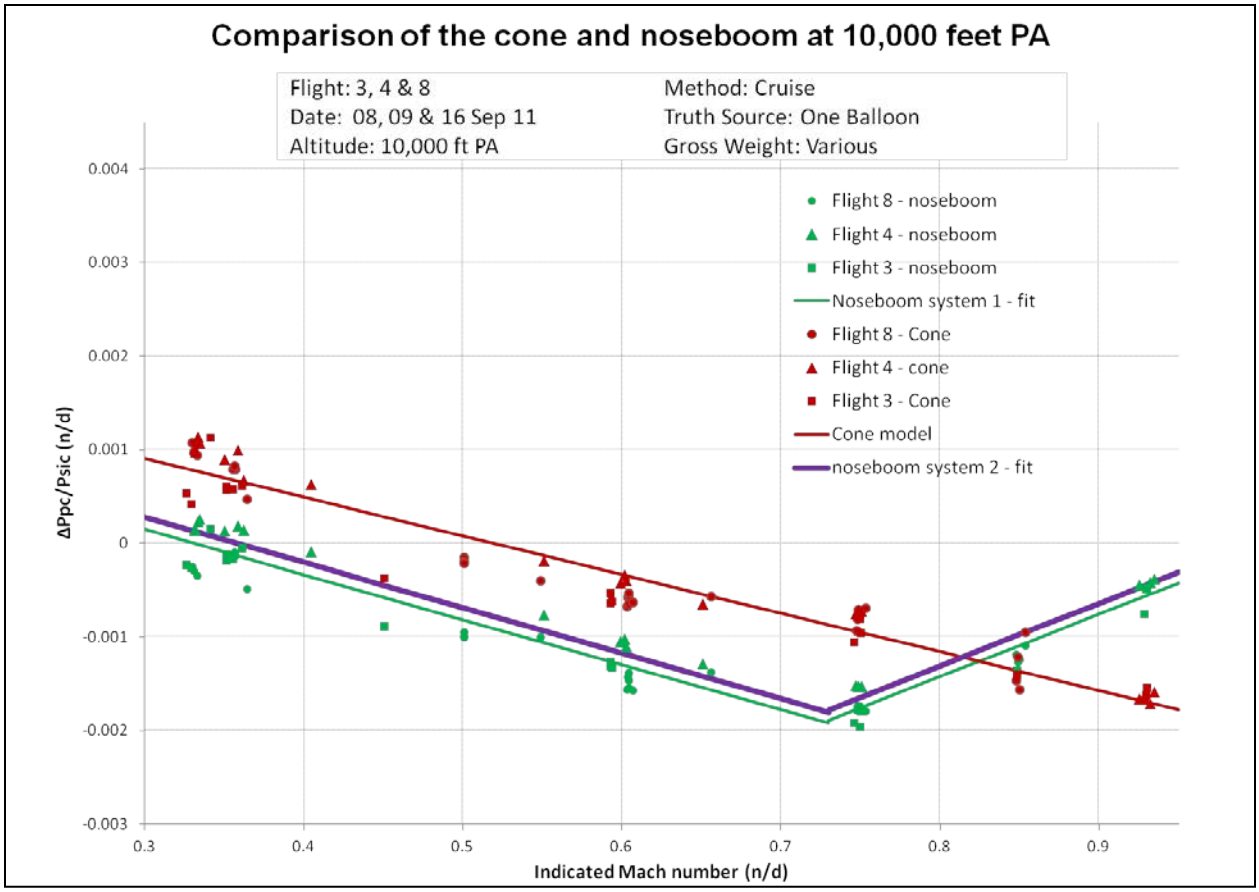

Figure 13 Comparison of the Cone and Noseboom at 10,000 feet PA

Cruise Technique Truth Sources

At 2,300 feet PA, the results for the cruise point with one balloon as the truth source were compared to the tower flyby results (figure 14). For the cone and the noseboom, the difference in static source error correction between the tower flyby and the cruise results was less than 0.00015, which was determined by finding the maximum difference between the line fits for the tower flyby and for the cruise techniques. This difference corresponded to less than 4 feet. Random uncertainty was 3.86×10^{-5} for the noseboom when using the cruise with one balloon technique, but only 1.91×10^{-5} for the tower flyby technique. For the cone, the random uncertainty was respectively 4.73×10^{-5} and 2.52×10^{-5}. This showed that the tower flyby technique only slightly reduced the random uncertainty. Also, the fact that two very different techniques gave very similar results increased the confidence in there being a small systematic uncertainty.

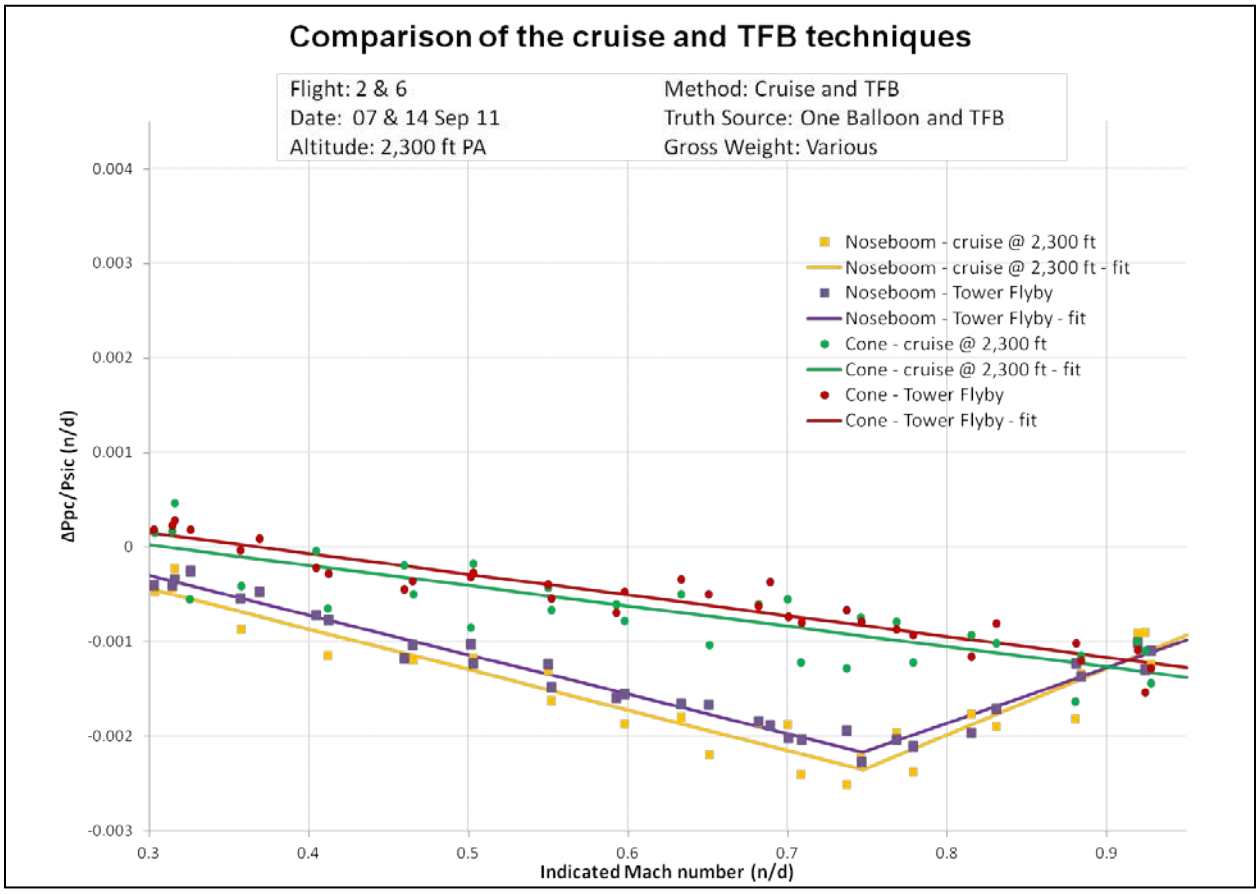

Figure 14 Comparison of the Cruise and Tower Flyby Techniques

At 10,000 feet PA, the results for the cruise points with one balloon and with two balloons as the truth source were compared (figure 15). Again, the difference between both results was less than 0.0002, or about 5 feet at 10,000 feet PA. For the noseboom, the random uncertainty was 2.31×10^{-5} with one balloon and 3.67×10^{-5} with two balloons. The intent of using a second balloon was to decrease the maximum systematic uncertainty from having pressure reference at both ends of the used airspace instead of only one. Yet, the systematic uncertainty was not significantly changed while uncertainty was increased. Using two balloons instead of one did not increase the accuracy of the noseboom or cone calibration.

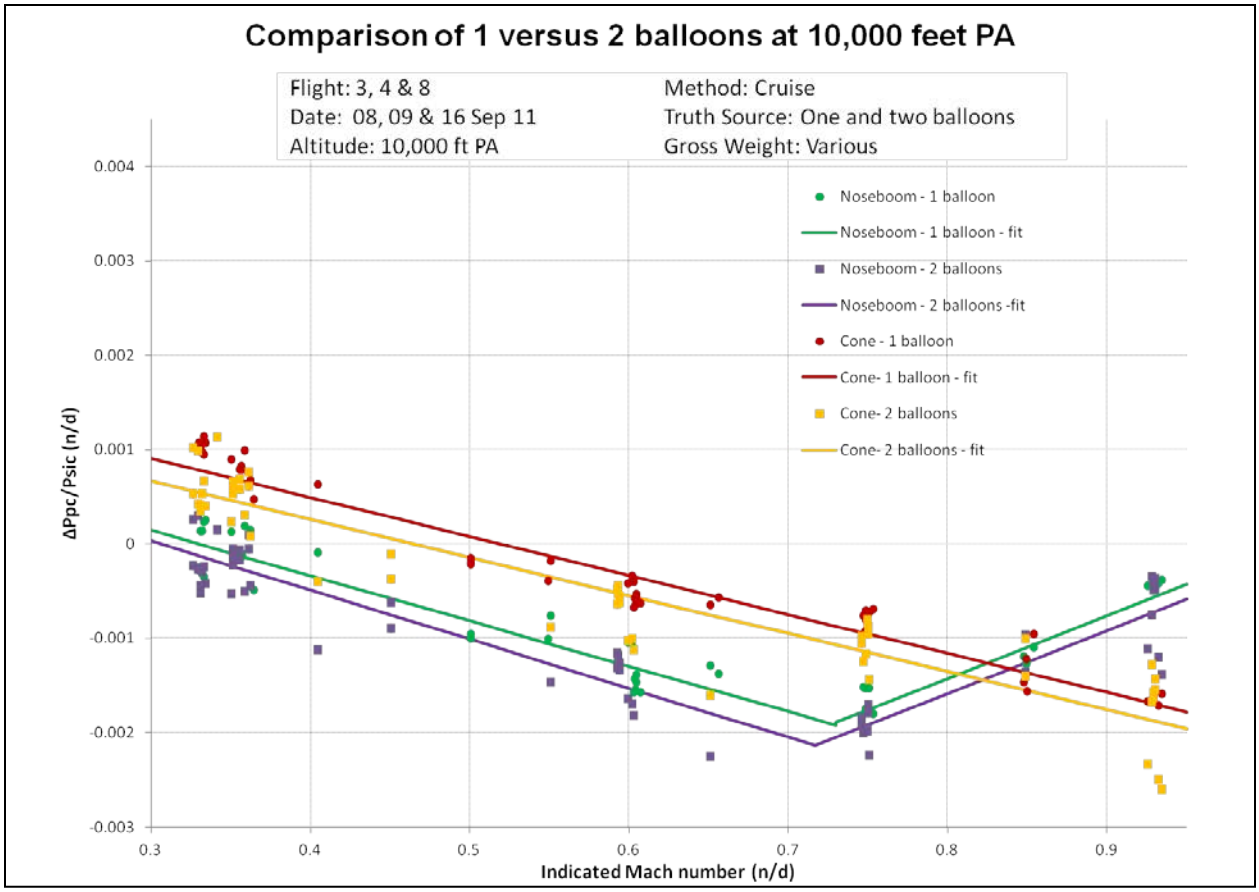

Figure 15 Comparison of One Versus Two Balloons

The Atmospheric Analysis, as well as the Self-Survey, did not provide many usable results. Specifically, for flight number five, the model gave unreasonable values (with negative pressure sometimes). This was probably due to the fact that the weather that day was changing rapidly, with a meteorological front approaching the area. The presence of clouds pushed the flight profile away from the intended path. The consequence was that only one of the last two survey passes was performed at the end of the flight, and that pass was offset in position from the first two. This probably led to confounding in the model, with both time and position changing at the same time, thus not being independent. Although the Atmospheric Analysis could not be performed, the changes in ambient pressure with time and position were still small enough to allow the use of the data with the one or two balloon truth sources.

For all the other flights, the weather conditions were stable, with changes in pressure smaller than 0.02 inches of mercury (inHg) over the airspace and timeframe of the flight test day. The atmospheric models gave results similar to the one balloon truth source, yet were devoid of physical or statistical significance. First, because Atmospheric Analysis passes were only flown on one axis, pressure changes could only be observed on that axis. Yet, as shown in figure 16, isobars are not parallel straight lines. Since the model was created as a linear model, it was only valid on the axis on which the passes were flown. Then, if a test point was flown outside that axis, the model could not be used. In addition, the mathematical model resulting from the statistical analysis was not physically significant. Indeed, the model was found by assuming that changes of pressure with position or time were linear, which is rarely true, as shown again by the example in figure 16. Second, for some flights, time and or position were found to be insignificant in the model and had to be removed from the model's variables. Finally, the model itself could give unrealistic values as soon as the time or position was outside what had been

mapped during the Atmospheric Analysis passes. As an example, for flight seven, the model for pressure was the following:

Pressure (inHg) = -26.818364 – 0.000396 * Altitude + 0.000002 * Time – 0.058016 * Dlat + 0.059654 * Dlon,

with 'Time' being the time of year in seconds (hence having a value of about 22347000 seconds for that flight); Altitude was the DGPS altitude in feet (around 30,000 feet for that flight); Dlat and Dlon were the latitude and longitude difference in degrees from the reference point, which was positioned at the middle of the Atmospheric Analysis passes.

From that equation, a change of 30 nautical miles in latitude or longitude resulted in about 2 inHg change in pressure, which is not consistent with actual pressure changes that day. Still from that equation, if latitude and longitude changed as a result of flying on the same axis as the Atmospheric Analysis passes (heading of 030 degrees north), the pressure change given on the model matched reality, i.e., about 0.005 inHg for 30 nautical miles.

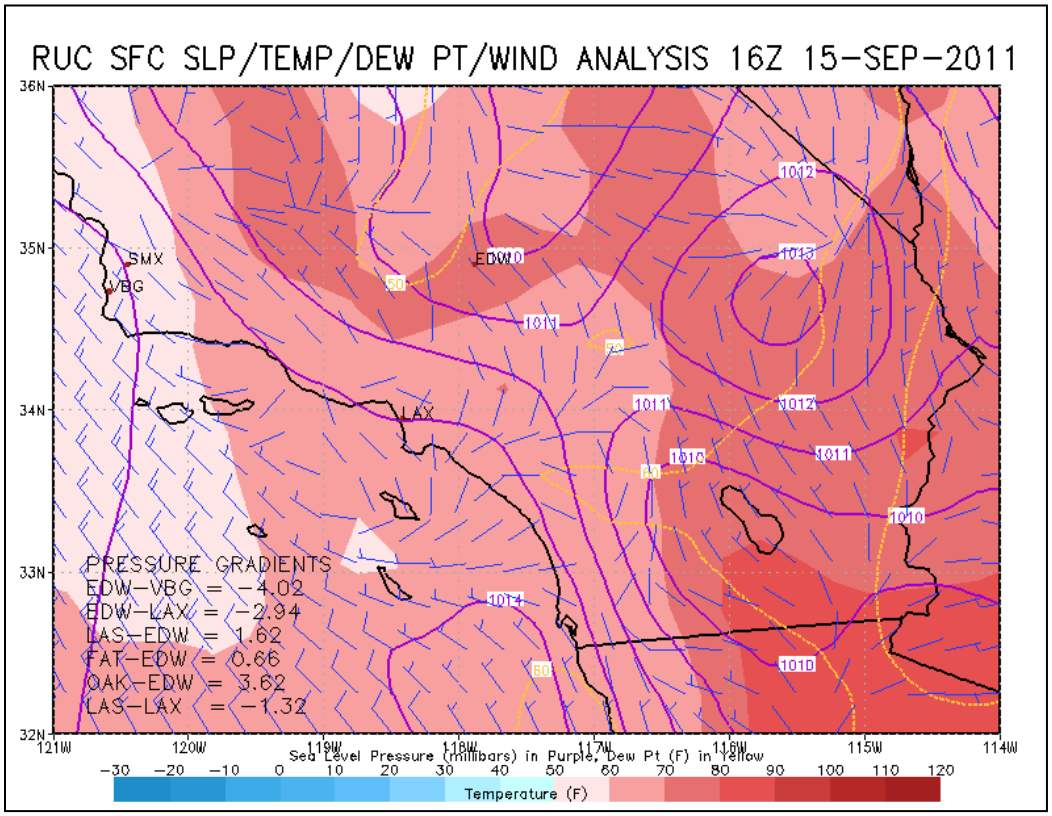

Figure 16 Lines of Constant Pressure at the Surface (mbar), Around Edwards AFB, California, on 15 September 2011

The results for static pressure calibration using the Atmospheric Analysis and Self-Survey are presented for flight three, which was a 10,000 feet profile (figure 17). The difference between one balloon and the Atmospheric Analysis as truth sources was of the same order of magnitude as between one and two balloons, both in bias and in standard deviation.

The Atmospheric Analysis did not provide any improvement over the one balloon as a truth source. Yet, using the Atmospheric Analysis passes could be used to characterize the atmosphere variability in the absence of other meteorological data. This would provide an estimate of the largest error in the reference ambient pressure, hence providing a criterion on whether to utilize the data or not.

The Self-Survey technique did not provide any improvement over the one balloon as a truth source in terms of bias or standard deviation. Yet, this technique presented the advantage that no balloon was required as a truth source. It is important to remember here that the Self-Survey technique was identical to the Atmospheric Analysis with the exception that the model's offset was corrected by using a known correction at the airspeed used to fly the survey passes, instead of using a balloon. The Self-Survey technique could then be very advantageous if the Pitot-static system was calibrated for one airspeed only, but required calibration at other airspeeds.

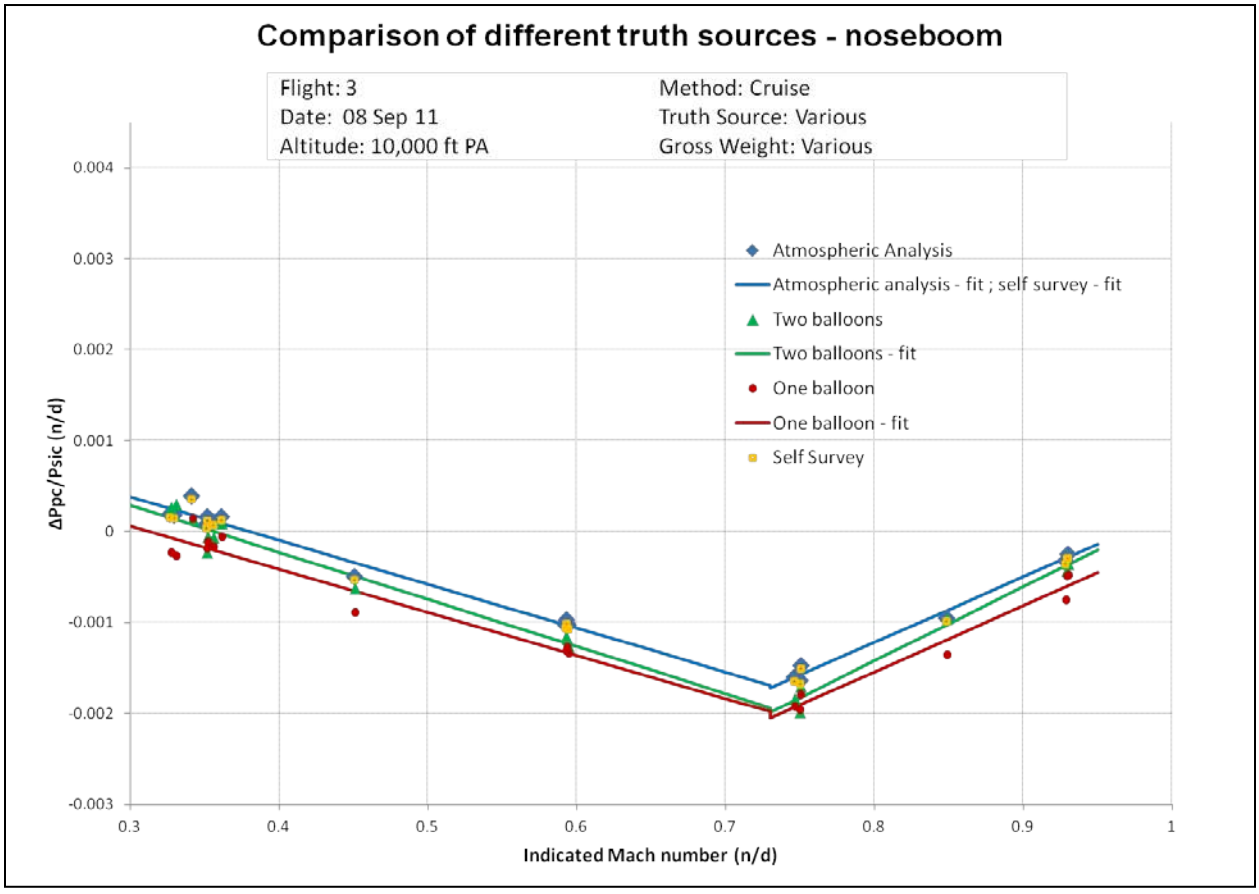

Figure 17 Comparison of Different Truth Sources

Cruise Technique at Different Altitudes

The static source error correction determined from the cruise technique was significantly different when altitude was changed, as shown in figures 18 and 19. All numerical values are summarized in table 13. At 2,300 feet PA, the random uncertainty was small for the noseboom and for the cone. At 10,000 feet PA, the mean static source error correction was slightly offset compared to the 2,300 feet PA values. The random uncertainty was almost unchanged. Finally, at 30,000 feet PA, the offset (from the 2,300 feet values) increased significantly and the random uncertainty was tripled for the noseboom and for the cone. Values are also given in terms of equivalent altitude correction for ease of interpretation. It

must be remembered that at different altitudes but with an identical $\Delta P_{pc}/P_{sic}$ value, resulting altitude corrections in feet will be different. It was expected that the $\Delta P_{pc}/P_{sic}$ values would not change with altitude. It was not the case. Curves of $\Delta P_{pc}/P_{sic}$ against V_{eic}, or instrument-corrected equivalent airspeed are also provided in figures C50 and C51. Plotting against V_{eic} changed the way the different curves compared to one another. For the cone, the differences were larger, but for the noseboom, they were reduced. More specifically, for the noseboom, the shape of each curve was similar, and only the equivalent airspeed at which the 'kink in the curve' occurred changed. Yet, the difference in the slopes of the curves for different altitudes reached 62 percent, resulting in $\Delta P_{pc}/P_{sic}$ differences of 0.0008.

Table 13 Summary of Results for Static Source Error Correction

System	Noseboom		Cone	
Altitude (ft)	Bias compared to the 2,300 feet results ($\Delta P_{pc}/P_{sic}$ and feet equivalent)	Random uncertainty ($\Delta P_{pc}/P_{sic}$)	Bias compared to the 2,300 feet results ($\Delta P_{pc}/P_{sic}$ and feet equivalent)	Random uncertainty ($\Delta P_{pc}/P_{sic}$)
2,300	N/A	0.0000386	N/A	0.0000473
10,000	0.00056/15	0.0000232	0.00078/20	0.0000275
30,000	0.0016/40	0.0000843	0.0037/95	0.0001086

The consequence was that although normalized for pressure altitude, the static source error correction $\Delta P_{pc}/P_{sic}$ obtained at one altitude could not be used to calibrate the Pitot-static cone or noseboom systems at all altitudes. The usual assumption when using the cone was that the cone calibration was independent of altitude and that one calibration at one altitude was sufficient. That assumption was not valid. The calibration must be performed at several altitudes for better precision, both for the noseboom and the cone. The spacing between altitudes will depend on the accuracy required for the calibration.

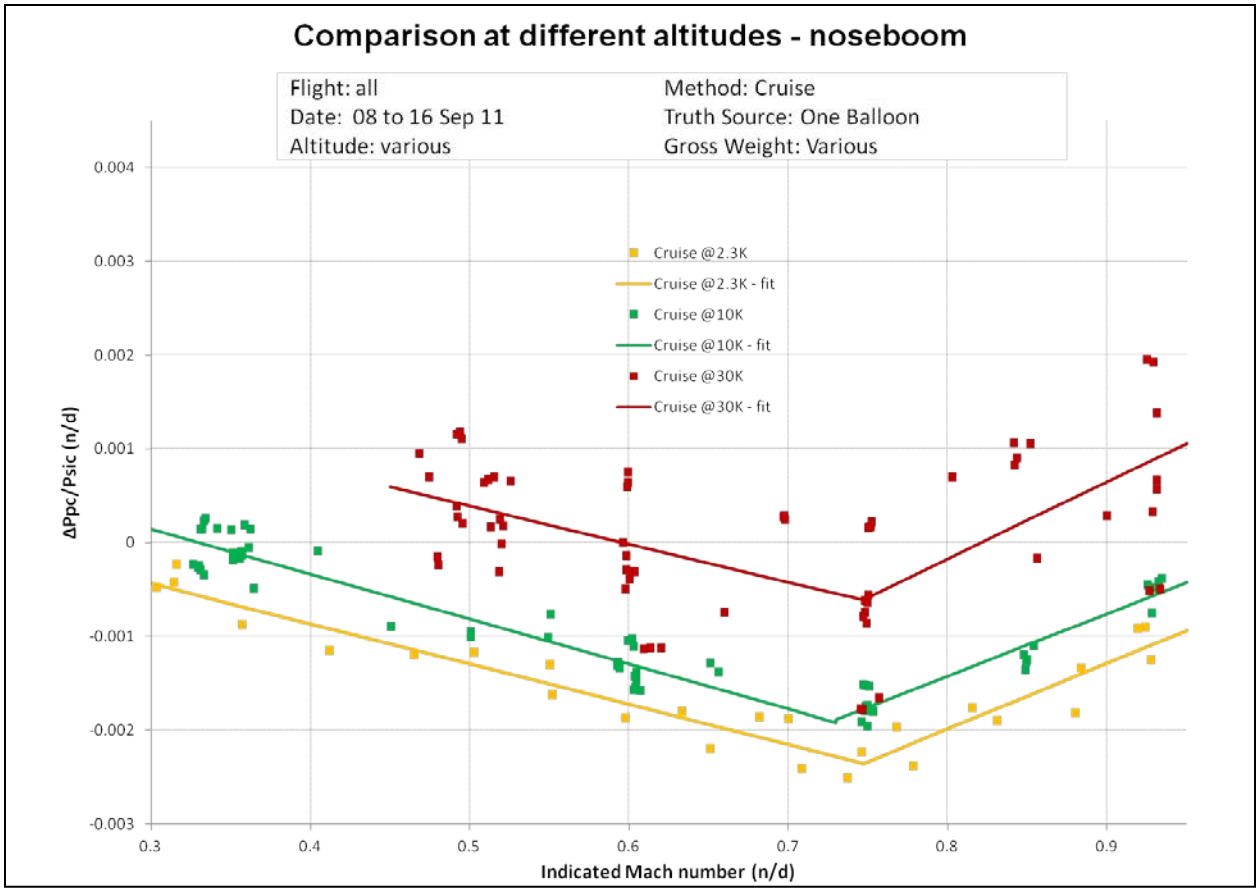

Figure 18 Comparison at Different Altitudes - Noseboom

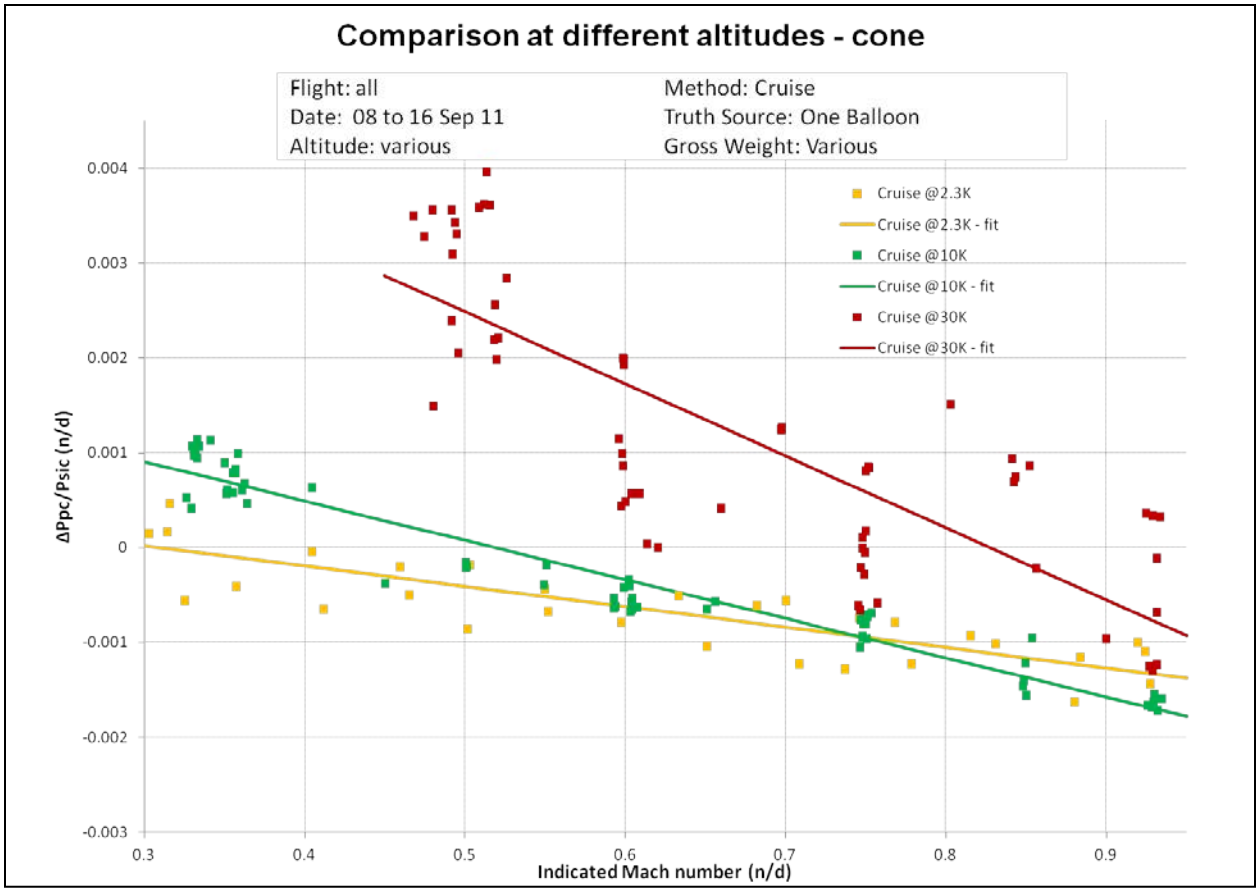

Figure 19 Comparison at Different Altitudes - Cone

Comparison of Cruise and Level Acceleration-Deceleration Techniques

At 10,000 feet PA, LADs gave results similar to the cruise points. These results are shown in figure 20 for the noseboom, and figure C52 for the cone. Taken separately, the level accelerations gave different results from the level decelerations, but combined, the LAD would bracket the model found using the cruise points. Then, fitting a model through all the level accelerations and decelerations at that altitude gave a result very similar to the cruise points fit. Indeed, the mean static source error correction at each airspeed was offset by a maximum of 0.00015 (4 feet) for the noseboom and 0.0005 (13 feet) for the cone, with the random uncertainty being largely decreased at 0.36×10^{-5} and 0.43×10^{-5}, respectively (versus 2.32×10^{-5} and 2.75×10^{-5} for the cruise points). At 30,000 feet PA, similar results were found, although the difference between the cruise points and the LADs was larger at about 0.00038. This was essentially due to a much larger scatter, which affected both techniques. Corresponding results are shown in figure 21 for the noseboom and C53 for the cone.

These results showed that the LAD technique could provide results within 0.0005 $\Delta P_{pc}/P_{sic}$ of the cruise technique, with a much lower cost. In addition, this showed that the error associated with the level accelerations and decelerations was similar for the cone and the noseboom.

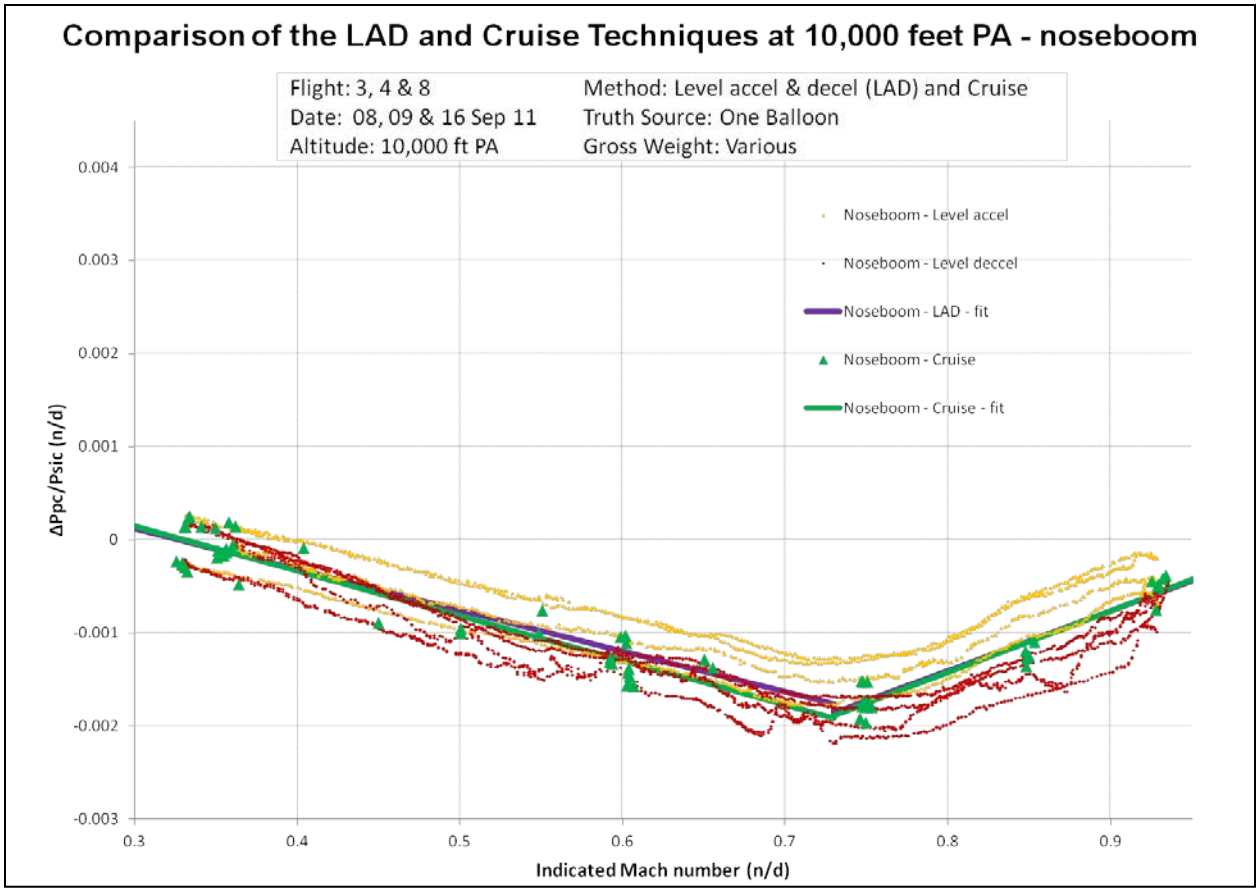

Figure 20 Comparison of the LAD and Cruise Techniques at 10,000 Feet PA

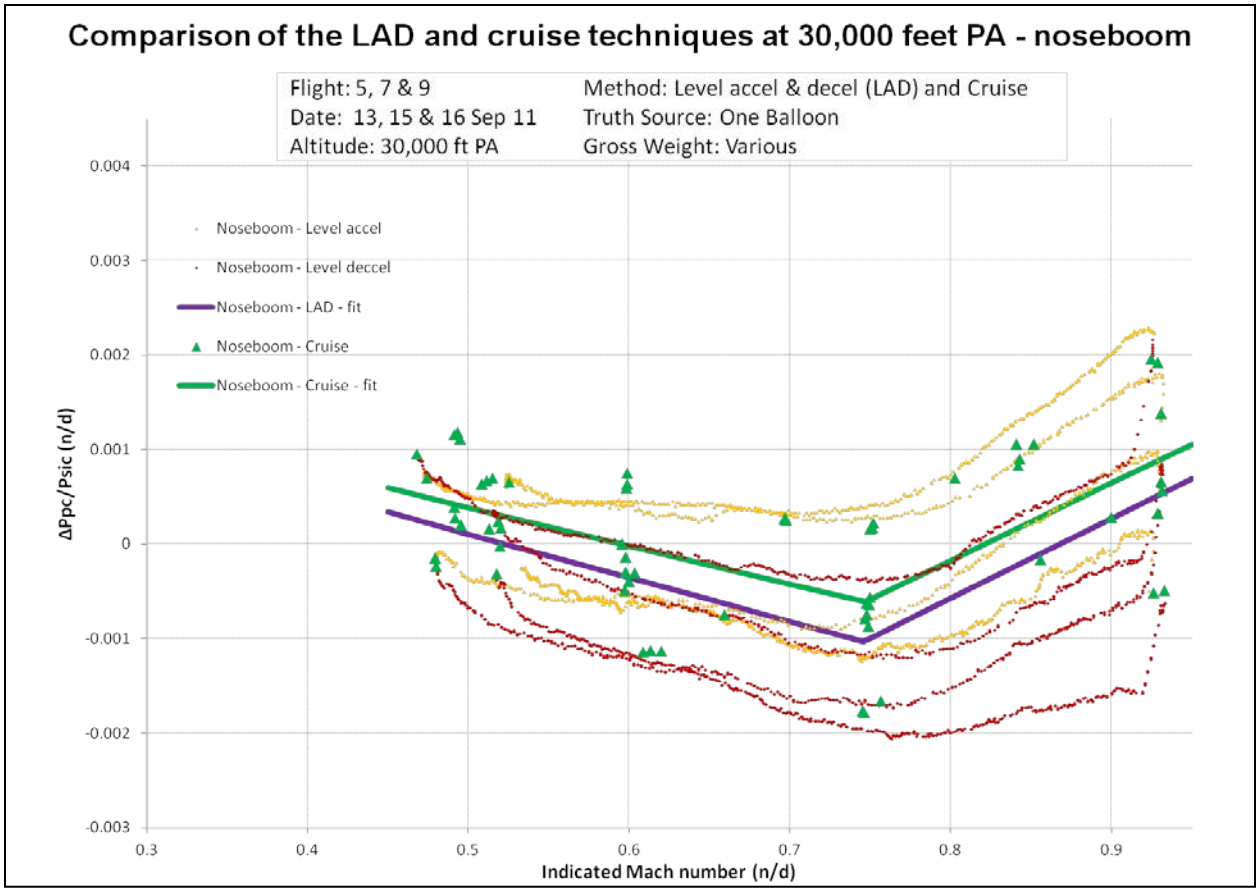

Figure 21 Comparison of the LAD and Cruise Techniques at 30,000 Feet PA

Level Acceleration-Deceleration Techniques at Different Weights

For cruise and for LAD techniques, it was anticipated that AoA could have an impact on the static source error correction. In level, un-accelerated flight, at a given pressure altitude and indicated airspeed, AoA is a function of weight only. Many points would be required to isolate the effect of AoA from altitude, compressibility, and thrust effects. Therefore, only the weight effect was considered. For cruise points, each speed being flown at a different weight, and each point being affected by an uncertainty, it was hard to evaluate the effect of weight. For LADs, evaluating the effect of weight was much easier because each LAD covered the entire speed range, and was flown toward either the end or the beginning of the flight. Each LAD was then flown at a very different weight. At 10,000 feet PA, it was found that the weight did not have an effect on the measured value of the static source error correction, both for the cone and the noseboom (figures 22 and 23). Only one LAD at each weight was flown, and the comparison therefore lacked statistical significance, yet no weight trend was noticed when looking at the cruise points or at the LAD at 10,000 and 30,000 feet PA.

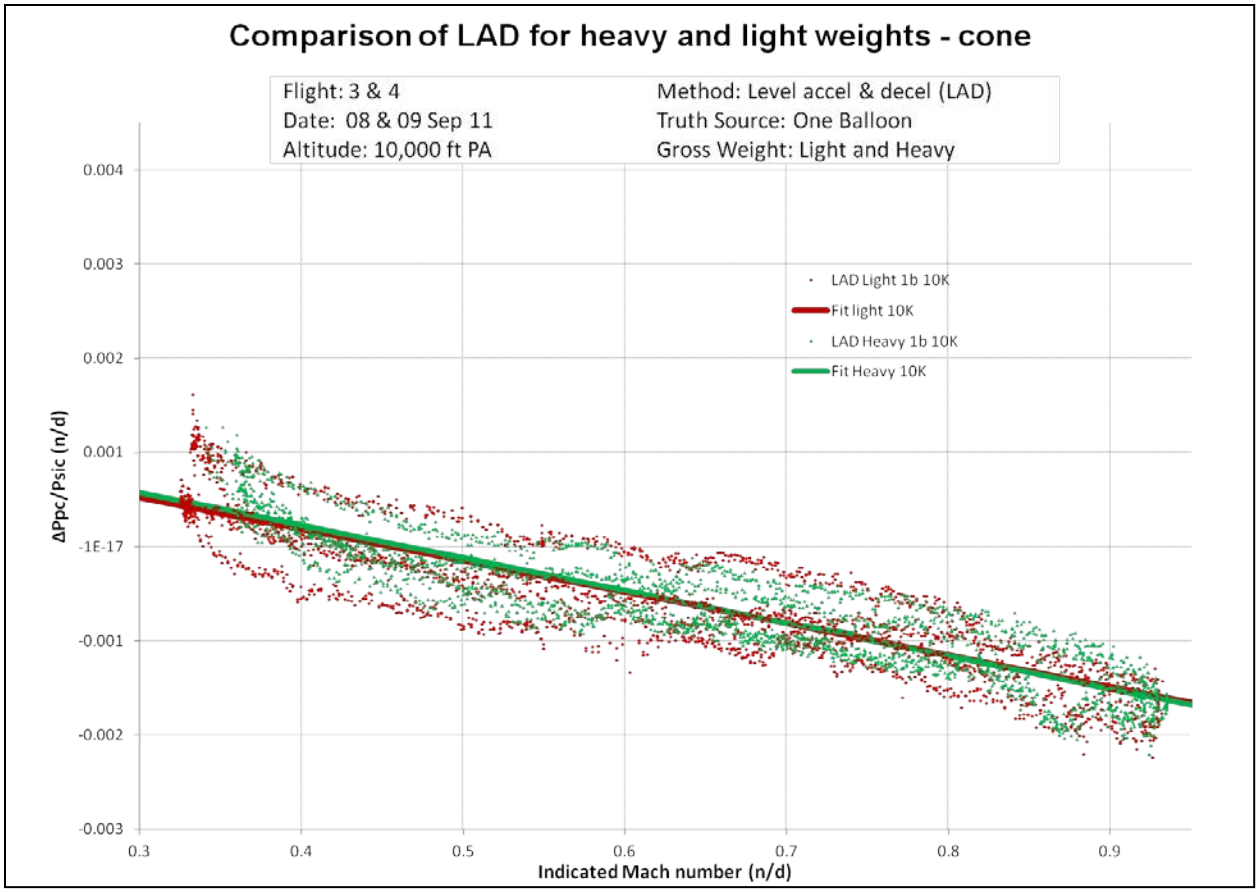

Figure 22 Comparison of LAD for Heavy and Light Weights - Cone

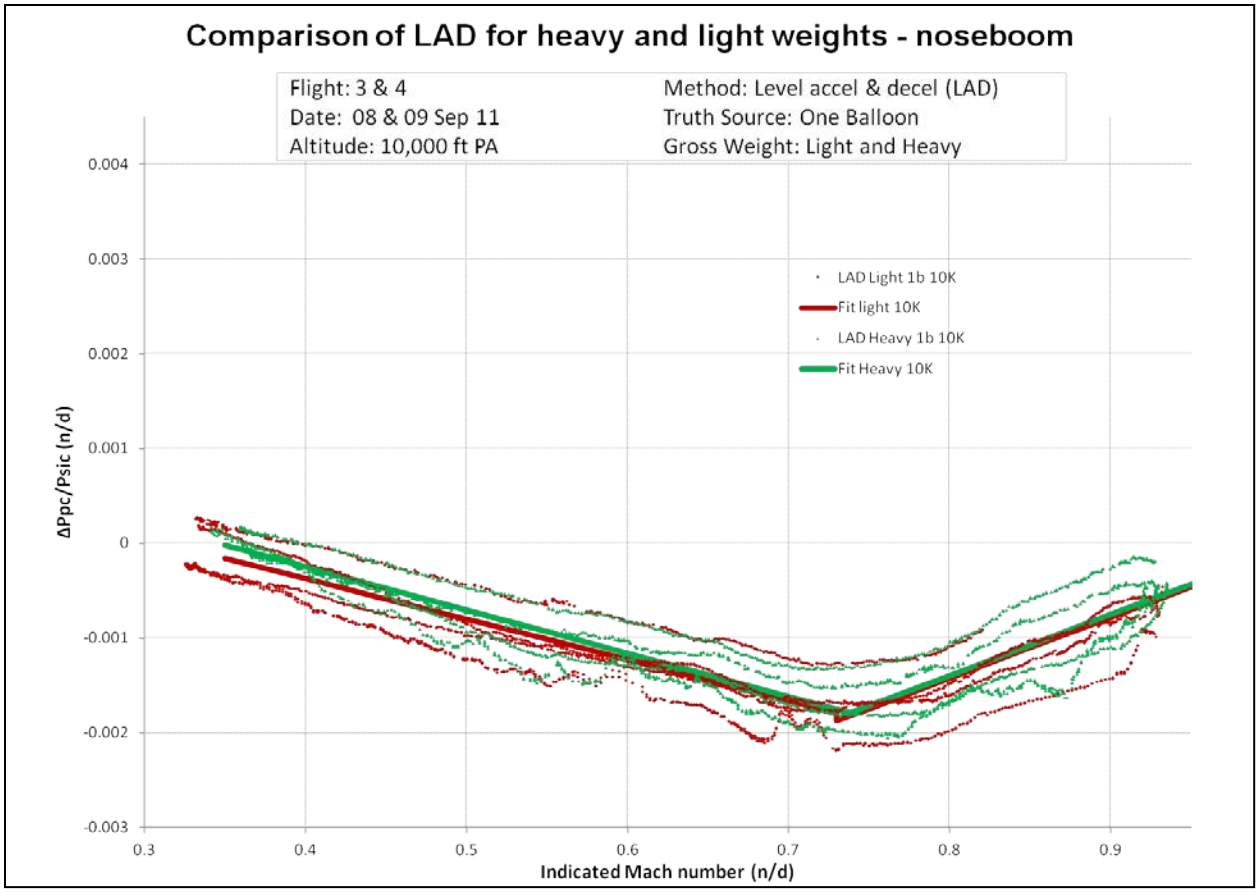

Figure 23 Comparison of LAD for Heavy and Light Weights – Noseboom

Repeatability of the Level Acceleration-Deceleration Calibrations

At 10,000 feet PA, four LAD were flown during two different sorties (flights three and four), on two different days, with a 'heavy' and 'light' weight flown on each sortie. The models resulting from each LAD were similar (figure 24). Indeed, the maximum difference in static source error correction at any given Mach number was 0.0005, which equates to about 13 feet, with a random uncertainty between the models of 0.58×10^{-5}. This was better than the cruise points at 10,000 feet PA, for which the random uncertainty was found to be 2.32×10^{-5}.

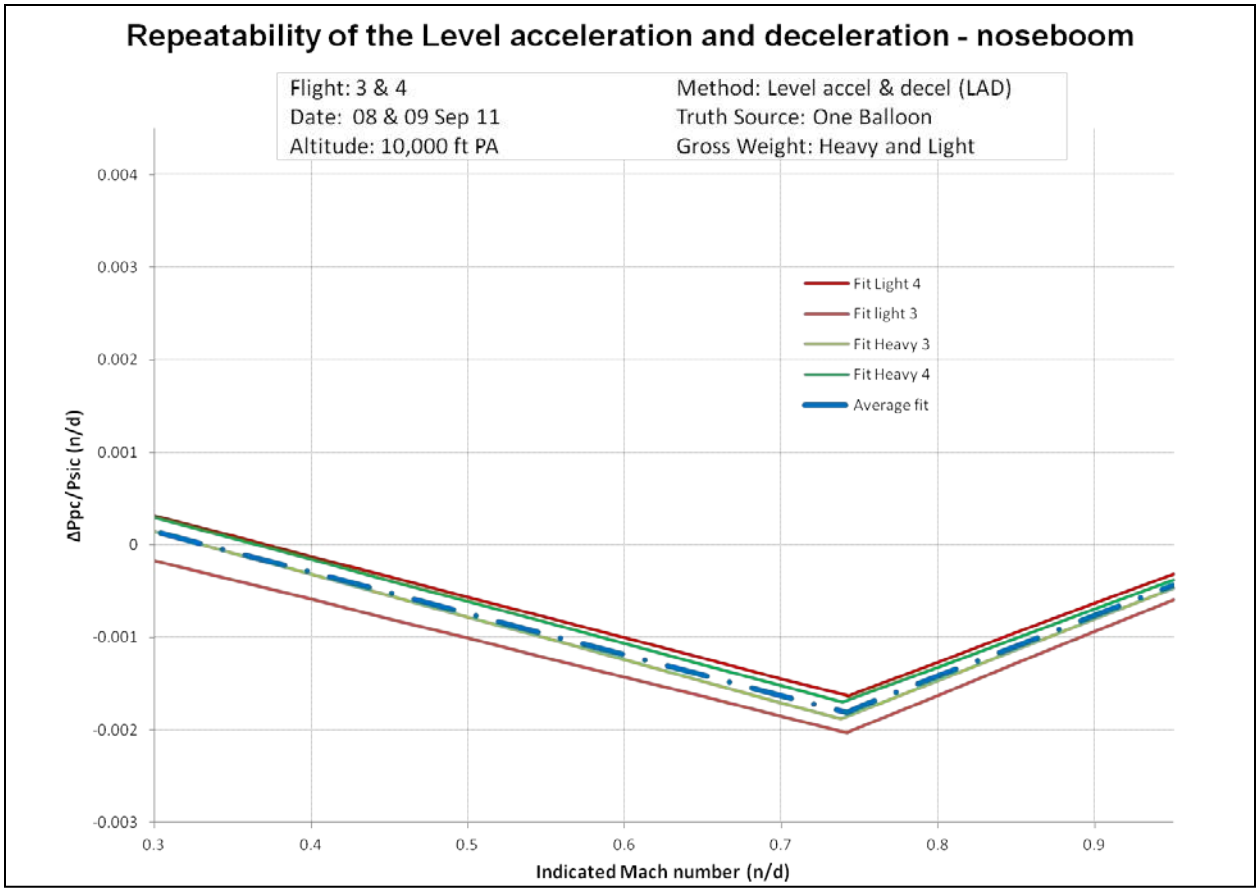

Figure 24 Repeatability of the LAD

Different Temperature Truth Sources for the Speed Techniques

For the speed technique, it was necessary to determine the truth ambient temperature. This could be obtained either by using the test total temperature probe and its associated recovery factor and bias, which were determined by a different FTT as described before, or by using ambient temperature from one balloon. The random uncertainty was similar for both truth sources (figure 25). Using a balloon for the speed techniques was, therefore, unnecessary if the temperature probe was properly calibrated.

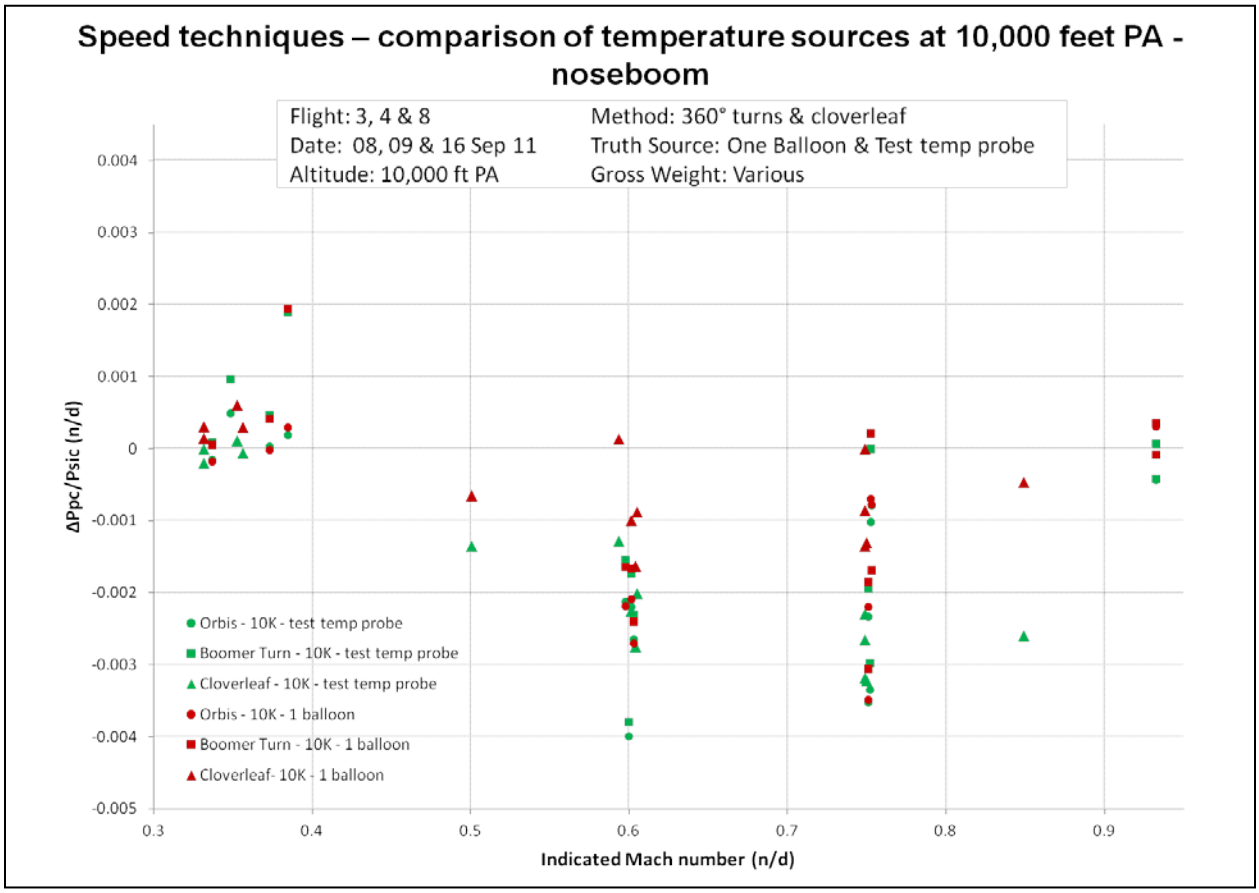

Figure 25 Speed Techniques – Comparison of Temperature Sources at 10,000 Feet PA

Comparison of Cruise and the Speed Techniques

At 10,000 feet PA, the speed technique results were much more scattered than the cruise technique results (figure 26). Looking at the results for the points flown at 0.75M, the $\Delta P_{pc}/P_{sic}$ results showed a variation of 0.0005 for the cruise technique, 0.0009 for the cloverleaf (four points flown), and 0.003 for the 360-degree turns, either with the Boomer Turn or the Orbis data reduction techniques (four points flown), which equated to 70 feet.. Except for one point at 11 AoA, the results for the two data reduction techniques for turns were similar. Because only four different airspeeds were used for the turn points, a model could not be developed. For the cloverleaf, five different airspeeds were used and two of these were only flown once, so no model could be developed. Yet, flying additional points to define that model was not necessary since it was already concluded that the uncertainty inherent to that technique was unacceptable, and also since this flight test technique was found to be the least efficient in terms of time, fuel, and ease of accomplishment.

A possible explanation to the large amount of scatter found when using the turn techniques can be that these techniques are very sensitive to speed errors. Indeed, an error in GPS speed measurement of 0.5 knot led to an error in altitude of 20 feet, or in $\Delta P_{pc}/P_{sic}$ of 0.0008 at 10,000 feet. According to the specifications, the G-Lite gave ground speed within 0.5 knot, and would therefore account for half of the maximum $\Delta P_{pc}/P_{sic}$ variation observed for the 0.75M points. Another explanation was temperature sensitivity, with 1 degree Celsius error on the ambient temperature resulting in 25 feet altitude error or in $\Delta P_{pc}/P_{sic}$ of 0.001 at 10,000 feet. Figure 9 (in the section related to the temperature probe calibration)

showed that at one airspeed, the post calibration residual error could attain 0.8 degrees Celsius between two test points. These turn techniques also assume constant wind and ambient air temperature during the maneuver, so any changes in winds with time or over the airspace where the maneuver was performed will also contribute to the error.

The turn techniques had uncertainties of approximately 70 feet, probably because of their sensitivity to ground speed and temperature measurements or to changes in assumed constant winds and ambient temperature.

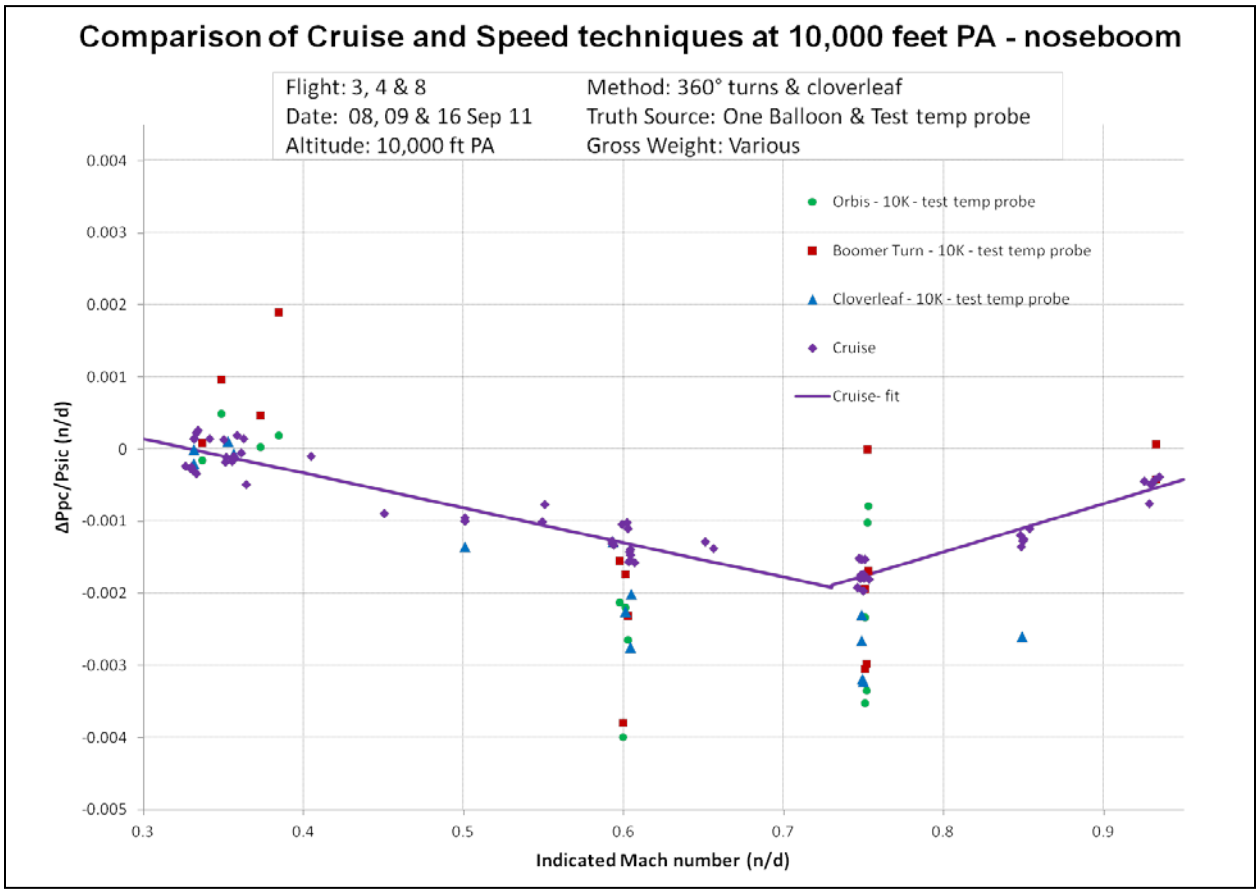

Figure 26 Comparison of Cruise and Speed Techniques at 10,000 Feet PA

Speed Techniques at Different Altitudes

As for the cruise technique, the mean values of static source error correction were different at 30,000 feet and 10,000 feet PA (figure 27). The scatter was similar at 30,000 feet and 10,000 feet PA, which was different than was observed for cruise.

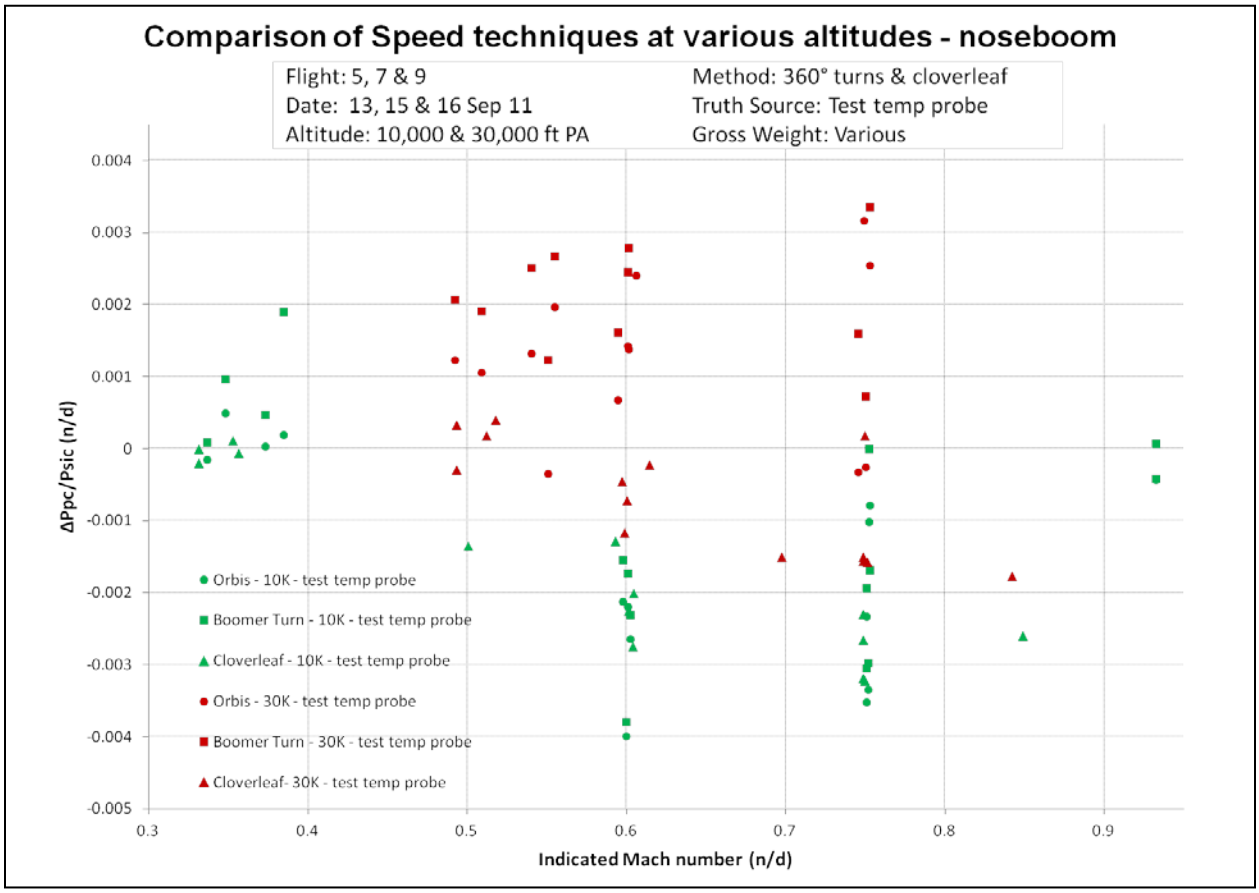

Figure 27 Comparison of Speed Techniques at Different Altitudes

Conclusions for the Static Source Error Correction Calibration Techniques

The noseboom and the cone could be calibrated with the same level of precision. The calibration for both the noseboom and the cone was a function of altitude. The noseboom and the cone should then be calibrated at various altitudes for better results. The LAD method was found to give a similar result as the cruise points. Using one or two balloons did not change the results significantly. Using the tower flyby technique gave similar results as using the cruise technique with one balloon as a truth source, at the tower flyby altitude. The Atmospheric Analysis was accomplished by using the Atmospheric Analysis passes coupled with a balloon to correct for the bias. Both the Atmospheric Analysis and the Self-Survey analysis gave unsatisfactory results, as the model created by these analyses was either mathematically or physically incorrect. The speed calibration techniques, which included the cloverleaf, the Orbis, and the Boomer Turn methods, gave static source error correction with a much larger scatter than the altitude techniques (tower flyby, cruise, and LAD).

The FTT truth source combination with the least cost was the level acceleration and deceleration method combined with the one balloon rawinsonde.

Furthermore, it was given a “simple and quick” data reduction efficiency rating and a level two Bedford workload rating. The highest total cost was the cloverleaf and Atmospheric Analysis combination.

REFERENCES

1. Lawless, Al, *Orbis Matching, Precision Pitot-Statics Calibration*, Presented at the Society of Flight Test Engineers Symposium, National Harbor, Maryland, September 2010.

2. Ramos, M. M., et al., *Statistical Pitot-Static Calibration Technique Using Turns and Self-Survey Method*, 42nd International Society of Flight Test Engineers Symposium, Seattle, Washington, August 2011.

3. AFFTC-TP-10-74, *AFFTC F-16D Pacer Calibration Plan*, Air Force Flight Test Center, Edwards AFB, California, August 2010 (Test plan can be found at the USAF Test Pilot School at Edwards AFB, California.)

4. Temporary-2 Modification Number M07B391D, *Pacer Wingtip Total Air Temperature Probe Interface*, Air Force Flight Test Center, Edwards AFB, California, July 2011.

5. F-16 C/D Support Fleet, *Modification Flight Manual Change 5*, Air Force Flight Test Center, Edwards AFB, California, September 2007.

6. AFFTC Instruction 11-1, *Flying Operations, Air Operations*, Air Force Flight Test Center, Edwards AFB, California, January 2004.

7. Technical Report 5755, *Total Temperature Sensors*, Goodrich Sensor Systems, January 1994.

8. Clark, J., et al., *The Effects of Aircraft Acceleration and Deceleration on Static Source Error Corrections*, 42nd Annual SFTE Symposium, Society of Flight Test Engineers, Seattle, Washington, August 2011.

9. ASD/ENAI-81-6G, *Technical Exhibit*, January 1994.

10. DeAnda, Albert G., AFFTC-TIH-81-5, *AFFTC Standard Airspeed Calibration Procedures*, Flight Dynamics Division, Air Force Flight Test Center, Edwards AFB, California, June 1981.

11. NOAA-S/T 76-1562, *U.S. Standard Atmosphere*, 1976, Joint Report of the National Oceanic and Atmospheric Administration (NOAA), National Aeronautics and Space Administration (NASA), and the United States Air Force, U.S. Government Printing Office, Washington, D.C., October 1976.

This page was intentionally left blank.

APPENDIX A - SORTIE PROFILES

Table A1 Sortie Profiles

Flight Number	Date	Takeoff Time	Sortie Duration (hours)	Test Altitude	Sortie Profile
1	6 Sep 11	2044Z	1.4	10,000 feet PA 30,000 feet PA	Instrumentation Check Flight 360-Degree Turns
2	7 Sep 11	1459Z	1.9	100 feet AGL	Tower Flyby Only
3	8 Sep 11	1528Z	2.0	10,000 feet PA	All Up-and-Away Techniques
4	9 Sep 11	1435Z	2.1	10,000 feet PA	All Up-and-Away Techniques
N/A	9 Sep 11	1515Z	1.0	N/A	T-38 Flight, Photo Chase
5	13 Sep 11	1455Z	1.6	30,000 feet PA	All Up-and-Away Techniques
6	14 Sep 11	1427Z	2.1	100 feet AGL 30,000 feet PA	Tower Flyby, then 360-Degree Turns
7	15 Sep 11	1422Z	2.1	30,000 feet PA	All Up-and-Away Techniques
8	16 Sep 11	1442Z	1.9	10,000 feet PA	All Up-and-Away Techniques
9	16 Sep 11	1928Z	2.3	30,000 feet PA	All Up-and-Away Techniques

This page was intentionally left blank.

APPENDIX B - DETAILED TEST ITEM DESCRIPTION

Pacer aircraft USAF S/N 87-0391 was a modified Block 40 F-16D that implemented the following systems:

1- Teletronics Technology Corporation (TTC) Data Acquisition System (DAS) pacer modification

2- Advanced Range Data System (ARDS) pod

3- Beacon

4- Trailing cone

5- G-Lite

6- Gun port plug

7- Video recorder

8- Flight test YAPS noseboom

9- Telemetry

The aircraft received a TTC DAS pacer modification that allowed for highly accurate Pitot-static pressure measurements. The basic pacer system was a Pulse Code Modulation (PCM) data acquisition system with onboard recording capability. The pacer system collected and recorded Pitot-static, total air temperature, voice, Inter-Range Instrumentation Group (IRIG)-B time code, PCM, and Avionics 1553 multiplex (MUX) bus data.

Figure B1 contains a schematic of the production F-16D noseboom air data system. This modified figure depicts where the pacer dual Paroscientific digital pressure transducers were connected (labeled 'Pacer Air Data System (ADS) connections'). The pacer air data system included a flight test Pitot-static probe mounted on the nose that provided a dual source of static and total pressures. A production, five-hole air data probe was mounted on the forward right fuselage and provided the production Pneumatic Sensor Assembly (PSA) with another source of static and total pressures. The PSA used these pressures to estimate aircraft angle-of-attack. Two additional cone-type production angle-of-attack transducers were installed, one on either side of the forward fuselage. A flight test total air temperature probe was mounted on the underside of the left forebody strake, but data from this probe were not used. The production total air temperature probe mounted on the right side of the fuselage and the modified total air temperature probe mounted on the left wingtip provided the pacer air data system with total air temperature measurements.

The pressures for the pacer system were measured using five pressure transducers: four were located in the left hand forward equipment bay and one was installed in the tip of the vertical stabilizer for the trailing cone. The transducers used during the test were S/Ns 119285 (static pressure) and 114132 (total pressure) for System One and 119287 (static pressure) and 114132 (total pressure) for System Two. The section 'Pacer Air Data Instrumentation Upgrade – Trailing Cone' contains additional details about the trailing cone system. Data measured with these transducers were collected by the DAS located in the gun breech area. The sensitive transducers provided input signals to the TTC pacer system, which output engineering unit data to pacer cockpit displays and a TTC data recorder in the aft cockpit.

The pacer instrumentation system was calibrated over an airspeed range of 170 to 600 KCAS (0.95 Mach number). The noseboom systems were calibrated with the de-ice heat on. The flight test total temperature probe was heated, and the heat was turned on automatically when the weight-on-wheels signal showed no weight-on-wheels.

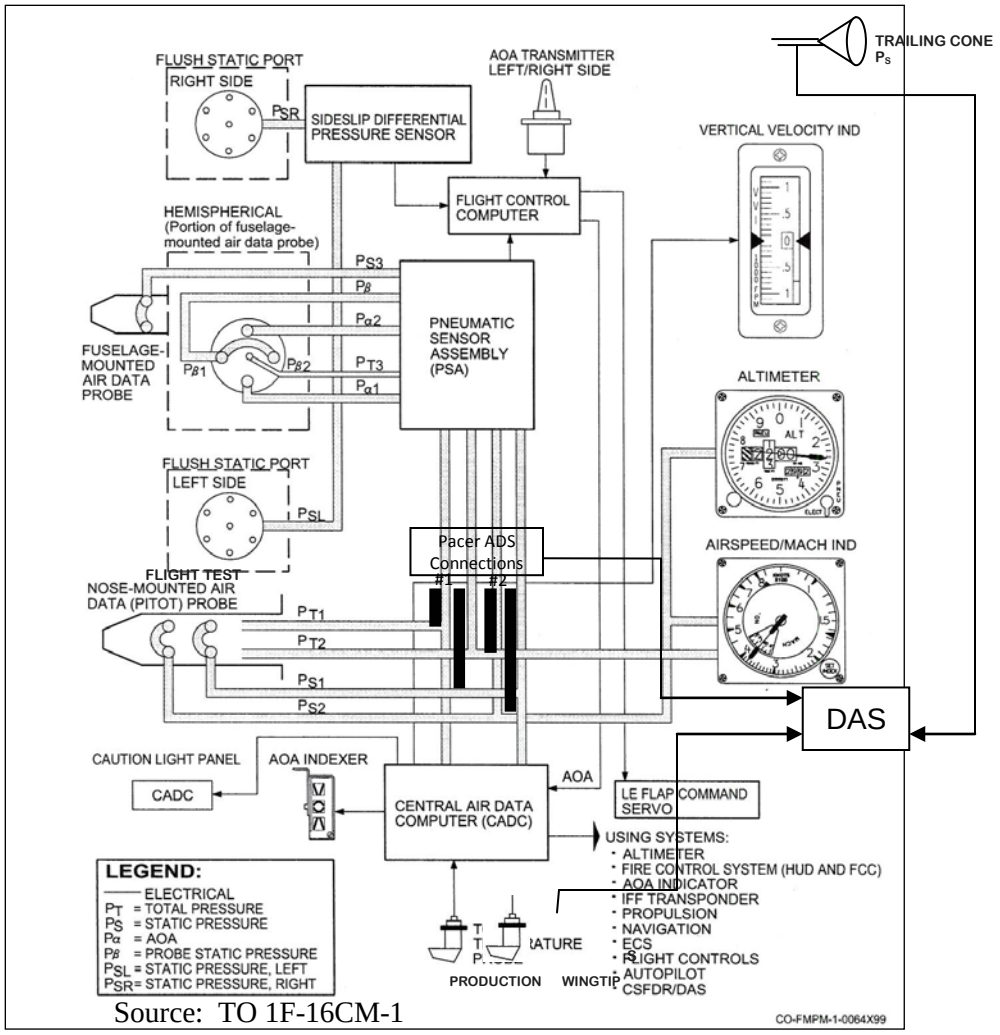

Source: TO 1F-16CM-1

Figure B1 Schematic of Pacer Air Data System

DAS SYSTEM DESCRIPTION

The TTC DAS consisted of various components to measure, record and transmit approximately 40 data parameters. Internal and external transducers collected and conditioned the data as necessary for recording on an in-flight, solid-state data recorder, or it could be sent to ground-based equipment via telemetry transmission. The DAS used AC and DC power from the aircraft. Current load protection was provided by a circuit breaker located in the right strake.

TEST EQUIPMENT

The main components of the DAS were located in the gun breech area of the F-16. The following sections provide a brief description of the equipment added to the modified aircraft.

YAPS NOSEBOOM

The pacer aircraft was modified with a YAPS flight test noseboom comprised of a Lockheed Martin boom (Model number 16IH001) and a Rosemount Pitot-static tube (Model number 855EJ). The Pitot-static tube was aerodynamically compensated and had five static ports on both the top and bottom of the tube.

PC/104

The PC/104 computer system received RS-232 data from the trailing cone pressure transducer and recorded those data onto a PCMCIA Type II flashcard in standard PC text file format. The PC/104 had one PCMCIA flash card memory slot accepting up to a 240MB memory card. The system had a run indication to show when a print command was received by the PC/104. The print output was recorded in standard text file format on the PCMCIA flash card. Two dated files were recorded on each mission: one with an '.F16' extension, which was comma and quotation delimited, and one with a '.RAW' extension. These files could be read by any PC with a PCMCIA reader, and read with any text editor. The files contained one line of data per record.

DAS CONTROL PANELS AND DISPLAYS

Front Cockpit Modifications:

Table B1 Front Cockpit DAS Control Panels and Displays with Locations

Component	Location
Flight Test Control Panel	Right Console
Angle-of-Sideslip (AoSS) Gauge	Right Side of Instrument Panel
Video Control Panel	Left Console

Flight Test Control Panel.

The Instrumentation MASTER POWER was located on the right console in the forward cockpit. It controlled electrical power to all modified equipment (figure B2).

Figure B2 Flight Test Control Panel

AoSS Gauge.

An AoSS was installed on the right side of the forward instrument panel in both cockpits (figure B3). Input was taken from the beta vanes on the YAPS boom.

Figure B3 AoSS Gauge

Rear Cockpit Modifications:

The following figure (B4) shows the locations of the pacer's rear cockpit modifications:

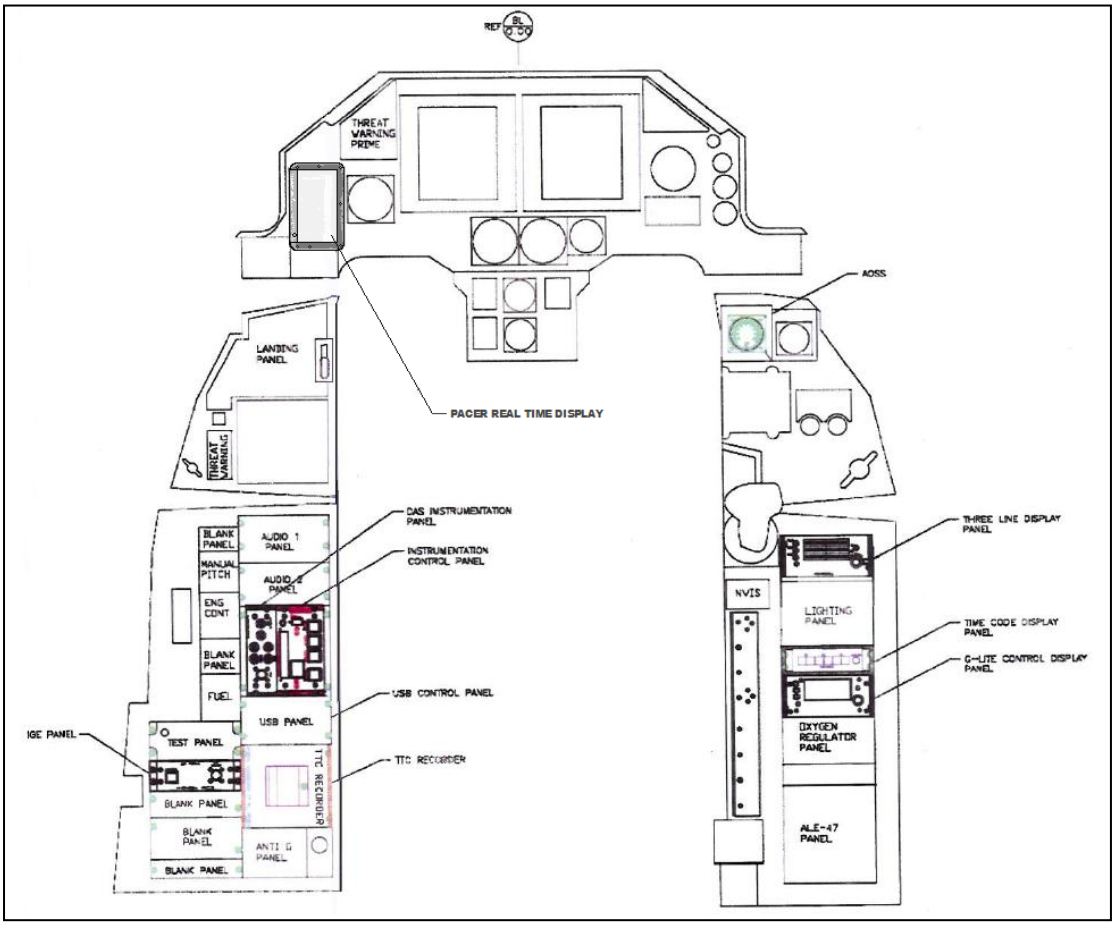

Figure B4 Pacer Rear Cockpit Pacer Instrumentation

Range Time (IRIG-B) Display.

An IRIG-B range time display (figure B5) was located in the rear cockpit (RCP), right console. It contained a six-digit decimal display indicating GPS time in hours (00-23), minutes (00-59), and seconds (00-59) received from the differential GPS (DGPS) system. A TrueTime 705-205 GPS IRIG-B receiver provided time, frequency, and position information as derived from signals transmitted by global positioning satellites and was usable on a worldwide basis. The IRIG time was available within 3 minutes when the antenna had an unobstructed view to the sky. The receiver was located on the ammo pallet on the top shelf.

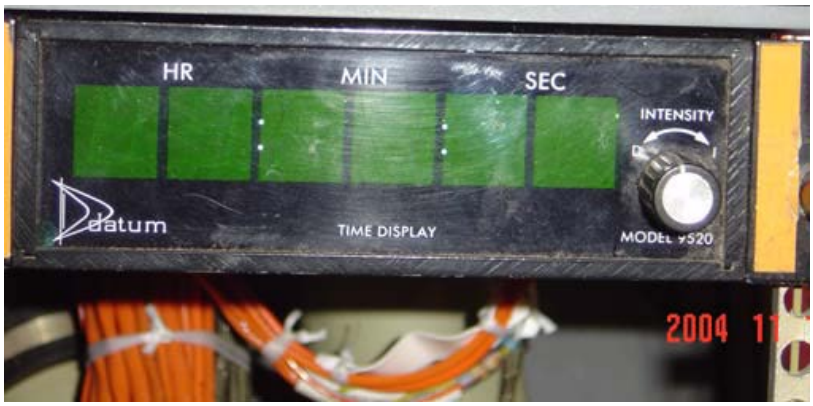

Figure B5 IRIG-B Display Rear Cockpit

Instrumentation Control Panel (ICP).

The ICP was located on the left console in the rear cockpit (figure B6). The ICP controlled the TTC DAS solid-state data recorder located in the rear cockpit. The ICP also controlled and showed the recording system status (RECORD/STOP), the data recording PAUSE function, the telemetry transmitter status (ON/OFF) and event number. Squeezing the CAMERA/GUN trigger in either cockpit to the first detent also marked an event. A 16-place alphanumeric display window was located forward of the event counter display. This display showed memory remaining on the PCMCIA as a percentage. The Dimmer rocker switch controlled the brightness of the Event and 16-place alphanumeric display, but not the push-button text. The ICP received DC power through the Instrumentation MASTER POWER located on the right console of the front cockpit.

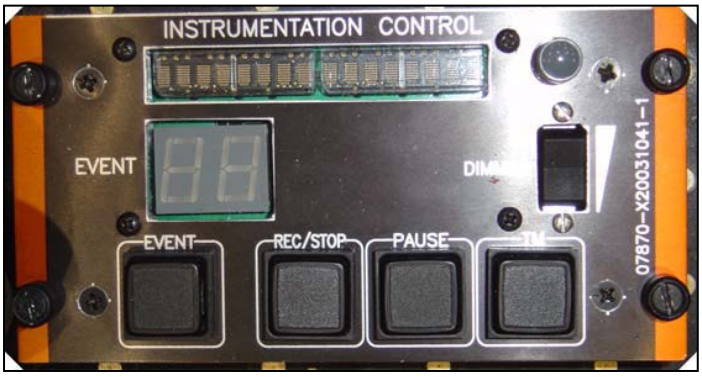

Figure B6 Instrumentation Control Panel

TTC Solid-State Data Recorder.

The rear cockpit contained a TTC solid-state recorder, which was installed on the left console (figure B7). The recorder recorded all instrumentation parameters acquired by the DAS; voice and time were recorded as part of the data stream. The instrumentation MASTER POWER switch provided power to the recorder.

Figure B7 TTC Solid-State Data Recorder,
Rear, Left Console

DAS Instrumentation Panel.

The instrumentation panel was located on the left console in the rear cockpit (figure B8) and provided crew interface for PCM data, DGPS, and video; it was not used during flight. The GPS connector was a DGPS antenna feed from the ammunition bay, panel-mounted DGPS antenna. The video connector provided a video input to the solid-state recorder.

Figure B8 DAS instrumentation panel

Instrument Ground Equipment Panel.

The Instrument Ground Equipment Panel (IGE) was located on the left console in the rear cockpit (figure B9). The IGE displayed the DGPS and PCM system status. The text ‘GPS’ was displayed when the DGPS was acquiring satellites. The text ‘PCM’ was displayed when data were ready to record to PCMCIA media.

Figure B9 IGE Panel

GPS-AIDED INERTIAL NAVIGATION REFERENCE-LITE DGPS

A GPS-Aided Inertial Navigation Reference-Lite (G-Lite) DGPS receiver/recorder was installed in the aircraft (figure B10), which used a special DGPS antenna. The G-Lite DGPS receiver/recorder was installed at the base of vertical stabilizer. A two-line display without shock mounts was also installed. The G-Lite provided higher-accuracy position data than the ARDS pod.

Figure B10 Installed G-Lite DGPS

REAL TIME DISPLAY

The Real Time Display (figure B11) was a small computer located under the left glare shield and was software programmable to show a variety of displays and formats. This display allowed the flight crew to view data in engineering units being collected in real time. Typically, airspeed, altitude, and Mach number were selected from either system one, system two, or the trailing cone; the display showed altitude to the nearest foot, airspeed to a tenth of a knot, and the Mach number to two decimal places. IRIG time, temperature, and other parameters were displayed as well. The basic display format incorporated tabbed window layers; each tab could have different data, layouts, controls, and formats. The display communicated with a PC/104 computer or Real Time Display Main Processor (RTD-MP) via a Universal Serial Bus (USB) to the RS422 converter. The RTD-MP retrieved data from the DAS that was requested by the RTD-MP based on requirements for the active screen.

Figure B11 Pacer Real Time Display

PACER 3-LINE DISPLAY

The pacer 3-Line Display (figure B12) was located in the RCP on the right console and was a software programmable, 16-character per line, alphanumeric, 5x7 dot matrix, light emitting diode display. It provided real time flight test data displayed in engineering units and could be frozen to record data. It was designed to be flexible and efficient by providing the ability to display up to five lines of data in just three lines of displays. The basic display format could accommodate three lines of data. The top two push buttons (labeled 'TGL') were programmed to perform a toggle function, allowing their respective lines to display a second set of data. The display communicated with a PC/104 computer also known as Real Time Display Main Processor (RTD-MP) via RS422. The RTD-MP retrieved data from the Data Acquisition System (DAS) and sent it to a uniquely assigned display line.

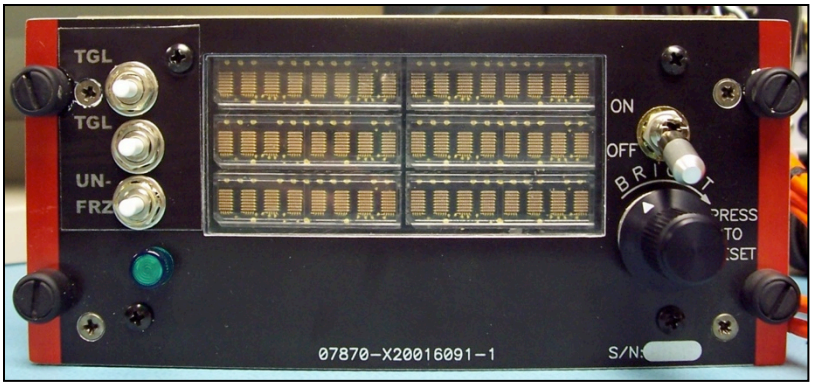

Figure B12 Pacer 3-Line Display

PACER AIR DATA INSTRUMENTATION (PADI) UPGRADE-TRAILING CONE

The Space Age Control trailing cone tube, P/N 4510-01 Revision A, and the trailing cone, P/N 4492-01 Revision D, comprised the pacer trailing cone system, shown in figure B13, and was installed on the aircraft for the dual purpose of providing high-accuracy pressure altitude data for use in calibrating the pacer noseboom system and for use in calibrating the air data systems on other test aircraft. The two different trailing cones used during the test were S/Ns 119288 and 109052, respectively.

The system was a fixed-length, non-retractable, non-jettisonable system that was dragged on the runway during takeoff and landing (figure B13). The system consisted of an anchor fixture attached to the tip of the vertical stabilizer (figure B14), a high-accuracy pressure transducer, Nylaflow® pressure tubing reinforced with a steel cable, a heat-resistant Kevlar® fire sleeve, a stainless steel static pressure sensing sleeve and a drag cone. The system worked by sensing the free stream static pressure away from the influence of the aircraft via orifices in the static sensing sleeve. The sensed pressure was transmitted through the Nylaflow® pressure tubing to the pressure transducer. Data from this transducer were collected by the DAS and recorded along with the other pressure and data parameters. The static sleeve and pressure tubing were stabilized by the drag cone. The steel reinforcing cable supported the drag loads of the cone.

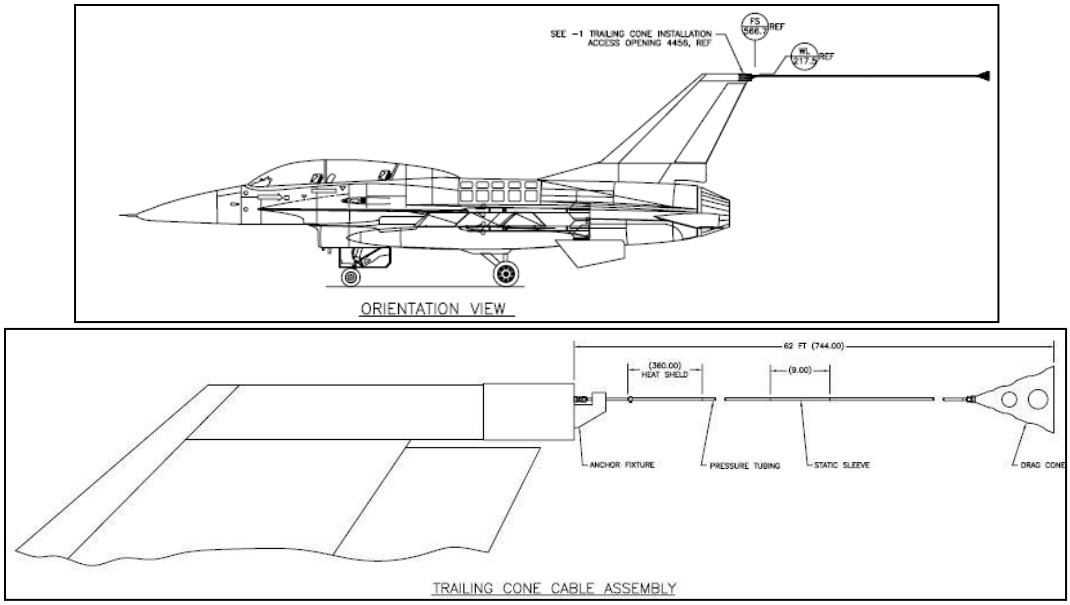

Figure B10 F-16 Pacer Trailing Cone Installation

The trailing cone assembly had a length of approximately 52 feet between the anchor point and the sensing static sleeve. The overall length of the assembly was approximately 62 feet. The first 30 feet of the Nylaflow® tubing was covered with 0.125-inch thick Kevlar® fire sleeve to protect against heat damage from the engine exhaust. The fire sleeve was fastened to the tubing with a hose clamp near the anchor point. The other end of the fire sleeve was sealed with epoxy to prevent fraying but was not fastened to the tube. The 10 inch diameter trailing cone was made of carbon fiber, weighed approximately one pound, and was painted flight test orange to enhance visibility. The circular edge of the trailing cone was covered in epoxy to prevent damage during taxi, takeoff, and landing and proved effective in allowing 4 to 5 flights with a single cone before replacement was necessary to prevent cone failure in flight. The change in cones during the test was deemed to have no effect on data quality, as the cone only provided stabilization for the trailing cone tubing.

The threat warning antenna was removed from the aft tip of the vertical stabilizer to accommodate the trailing cone system anchor fixture. The anchor fixture was installed on the rear-facing bulkhead and was painted flight test orange. A zero to 15 pounds per square inch absolute, pressure transducer with accuracy of 0.01 percent of full scale was installed inside the anchor fixture. This level of accuracy was equivalent to approximately ±11 feet at 40,000 feet pressure altitude. Data from the pressure transducer were time-stamped and recorded on the PCMCIA card in the TTC recorder.

Figure B14 Anchor Fixture

ADVANCED RANGE DATA SYSTEM (ARDS)

An Advanced Range Data System (ARDS) (AN/ARQ-52-V17) was attached on wingtip station nine and used as a backup source of TSPI data in the event of a G-Lite DGPS failure (figure B15). The ARDS pod on the wingtip was assumed to have negligible effect on the aircraft's Pitot-static system.

Figure B15 Advanced Range Data System (ARDS) Pod on Right Wingtip

APPENDIX C – DATA PRODUCTS

Table C1 Full Temperature Recovery Factor Calibration Data

							Wing-Tip - Element 1			Wing-Tip - Element 2			Production Probe		
	Weight	Truth	Mc Source	Altitude	Flight #	# of Points	K_R	b_K	$S_{y,x}$	K_R	b	S_{xy}	K_R	b_K	$S_{y,x}$
Cruise	All	1 Balloon	1 Balloon	10,000	3	16	0.9921	-0.0118	0.0025	0.9896	-0.0131	0.0025	0.9323	0.0232	0.0090
Cruise	All	1 Balloon	1 Balloon	10,000	4	20	0.9967	-0.0159	0.0025	0.9946	-0.0173	0.0026	0.9396	0.0190	0.0103
Cruise	All	1 Balloon	1 Balloon	10,000	8	28	0.9912	-0.0145	0.0020	0.9898	-0.0130	0.0020	0.9748	0.0203	0.0061
Cruise	All	1 Balloon	1 Balloon	10,000	3, 4 & 8	64	0.9936	-0.0144	0.0026	0.9917	-0.0146	0.0026	0.9497	0.0221	0.0116
Cruise	All	2 Balloons	2 Balloons	10,000	3	18	0.9908	-0.0111	0.0026	0.9882	-0.0124	0.0026	0.9284	0.0240	0.0090
Cruise	All	2 Balloons	2 Balloons	10,000	4	20	0.9929	-0.0145	0.0024	0.9907	-0.0159	0.0025	0.9357	0.0203	0.0107
Cruise	All	2 Balloons	2 Balloons	10,000	3 & 4	38	0.9921	-0.0130	0.0028	0.9897	-0.0144	0.0028	0.9322	0.0220	0.0097
Cruise	All	1 Balloon	1 Balloon	30,000	5	11	1.0024	-0.0042	0.0055	0.9998	-0.0030	0.0057	1.0016	0.0231	0.0094
Cruise	All	1 Balloon	1 Balloon	30,000	7	27	0.9858	-0.0060	0.0033	0.9839	-0.0048	0.0035	0.9320	0.0452	0.0126
Cruise	All	1 Balloon	1 Balloon	30,000	9	23	0.9970	-0.0018	0.0029	0.9950	-0.0008	0.0032	0.9611	0.0444	0.0113
Cruise	All	1 Balloon	1 Balloon	30,000	5, 7 & 9	61	0.9937	-0.0043	0.0062	0.9916	-0.0032	0.0062	0.9550	0.0418	0.0141
Cruise	All	2 Balloons	2 Balloons	30,000	5	11	1.0016	-0.0053	0.0054	0.9990	-0.0041	0.0056	1.0008	0.0220	0.0094
Cruise	All	2 Balloons	2 Balloons	30,000	7	28	0.9841	-0.0056	0.0038	0.9822	-0.0044	0.0039	0.9309	0.0452	0.0129
Cruise	All	2 Balloons	2 Balloons	30,000	9	23	0.9819	0.0026	0.0036	0.9799	0.0035	0.0036	0.9461	0.0487	0.0148
Cruise	All	2 Balloons	2 Balloons	30,000	5, 7 & 9	62	0.9877	-0.0029	0.0058	0.9856	-0.0018	0.0058	0.9492	0.0430	0.0149
Level Accel/Decel	Heavy	1 Balloon	1 Balloon	10,000	3	30	0.9870	-0.0096	0.0029	0.9846	-0.0110	0.0031	0.9281	0.0264	0.0177
Level Accel/Decel	Light	1 Balloon	1 Balloon	10,000	3	30	0.9911	-0.0078	0.0032	0.9889	-0.0091	0.0034	0.9357	0.0265	0.0174
Level Accel/Decel	Heavy	1 Balloon	1 Balloon	10,000	4	26	0.9912	-0.0114	0.0030	0.9889	-0.0125	0.0033	0.9389	0.0234	0.0193
Level Accel/Decel	Light	1 Balloon	1 Balloon	10,000	4	29	0.9933	-0.0139	0.0033	0.9916	-0.0155	0.0034	0.9412	0.0209	0.0188
Level Accel/Decel	All	1 Balloon	1 Balloon	10,000	3 & 4	114	0.9912	-0.0108	0.0037	0.9891	-0.0122	0.0038	0.9359	0.0244	0.0179
Level Accel/Decel	Heavy	1 Balloon	1 Balloon	10,000	3 & 4	56	0.9892	-0.0106	0.0028	0.9871	-0.0119	0.0030	0.9325	0.0251	0.0179
Level Accel/Decel	Light	1 Balloon	1 Balloon	10,000	3 & 4	59	0.9915	-0.0107	0.0045	0.9894	-0.0121	0.0047	0.9379	0.0238	0.0182
Level Accel/Decel	Heavy	2 Balloons	2 Balloons	10,000	3	30	0.9876	-0.0081	0.0030	0.9853	-0.0096	0.0031	0.9287	0.0279	0.0178
Level Accel/Decel	Light	2 Balloons	2 Balloons	10,000	3	30	0.9909	-0.0074	0.0030	0.9887	-0.0087	0.0032	0.9354	0.0269	0.0172
Level Accel/Decel	Heavy	2 Balloons	2 Balloons	10,000	4	26	0.9897	-0.0147	0.0030	0.9874	-0.0158	0.0032	0.9375	0.0201	0.0193
Level Accel/Decel	Light	2 Balloons	2 Balloons	10,000	4	29	0.9923	-0.0176	0.0032	0.9906	-0.0193	0.0033	0.9402	0.0170	0.0186

Table C1 Full Temperature Recovery Factor Calibration Data (Concluded)

Method	Weight	Truth	Mc Source	Altitude	Flight #	# of Points	Wing-Tip - Element 1			Wing-Tip - Element 2			Production Probe		
							K_r	b_k	$s_{y,x}$	Kr	b	Sxy	Kr	b	Sxy
Level Accel/Decel	All	2 Balloons	2 Balloons	10,000	3 & 4	114	0.9908	-0.0121	0.0051	0.9888	-0.0135	0.0051	0.9355	0.0231	0.0181
Level Accel/Decel	Heavy	2 Balloons	2 Balloons	10,000	3 & 4	56	0.9891	-0.0115	0.0040	0.9870	-0.0127	0.0039	0.9324	0.0243	0.0180
Level Accel/Decel	Light	2 Balloons	2 Balloons	10,000	3 & 4	59	0.9905	-0.0122	0.0061	0.9884	-0.0136	0.0063	0.9369	0.0223	0.0184
Level Accel/Decel	Heavy	1 Balloon	1 Balloon	30,000	5	26	0.9879	0.0052	0.0067	0.9860	0.0057	0.0069	0.9557	0.0454	0.0157
Level Accel/Decel	Heavy	1 Balloon	1 Balloon	30,000	7	18	0.9942	-0.0107	0.0093	0.9936	-0.0103	0.0096	0.9505	0.0350	0.0241
Level Accel/Decel	Light	1 Balloon	1 Balloon	30,000	7	18	0.9838	-0.0025	0.0043	0.9820	-0.0006	0.0044	0.9420	0.0455	0.0216
Level Accel/Decel	Light	1 Balloon	1 Balloon	30,000	9	22	0.9997	0.0033	0.0067	0.9982	0.0044	0.0070	0.9542	0.0516	0.0243
Level Accel/Decel	Heavy	1 Balloon	1 Balloon	30,000	5 & 7	43	0.9929	-0.0019	0.0095	0.9904	-0.0010	0.0096	0.9545	0.0412	0.0200
Level Accel/Decel	All	1 Balloon	1 Balloon	30,000	5, 7 & 9	83	0.9900	0.0008	0.0094	0.9879	0.0019	0.0095	0.9484	0.0465	0.0217
Level Accel/Decel	Light	1 Balloon	1 Balloon	30,000	7 & 9	40	0.9890	0.0025	0.0091	0.9875	0.0039	0.0090	0.9438	0.0513	0.0228
Level Accel/Decel	Heavy	2 Balloons	2 Balloons	30,000	5	26	0.9869	0.0045	0.0066	0.9850	0.0050	0.0068	0.9547	0.0448	0.0156
Level Accel/Decel	Heavy	2 Balloons	2 Balloons	30,000	7	18	0.9941	-0.0122	0.0098	0.9934	-0.0118	0.0101	0.9504	0.0334	0.0247
Level Accel/Decel	Light	2 Balloons	2 Balloons	30,000	7	18	0.9831	-0.0043	0.0044	0.9812	-0.0024	0.0044	0.9412	0.0437	0.0216
Level Accel/Decel	Light	2 Balloons	2 Balloons	30,000	9	22	0.9964	-0.0131	0.0069	0.9949	-0.0119	0.0072	0.9510	0.0351	0.0244
Level Accel/Decel	Heavy	2 Balloons	2 Balloons	30,000	5 & 7	43	0.9919	-0.0028	0.0098	0.9895	-0.0019	0.0099	0.9536	0.0403	0.0203
Level Accel/Decel	All	2 Balloons	2 Balloons	30,000	5, 7 & 9	83	0.9921	-0.0062	0.0089	0.9900	-0.0051	0.0089	0.9505	0.0394	0.0214
Level Accel/Decel	Light	2 Balloons	2 Balloons	30,000	7 & 9	40	0.9890	-0.0084	0.0059	0.9875	-0.0070	0.0062	0.9440	0.0403	0.0221
TFB	All	1 Balloon	1 Balloon	2,300	2	20	1.0178	0.0165	0.0206	1.0155	0.0147	0.0206	0.9591	0.0532	0.0249
TFB	All	1 Balloon	1 Balloon	2,300	6	12	0.9919	-0.0074	0.0065	0.9893	-0.0079	0.0064	0.9236	0.0344	0.0108
TFB	All	1 Balloon	1 Balloon	2,300	2 & 6	27	0.9954	0.0156	0.0245	0.9934	0.0140	0.0242	0.9338	0.0536	0.0275
TFB	All	2 Balloons	2 Balloons	2,300	2	21	1.0181	0.0137	0.0195	1.0158	0.0119	0.0195	0.9598	0.0488	0.0219
TFB	All	2 Balloons	2 Balloons	2,300	6	12	0.9857	-0.0038	0.0070	0.9833	-0.0045	0.0069	0.9254	0.0323	0.0100
TFB	All	2 Balloons	2 Balloons	2,300	2 & 6	27	1.0010	0.0092	0.0228	0.9988	0.0077	0.0224	0.9419	0.0446	0.0244
TFB	All	TFB	TFB	2,300	2	21	0.9823	-0.0348	0.0199	0.9802	-0.0367	0.0200	0.9274	-0.0002	0.0240
TFB	All	TFB	TFB	2,300	6	12	0.9863	-0.0153	0.0059	0.9839	-0.0160	0.0059	0.9280	0.0204	0.0110
TFB	All	TFB	TFB	2,300	2 & 6	33	0.9857	-0.0285	0.0191	0.9836	-0.0300	0.0195	0.9294	0.0066	0.0224

Note: Standard Error ($S_{y,x}$), Recovery Factor (K_R), Bias (b_K)

Table C 2 Temperature Recovery Correction Calibration Data

Method	Weight	Truth	Mc Source	Altitude	Flight #	# of Points	Wing-Tip - Element 1		Wing-Tip - Element 2		Production Probe	
							Bias*100	MSE*100	Bias*100	MSE*100	Bias*100	MSE*100
Cruise	All	1 Balloon	1 Balloon	10,000	3, 4 & 8	64	-0.1878	0.0024	-0.2027	0.0024	0.1945	0.0461
Cruise	All	2 Balloons	2 Balloons	10,000	3 & 4	64	-0.1757	0.0015	-0.2169	0.0020	0.0741	0.0400
Cruise	All	1 Balloon	1 Balloon	30,000	5, 7 & 9	61	0.0198	0.0076	0.0220	0.0074	0.5252	0.0508
Cruise	All	2 Balloons	2 Balloons	30,000	5, 7 & 9	61	-0.0075	0.0069	-0.0051	0.0070	0.4999	0.0600
Level Accel/Decel	All	1 Balloon	1 Balloon	10,000	3 & 4	114	-0.1279	0.0060	-0.1695	0.0081	0.0829	0.1746
Level Accel/Decel	All	2 Balloons	2 Balloons	10,000	3 & 4	114	-0.1542	0.0105	-0.1957	0.0124	0.0565	0.1770
Level Accel/Decel	All	1 Balloon	1 Balloon	30,000	5, 7 & 9	83	0.0816	0.0239	0.0825	0.0245	0.5292	0.1437
Level Accel/Decel	All	2 Balloons	2 Balloons	30,000	5, 7 & 9	83	-0.0271	0.0218	-0.0262	0.0216	0.4199	0.1374
Level Accel/Decel	Heavy	1 Balloon	1 Balloon	10,000	3 & 4	56	-0.1394	0.0017	-0.1800	0.0028	0.0608	0.0873
Level Accel/Decel	Heavy	2 Balloons	2 Balloons	10,000	3 & 4	56	-0.1552	0.0033	-0.1958	0.0040	0.0449	0.0884
Level Accel/Decel	Heavy	1 Balloon	1 Balloon	30,000	5 & 7	43	0.0611	0.0125	0.0545	0.0127	0.4751	0.0599
Level Accel/Decel	Heavy	2 Balloons	2 Balloons	30,000	5 & 7	43	0.0355	0.0133	0.0288	0.0134	0.4494	0.0617
Level Accel/Decel	Light	1 Balloon	1 Balloon	10,000	3 & 4	59	-0.1256	0.0044	-0.1669	0.0055	0.1011	0.0902
Level Accel/Decel	Light	2 Balloons	2 Balloons	10,000	3 & 4	59	-0.1613	0.0076	-0.2025	0.0088	0.0654	0.0924
Level Accel/Decel	Light	1 Balloon	1 Balloon	30,000	7 & 9	40	0.1006	0.0104	0.1131	0.0103	0.5911	0.0783
Level Accel/Decel	Light	2 Balloons	2 Balloons	30,000	7 & 9	40	-0.0977	0.0047	-0.0853	0.0052	0.3918	0.0734
TFB	All	TFB	TFB	2,300	2 & 6	33	-0.4994	0.0392	-0.5432	0.0412	-0.2725	0.0721
TFB	All	1 Balloon	1 Balloon	2,300	2 & 6	27	0.3927	0.0497	0.3467	0.0488	0.5816	0.0805
TFB	All	2 Balloons	2 Balloons	2,300	2 & 6	27	0.3161	0.0430	0.2719	0.0418	0.4992	0.0631

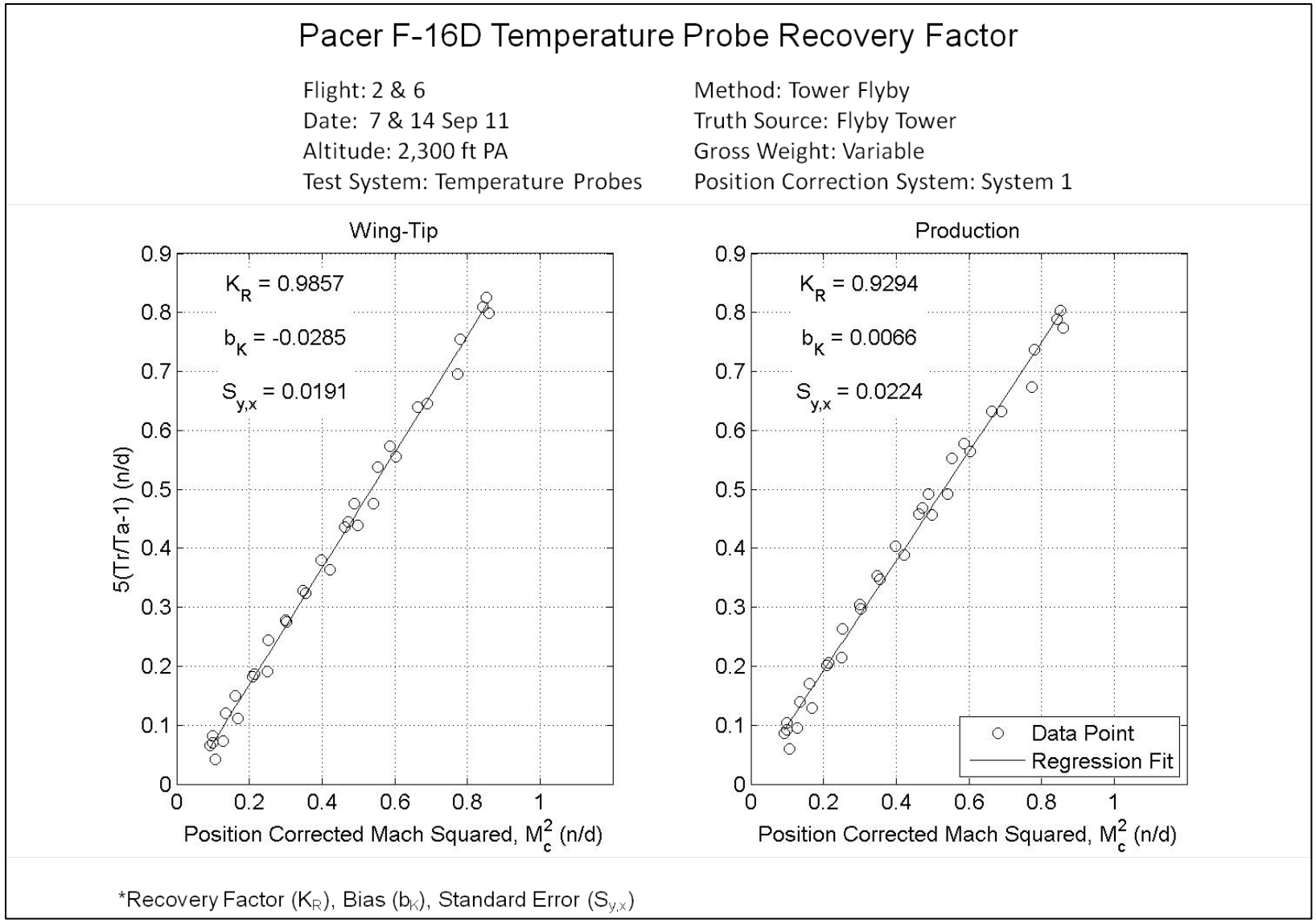

Figure C1 Temperature Recovery Factor - Tower Flyby - Flyby Tower

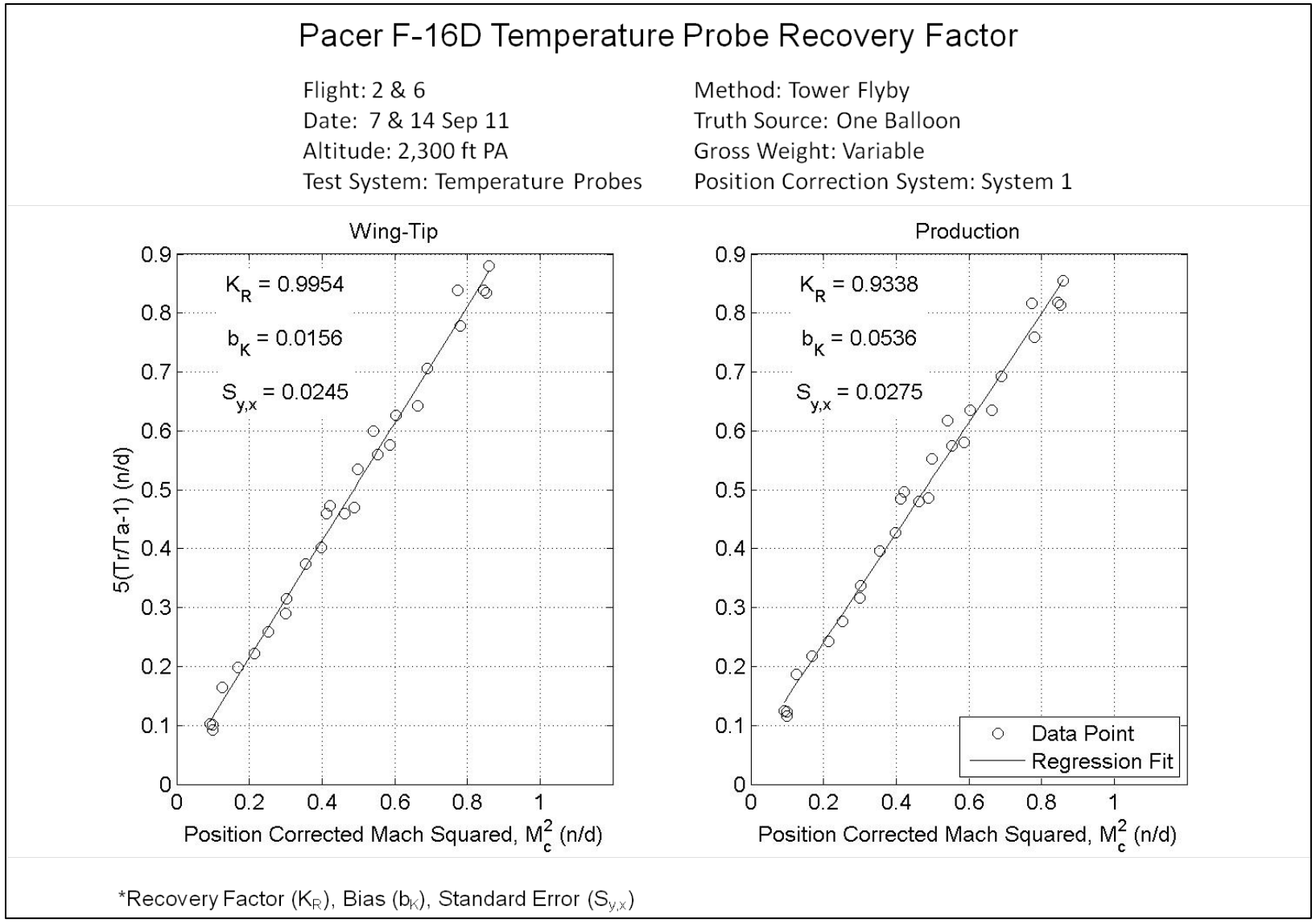

Figure C2 Temperature Recovery Factor - Tower Flyby – One Balloon

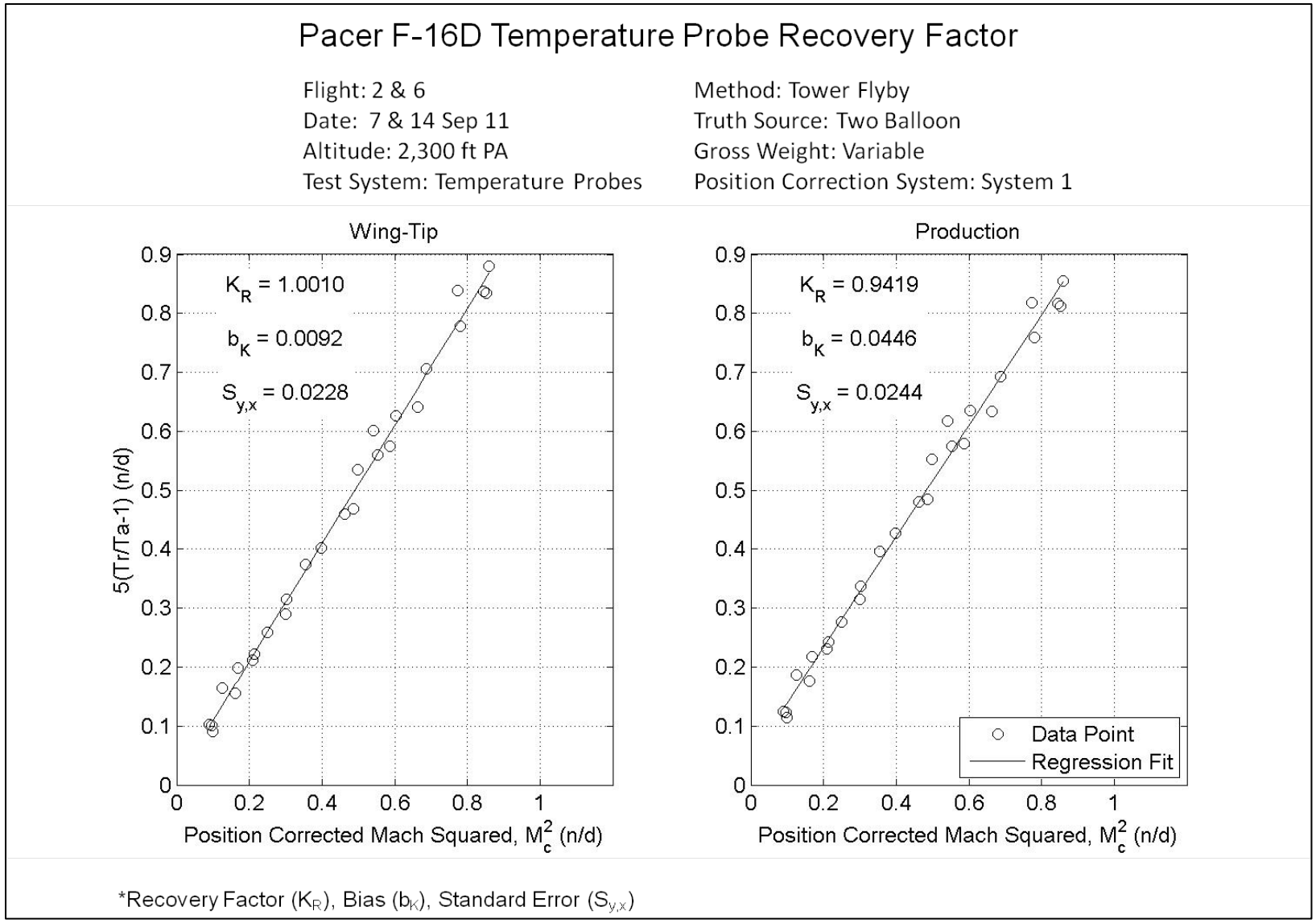

Figure C3 Temperature Recovery Factor - Tower Flyby – Two Balloon

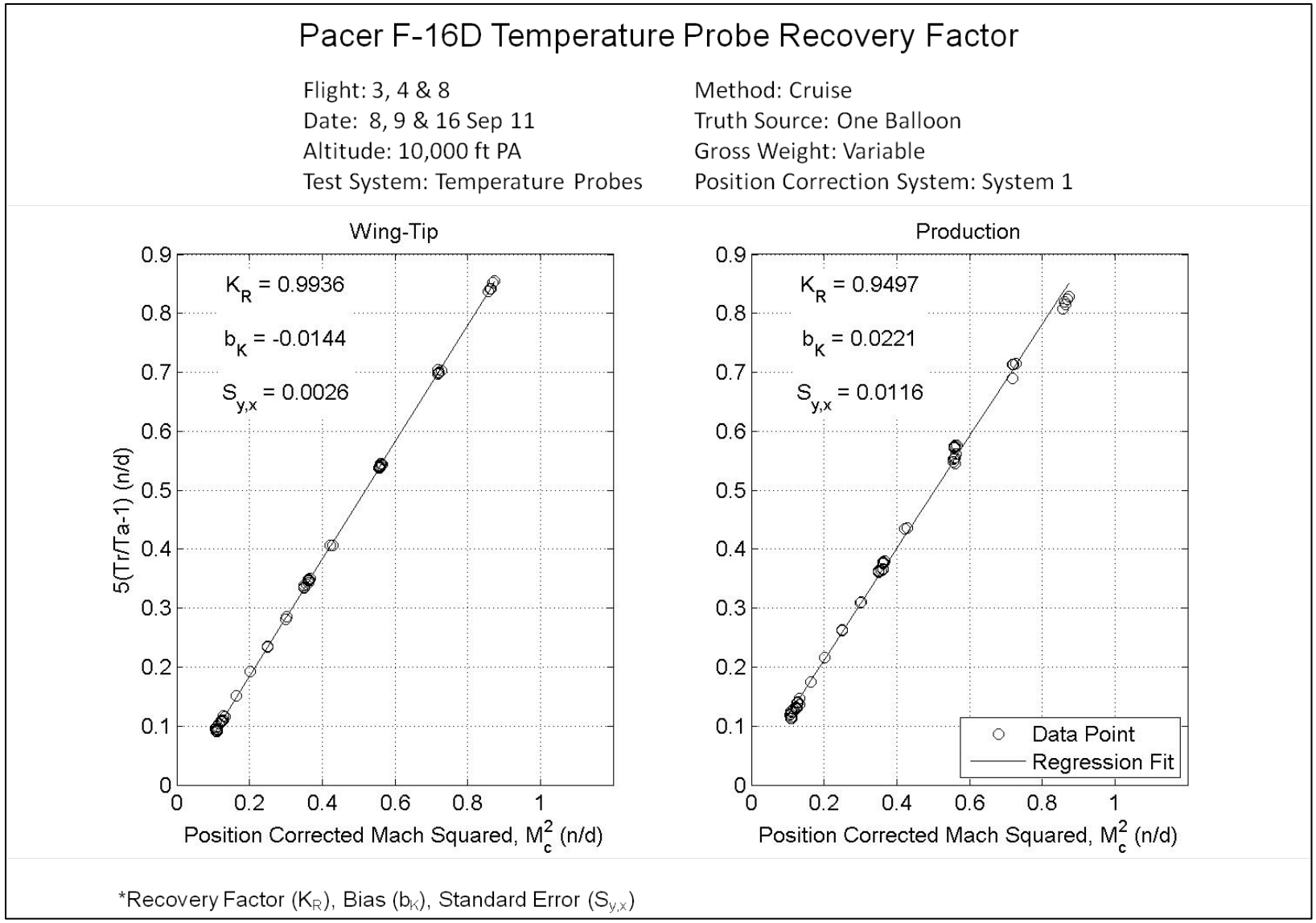

Figure C4 Temperature Recovery Factor - Cruise – 10,000 Feet – One Balloon

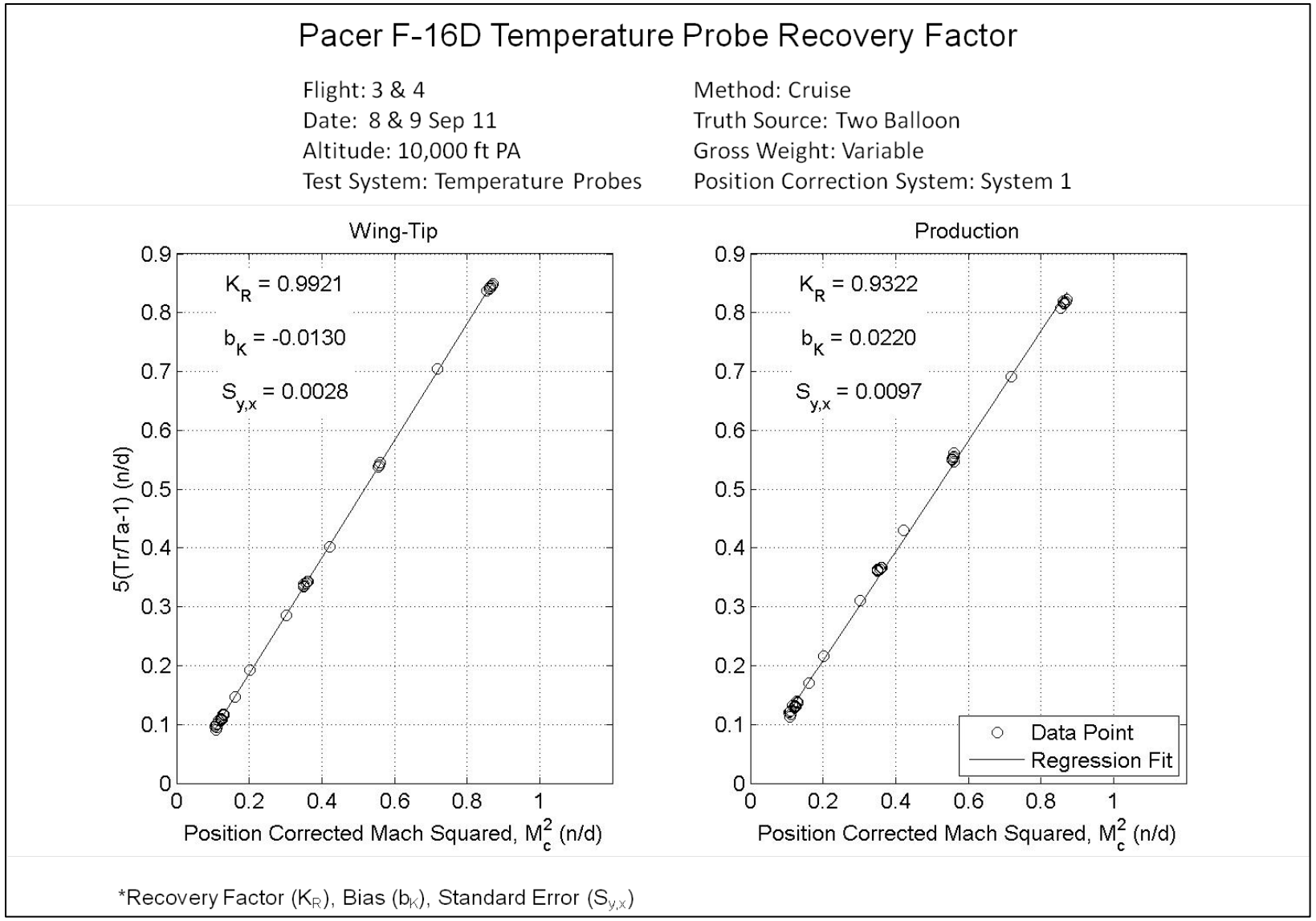

Figure C5 Temperature Recovery Factor - Cruise – 10,000 Feet – Two Balloons

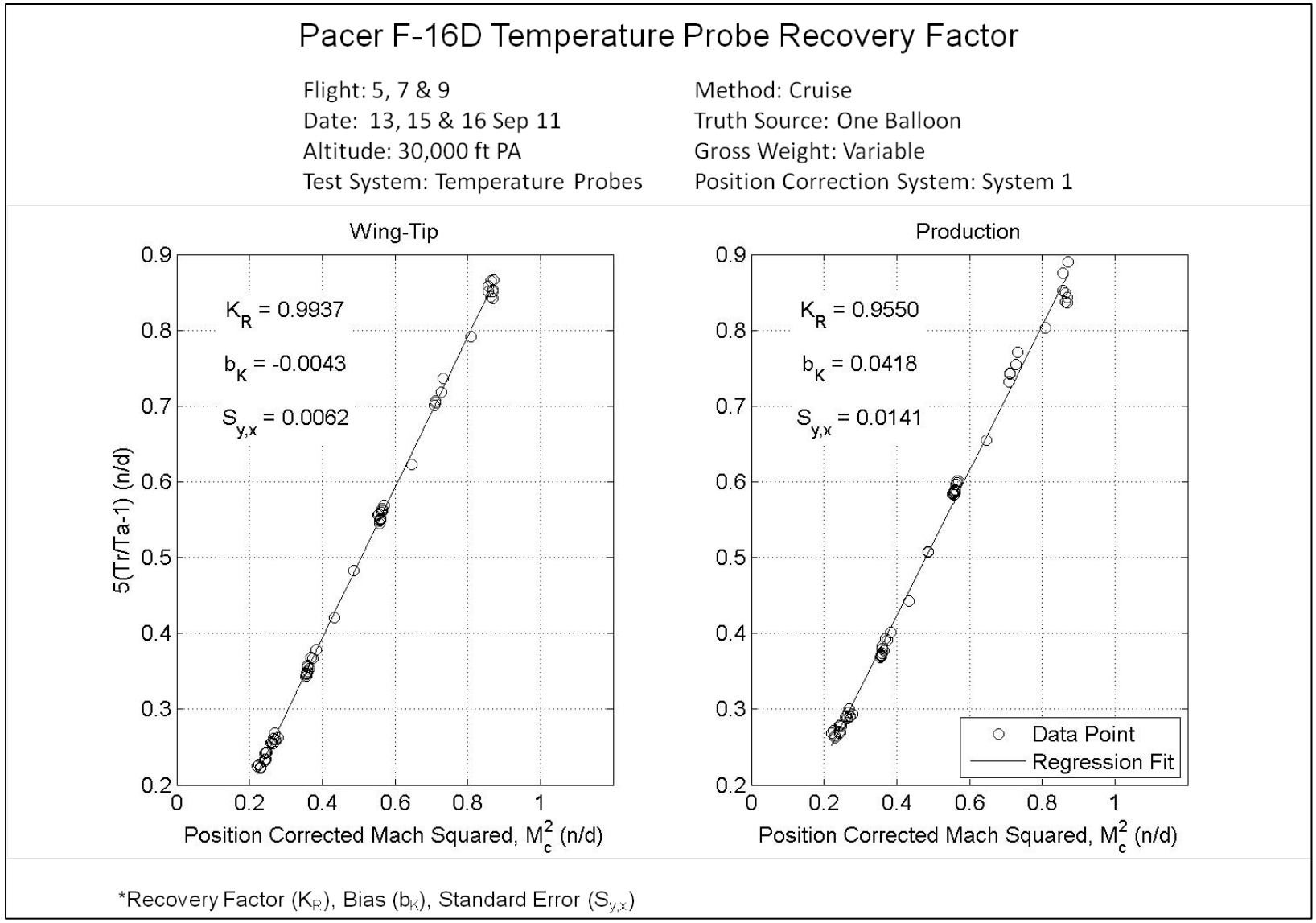

Figure C6 Temperature Recovery Factor - Cruise – 30,000 Feet – One Balloon

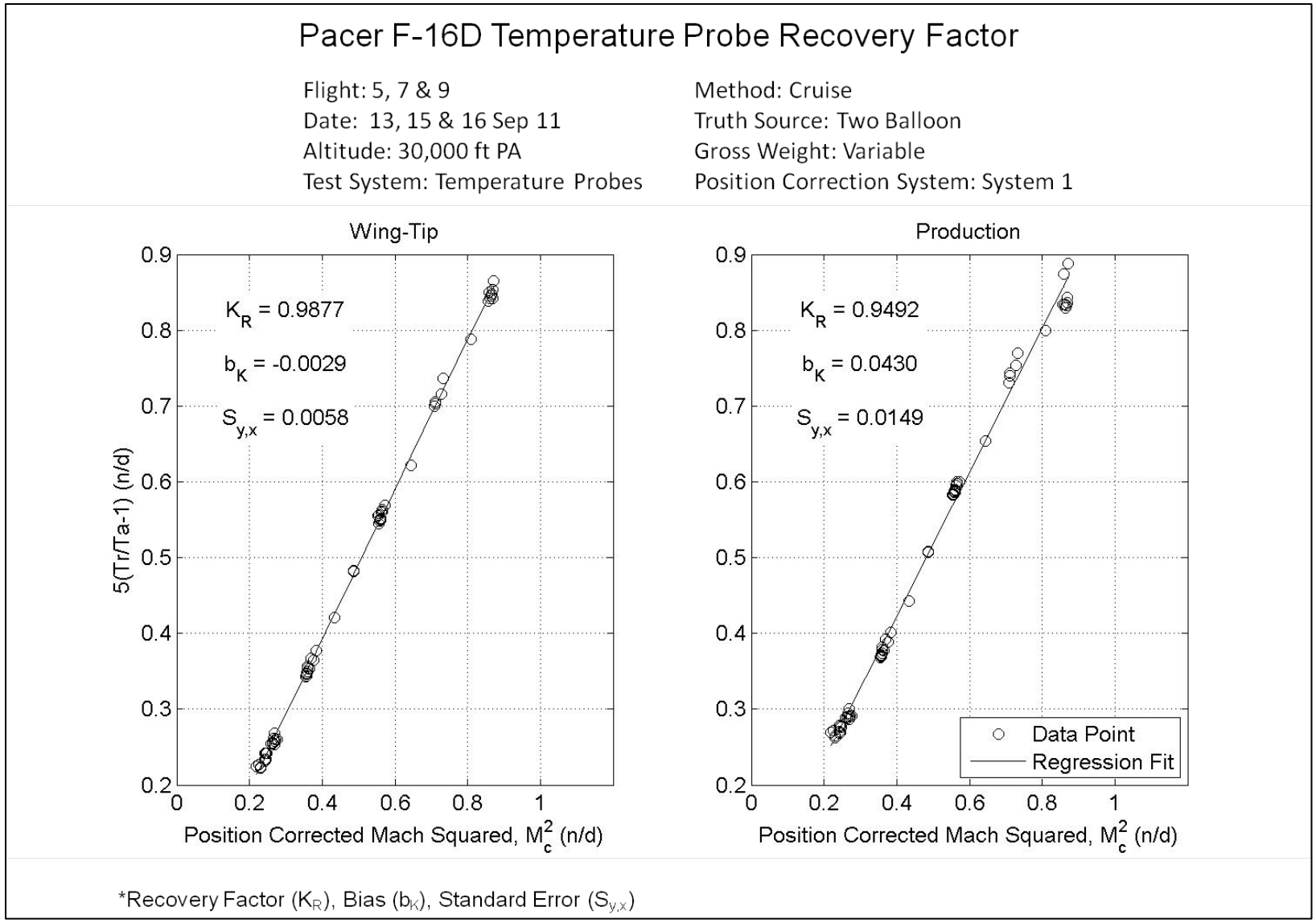

Figure C7 Temperature Recovery Factor - Cruise – 30,000 Feet – Two Balloons

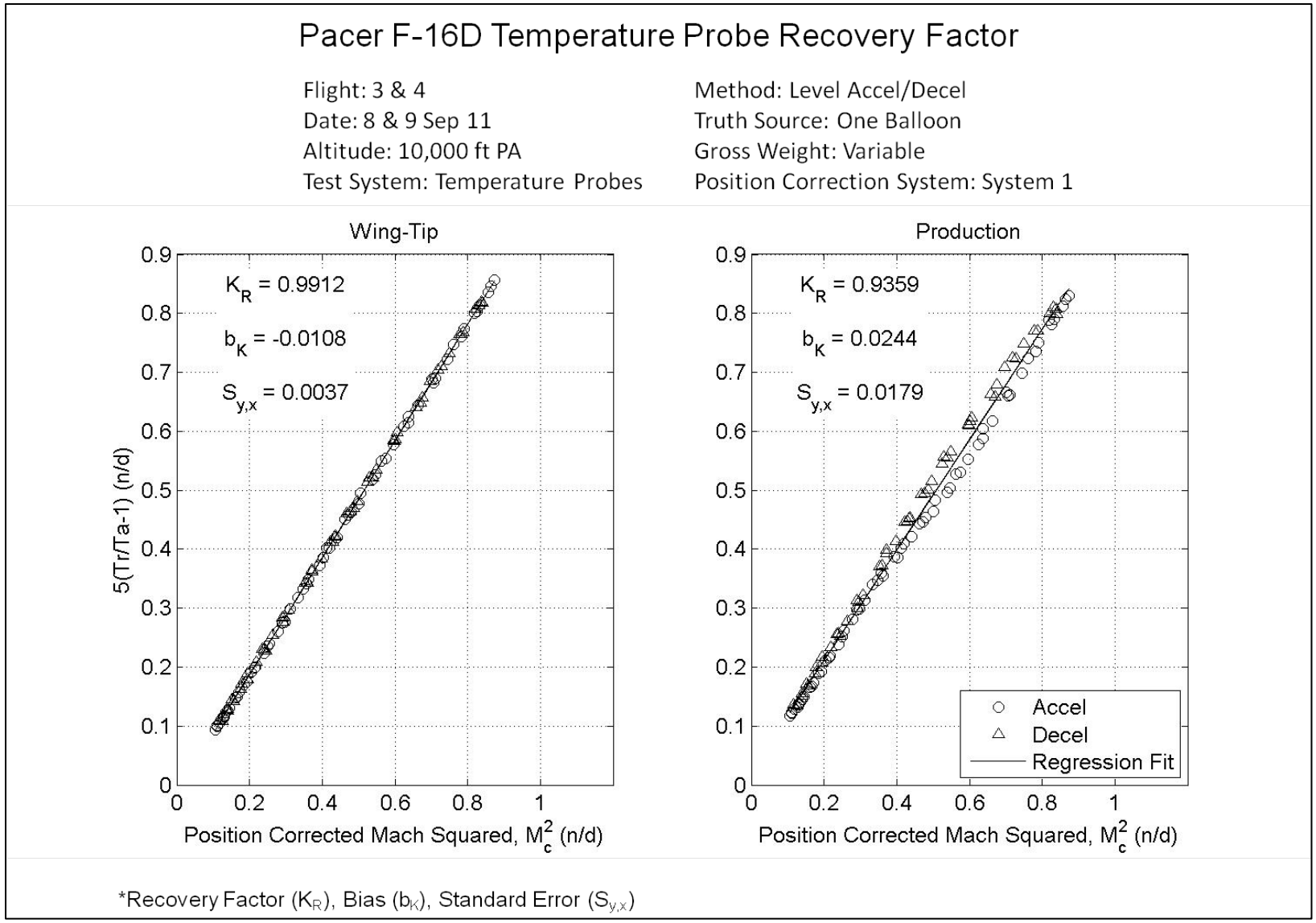

Figure C8 Temperature Recovery Factor – Level Accel/Decel – 10,000 Feet – One Balloon

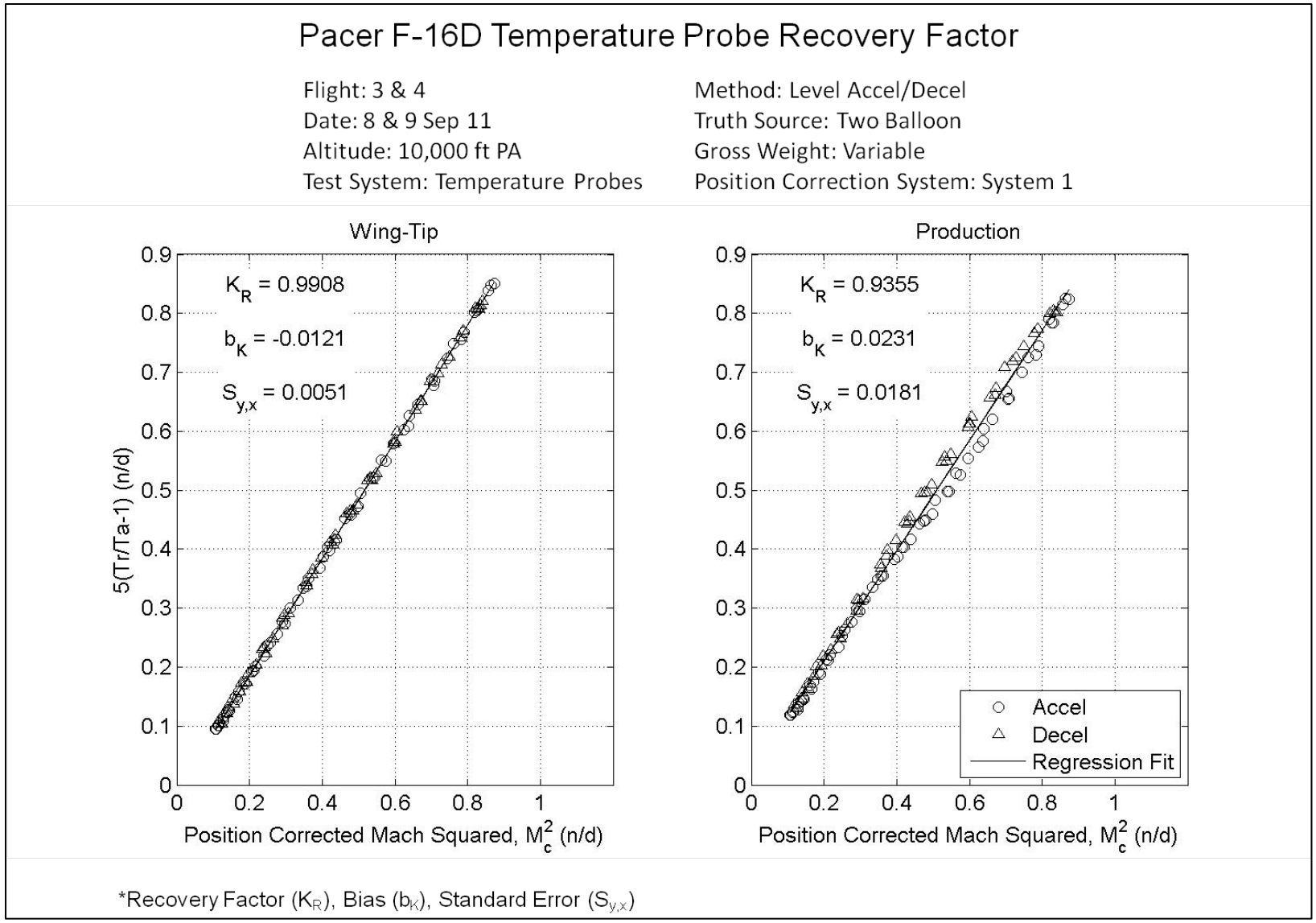

Figure C9 Temperature Recovery Factor – Level Accel/Decel – 10,000 Feet – Two Balloons

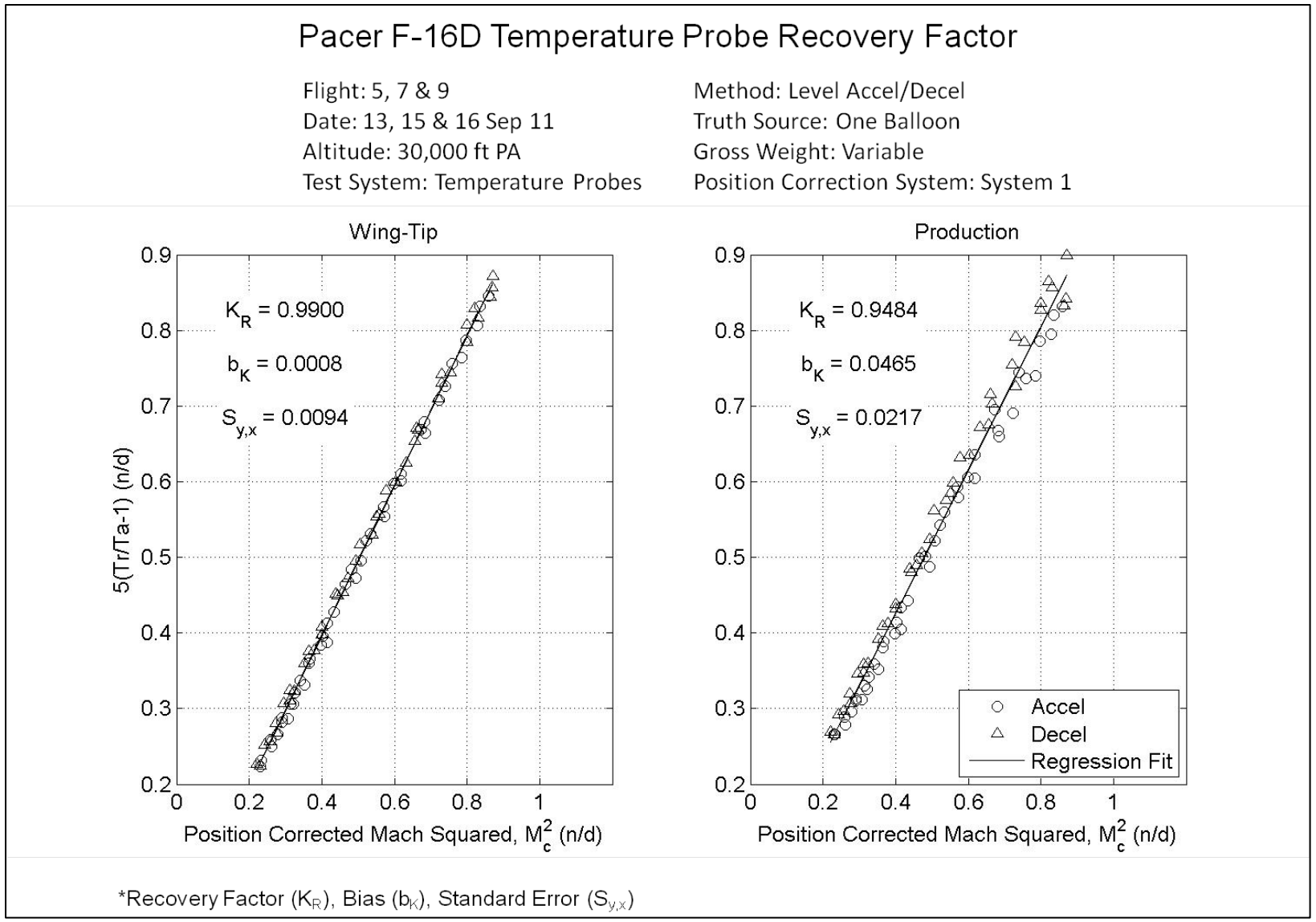

Figure C10 Temperature Recovery Factor – Level Accel/Decel – 30,000 Feet – One Balloon

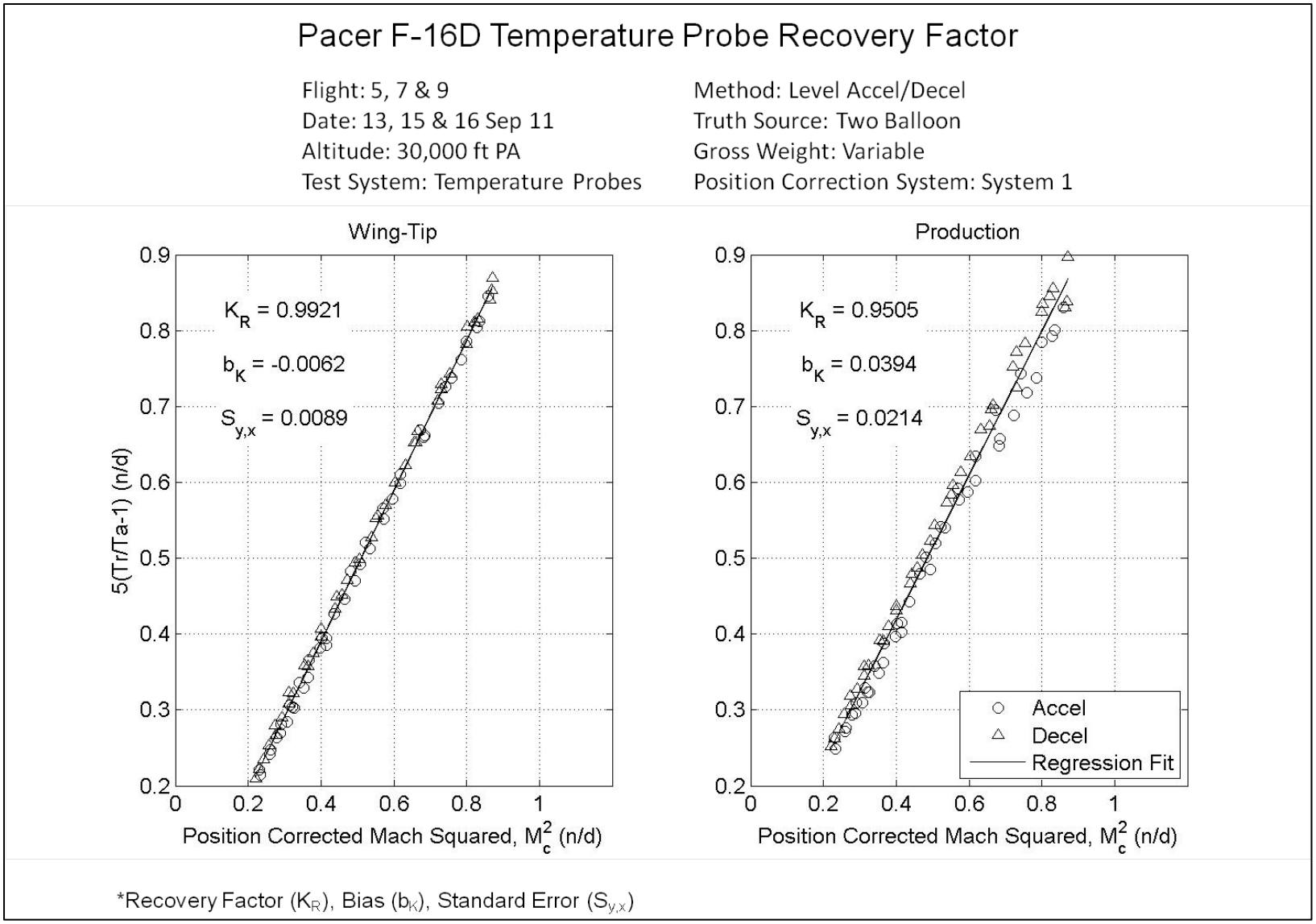

Figure C11 Temperature Recovery Factor – Level Accel/Decel – 30,000 Feet – Two Balloons

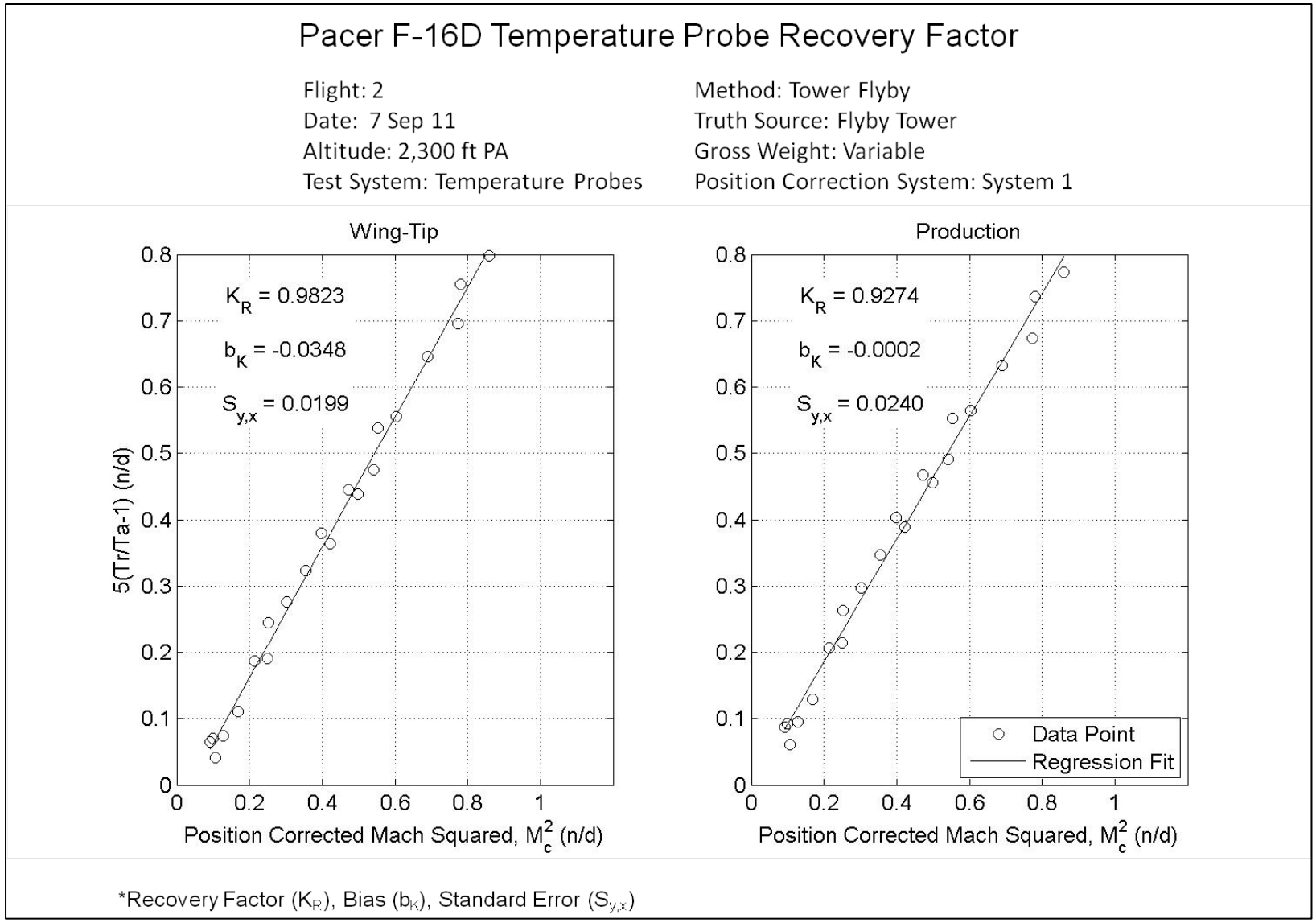

Figure C12 Temperature Recovery Factor – Tower Flyby – Flyby Tower – Flight 2

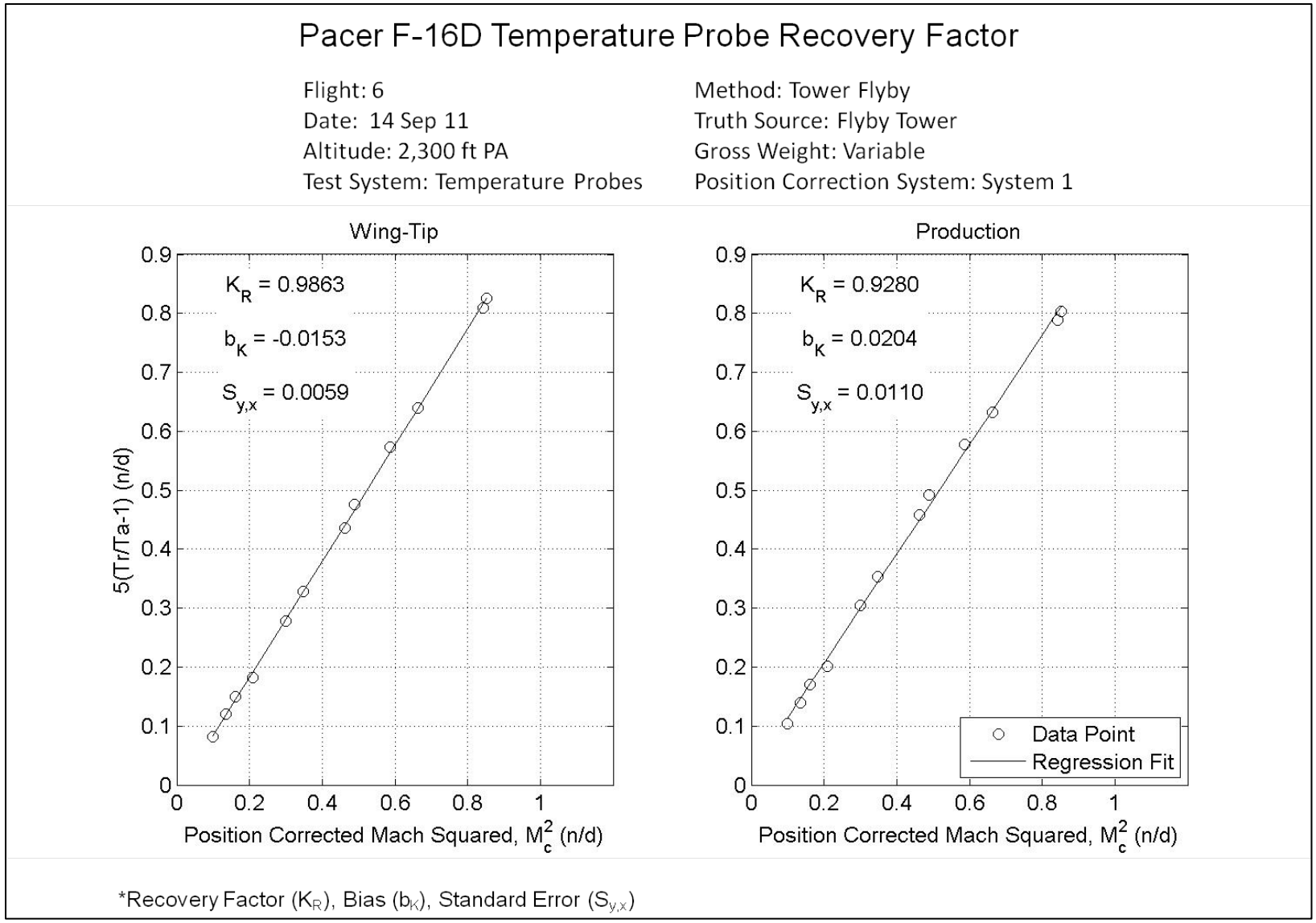

Figure C13 Temperature Recovery Factor – Tower Flyby – Flyby Tower – Flight 6

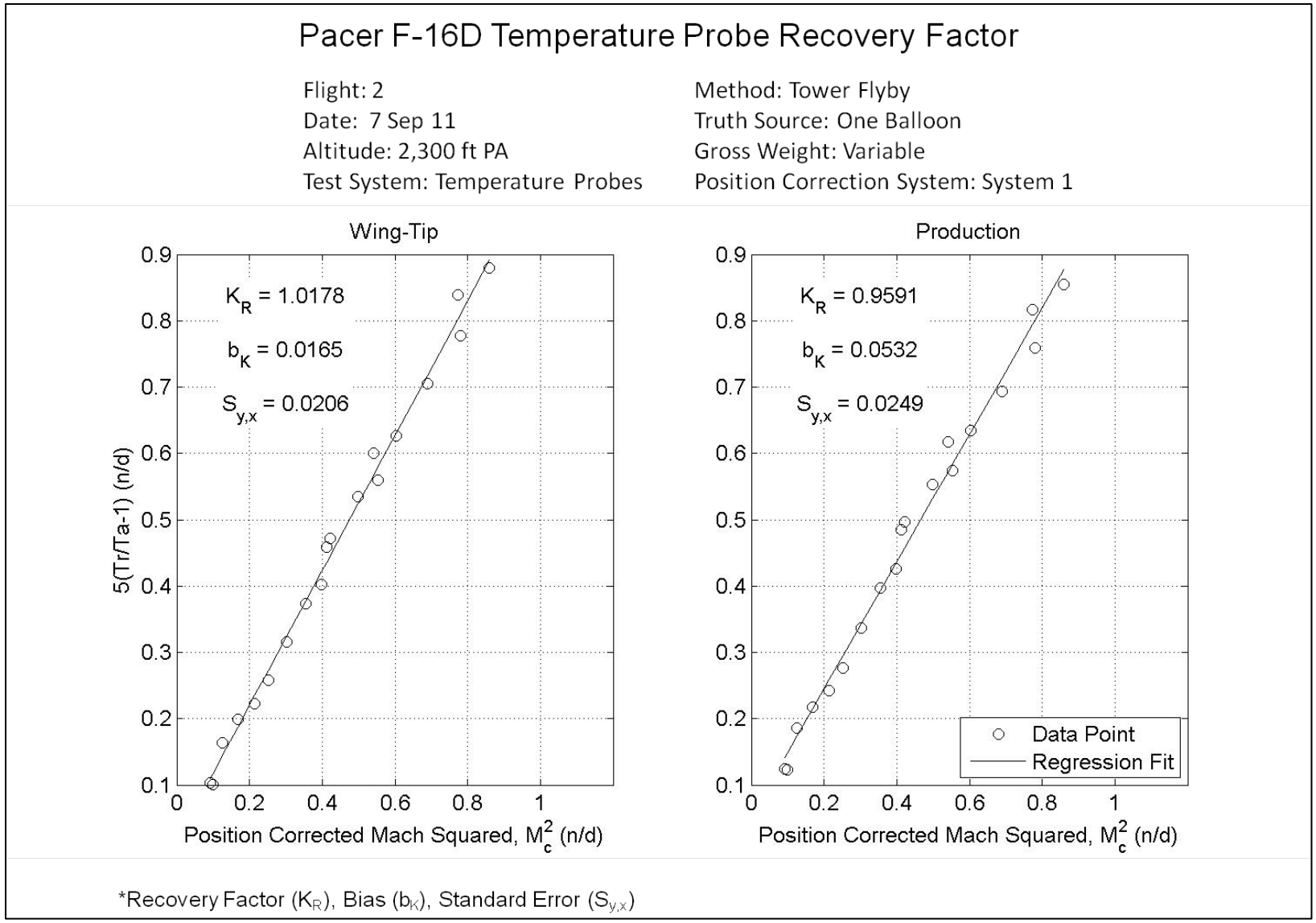

Figure C14 Temperature Recovery Factor – Tower Flyby – One Balloon – Flight 2

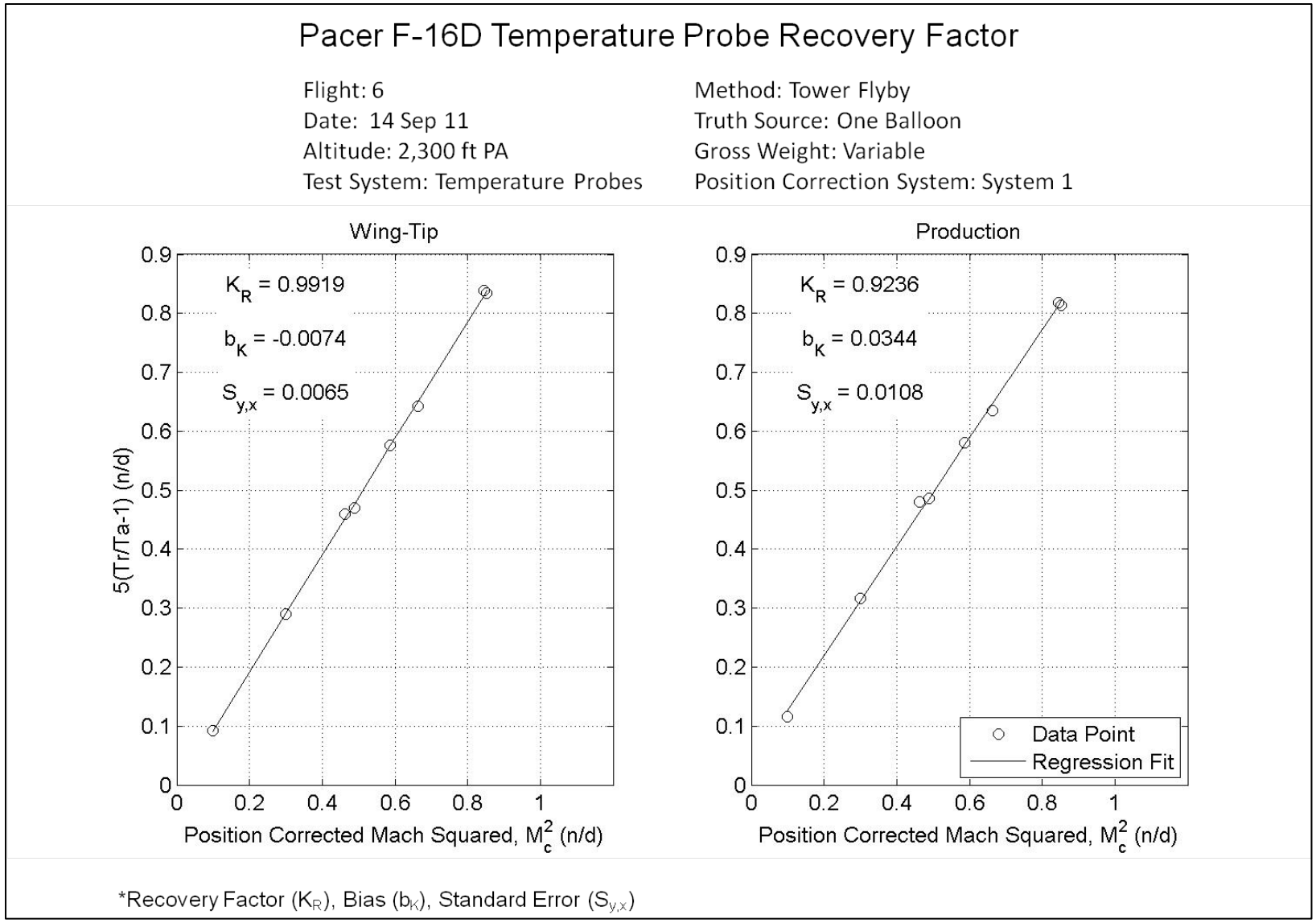

Figure C15 Temperature Recovery Factor – Tower Flyby – One Balloon – Flight 6

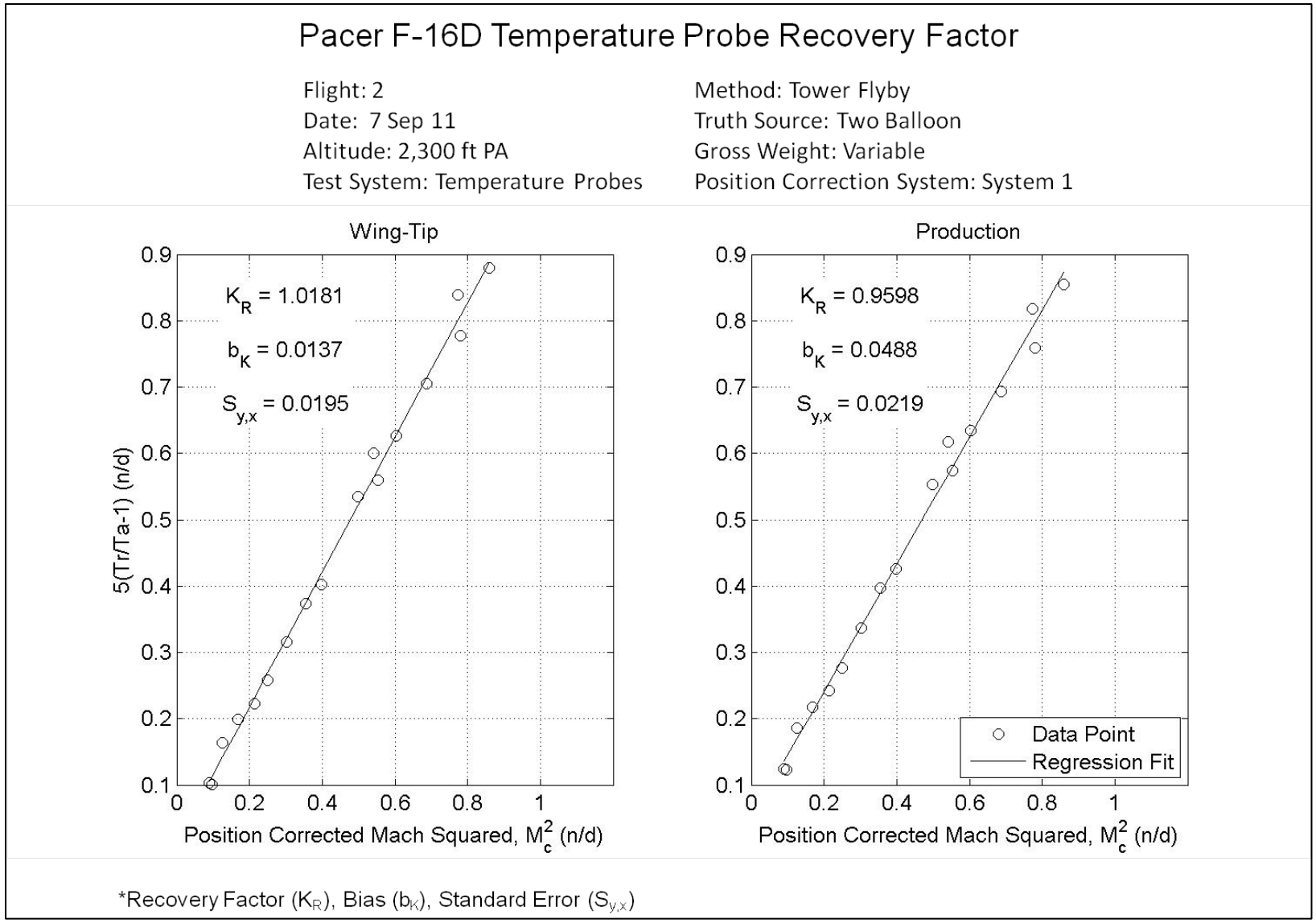

Figure C16 Temperature Recovery Factor – Tower Flyby – Two Balloons – Flight 2

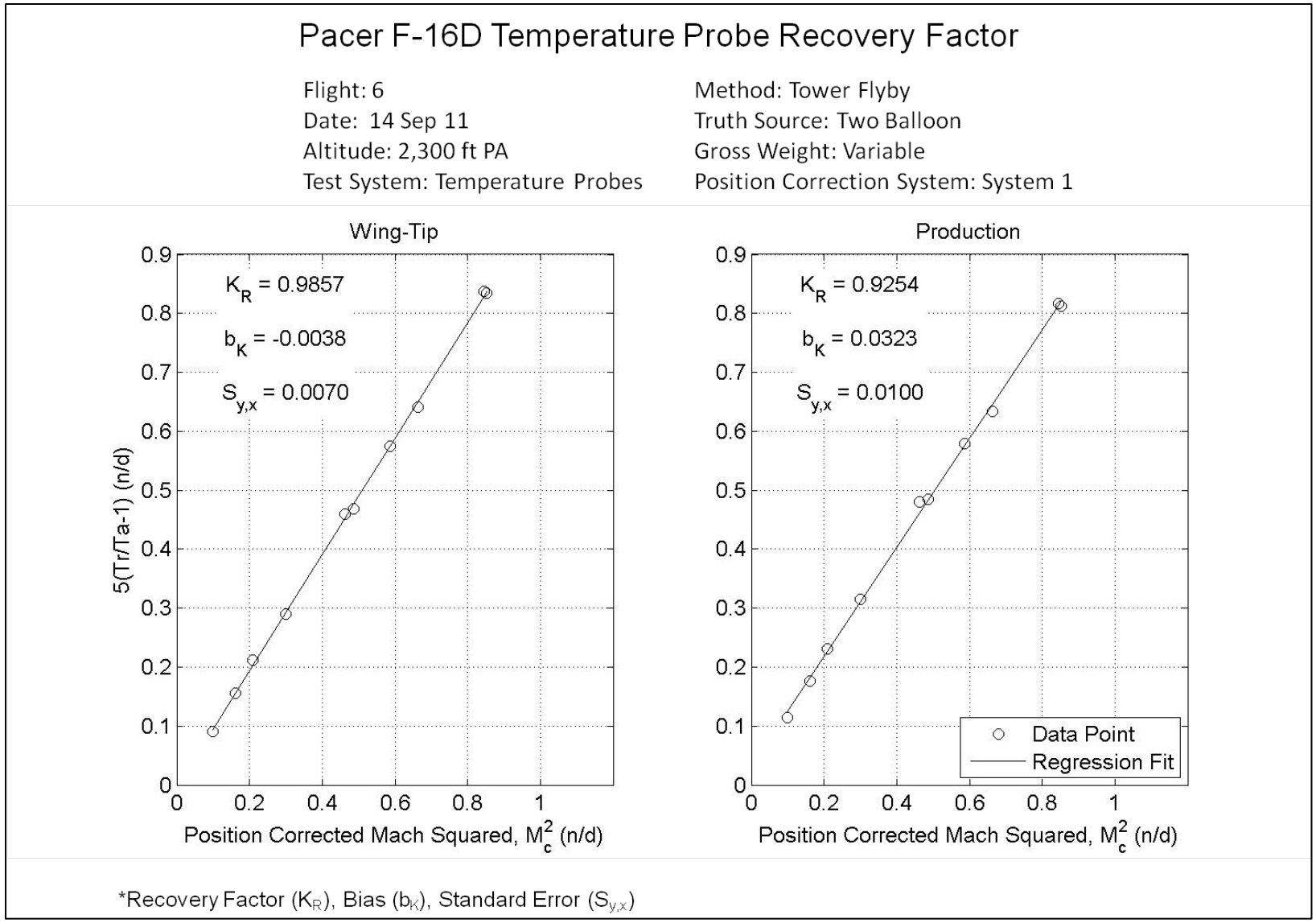

Figure C17 Temperature Recovery Factor – Tower Flyby – Two Balloons – Flight 6

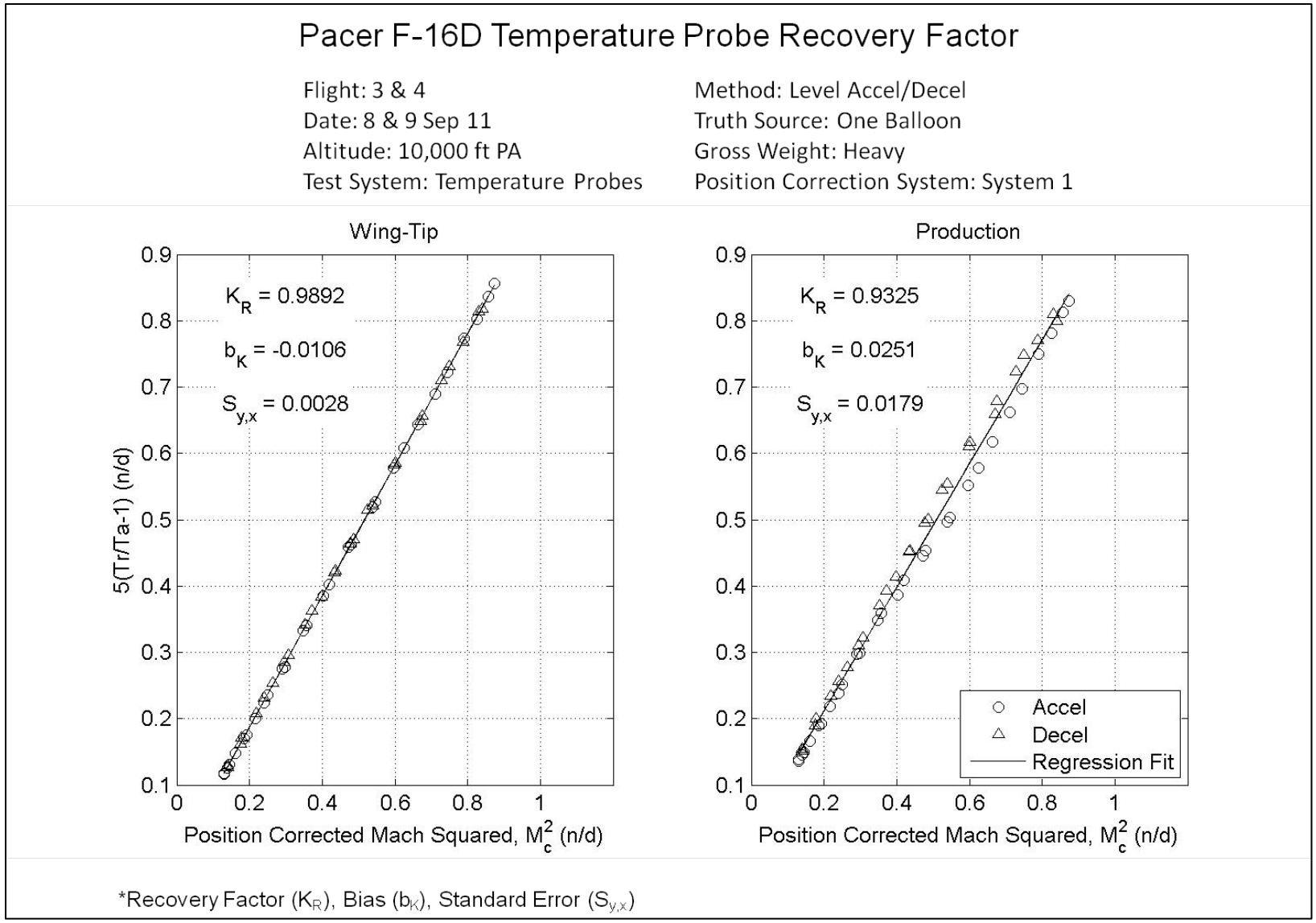

Figure C18 Temperature Recovery Factor – Level Accel/Decel – 10,000 Feet – One Balloon – Heavy

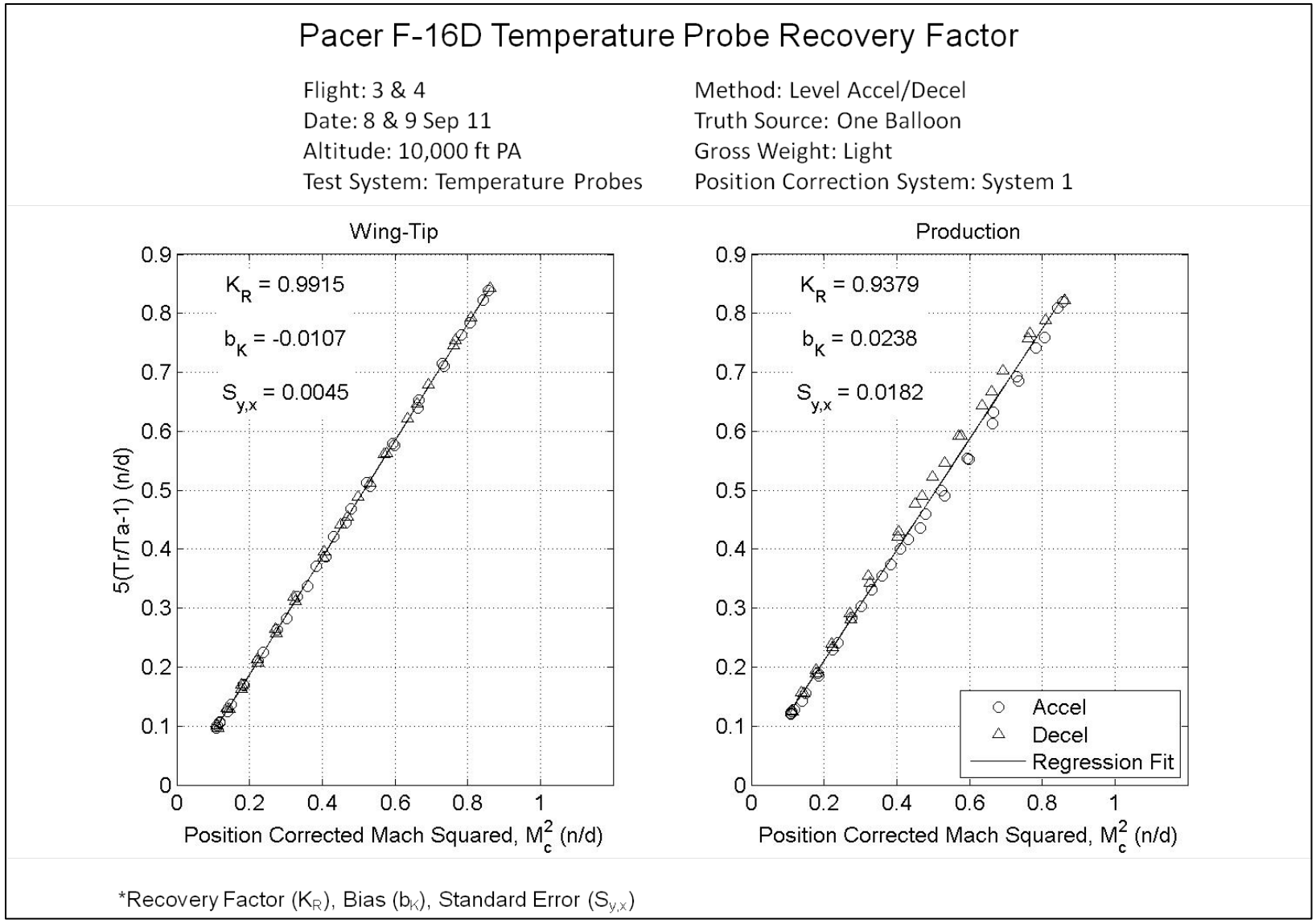

Figure C19 Temperature Recovery Factor – Level Accel/Decel – 10,000 Feet – One Balloon – Light

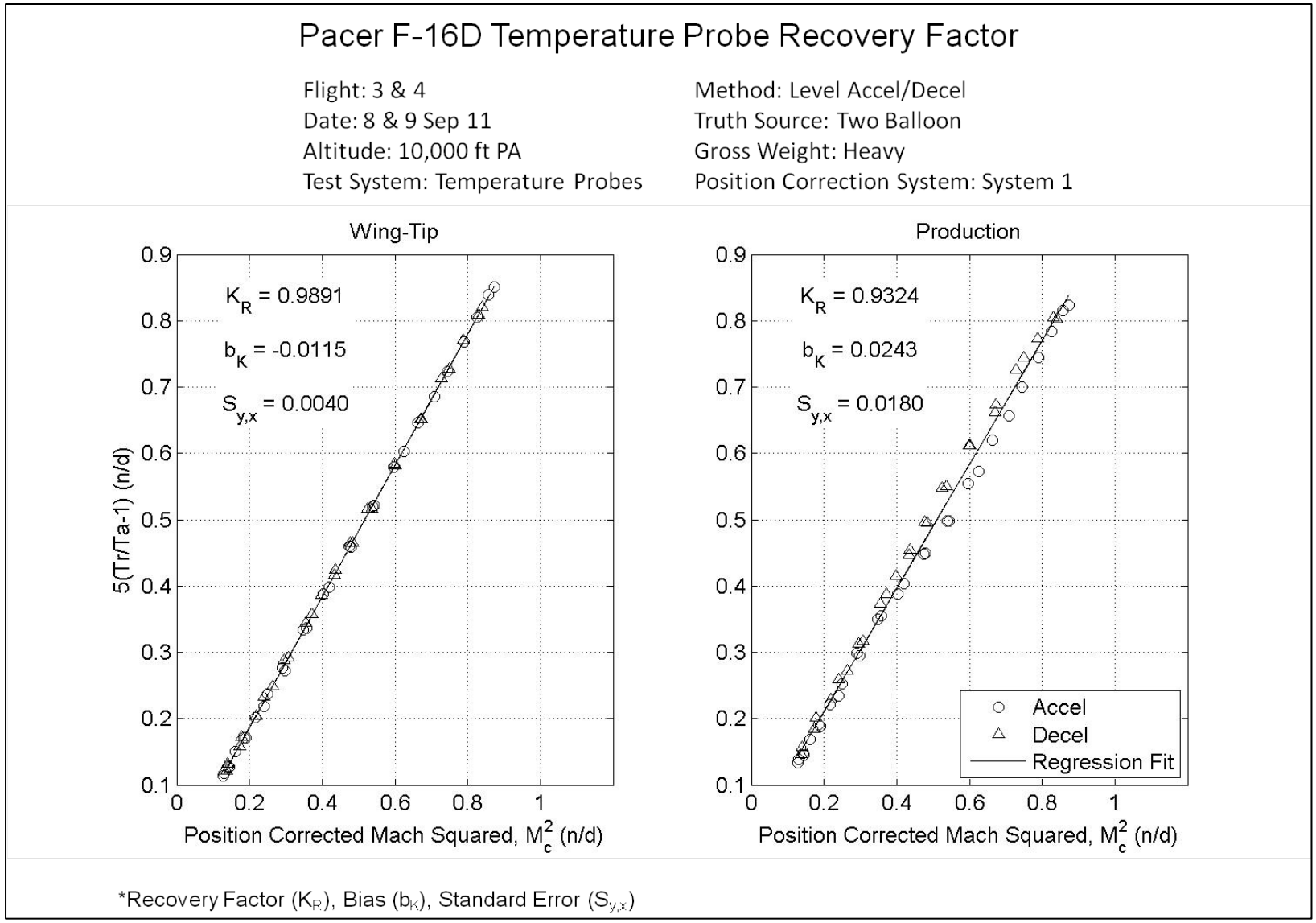

Figure C20 Temperature Recovery Factor – Level Accel/Decel – 10,000 Feet – Two Balloons – Heavy

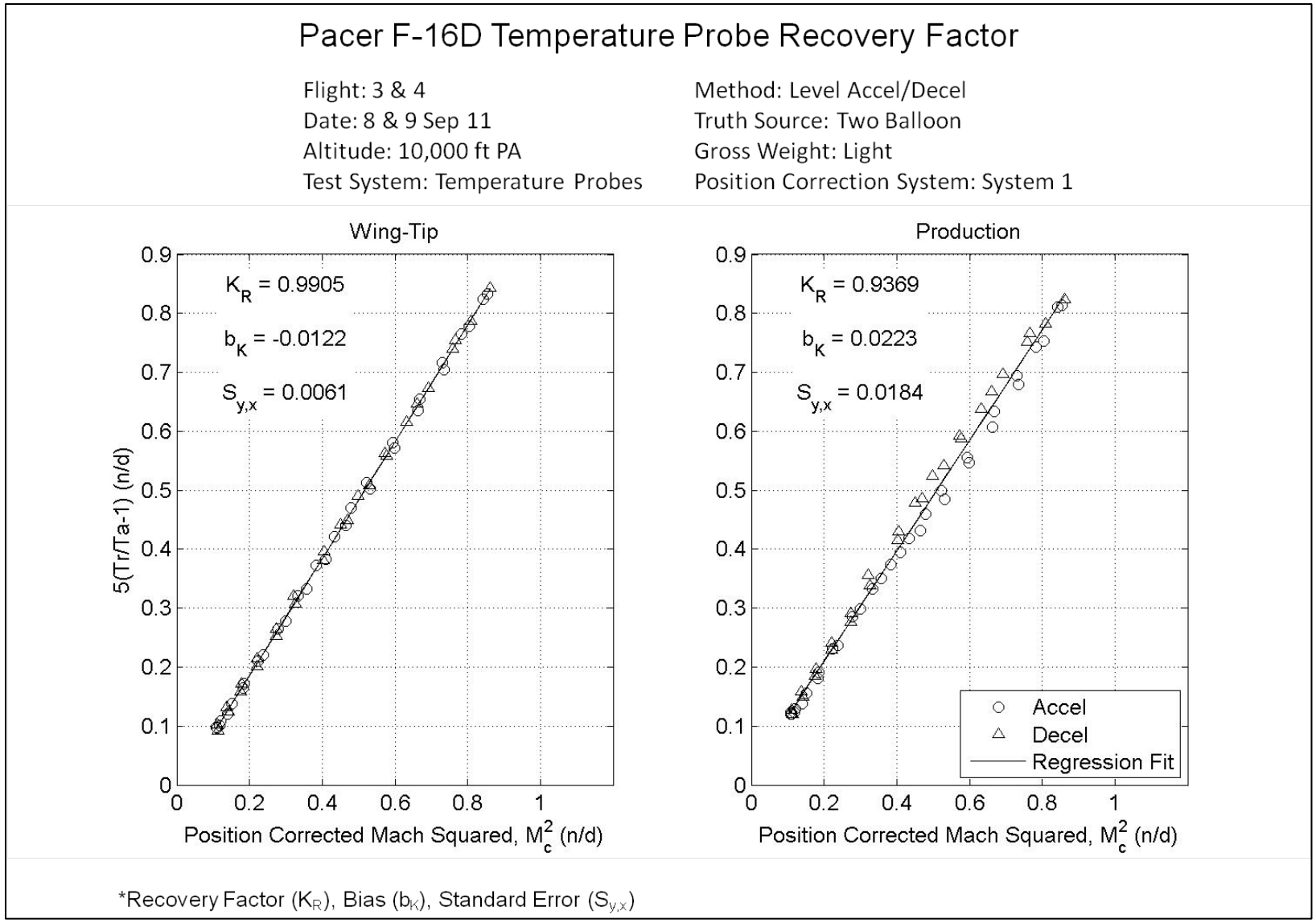

Figure C21 Temperature Recovery Factor – Level Accel/Decel – 10,000 Feet – Two Balloons – Light

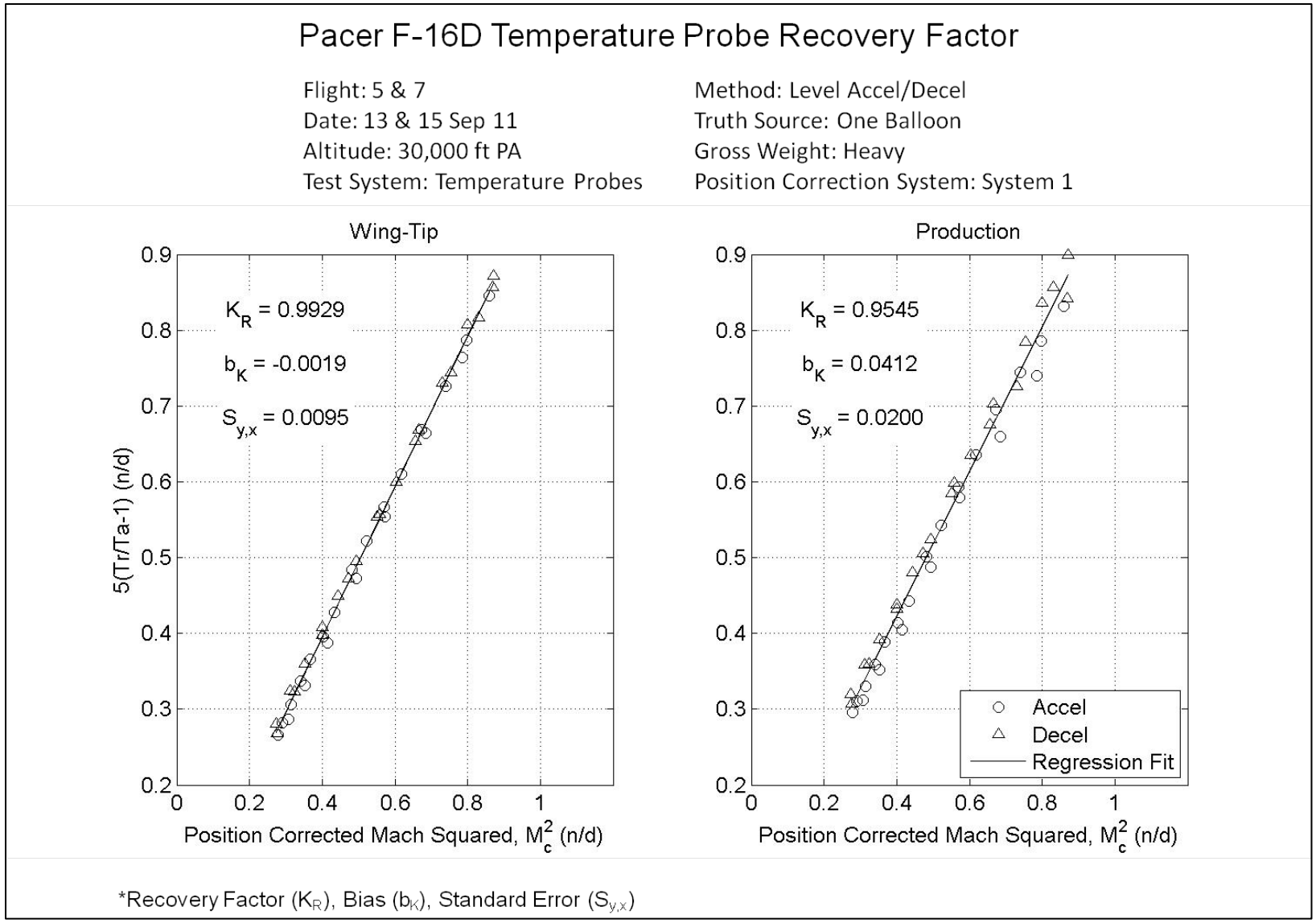

Figure C22 Temperature Recovery Factor – Level Accel/Decel – 30,000 Feet – One Balloon – Heavy

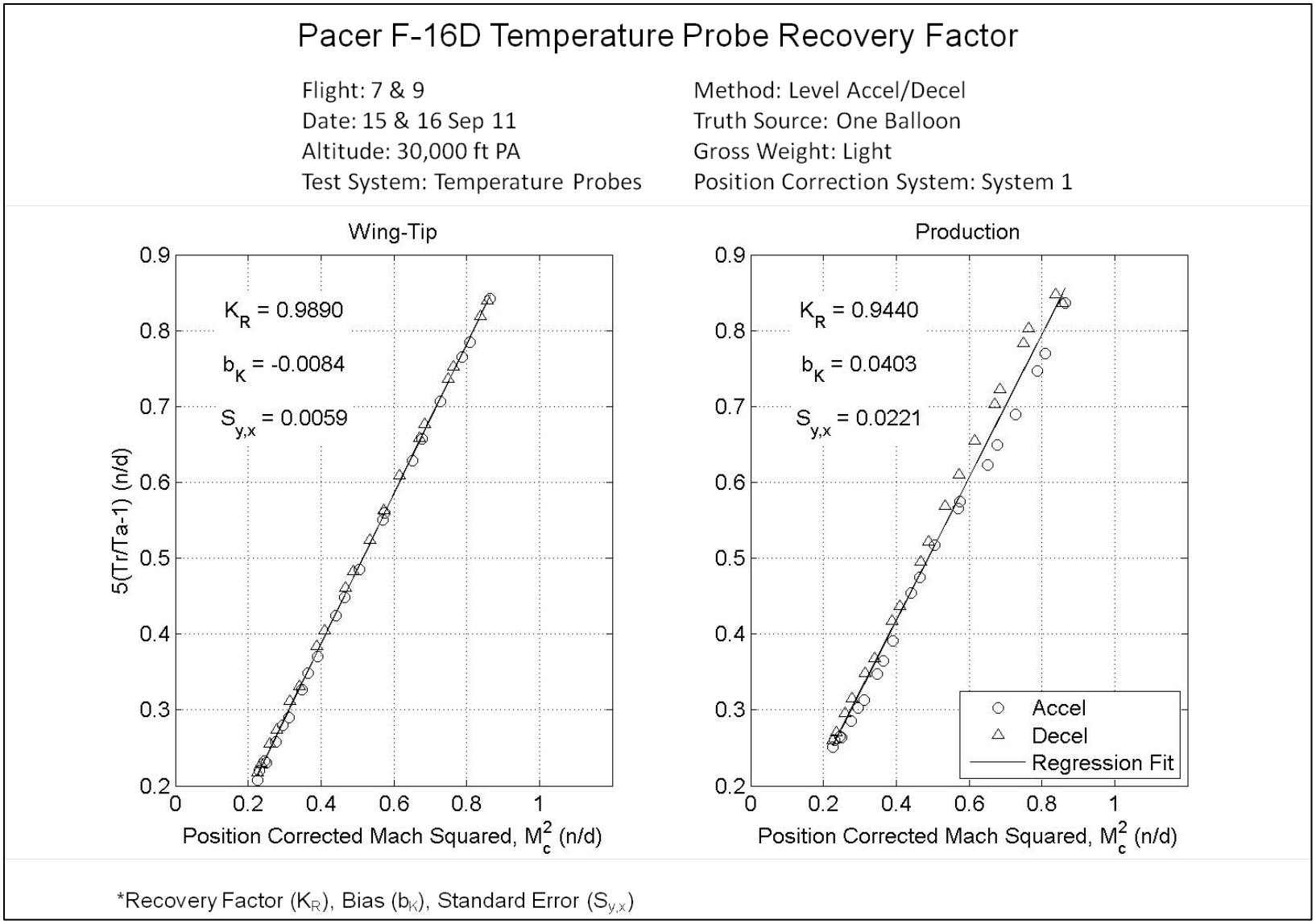

Figure C23 Temperature Recovery Factor – Level Accel/Decel – 30,000 Feet – One Balloon – Light

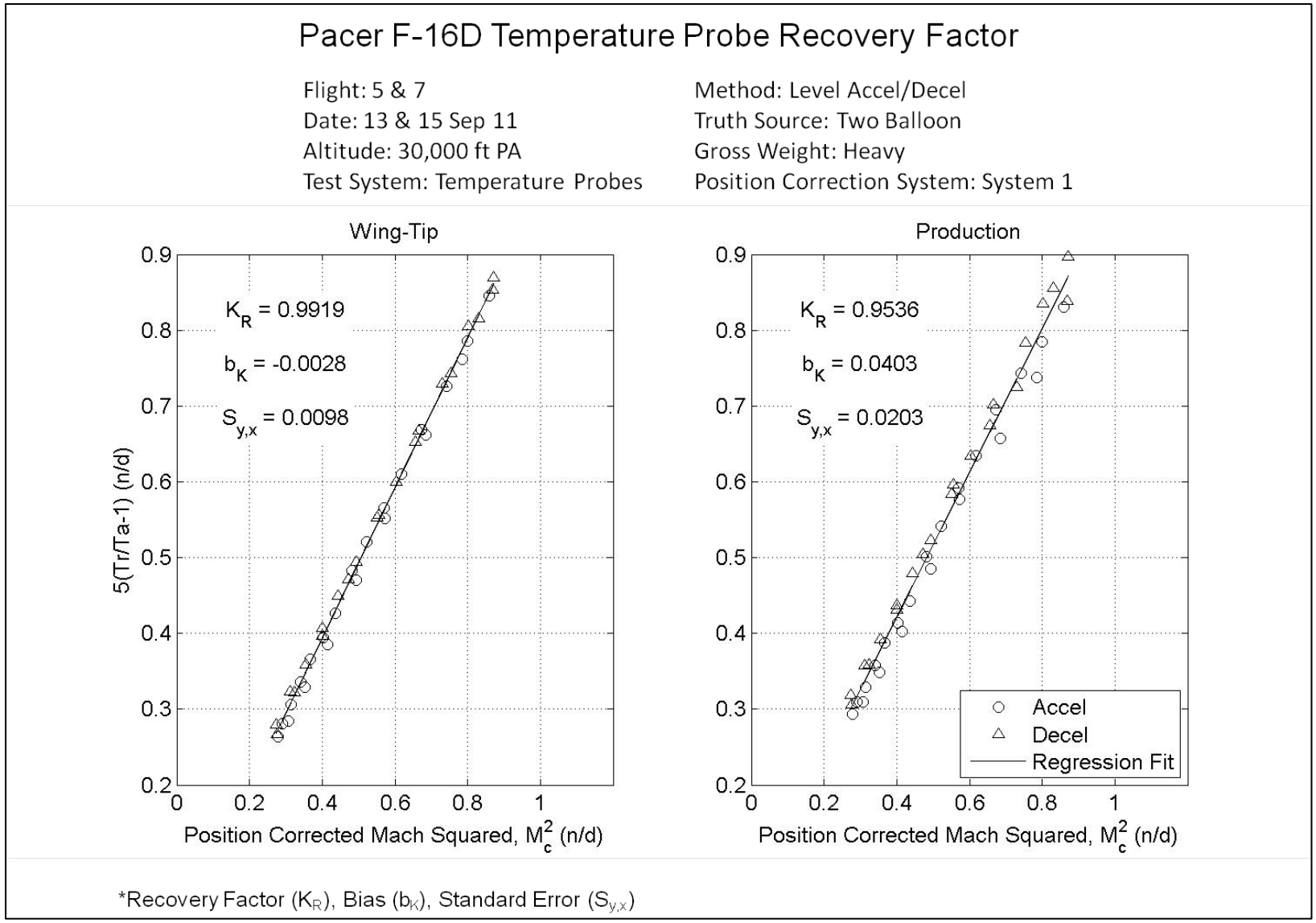

Figure C24 Temperature Recovery Factor – Level Accel/Decel – 30,000 Feet – Two Balloons – Heavy

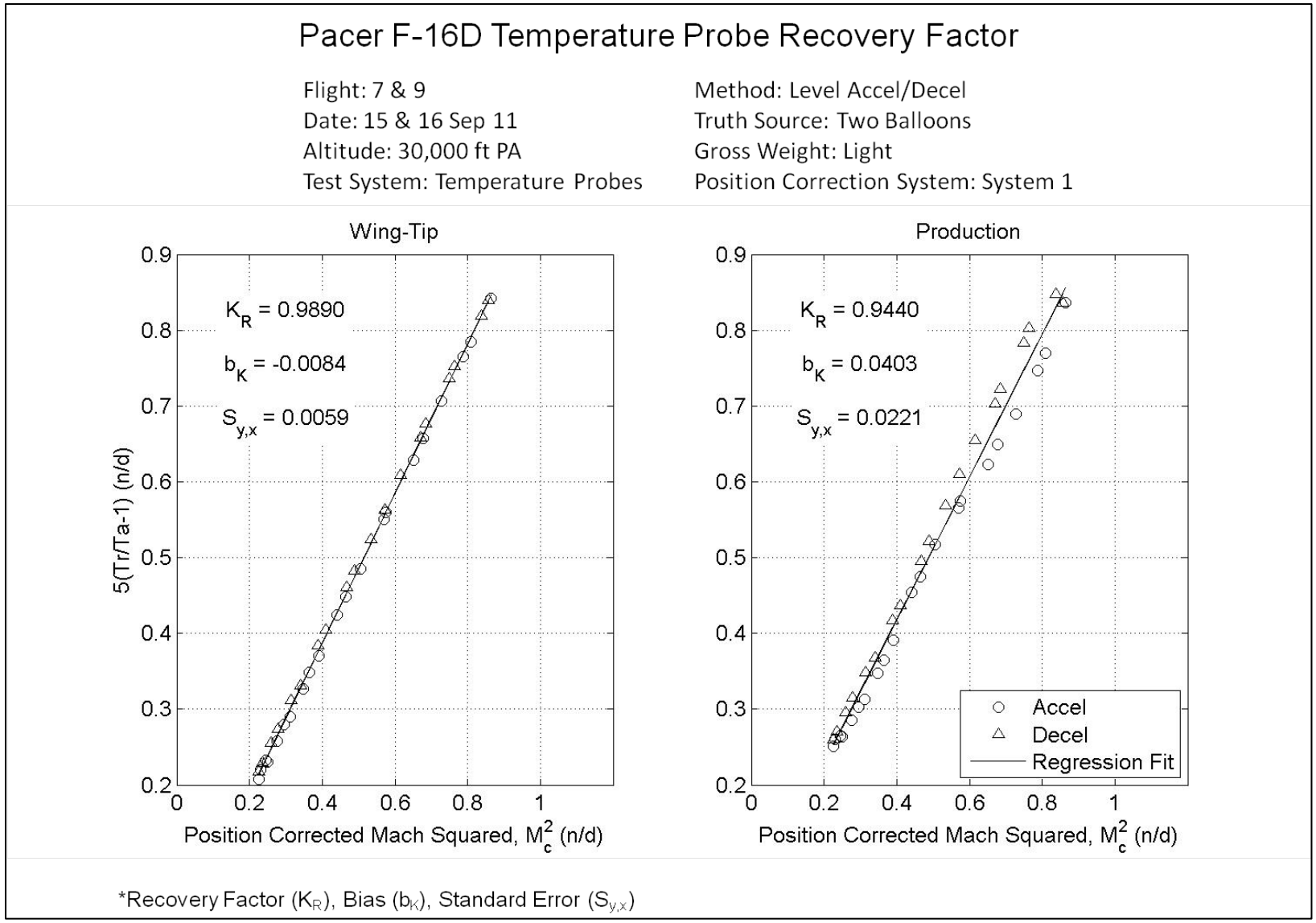

Figure C25 Temperature Recovery Factor – Level Accel/Decel – 30,000 Feet – Two Balloons – Light

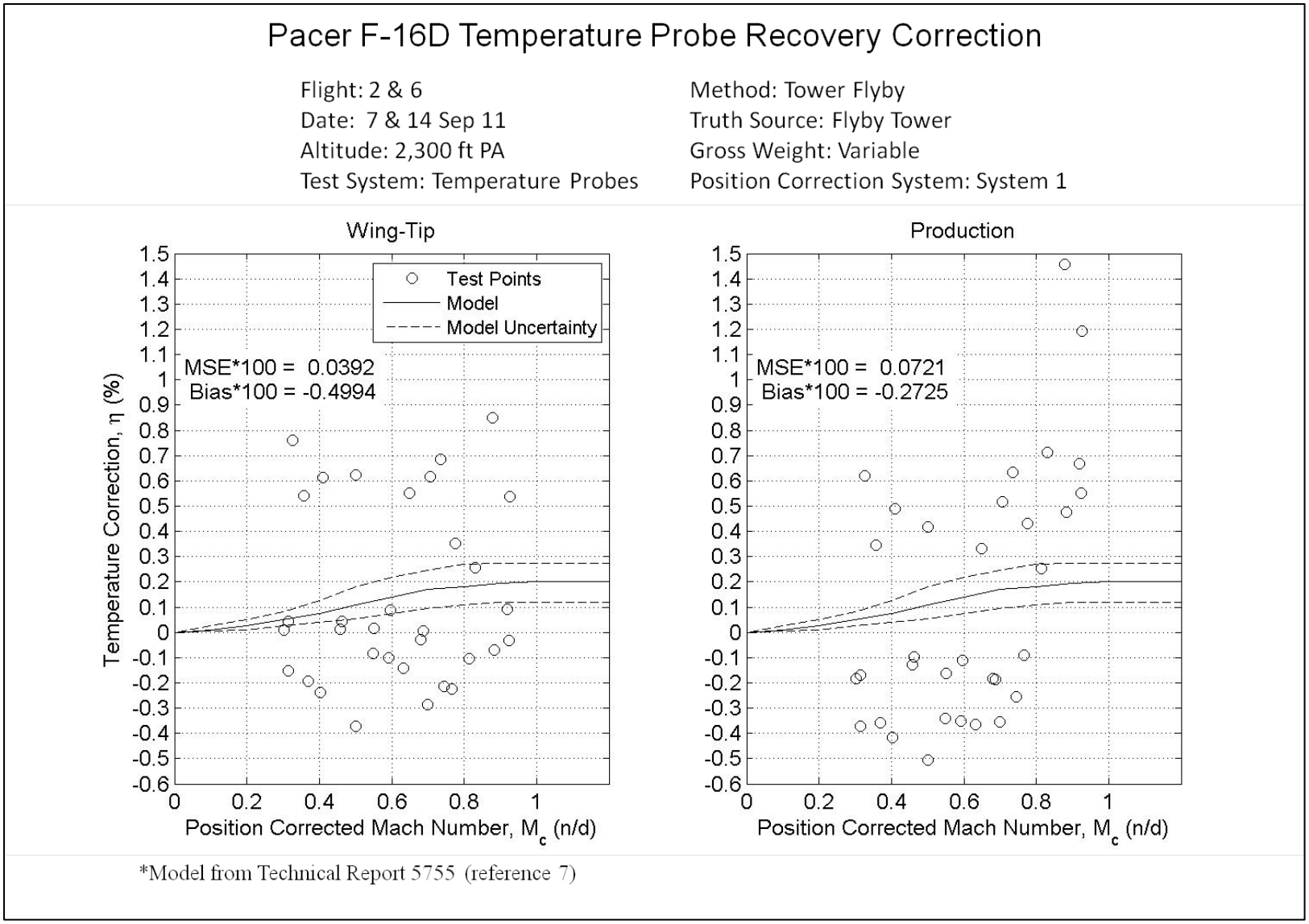

Figure C26 Temperature Recovery Correction – Tower Flyby – Flyby Tower

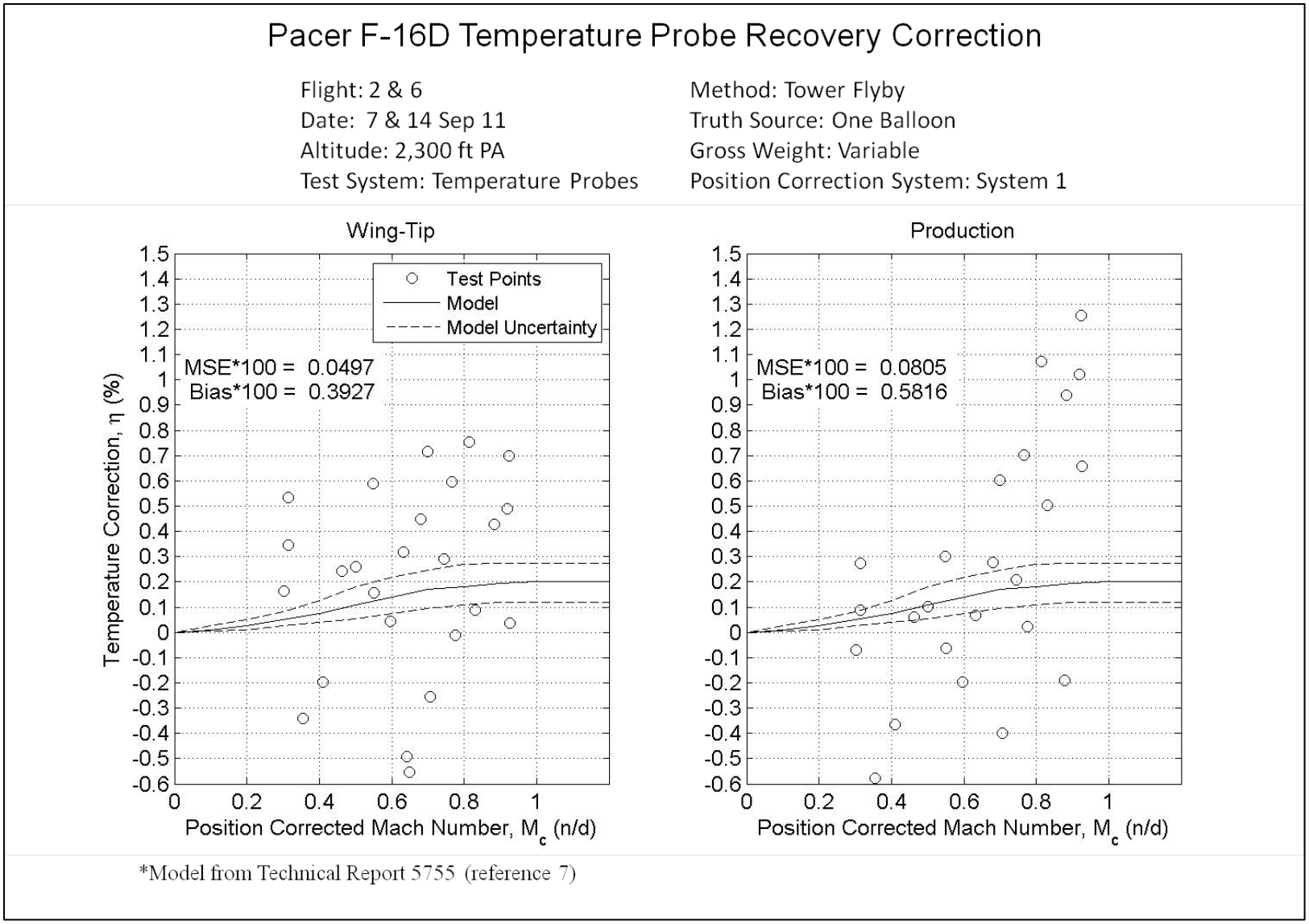

Figure C27 Temperature Recovery Correction – Tower Flyby – One Balloon

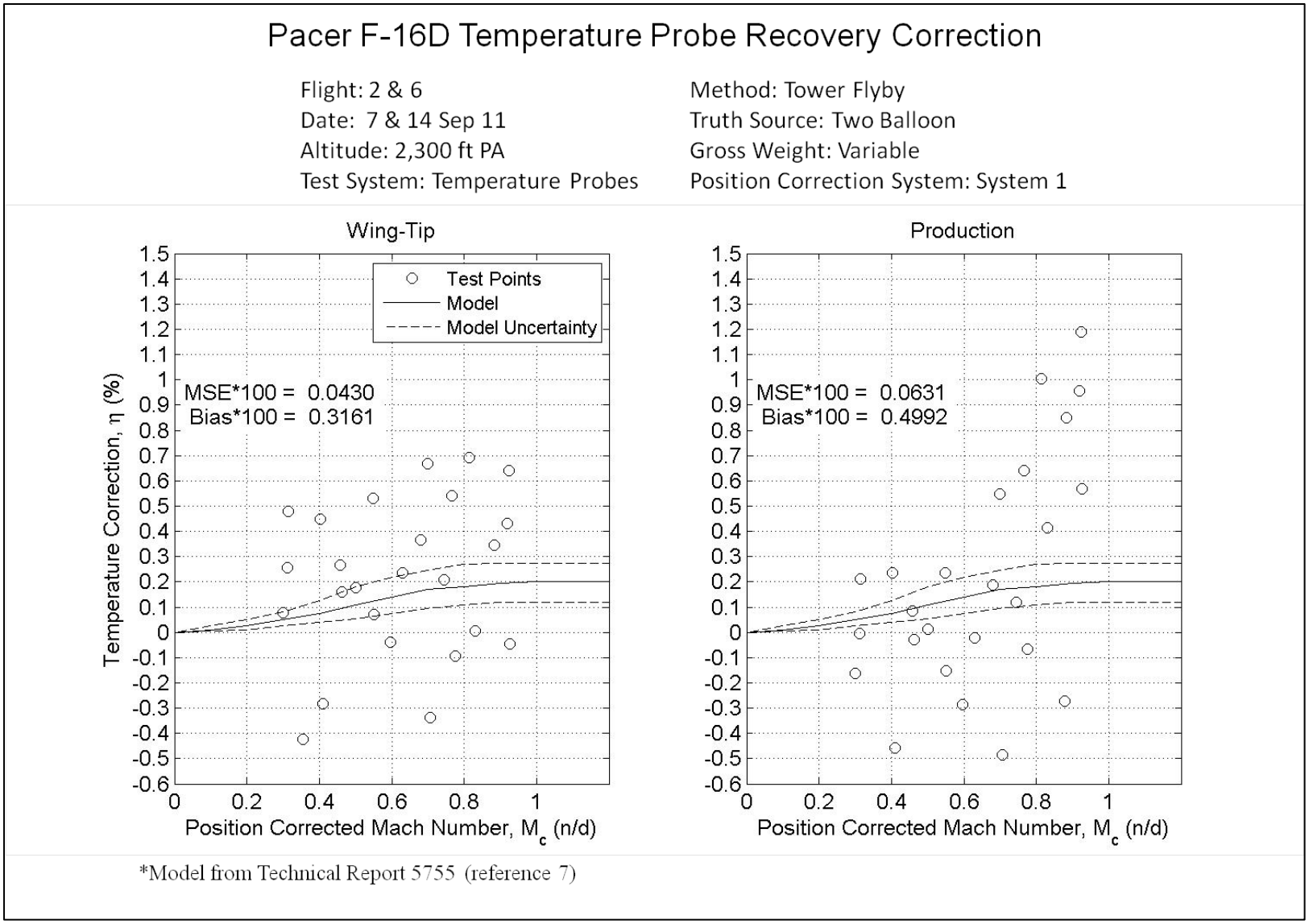

Figure C28 Temperature Recovery Correction – Tower Flyby – Two Balloons

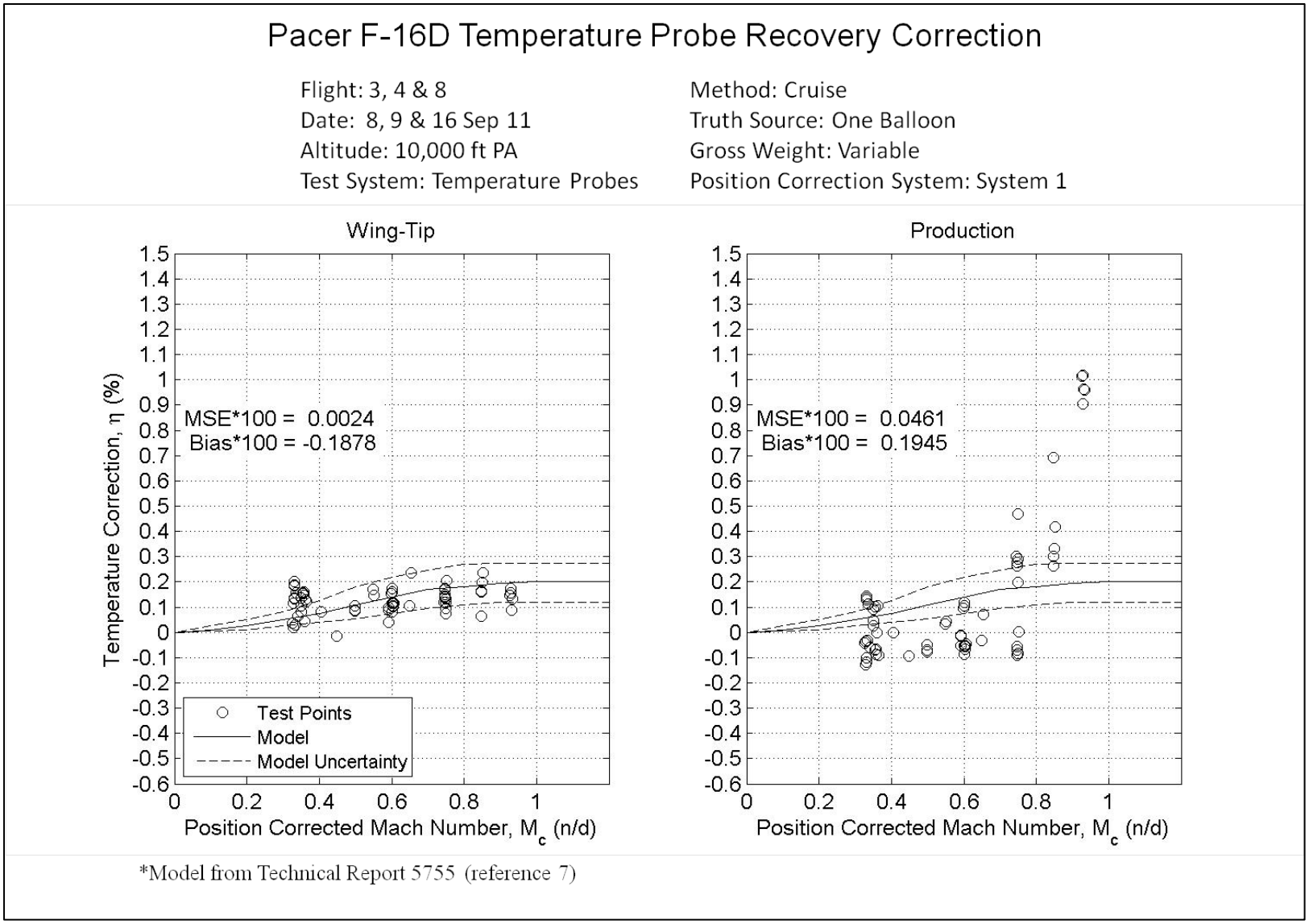

Figure C29 Temperature Recovery Correction – Cruise – 10,000 Feet – One Balloon

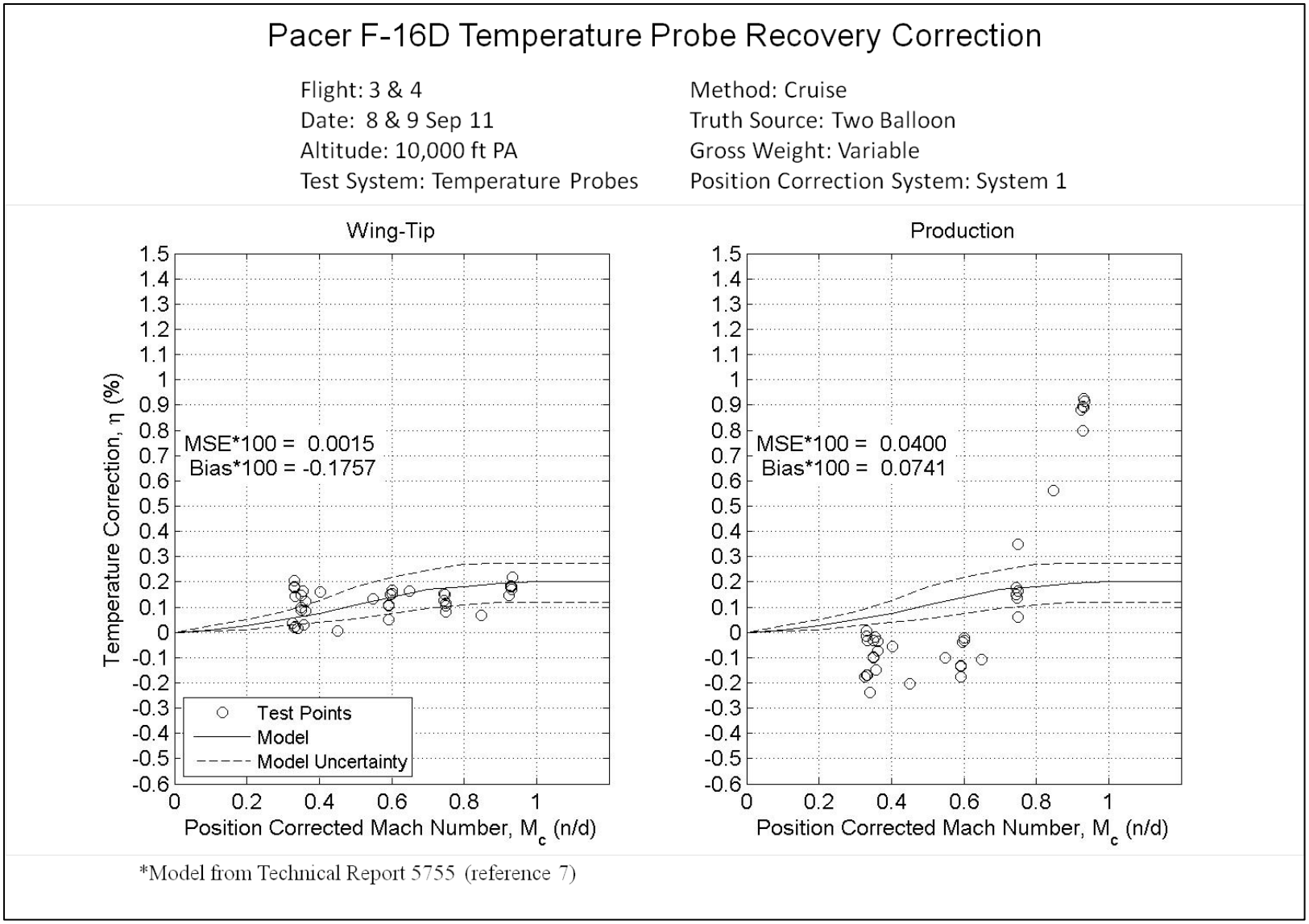

Figure C30 Temperature Recovery Correction – Cruise – 10,000 Feet – Two Balloons

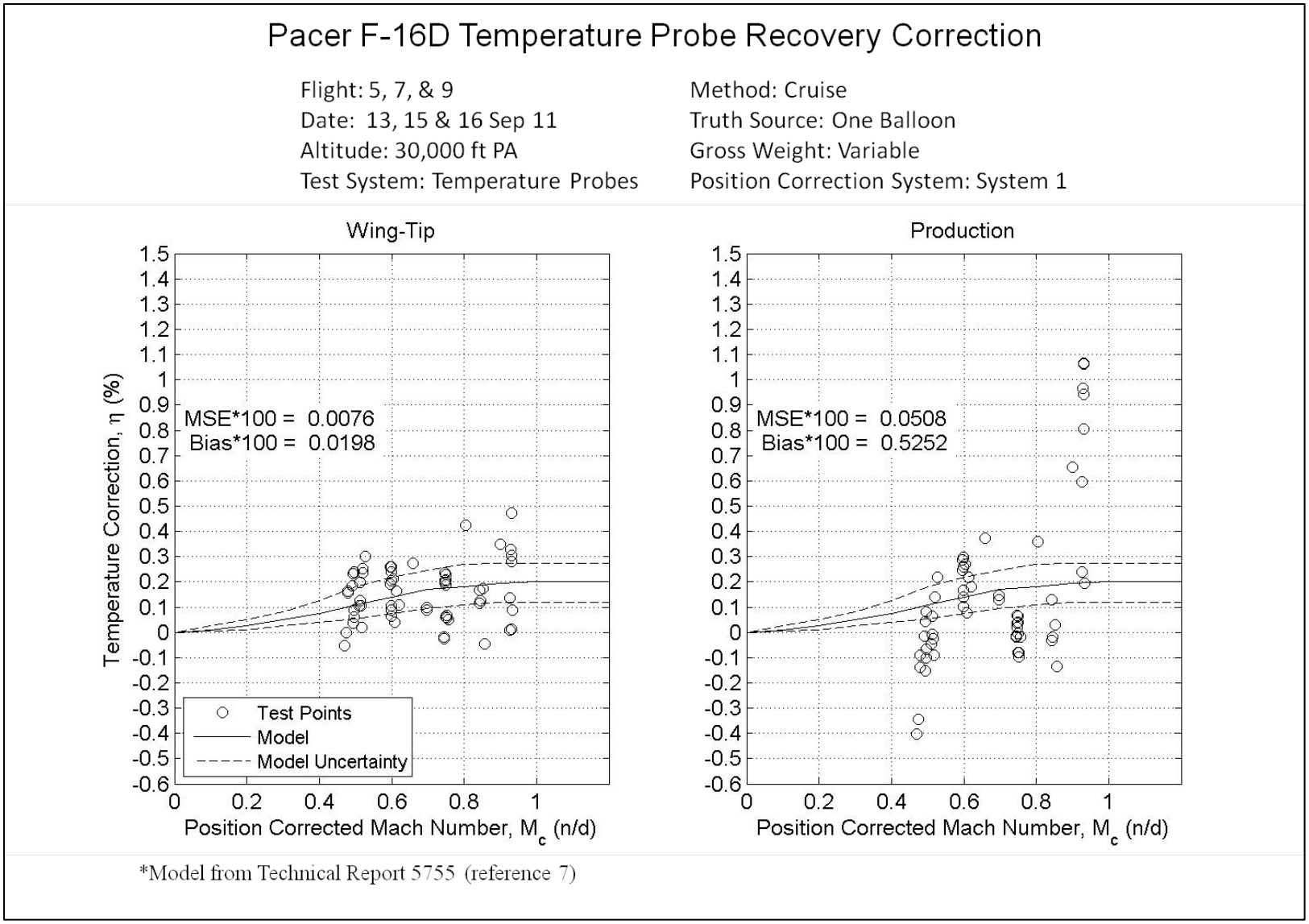

Figure C31 Temperature Recovery Correction – Cruise – 30,000 Feet – One Balloon

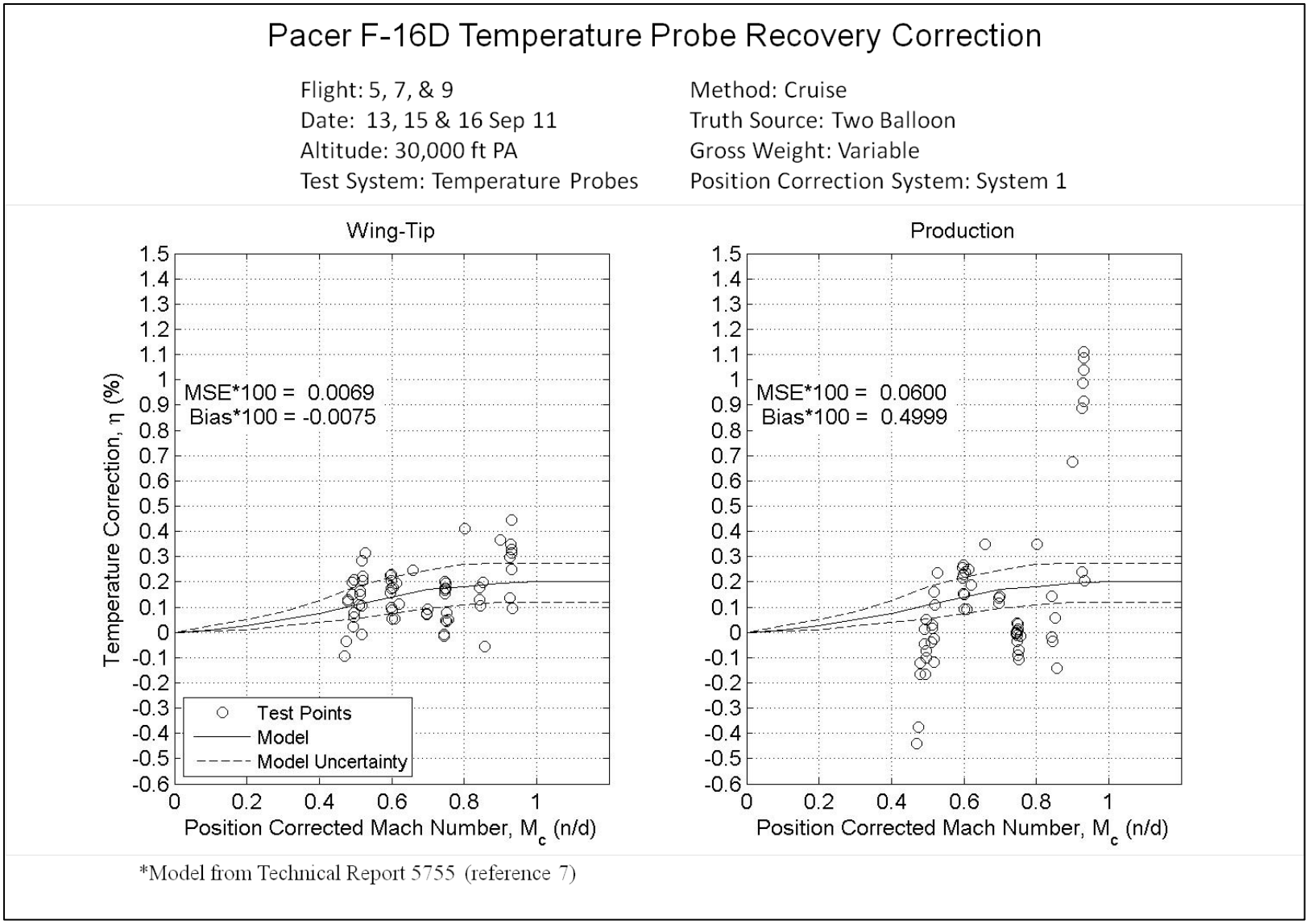

Figure C32 Temperature Recovery Correction – Cruise – 30,000 Feet – Two Balloons

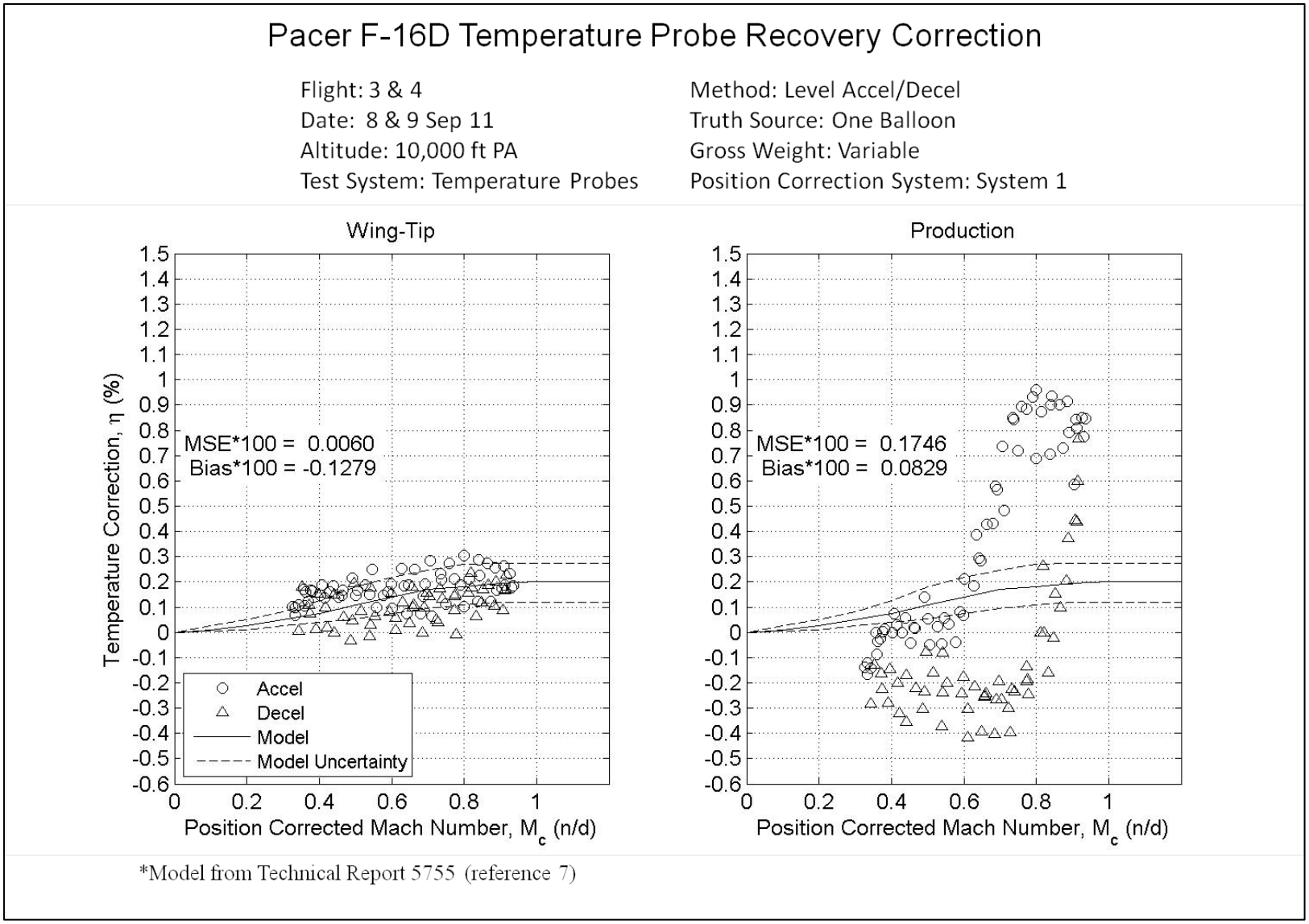

Figure C33 Temperature Recovery Correction – Level Accel/Decel – 10,000 Feet – One Balloon

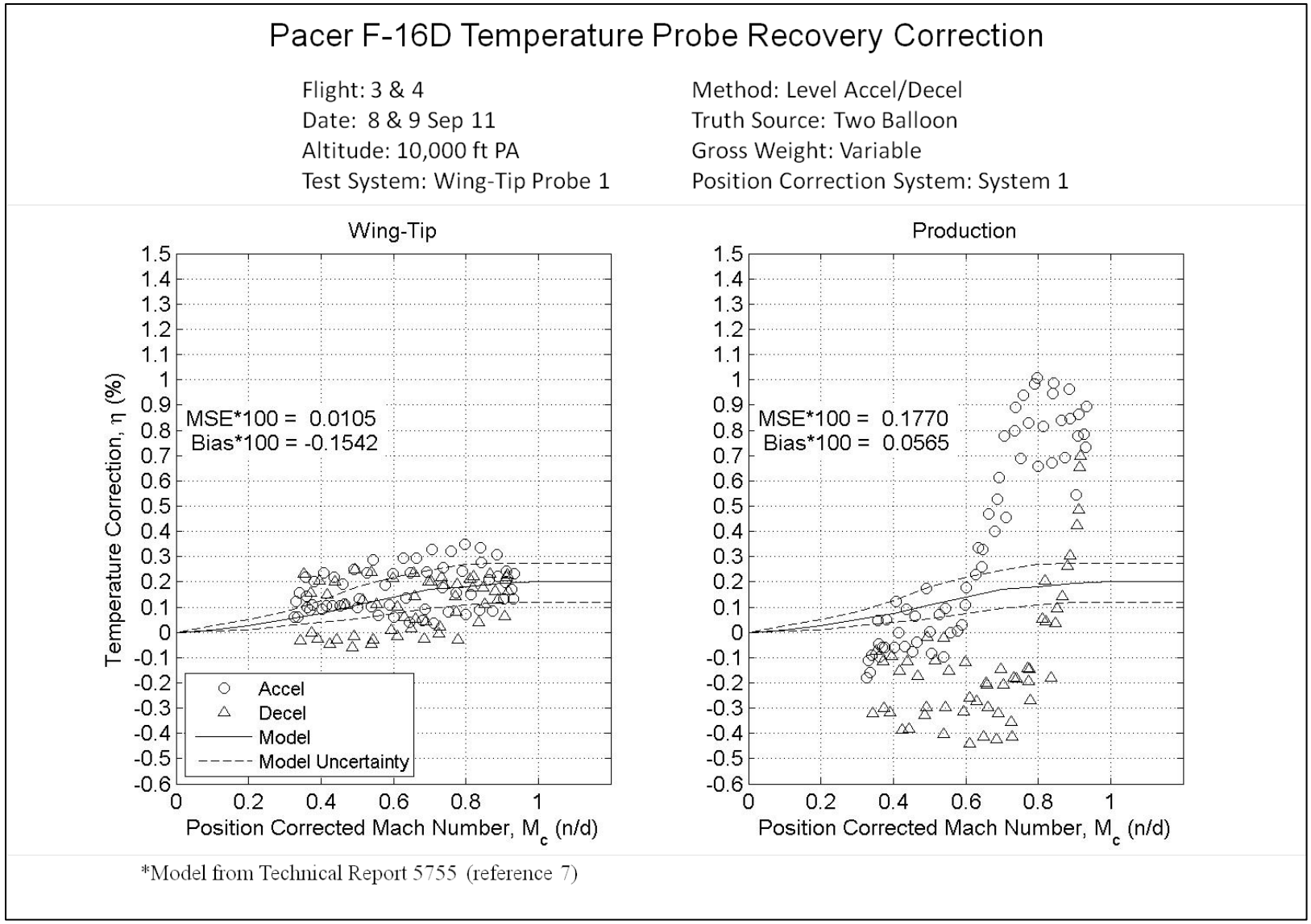

Figure C34 Temperature Recovery Correction – Level Accel/Decel – 10,000 Feet – Two Balloons

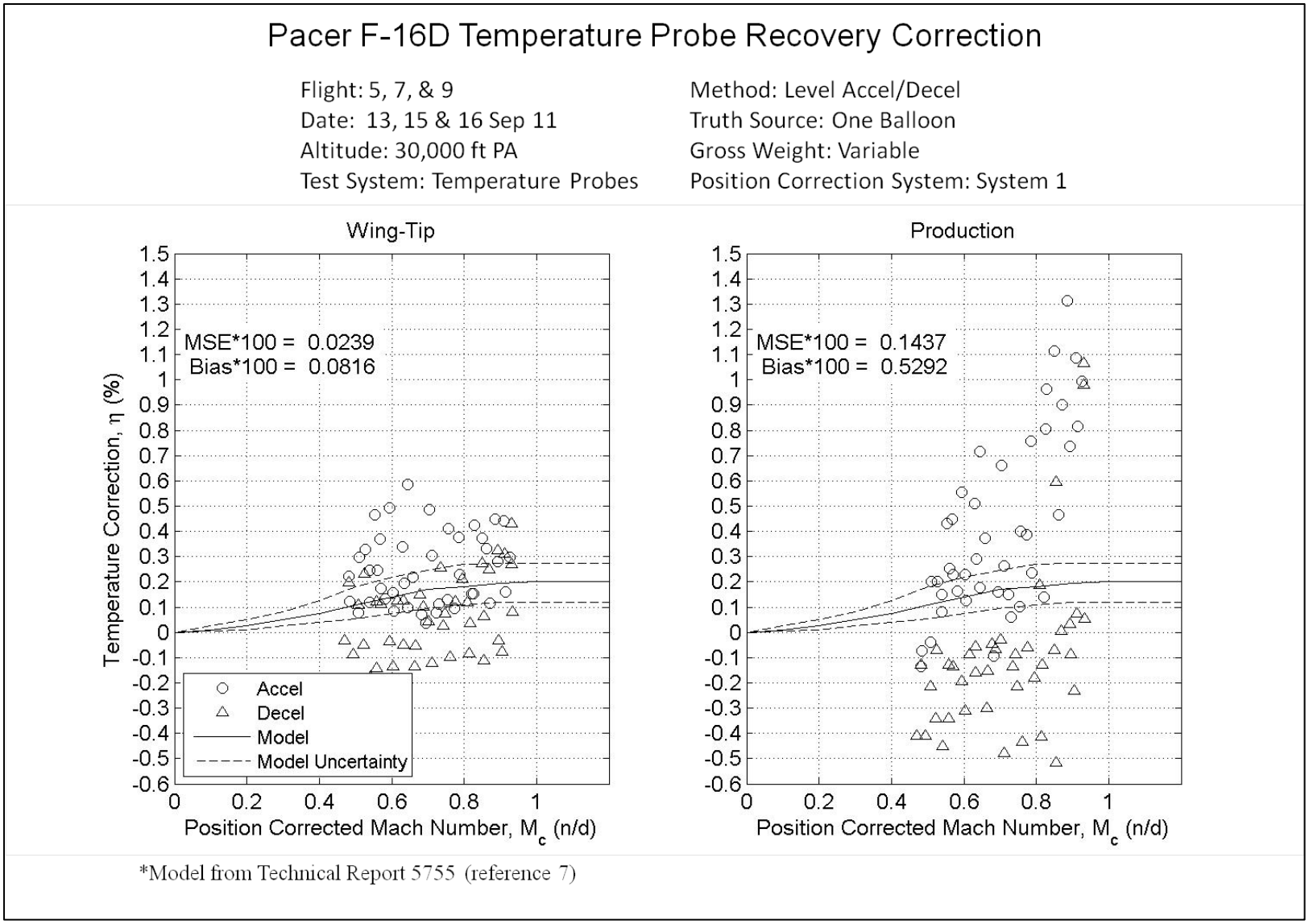

Figure C35 Temperature Recovery Correction – Level Accel/Decel – 30,000 Feet – One Balloon

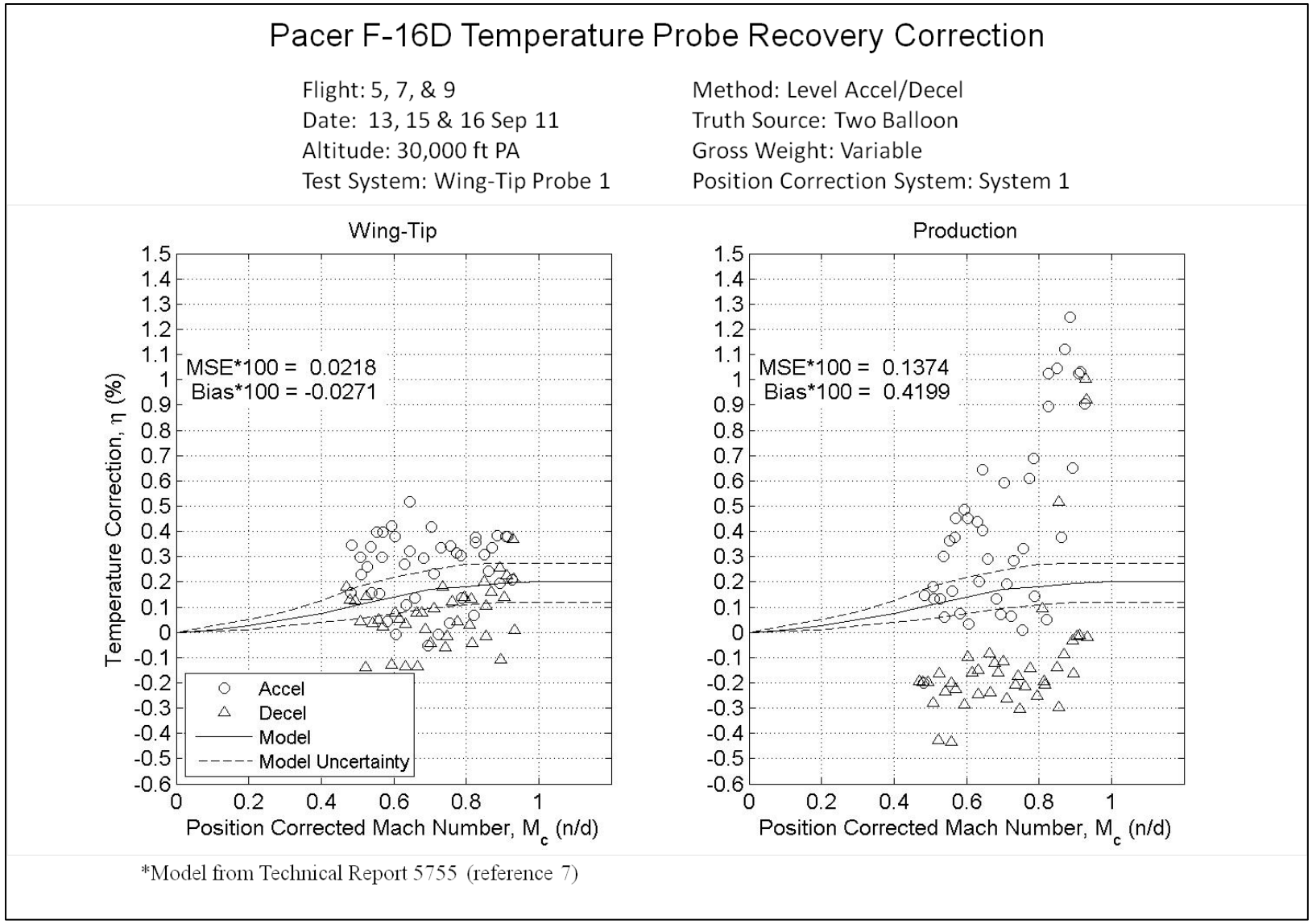

Figure C36 Temperature Recovery Correction – Level Accel/Decel – 30,000 Feet – Two Balloons

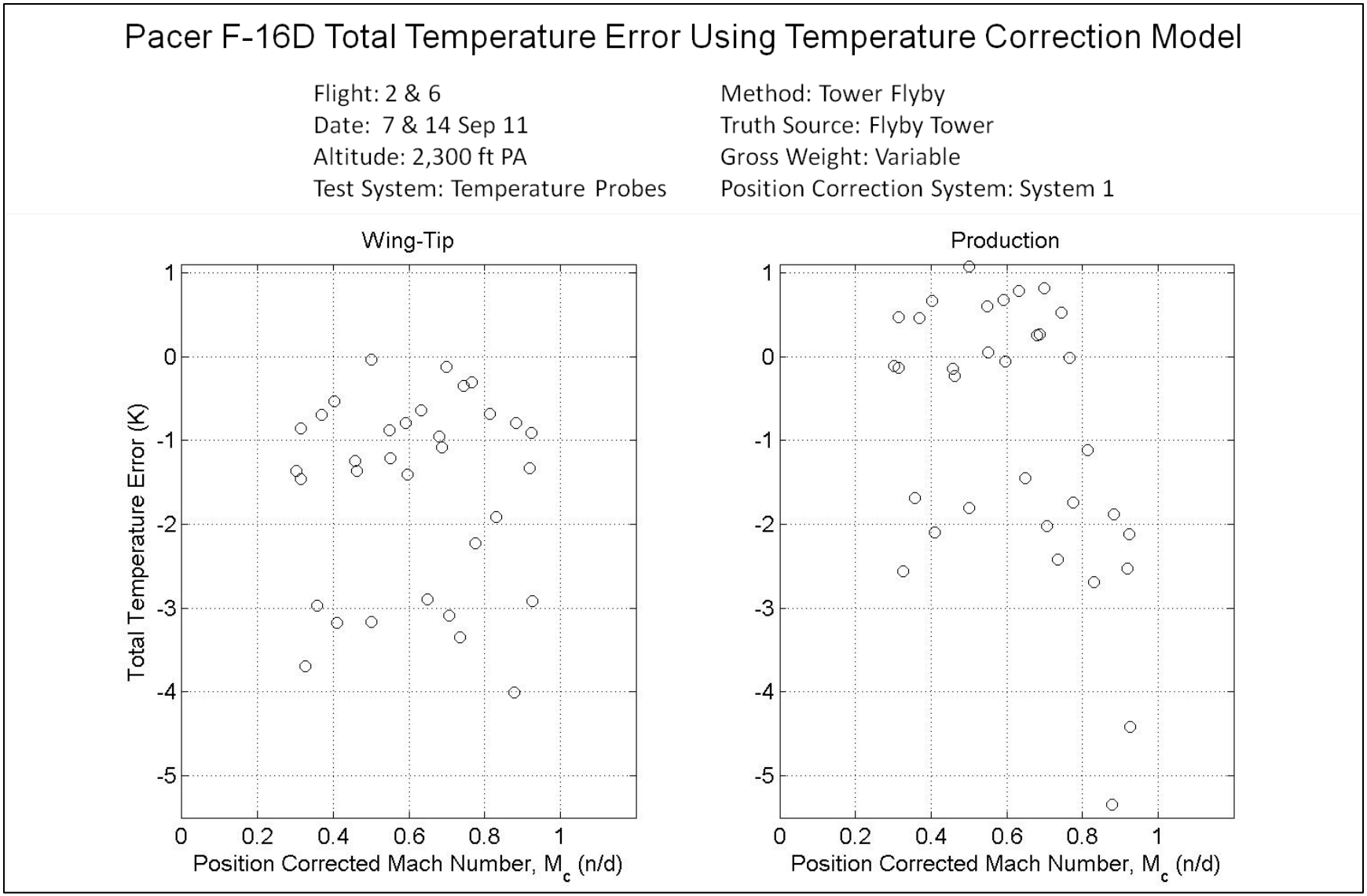

Figure C37 Total Temperature Error – Tower Flyby – Flyby Tower

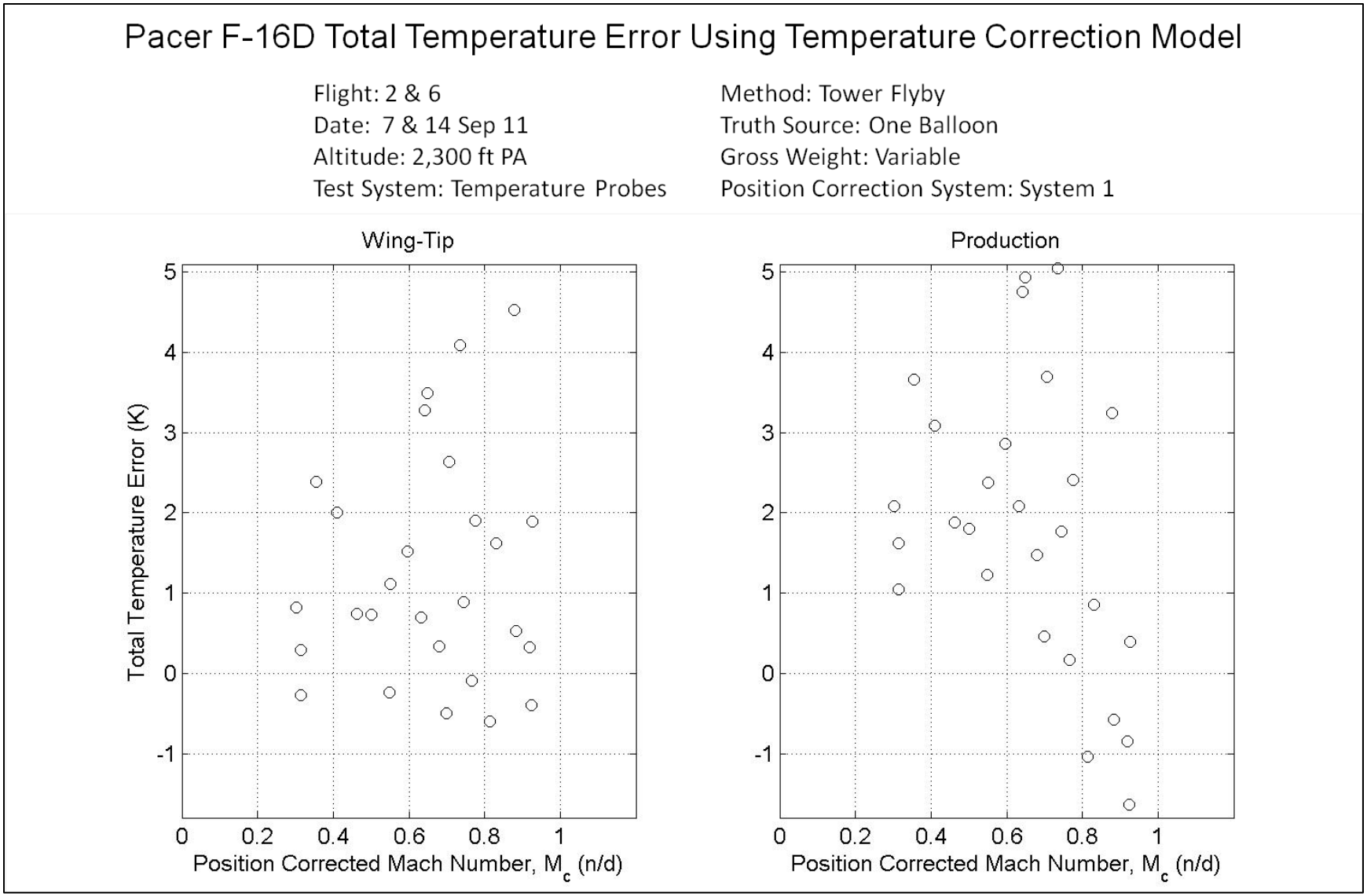

Figure C38 Total Temperature Error – Tower Flyby –One Balloon

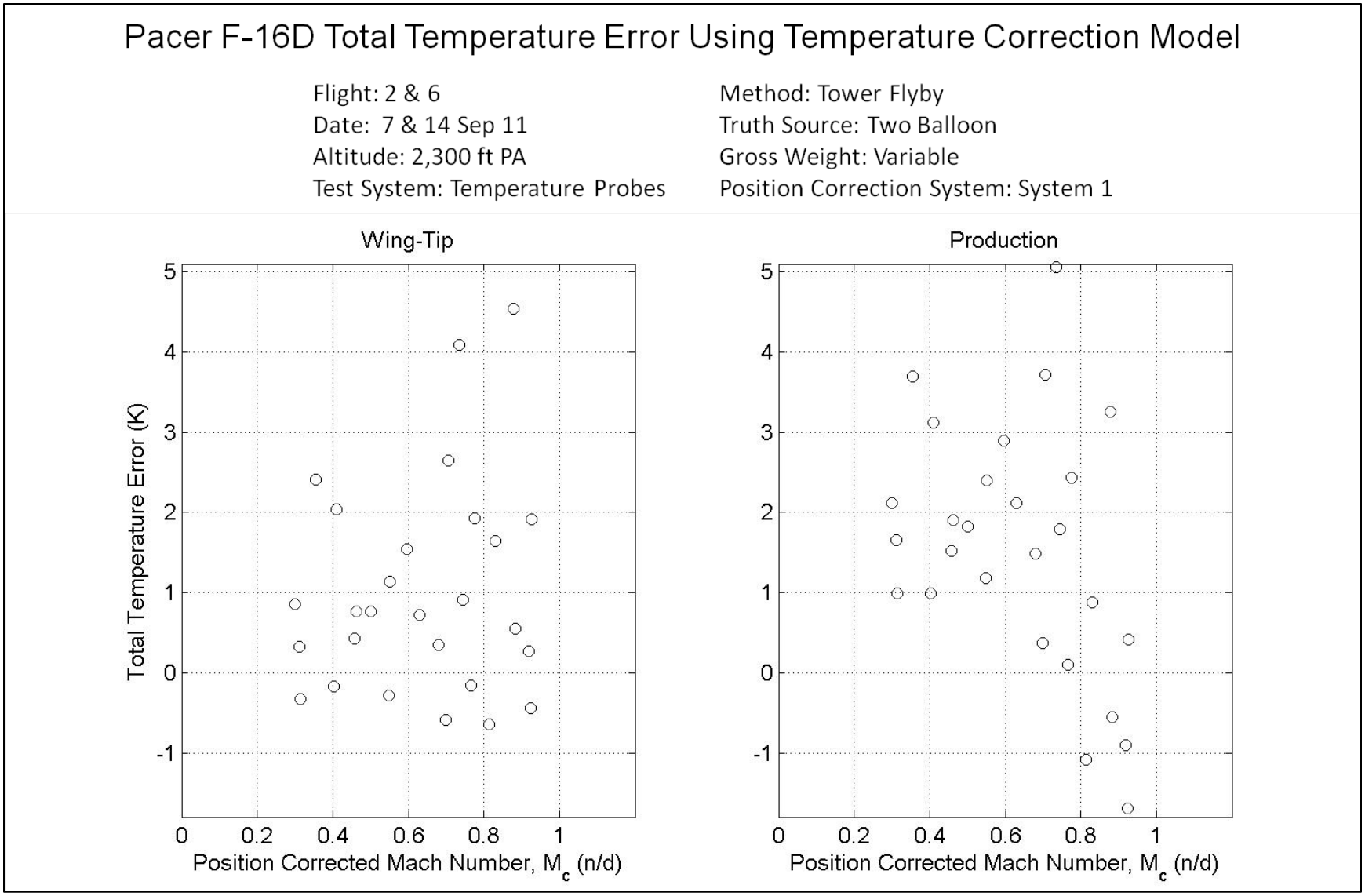

Figure C39 Total Temperature Error – Tower Flyby –Two Balloons

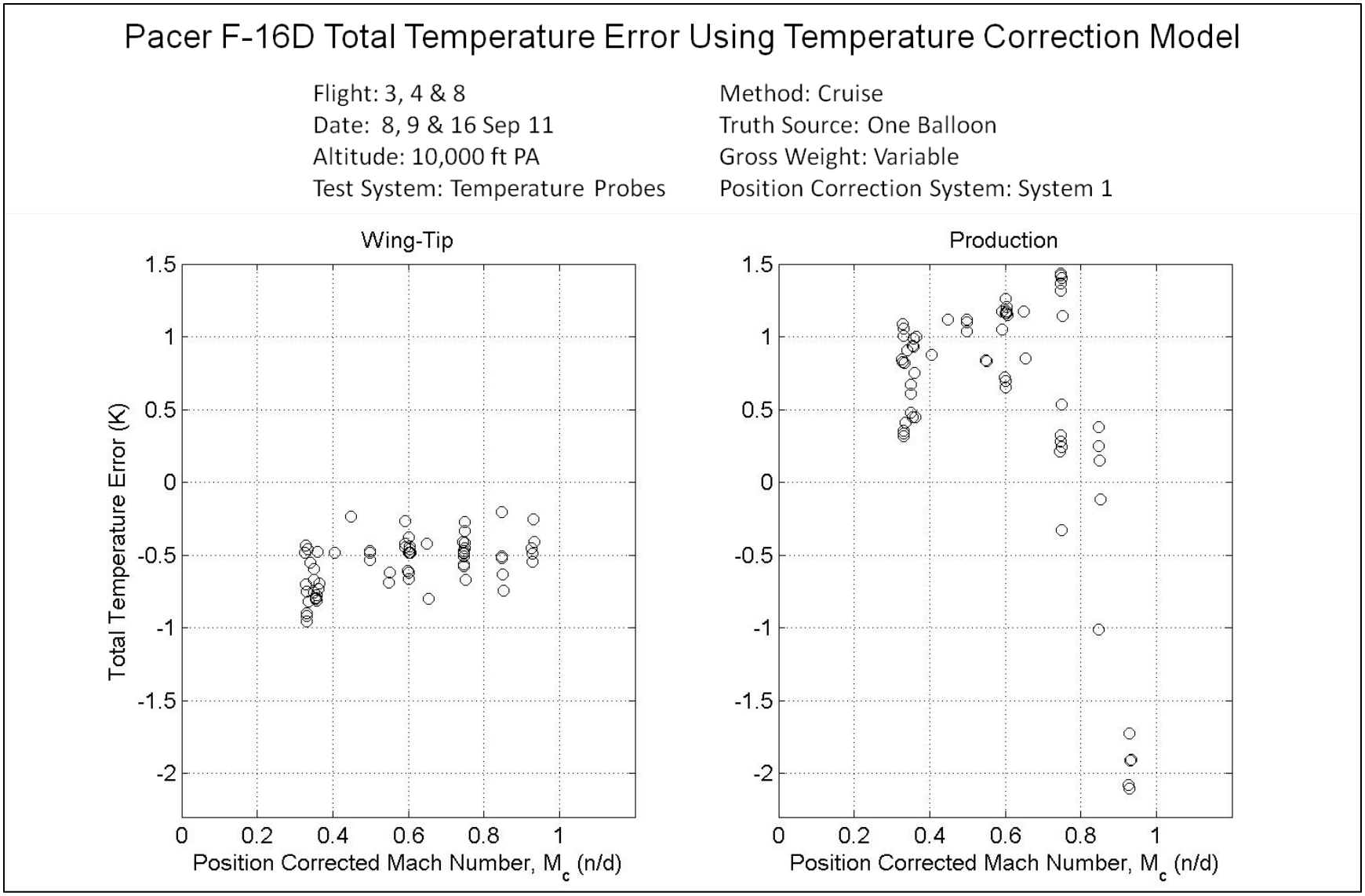

Figure C40 Total Temperature Error – Cruise – 10,000 Feet – One Balloon

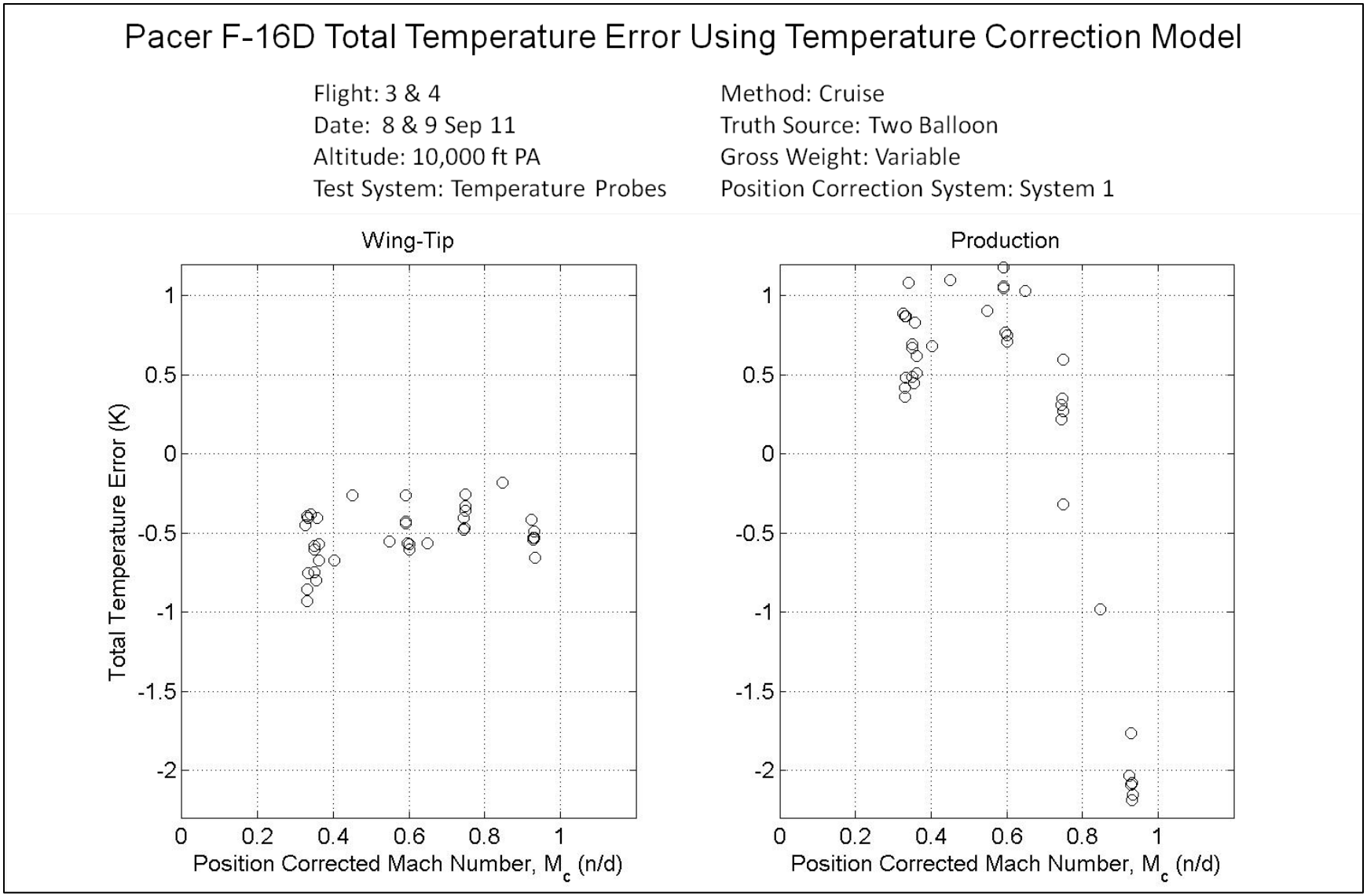

Figure C41 Total Temperature Error – Cruise – 10,000 Feet – Two Balloons

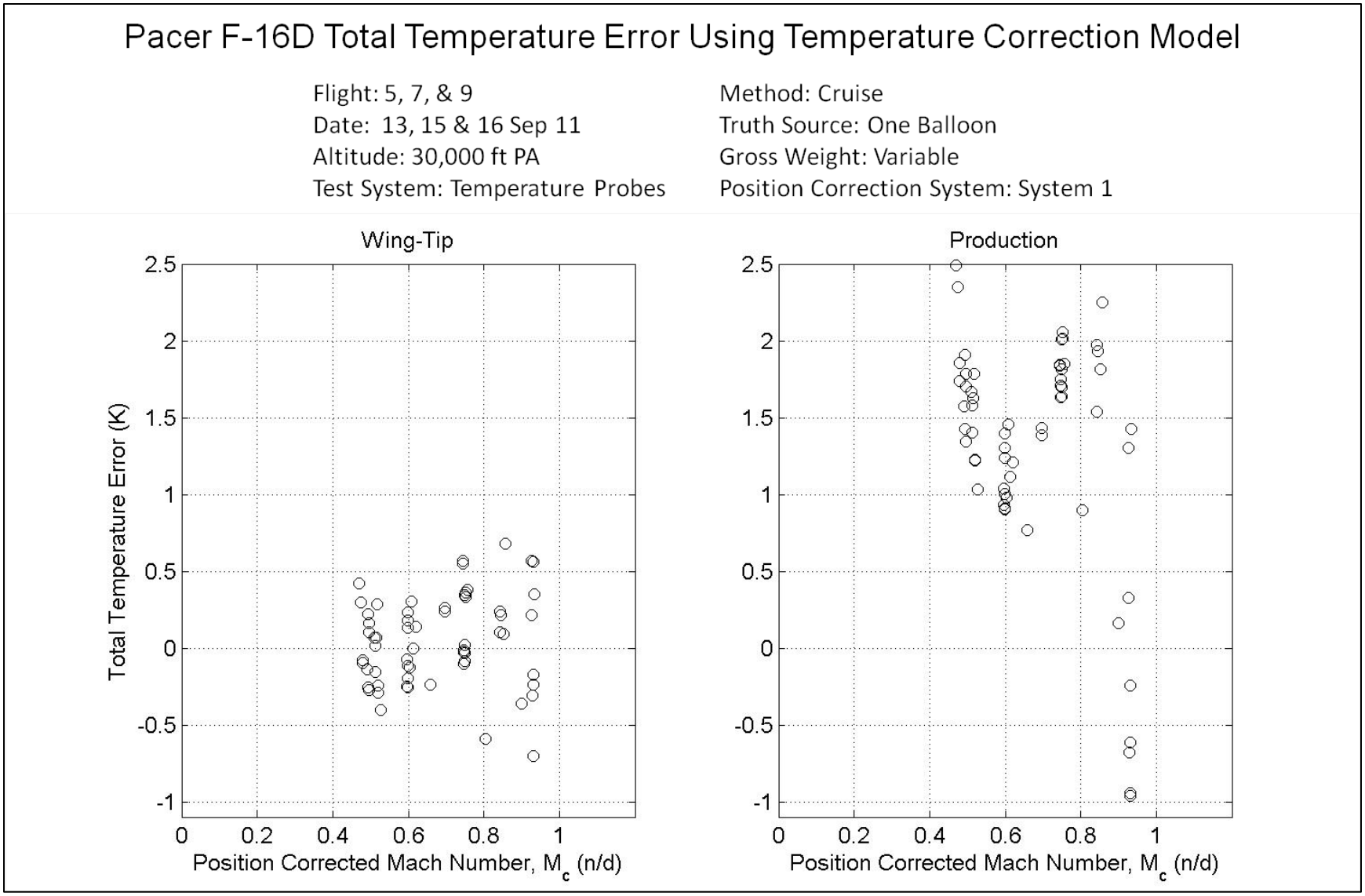

Figure C42 Total Temperature Error – Cruise – 30,000 Feet – One Balloon

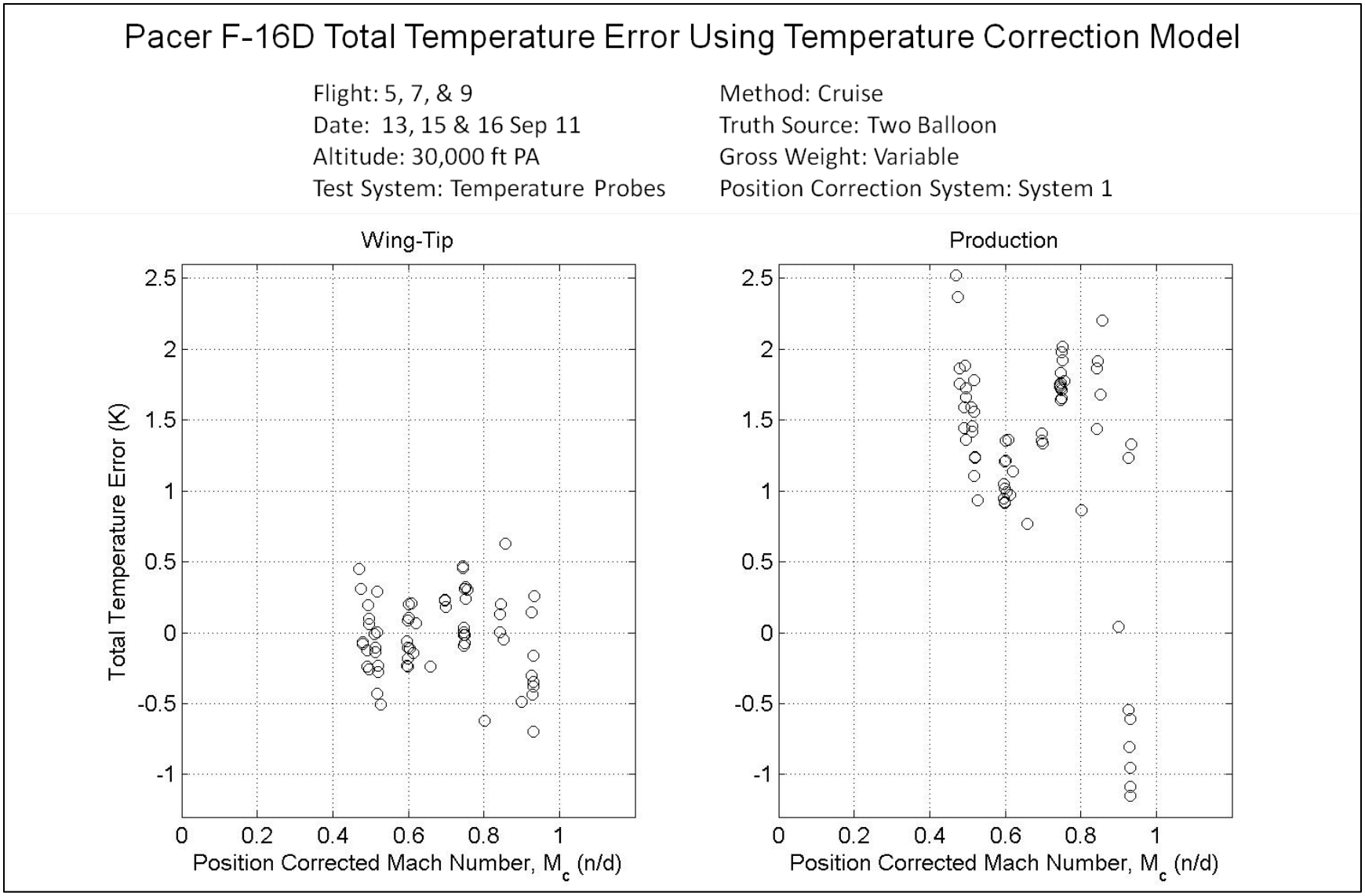

Figure C43 Total Temperature Error – Cruise – 30,000 Feet – Two Balloons

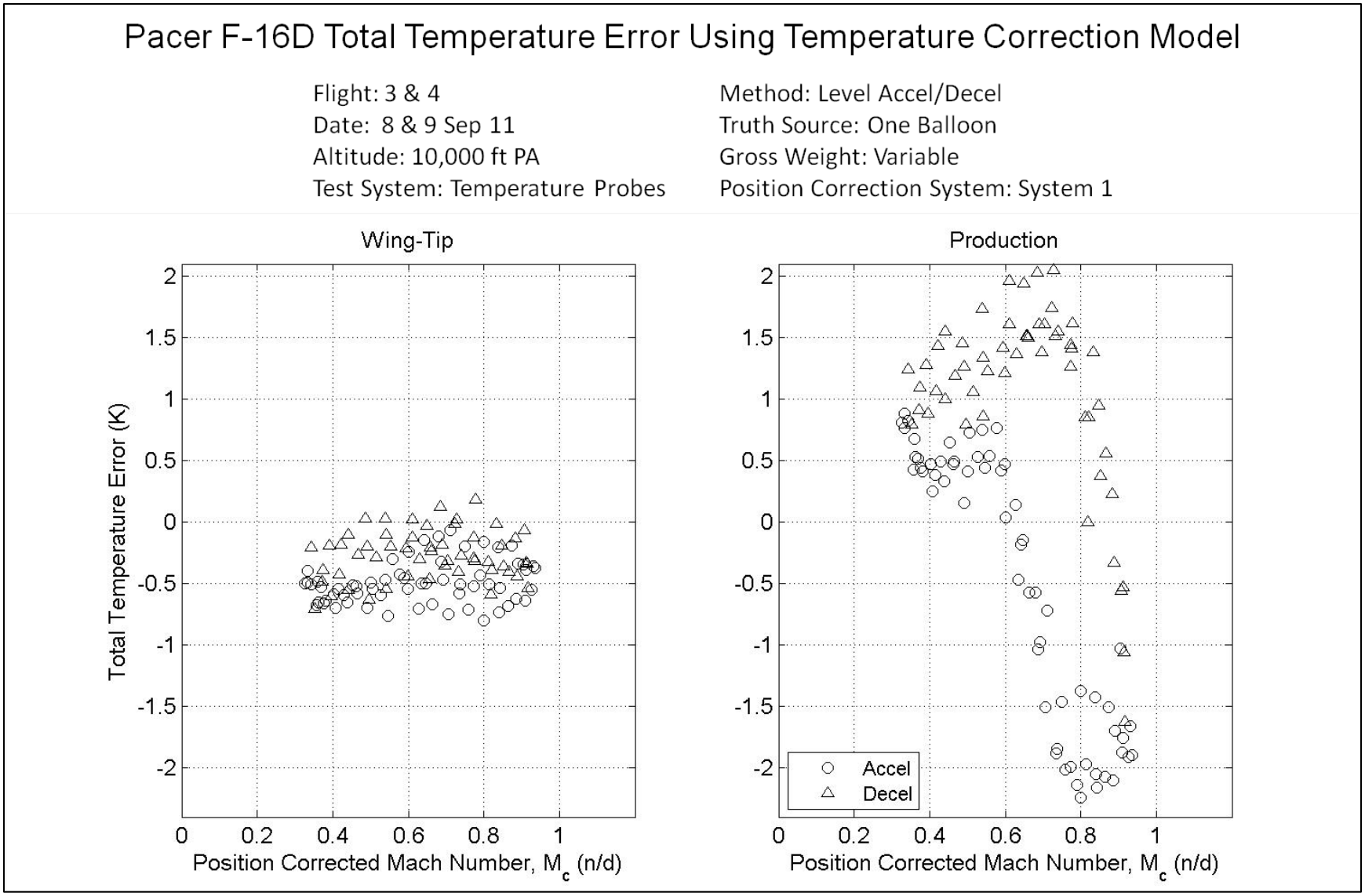

Figure C44 Total Temperature Error – Level Accel/Decel – 10,000 Feet – One Balloon

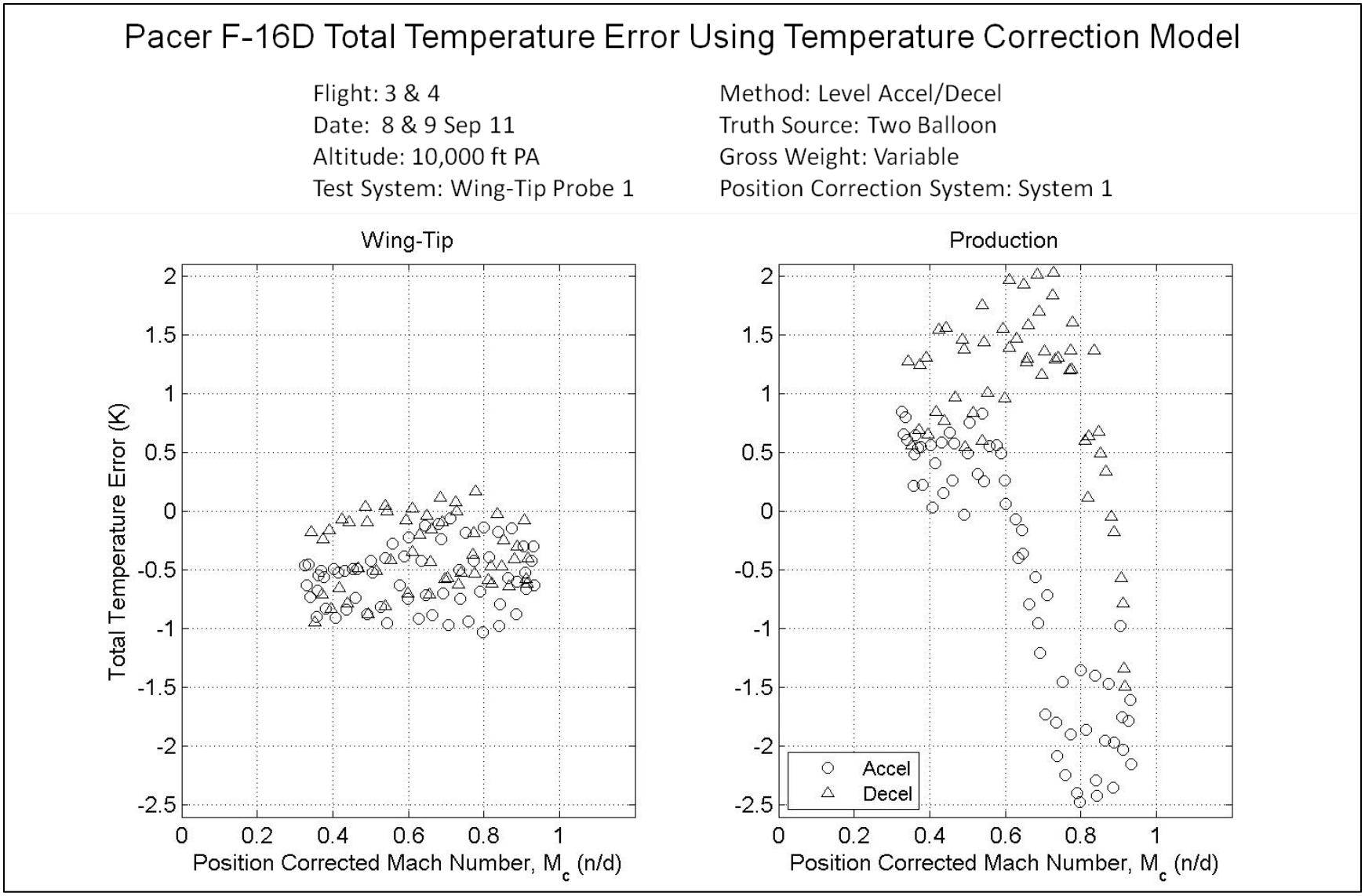

Figure C45 Total Temperature Error – Level Accel/Decel – 10,000 Feet – Two Balloons

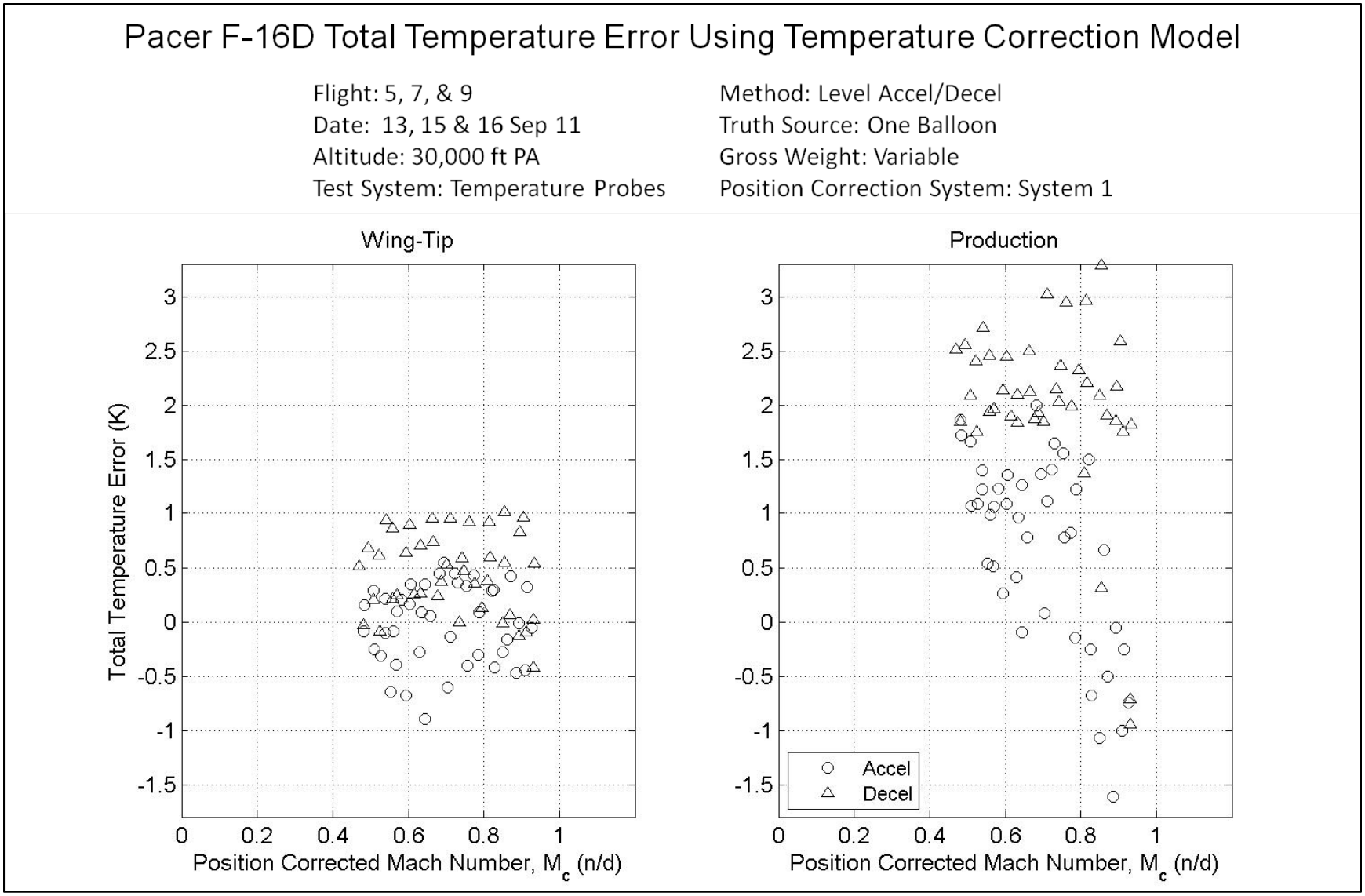

Figure C46 Total Temperature Error – Level Accel/Decel – 30,000 Feet – One Balloon

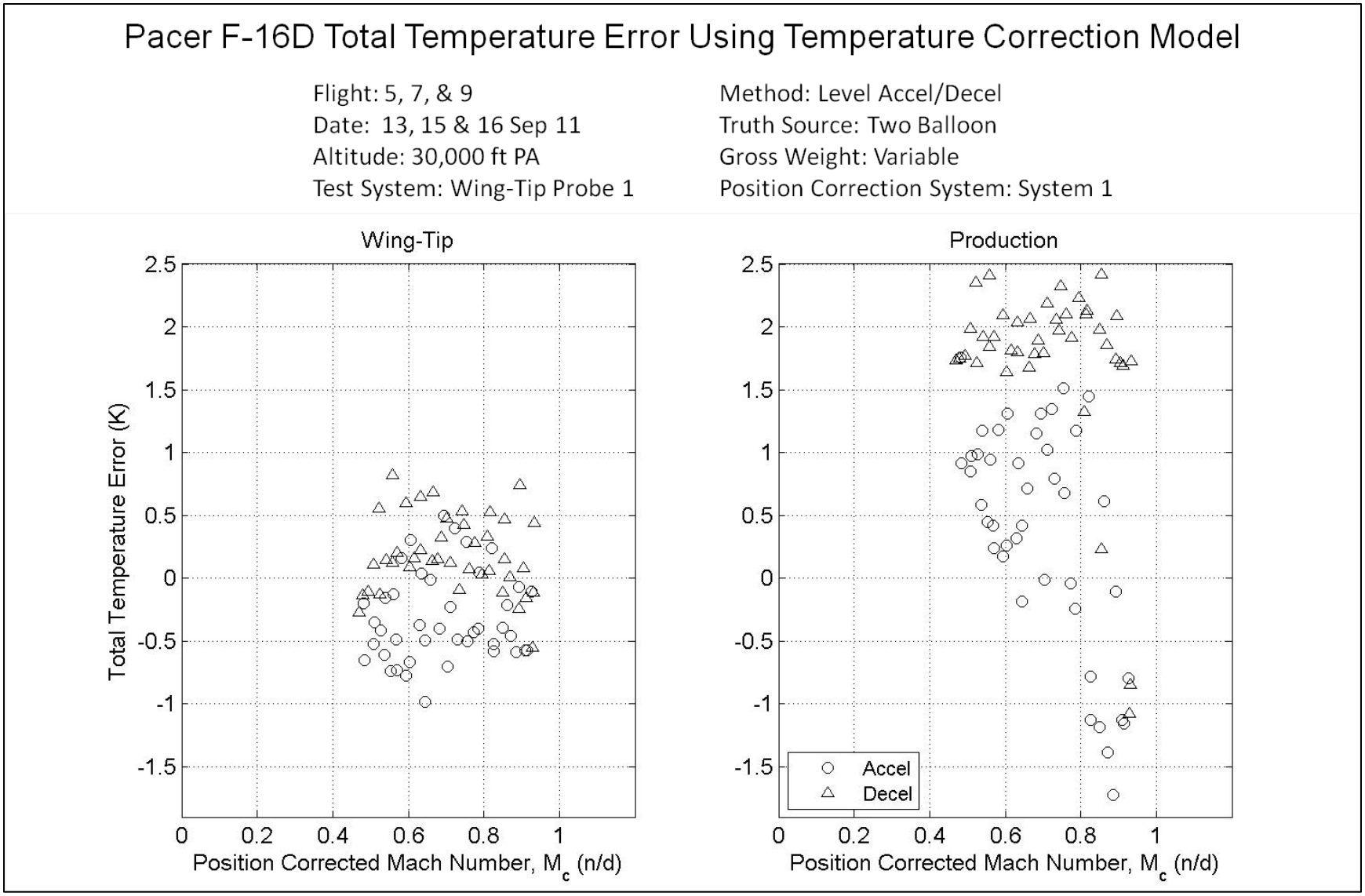

Figure C47 Total Temperature Error – Level Accel/Decel – 30,000 Feet – Two Balloons

Table C3 Position Error Correction Standard Deviations

FTT & Data Reduction	Truth Source	Altitude (feet)	System	Random Uncertainty of $\frac{\Delta P_{pc}}{P_{sic}}$
Cruise	1 balloon	10,000	Noseboom	0.0000232
Cruise	1 balloon	10,000	Cone	0.0000275
Cruise	1 balloon	2,300	Noseboom	0.0000386
Cruise	1 balloon	2,300	Cone	0.0000473
Tower Flyby	Tower flyby	2,300	Noseboom	0.0000191
Tower flyby	Tower flyby	2,300	Cone	0.0000252
Cruise	2 balloon	10,000	Noseboom	0.0000367
Cruise	2 balloon	10,000	Cone	0.0000475
Cruise	Self-Survey	10,000	Noseboom	0.0000189(*)
Cruise	Atmospheric Analysis	10,000	Noseboom	0.0000189(*)
Cruise	1 balloon	30,000	Noseboom	0.0000843
Cruise	1 balloon	30,000	Cone	0.0001086
Cruise	2 balloons	30,000	Noseboom	0.0000995
Cruise	2 balloons	30,000	Cone	0.0001280
LAD	1 balloon	10,000	Noseboom	0.0000036
LAD	1 balloon	10,000	Cone	0.0000043
LAD	1 balloon	30,000	Noseboom	0.0000124
LAD	1 balloon	30,000	Cone	0.0000115

* based on flight number 3 only

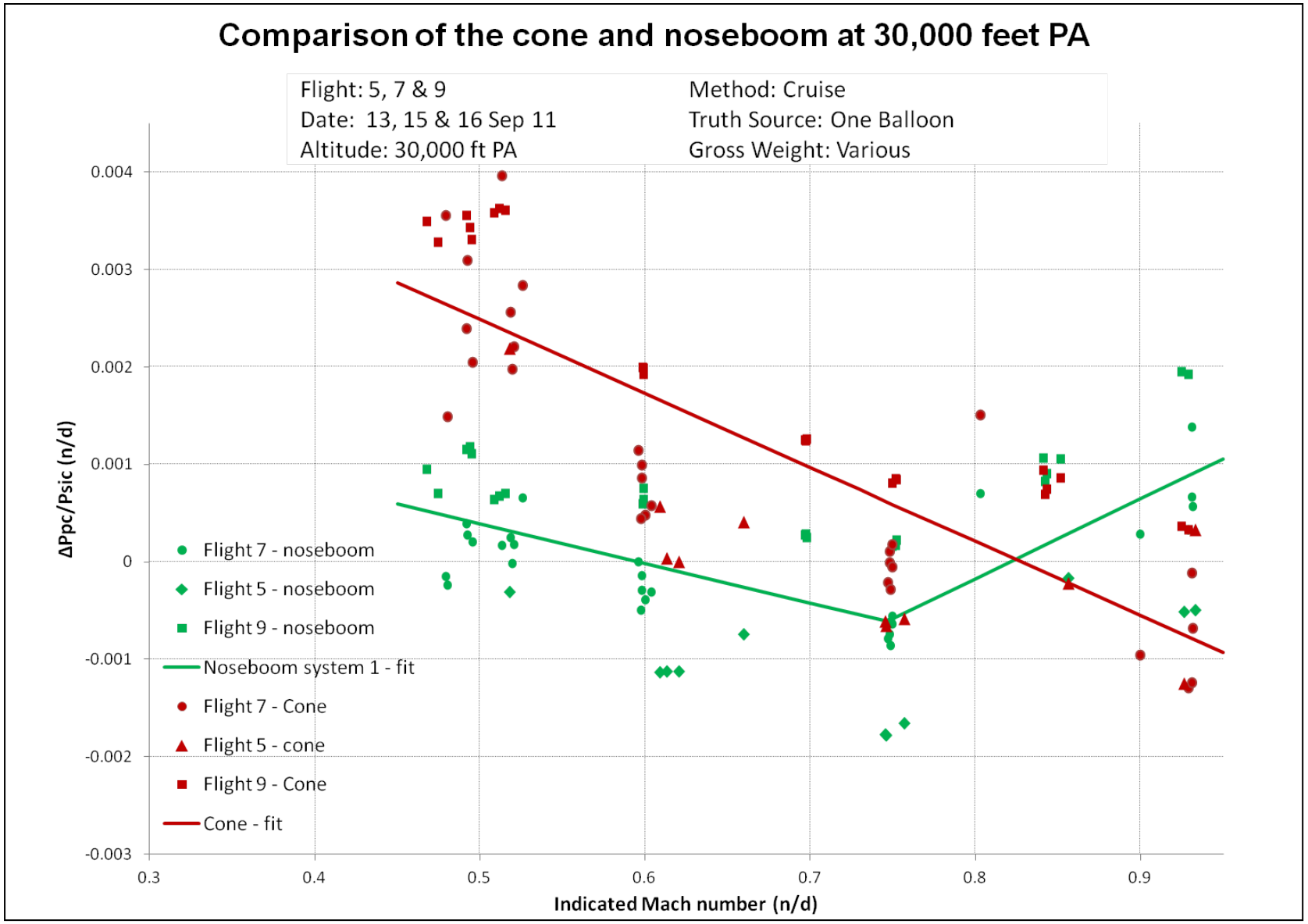

Figure C48 Comparison of the Cone and Noseboom at 30,000 Feet PA

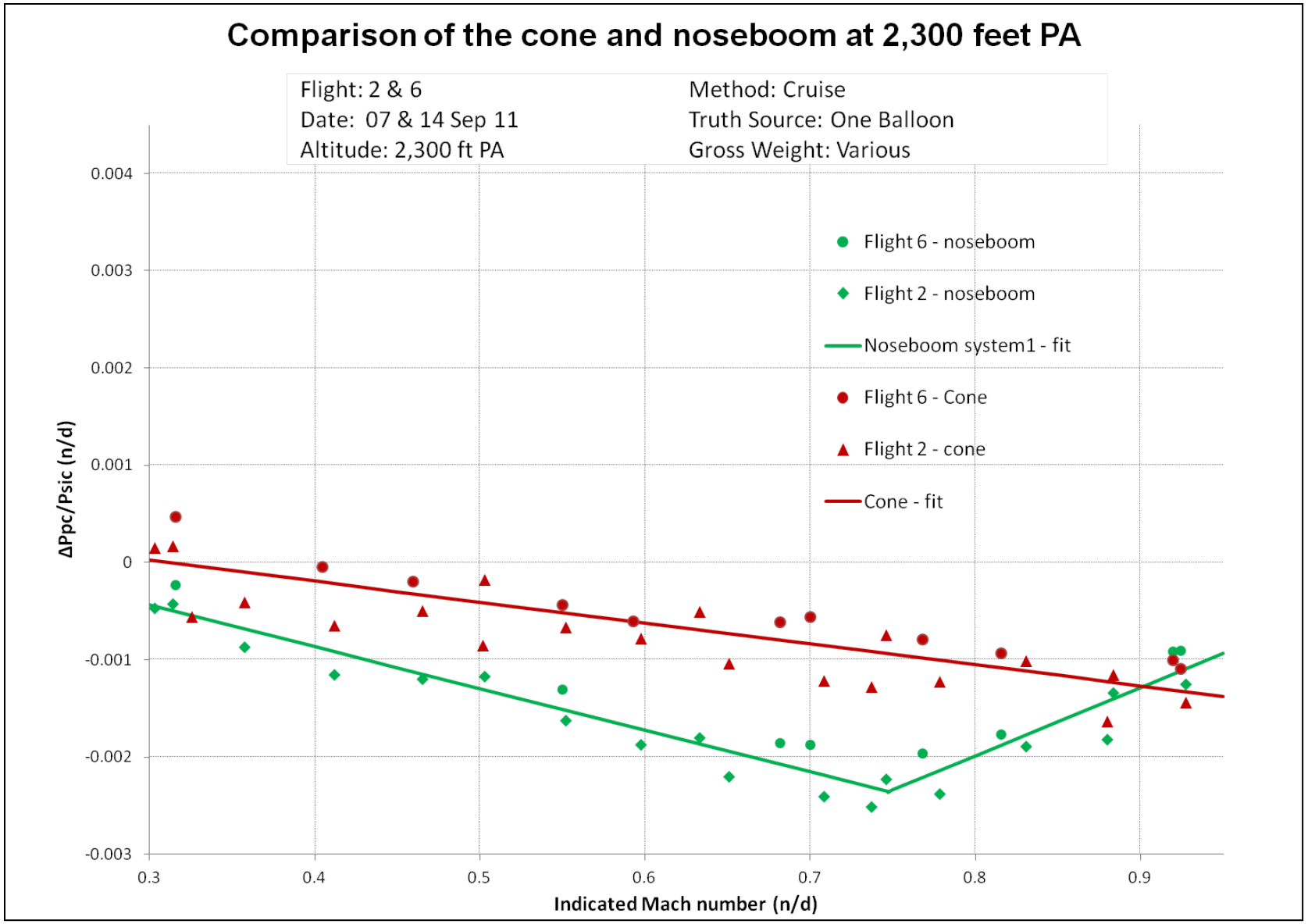

Figure C49 Comparison of the Cone and Noseboom at 2,300 Feet PA

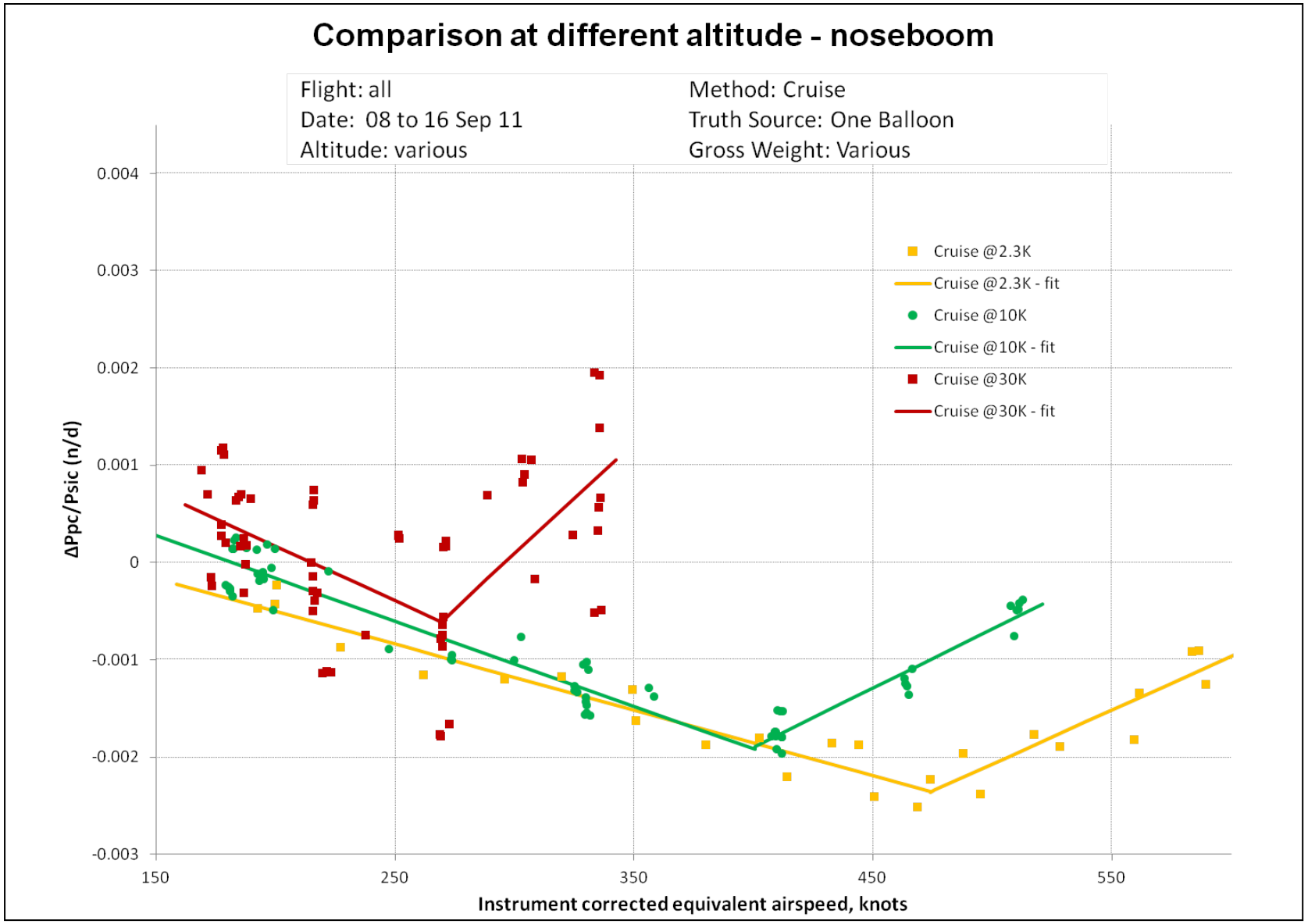

Figure C50 Comparison at Different Altitude - Noseboom

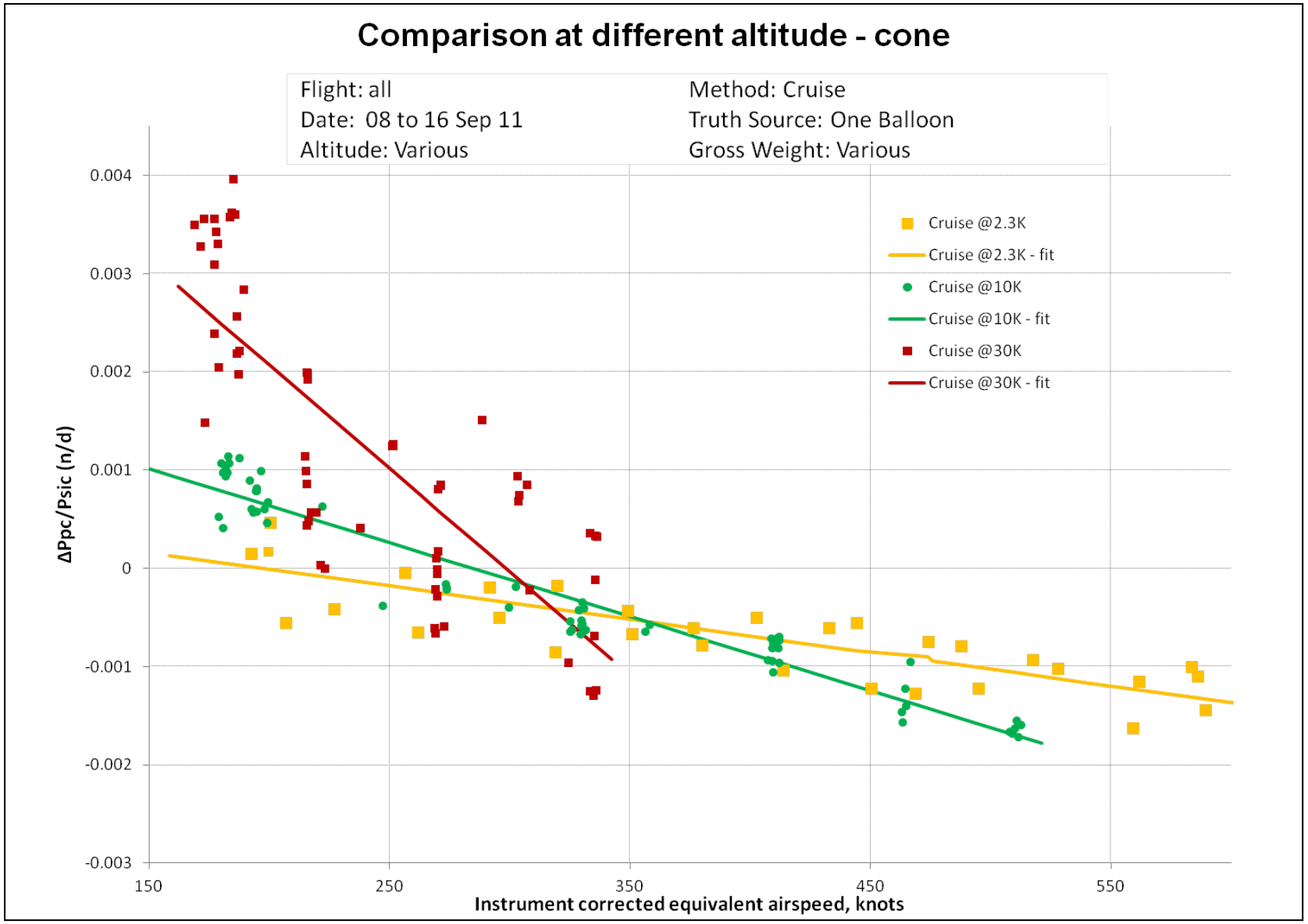

Figure C51 Comparison at Different Altitude - Cone

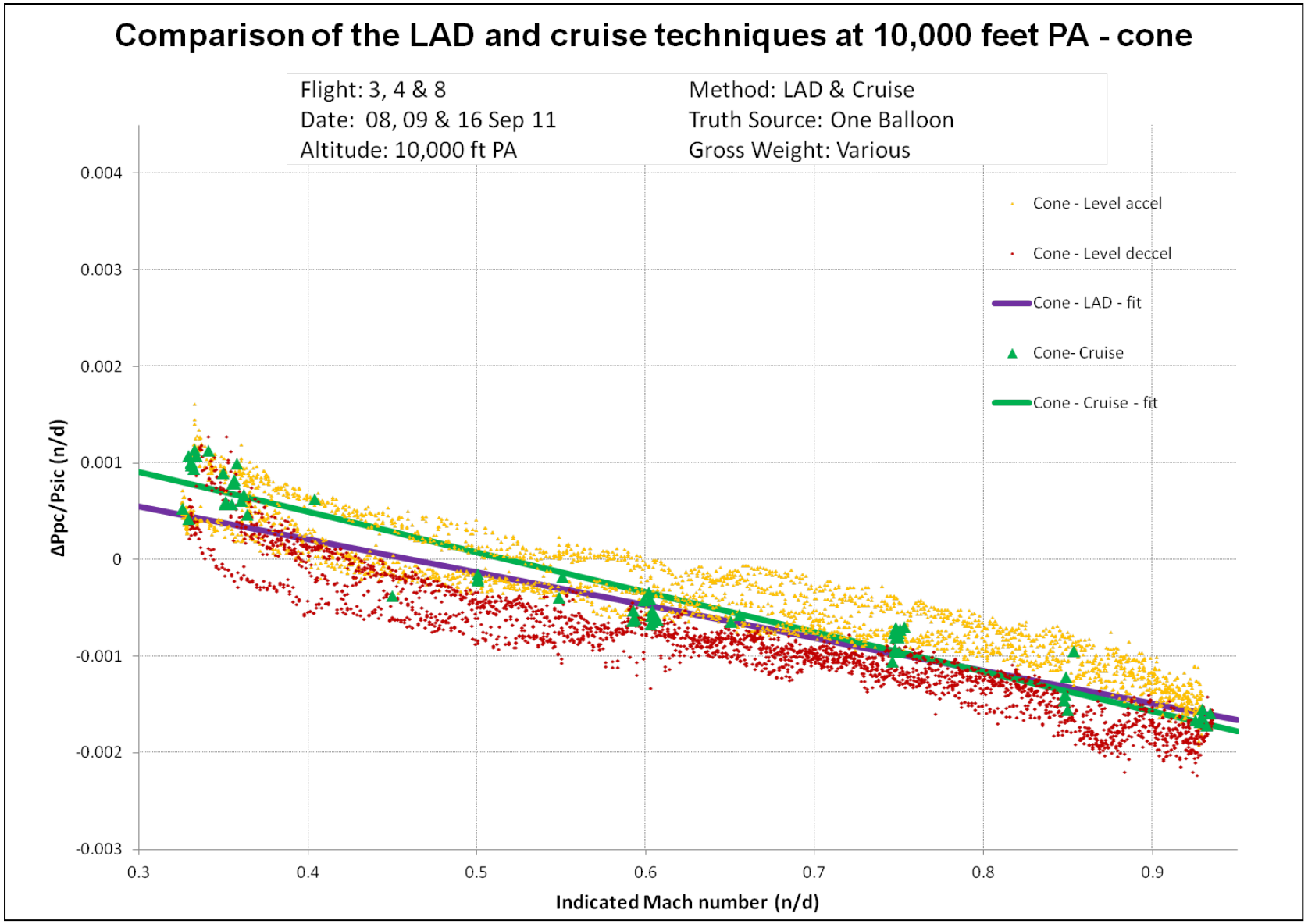

Figure C52 Comparison of the LAD and Cruise Techniques at 10,000 Feet PA - Cone

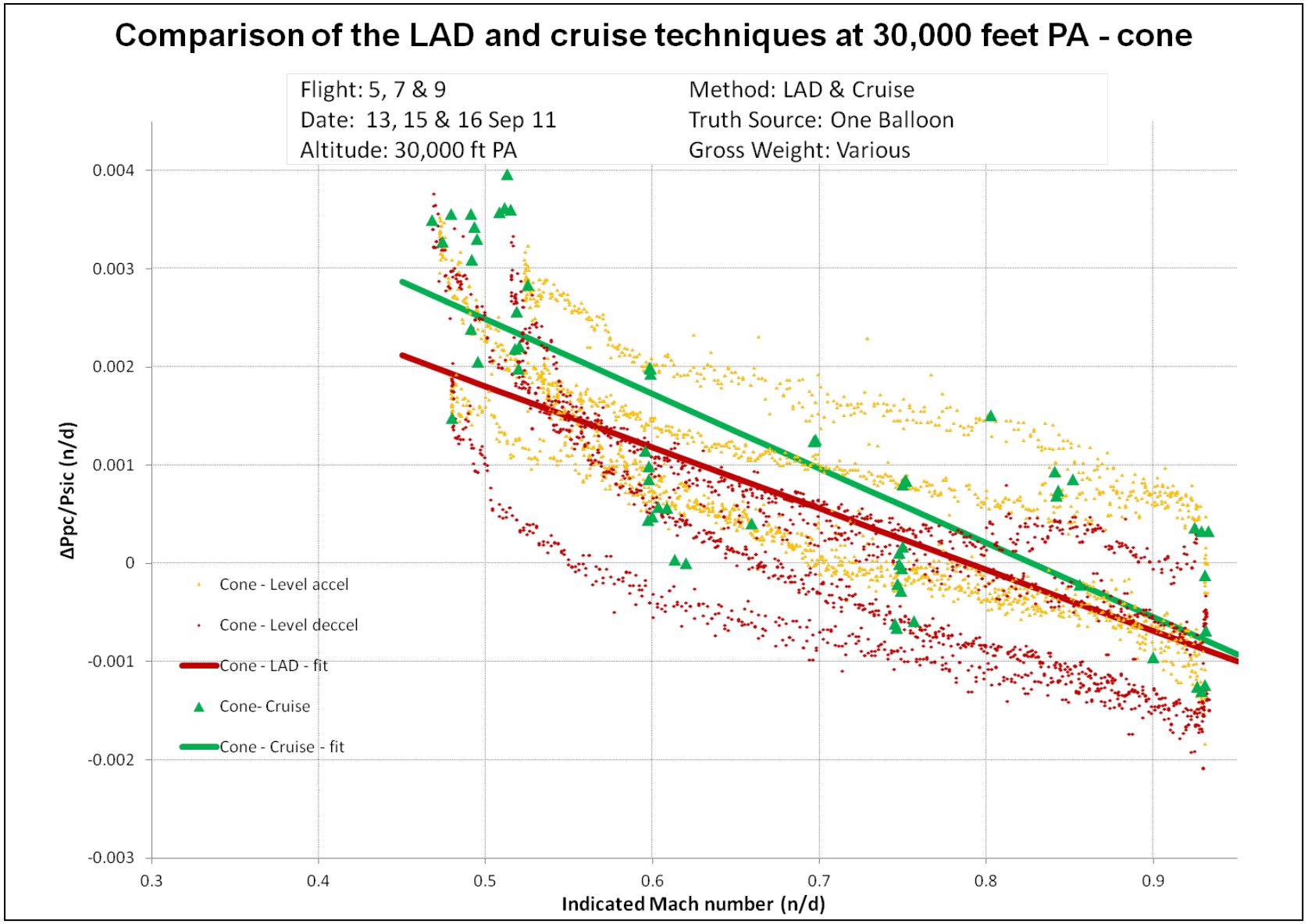

Figure C53 Comparison of the LAD and Cruise Techniques at 10,000 Feet PA - Cone

This page was intentionally left blank.

APPENDIX D – DATA ANALYSIS PROCEDURES

OVERVIEW

Each Pitot-static system (System one and System two) had two Paroscientific Pressure Transducers (a total pressure transducer and a static pressure transducer) that were connected to the flight test Pitot-static noseboom. An additional Paroscientific Pressure Transducer was installed in the vertical tail of the pacer aircraft for use with the trailing cone. The flight test total air temperature probe located on the left wingtip rail (station 1) was used to measure total temperature. The production total air temperature probe was also used. A GPS-Aided Inertial Navigation Reference-Lite (G-Lite) C2B hybrid Global Positioning System (GPS)/Inertial Navigation Unit (INU) system was used to measure and record latitude, longitude, geometric altitude, velocities and Euler angles. An Advanced Range Data System (ARDS) pod, located on the right wing tip (station 9) served as a backup in case the G-Lite system did not work properly. This backup was used for sortie number 7 since the G-Lite data file was empty following the sortie. Weather balloons and/or flyby tower readings were used as a truth source for ambient pressure and temperature.

COMMON VARIABLES

Pressure Transducer Data Analysis:

The indicated total and static pressures (in inches of mercury) that were measured by the pressure transducers were corrected for instrument errors by the transducers themselves, so that the output of the transducers was instrument-corrected pressures:

$$P_{tic} = P_{ti} + \Delta P_{tic} \tag{D1}$$

$$P_{sic} = P_{si} + \Delta P_{sic} \tag{D2}$$

where P_{tic} is the instrument-corrected total pressure, P_{ti} is the indicated total pressure, ΔP_{tic} is the total pressure instrument error correction, P_{sic} is the instrument-corrected static pressure, $P_{si,}$ is the indicated static pressure, and ΔP_{sic} is the static pressure instrument error correction. Appropriate subscripts will be applied to these and following equations that define the source of the variable: *nb* for the first system in the noseboom, *cone* for the trailing cone, and *nb2* for the second system in the noseboom.

The instrument-corrected differential pressure is equal to the difference between the instrument-corrected total and static pressures:

$$q_{cic} = P_{tic} - P_{sic} \tag{D3}$$

Position-Corrected Total Pressure:

The total pressure error $\Delta P_{T,nb}$ was assumed to be equal to zero as it was assumed that errors did not affect the total pressure probe at normal flight angles of attack.

Height Translations:

The indicated or measured values from the pacer aircraft were measured at different geometric heights, depending on the placement of the instrumentation on the aircraft. This geometric height

difference translated to a change in pressure altitude (geometric altitude and pressure altitude were assumed to be the same over a short distance), or ultimately a change in measured pressure. To account for this pressure change due to differences in instrumentation heights, translations were performed so that all the variables in each computation (with the exception of temperature, which has an insignificant temperature change for the height of the translation) would be calculated at the same pressure altitude. The following paragraphs provide all the required height translations for the flight maneuvers, along with additional translations that may be useful if a customer wishes to translate calibration results to different locations.

F-16D PACER

The following figure, figure D1, shows the reference locations for the translations in inches for the F-16D aircraft:

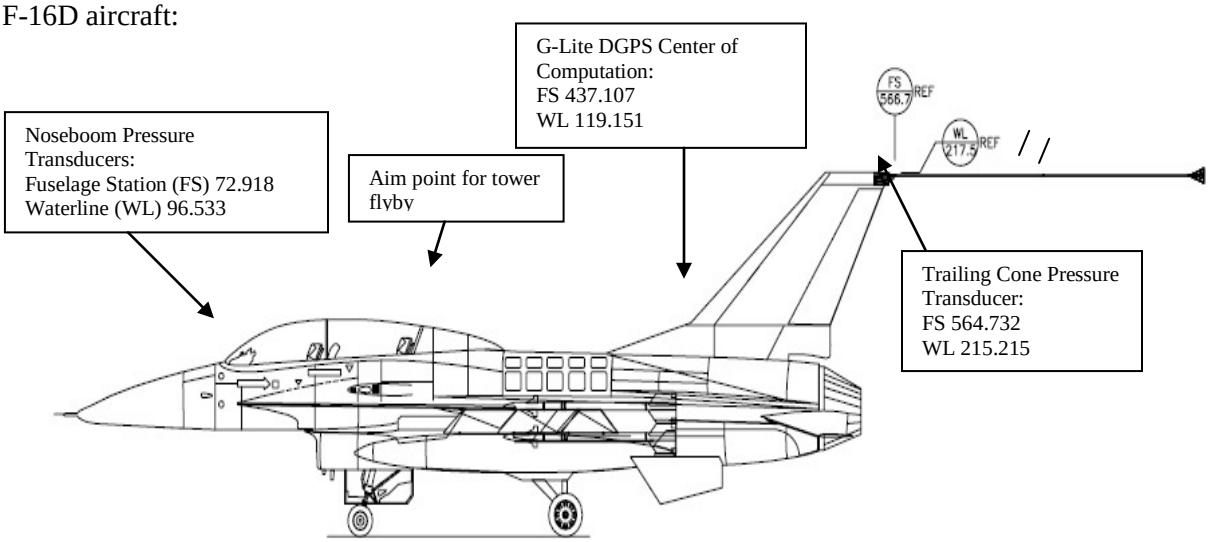

Figure D1 Reference Locations

The translations between two locations were calculated with the following generic equation, with constants being given in inches:

$$\Delta h_{1\ to\ 2} = [(WL_2 - WL_1)\cos\theta_{INS} - (FS_2 - FS_1)\sin\theta_{INS}]/12$$

The translation from the location of the noseboom pressure transducers to the location of the G-Lite DGPS center of computation was calculated with the following equation:

$$\Delta h_{nb\ to\ G-Lite} = \Delta h_{nb2\ to\ G-Lite} = \left[(22.62)\cos\theta_{INS} - (364.19)\sin\theta_{INS}\right]/12 \quad \text{(D4)}$$

The translation from the location of the G-Lite DGPS center of computation to the location of the trailing cone pressure transducer was calculated with the following equation:

$$\Delta h_{G-Lite\ to\ cone} = \left[(96.06)\cos\theta_{INS} - (127.62)\sin\theta_{INS}\right]/12 \quad \text{(D5)}$$

The translation from the location of the noseboom pressure transducers to the location of the trailing cone pressure transducer was calculated with the following equation:

$$\Delta h_{nb\ to\ cone} = \Delta h_{nb2\ to\ cone} = \left[(118.62)\cos\theta_{INS} - (491.81)\sin\theta_{INS}\right]/12 \quad \text{(D6)}$$

TOTAL AIR TEMPERATURE PROBE RECOVERY FACTOR AND TEMPERATURE CORRECTION

Comparison of the LAU-129 temperature probe and the production temperature probe was made by collecting data from both probes with all combinations of methods and truth sources listed in table D1. Methods used to determine calibration data were tower flyby, stabilized cruise, and LAD. The truth sources used were flyby tower ambient temperature readings, one balloon atmospheric data, and multiple balloon atmospheric data. Two sets of calibration parameters were determined; the temperature recovery factor and bias, and the temperature recovery correction and bias.

Table D1 Temperature Calibration Data Analysis Combinations

Calibration Technique	Truth Source
Tower Flyby Stabilized Cruise	Measured Ambient Temperature at Flyby Tower
Tower Flyby Stabilized Cruise	One Balloon Atmospheric Data
Tower Flyby Stabilized Cruise	Multiple Balloon Atmospheric Model
Stabilized Cruise	One Balloon Atmospheric Data
Stabilized Cruise	Multiple Balloon Atmospheric Model
Level Acceleration/Deceleration	One Balloon Atmospheric Data
Level Acceleration/Deceleration	Multiple Balloon Atmospheric Model

The required data from each data point were measured total temperature from each temperature probe, the position corrected Mach number, and the ambient temperature from a truth source. The position-corrected Mach number was derived from the static pressure correction algorithms for that maneuver. For repeatability, tower flybys were flown on two different days to see if test days affected the results and LADs were flown at two aircraft weight categories (light and heavy) to see if weight affected the results. Detailed flight conditions and dates can be found in appendix A.

In conjunction with the flyby tower theodolite grid readings, the ambient temperature at the test aircraft's transducer altitude was determined using the following equation:

$$T_a = T_{S,ZGL} - 0.0019812\Delta h_{ZGL\ to\ AC} \quad \text{(D7)}$$

Truth source ambient temperature (T_a), in Kelvin, at the aircraft was calculated by taking the measured temperature at the flyby tower zero grid line (ZGL) altitude ($T_{S,ZGL}$), in feet, and subtracting the temperature decrease seen in standard atmosphere for the difference in height from the aircraft to the tower ZGL ($\Delta h_{ZGL\ to\ AC}$), in feet. This equation did not take into account terrestrial heating which could be larger than the applied correction.

The second truth source was the one balloon atmospheric data. The Edwards AFB weather balloon data were used. The weather balloon provided ambient temperatures at different geometric altitudes as it climbed up the atmosphere. To determine the ambient temperature at the test point, the temperature at the corresponding altitude from the balloon data was used. A linear interpolation was used to determine the ambient temperature at intermediate altitudes.

The last truth source was the multiple balloon atmospheric model. This method was similar to the one balloon method since at each data point, either the Edwards AFB or the NASA balloon was chosen as the truth source. The difference from the single balloon analysis was that the ground distance of the aircraft from each balloon launch location was determined and the balloon with the smaller distance was used as the truth source. The distances were calculated from geographic coordinates as follows:

$$d_{a,b} = 60\sqrt{(latitude_b - latitude_a)^2 + (longitude_b - longitude_a)cos(latitude_a)^2} \quad \text{(D8)}$$

The distance from a to b ($d_{a,b}$) is determined using the standard distance formula with the appropriate conversion of the geographic coordinates to nautical miles (nm). Latitudinal distance was 60 nm/deg and longitudinal distance was 60 nm/deg times the cosine of the center latitude.

Prior to determining the model fit the total temperature from the production probe was determined. The DAS only recorded CADC-derived ambient temperature data from the production temperature probe and the measured total temperature value was not available. To determine the measured total temperature the following equations were used, which were documented in the *Technical Exhibit*, ASD/ENAI-81-6G (reference 9):

$$T_t = T_a\left(1 + 0.2M_{c,CADC}^2\right) \quad \text{(D9)}$$

$$T_{m,prod} = (1 - \eta_{CADC})(T_t + 0.55555) \quad \text{(D10)}$$

The CADC uses its own Mach number ($M_{c,CADC}$) and the manufacturer provided temperature recovery correction model (η_{CADC}). The model and the Mach number were available to derive the measured total temperature from the production probe ($T_{m,prod}$). The self-heating error was taken into account in equation D10 for the production probe so the measured temperature was equal to the recovery temperature. The self-heating error of the wing-tip temperature probe was assumed to be negligible and the measured temperature equaled the recovery temperature (T_r). This assumption was used due to the inability to calculate actual self-heating errors for the test probe.

The wing-tip temperature probe had two sensor elements. Plots were only made for one sensor element. Results for the other element are available in appendix C.

The first of the two calibration parameters was the temperature recovery factor and the related bias. Temperature recovery factor (K_R) was defined as the difference in recovery temperature (T_r) and the static temperature (T_S) divided by the difference in total temperature (T_t) andT_S.

$$K_R = \frac{T_r - T_S}{T_t - T_S} \quad \text{(D11)}$$

To determine the recovery factor from the flight test, plots of the square of position corrected Mach number (M_c) versus $5\left(\frac{T_r}{T_a} - 1\right)$ were created. The corresponding slope was the recovery factor and the intercept the bias (b_K). Equation D12 shows the full relationship of the recovery factor and the total and ambient temperatures.

$$5\left(\frac{T_r}{T_a} - 1\right) = K_R M_c^2 + b_K \quad \text{(D12)}$$

Position-corrected Mach number was determined from Pitot-static calibration results from Specific Test Objective 3. Calibration data from the same method and truth source combination was used.

The second calibration parameter was the temperature recovery correction and the associated bias. The temperature recovery correction (η) was defined as the difference between T_t and T_r divided byT_t.

$$\eta = \frac{T_t - T_r}{T_t} = 1 - \frac{T_r}{T_t} \tag{D13}$$

Plots of η versus M_c were created to compare the two temperature probes. Temperature recovery correction from test data (η_{test}) was calculated using the following equation, which was derived from the total and static temperature and equation D13:

$$\eta_{test} = \left[1 - \frac{T_r}{T_a}\frac{1}{(0.2M_c^2+1)}\right] \times 100 \tag{D14}$$

Once the test temperature recovery correction was determined, the bias, b_η, was chosen which minimized the mean squared error. MATLAB® function 'fminunc.m' was used to minimize the mean squared error. The bias was inserted as follows to determine the total temperature derived from the test data ($T_{t,derived}$):

$$T_{t,derived} = \frac{T_r}{1-(\eta - b_\eta)} \tag{D15}$$

For repeatability, the percent differences were calculated between data from different conditions. Percent difference was calculated using the following equation:

$$\%\, Difference = \frac{2(K_{R_1} - K_{R_2})}{(K_{R_1} + K_{R_2})} \tag{D16}$$

For the tower flyby the first recovery factor was from flight 2 and the second from flight 6. For the LAD, the first recovery factor was from heavyweight data while the second was from lightweight data.

To determine how well the recovery factor calibration model represents the actual data collected, the standard error of the estimate was calculated for each TAT probe and each calibration data analysis combination shown in table D1. The standard error was calculated using the following equation:

$$S_{y,x} = \sqrt{\frac{\sum y_i^2 - b\sum y_i - a\sum x_i y_i}{n-2}} \tag{D17}$$

Where y_i is the individual measured values of $5\left(\frac{T_r}{T_S} - 1\right)$, x_i is the measured values of M_c^2, n is the number of measurements taken, a is the temperature recovery factor from the linear regression, and b is the bias from the linear regression.

Since the temperature correction model recommended by the TAT probe manufacturer is not linear, the mean square error (MSE) was used to determine which probe best fits the model. The following equation was used to calculate the sum of the squared errors:

$$MSE = \frac{\sum (Y_i - y_i)^2}{n} \tag{D18}$$

Where Y_i is the temperature correction predicted by the manufacturer's model and y_i is the measured temperature correction.

STATIC PRESSURE CORRECTIONS

Comparison of the static pressure position correction calibration techniques were made by collecting data from both the flight test noseboom and the trailing cone system with all combinations of methods and truth sources. Methods used to determine the calibration were tower flyby, stabilized cruise, LAD, GPS cloverleaf, and 360-degree turns. The truth sources used were flyby tower ambient pressure and temperature readings, one-balloon atmospheric data, one-balloon with Atmospheric Analysis passes, Self-Survey, and multiple-balloon atmospheric data. The combinations of truth sources and calibration techniques are shown in table D2. The data reduction methods are described in the following paragraphs.

Table D2 Pressure Correction Data Analysis Combinations

Truth Source(s)	Techniques	Data Reduction	Calibrated System
Tower Flyby (Tower pressure altitude, theodolite, temperature)	Tower Flyby Stabilized Cruise	Standard	Noseboom
			Trailing Cone
1. One Balloon Atmospheric Data 2. Atmospheric Analysis 3. Multiple Balloon Atmospheric Model 4. Self-Survey	Stabilized Cruise	Standard	Noseboom
			Trailing Cone
	Level Accel/Decel	Standard	Noseboom
			Trailing cone
1. One Balloon Atmospheric Data 2. Wingtip Temperature Probe	GPS Cloverleaf Technique	Standard	Noseboom
Turns (INS Heading and GPS Speeds)	360-degree turns	Orbis	Noseboom
		Turn Method	

For repeatability, tower flybys were flown on two different days to see if test days affected the results and LADs were flown at two aircraft weight categories (light and heavy) to see if weight affected the results. Heavyweight was defined as having more than half of the usable fuel remaining and lightweight was defined as having less than half of the usable fuel remaining. The break between heavyweight and lightweight corresponded to 5,200 pounds of fuel for all sorties. The GPS cloverleaf and 360-degree turns were repeated at the airspeed corresponding to 11 degrees AoA, 0.60 Mach number, and 0.75 Mach number at both heavyweight and lightweight gross weight. Detailed flight conditions and dates can be found in appendix A.

TOWER FLYBY DATA ANALYSIS

The tower flyby method described in AFFTC-TIH-81-5, *AFFTC Standard Airspeed Calibration Procedures* (reference 10) was used in the calibration of the pacer noseboom and trailing cone at low altitudes. Data were also taken from both the flight test and production total air temperature probes during the tower flybys to determine the total temperature probe recovery factor of each probe. The data analysis method for this flight test maneuver is described in the following paragraphs.

STATIC SOURCE ERROR CORRECTION FOR THE TOWER FLYBYS

Readings of ambient air pressure and temperature measured at the zero grid line in the flyby tower were recorded every 5 minutes during the tower flyby calibration mission to ensure accurate temperature and pressure time histories.

The grid reading was taken at the point on the aircraft where the canopy met the aircraft spine behind the rear cockpit crewmember on the pacer aircraft was recorded by the observer (and a camera) in the flyby tower. This point's coordinates were not precisely known and the data were processed as if the noseboom location had been the aim point, thus introducing a maximum error of 0.8 feet in the tapeline altitude of the transducers. The grid reading was converted into a tapeline altitude difference between the zero grid line in the flyby tower and the noseboom transducers on the aircraft:

$$\Delta h_{ZGL\ to\ nb} = 31.48 \cdot GR \tag{D19}$$

where GR was the grid reading at the location previously described. The resultant $\Delta h_{ZGL\ to\ nb}$ was in units of feet of geometric, or tapeline, altitude above the zero grid line.

The translation from the location of the noseboom pressure transducers to the location of the trailing cone pressure transducer was then added to the tapeline altitude from the zero grid line to the noseboom pressure transducers to produce the tapeline altitude between the zero grid line and the trailing cone pressure transducer, $\Delta h_{ZGL\ to\ cone}$ in feet:

$$\Delta h_{ZGL\ to\ cone} = \Delta h_{ZGL\ to\ nb} + \Delta h_{nb\ to\ cone} \tag{D20}$$

The standard day temperature at the zero grid line (in Kelvin), $T_{a,SD,ZGL}$, was calculated using the standard day temperature profile described in NOAA-S/T 76-1562, *U.S. Standard Atmosphere*, (reference 11) for the 1976 U.S. Standard atmosphere for the troposphere and the pressure altitude at the zero grid line:

$$T_{a,SD,ZGL} = 288.15 - 0.0019812 \cdot H_{p_{ZGL}} \tag{D21}$$

The difference in tapeline altitude for the noseboom or trailing cone, $h_{ZGL\ to\ nb}$ or $h_{ZGL\ to\ cone}$, respectively, was converted to a difference in pressure altitude (in feet) by correcting for non-standard day temperature:

$$\Delta H_{p,ZGL\ to\ nb} = \Delta h_{ZGL\ to\ nb} \cdot \frac{T_{a,SD,ZGL}}{T_{a,ZGL}} \tag{D22}$$

$$\Delta H_{p,ZGL\ to\ cone} = \Delta h_{ZGL\ to\ cone} \cdot \frac{T_{a,SD,ZGL}}{T_{a,ZGL}} \tag{D23}$$

where $\Delta H_{p,ZGL\ to\ nb}$ and $\Delta H_{p,ZGL\ to\ cone}$ were the changes in pressure altitude between the zero grid line and the noseboom or trailing cone transducers, respectively.

The pressure altitude (in feet) at the location of the noseboom or trailing cone pressure transducers, $H_{c,nb}$ or $H_{c,cone}$, respectively, was calculated by adding $\Delta H_{p,ZGL\ to\ nb}$ or $\Delta H_{p,ZGL\ to\ cone}$, respectively, to the pressure altitude at the zero grid line:

$$H_{c,nb} = H_{p,ZGL} + \Delta H_{p,ZGL\ to\ nb} \tag{D24}$$

$$H_{c,cone} = H_{p,ZGL} + \Delta H_{p,ZGL\ to\ cone} \tag{D25}$$

The ambient air pressure (in inches of mercury) corresponding to $H_{c,nb}$ or $H_{c,cone}$ was calculated using the equation from the U.S. Standard Atmosphere, 1976 (reference 11), for pressure altitudes below 36,089 feet:

$$P_{a,nb} = 29.921252\left(1 - 6.87559 \times 10^{-6} \cdot H_{c,nb}\right)^{5.25588} \tag{D26}$$

$$P_{a,cone} = 29.921252\left(1 - 6.87559 \times 10^{-6} \cdot H_{c,cone}\right)^{5.25588} \tag{D27}$$

The static source error correction for the noseboom (in inches of mercury), $\Delta P_{pc,nb}$, or for the trailing cone, $\Delta P_{pc,cone}$, was:

$$\Delta P_{pc,nb} = P_{a,nb} - P_{sic,nb} \tag{D28}$$

$$\Delta P_{pc,cone} = P_{a,cone} - P_{sic,cone} \tag{D29}$$

The noseboom static source error correction coefficient to be added, $\Delta P_{pc,nb} / P_{sic,nb}$, and the trailing cone static source error correction coefficient, $\Delta P_{pc,cone} / P_{sic,cone}$, were then calculated:

$$\frac{\Delta P_{pc,nb}}{P_{sic,nb}} = \frac{P_{a,nb} - P_{sic,nb}}{P_{sic,nb}} = f\left(M_{ic,nb}\right) \tag{D30}$$

$$\frac{\Delta P_{pc,cone}}{P_{sic,cone}} = \frac{P_{a,cone} - P_{sic,cone}}{P_{sic,cone}} = f\left(M_{ic,nb}\right) \tag{D31}$$

STABILIZED POINT DATA ANALYSIS METHOD

Stabilized points were flown to obtain additional noseboom and trailing cone static source error correction data at a wide range of altitudes and subsonic airspeeds. The difference between the ambient pressure that was measured by the rawinsonde weather balloon and the static pressure measured by the pacer's noseboom and trailing cone at the same DGPS altitude was the static source error correction. The accuracy of this method depended on the currency of the rawinsonde data.

STATIC SOURCE ERROR CORRECTION FOR THE STABILIZED POINTS

The GPS tapeline altitude was recorded by the G-Lite DGPS in the F-16D pacer aircraft. This tapeline altitude was then translated from the location of the G-Lite DGPS to the location of the noseboom pressure transducers to produce the noseboom tapeline altitude in feet, $h_{G-Lite\,at\,nb}$, using the following equation:

$$h_{G-Lite\,at\,nb} = h_{G-Lite} + \Delta h_{G-Lite\,to\,nb} \tag{D32}$$

The tapeline altitude was also translated to the location of the trailing cone pressure transducer using the following equation:

$$h_{G-Lite\,at\,cone} = h_{G-Lite} + \Delta h_{G-Lite\,to\,cone} \tag{D33}$$

The rawinsonde balloon's GPS tapeline altitude was recorded every time the balloon recorded data. The tapeline altitude from the G-Lite DGPS at the location of the noseboom or trailing cone pressure transducers, $h_{G-Lite\,at\,nb}$ or $h_{G-Lite\,at\,cone}$, was linearly interpolated to the corresponding rawinsonde GPS tapeline altitude to lookup the rawinsonde ambient pressure ($P_{a,sonde\,at\,nb}$ or $P_{a,sonde\,at\,cone}$ in inches of mercury) at that tapeline altitude.

The difference between the rawinsonde ambient pressure at that GPS altitude and the noseboom instrument-corrected static pressure was the static source error correction (in inches of mercury):

$$\Delta P_{pc,nb} = P_{a,sonde\,at\,nb} - P_{sic,nb} \tag{D34}$$

alternatively, for the trailing cone:

$$\Delta P_{pc,cone} = P_{a,sonde\,at\,cone} - P_{sic,cone} \tag{D35}$$

The static source error correction coefficient is given by the following equation for the noseboom:

$$\frac{\Delta P_{pc,nb}}{P_{sic,nb}} = \frac{P_{a,nb} - P_{sic,nb}}{P_{sic,nb}} = f\left(M_{ic,nb}\right) \tag{D36}$$

or, for the trailing cone:

$$\frac{\Delta P_{pc,cone}}{P_{sic,cone}} = \frac{P_{a,cone} - P_{sic,cone}}{P_{sic,cone}} = f\left(M_{ic,nb}\right) \tag{D37}$$

LEVEL ACCELERATION AND DECELERATION DATA ANALYSIS METHOD

The algorithm was the same as the one used for the stabilized points (see previous section).

GPS CLOVERLEAF DATA ANALYSIS METHOD

True airspeed for each leg was determined using the G-Lite DGPS groundspeed and track angle. The difference between the Pitot-statics based true airspeed and the true airspeed calculated using the GPS velocity vectors and the wind vectors was then used to calculate the static source error correction as shown in the following data analysis method.

STATIC SOURCE ERROR CORRECTIONS TO BE ADDED FOR THE GPS CLOVERLEAF MANEUVERS

The instrument-corrected pressure altitude (in feet) using noseboom instrument-corrected static pressure and sea level ambient pressure was calculated. For pressure altitudes from sea level to 36,089 feet, $H_{ic,nb}$ was:

$$H_{ic,nb} = 145442.16\left[1-\left(\frac{P_{sic,nb}}{29.921252}\right)^{0.1902631}\right] \tag{D38}$$

or, for pressure altitudes from 36,089 to 65,617 feet:

$$H_{ic,nb} = 36089.239 - 20805.826\ln\left[4.4770774\left(\frac{P_{sic,nb}}{29.921252}\right)\right] \tag{D39}$$

The instrument-corrected Mach number, $M_{ic,nb}$, was then calculated using the noseboom total and static pressures. Again, the following equation was valid only for subsonic Mach numbers.

$$M_{ic,nb} = \left\{5\left[\left(\frac{P_{tic,nb}}{P_{sic,nb}}\right)^{2/7} - 1\right]\right\}^{1/2} \tag{D40}$$

Ambient air temperature (in Kelvin) from the instrument-corrected values, $T_{aic,nb}$, was calculated either by using the instrument-corrected total temperature from the flight test total temperature probe, $T_{ti_{FT}}$, the noseboom instrument-corrected Mach number, $M_{ic,nb}$, and the recovery factor, $K_{R_{FT}}$ and bias, b, determined when calibrating this temperature probe using tower flyby, cruise and LAD techniques:

$$T_{aic,nb} = T_{ti_{FT}}\left(1 + 0.2(K_{R_{FT}} M_{ic,nb}^2 + b)\right)^{-1} \tag{D41}$$

or by using the ambient temperature given by the balloon.

The standard day temperature (in Kelvin) was calculated using the standard day temperature profile (reference 11) and the calibrated pressure altitude. Below 36,089 feet pressure altitude, the equation was:

$$T_{a,SD,nb} = 288.15 - 0.0019812 \cdot H_{ic,nb} \tag{D42}$$

From 36,089 to 65,617 feet pressure altitude, the standard day temperature was constant:

$$T_{a,SD,nb} = 216.65\,K \tag{D43}$$

The following steps in the GPS cloverleaf analysis were an iterative process to solve for the corrected Mach number. Since the corrected Mach number could not be known until the static source error correction had been found, the following steps started by using a close guess of the corrected Mach number. A new variable, M^*_{nb} for the noseboom was used for the iterative process to prevent confusion between corrected Mach number and the iterative Mach number. Variables derived from this iterative Mach number were also marked with an asterisk to differentiate these iterative values from true values. The iterative process was applied until a convergence between the guess for M^*_{nb} and the Mach number resulting from this guess was within ±0.0001.

The first guess of the instrument-corrected Mach number ($M_{ic,nb}$) was used in the iterative Mach number:

$$M^*_{nb} = M_{ic,nb} \tag{D44}$$

This guess of the corrected Mach number was used to first solve for a term similar to the ambient air temperature (in Kelvin), $T^*_{a,nb}$:

$$T^*_{a,nb} = T_{ti_{FT}} \left(1 + 0.2(K_{R_{FT}} M^{*2}_{nb} + b)\right)^{-1} \tag{D45}$$

where $K_{R_{FT}}$ is the flight test total temperature probe recovery factor and b the bias that were previously determined in the tower flybys and in the level accelerations and decelerations.

A term similar to the local speed of sound (in knots) from the noseboom, a^*_{nb}, was then calculated:

$$a^*_{nb} = 661.4786\sqrt{\frac{T^*_{a,nb}}{288.15}} \tag{D46}$$

A term similar to the true airspeed (in knots) from the noseboom was equal to the iterative Mach number multiplied by the term similar to the local speed of sound:

$$V^*_{nb} = M^*_{nb} a^*_{nb} \tag{D47}$$

This iteration process was only used when using total temperature as a truth source. When using ambient temperature from the balloon, that step was not necessary.

A second iterative process within the first iterative process was used in the following steps to solve for the true airspeed error correction, the wind speed from the north, and the wind speed from the east for the noseboom and the trailing cone. Variables that were created and used in this second iterative process are marked with a double asterisk to differentiate these second iteration variables from the true variables and from the first iteration variables. The second iterative process was applied until a convergence

between the guess and the resulting value for the true velocity error correction, the wind speed from the north, and the wind speed from the east for the noseboom was within ±0.0001.

The terms that were similar to the true airspeed for the noseboom that resulted from equations D47 were added to the true velocity error correction term to produce the second iteration velocity term:

$$V_{nb}^{**} = V_{nb}^{*} + \Delta V_{nb}^{**} \tag{D48}$$

This second iterative velocity for the noseboom was broken down into its two components: true velocity from the north, $V_{N,nb}^{**}$, and true velocity from the east, $V_{E,nb}^{**}$:

$$V_{nb}^{**2} = V_{N,nb}^{**2} + V_{E,nb}^{**2} \tag{D49}$$

where the second iteration velocity from the north and second iteration velocity from the east could be broken down into their ground and wind components:

$$V_{N,nb}^{**} = V_{gN} + V_{wN,nb}^{**} \tag{D50}$$

$$V_{E,nb}^{**} = V_{gE} + V_{wE,nb}^{**} \tag{D51}$$

where V_{gN} was the ground speed from the north, $V_{wN,nb}^{**}$ was the wind speed from the north, V_{gE} was the ground speed from the east, and $V_{wE,nb}^{**}$ was the wind speed from the east. V_{gN} and V_{gE} were determined from the DGPS groundspeed, V_g, and track angle, σ_g, using the following equations:

$$V_{gN} = V_g \cos(\sigma_g) \tag{D52}$$

$$V_{gE} = V_g \sin(\sigma_g) \tag{D53}$$

V_{gN}, V_{gE}, V_g, and σ_g were fixed values from the GPS cloverleaf maneuvers and were not iterated.

Rearranging the equations, the following was obtained:

$$\Delta V_{nb}^{**}\left(2V_{nb}^{*} + \Delta V_{nb}^{**}\right) - V_{wN,nb}^{**}\left(2V_{gN} + V_{wN,nb}^{**}\right) - V_{wE,nb}^{**}\left(2V_{gE} + V_{wE,nb}^{**}\right) = \left(V_g^2 - V_{nb}^{*2}\right) \tag{D54}$$

The three passes of the GPS cloverleaf maneuver produced the three equations required to solve the three unknowns. In matrix format:

$$\begin{bmatrix} \left(2V_{nb}^{*} + \Delta V_{nb}^{**}\right)_1 & \left(2V_{gN} + V_{wN,nb}^{**}\right)_1 & \left(2V_{gE} + V_{wE,nb}^{**}\right)_1 \\ \left(2V_{nb}^{*} + \Delta V_{nb}^{**}\right)_2 & \left(2V_{gN} + V_{wN,nb}^{**}\right)_2 & \left(2V_{gE} + V_{wE,nb}^{**}\right)_2 \\ \left(2V_{nb}^{*} + \Delta V_{nb}^{**}\right)_3 & \left(2V_{gN} + V_{wN,nb}^{**}\right)_3 & \left(2V_{gE} + V_{wE,nb}^{**}\right)_3 \end{bmatrix} \begin{bmatrix} \Delta V_{nb}^{**} \\ V_{wN,nb}^{**} \\ V_{wE,nb}^{**} \end{bmatrix} = \begin{bmatrix} \left(V_g^2 - V_{nb}^{*2}\right)_1 \\ \left(V_g^2 - V_{nb}^{*2}\right)_2 \\ \left(V_g^2 - V_{nb}^{*2}\right)_3 \end{bmatrix} \tag{D55}$$

where the subscripts 1, 2, and 3 indicated the pass number.

The initial guesses for ΔV_{nb}^{**}, $V_{wN,nb}^{**}$ and $V_{wE,nb}^{**}$ were zero and were used to solve equations D55. The resulting values for ΔV_{nb}^{**}, $V_{wN,nb}^{**}$ and $V_{wE,nb}^{**}$ were used as new guesses to be used in equations D55. As previously mentioned, the second iterative process was applied until a convergence between the guess and the resulting value for the true velocity error correction, the wind speed from the north, and the wind speed from the east for the noseboom and the trailing was within ±0.0001. The final ΔV_{nb}^{**} was substituted into equations D48 to produce the second iteration velocity. This second iteration velocity was then used to compute the second iteration Mach number from the noseboom:

$$M_{nb}^{**} = \frac{V_{nb}^{**}}{a_{nb}^{*}} \tag{D56}$$

The second iteration Mach number that was found in equation D56 for the noseboom was used as the new guess for the first iteration Mach number:

$$M_{nb}^{*} = M_{nb}^{**} \tag{D57}$$

As previously mentioned, this iterative process was applied until a convergence between the guess for M_{nb}^{*} or M_{cone}^{*} and the Mach number resulting from this guess was within ±0.0001. This resulting Mach number was the corrected Mach number, $M_{c,nb}$ for the noseboom.

To find the static source error correction coefficient, the ambient pressure (in inches of mercury) was found using the corrected Mach number:

$$P_{a,nb} = P_{t,nb}\left(1 + 0.2M_{c,nb}{}^{2}\right)^{-7/2} \tag{D58}$$

The static source error correction (in inches of mercury) for the noseboom, $\Delta P_{pc,nb}$, was:

$$\Delta P_{pc,nb} = P_{a,nb} - P_{sic,nb} \tag{D59}$$

The static source error correction coefficient for the noseboom, was:

$$\frac{\Delta P_{pc,nb}}{q_{cic}} = \frac{P_{a,nb} - P_{sic,nb}}{q_{cic}} \tag{D60}$$

ORBIS DATA ANALYSIS METHOD

The Orbis method used GPS track to trace ground speed (reference 1). The indicated total and static pressure and temperature were used to find indicated true airspeed, then aircraft heading to trace the indicated true speed. The wind vector was determined from the vector between both circle centers. The wind vector and ground speed were then used to find actual true airspeed. From the true airspeed correction, assuming total pressure error is zero, static pressure error was obtained.

BOOMER TURN DATA ANALYSIS METHOD

The Boomer Turn data reduction started using the same principle as the Orbis method (reference 1). It was a velocity method but also used heading angle so that the Orbis iteration technique could be replaced by a single least square regression (reference 2).

The steps involved in the algorithm were as followed:

- Express ground speeds in terms of true airspeeds, true airspeed calibration error, aircraft heading, and wind airspeeds, and project on east and north axis
- Express the previous equations in a matrix form
- Use the multiple measurements done during the turn, then parse the data as needed to make them independent
- Use these data to perform a linear analysis of variances.

SELF-SURVEY AND ATMOSPHERIC ANALYSIS METHOD

The principle for this data reduction technique was to perform an analysis of variances on the measured static pressure using GPS altitude, horizontal position and time as factors. This analysis then provided a model of static pressure versus time and three-dimensional positions, which was used as a truth source for other calibration techniques (reference 2).

TWO BALLOONS ANALYSIS METHOD

The principle for this data reduction technique was to use the atmospheric data from two different balloons to create a model of the atmosphere. Because each balloon measured wind, it was possible to obtain a pressure gradient at the position of each balloon by applying the geostrophic equation. This analysis was performed by NASA and was provided to the test team. The equation is reproduced here for reference:

$$\vec{V}_{geo} = -\frac{g}{f}\frac{\partial z}{\partial y}\vec{x} + \frac{g}{f}\frac{\partial z}{\partial x}\vec{y} \tag{D61}$$

The $\vec{x}$ and $\vec{y}$ correspond to north and east, z was the geopotential height of constant pressure surface, g was the acceleration of gravity and f was the Coriolis factor.

First, the pressure gradient at each balloon was transformed to be expressed as the pressure change at a given geometric altitude for a horizontal displacement, instead of the geometric altitude change at a given pressure altitude for a horizontal displacement. The following equation was used

$$Grad_P = 29.921252 \times \left(\left(1 - 6.87559 \times 10^{-6} \times (geomalt + grad)\right)^{5.25588} - \left(\mathbf{1 - 6.87559 \times 10^{-6} \times (geomalt)}\right)^{\mathbf{5.25588}}\right) \tag{D62}$$

with $grad$ being the pressure gradient given in the balloon file, and $Grad_P$ the resulting, modified pressure gradient (as explained above), and *geomalt* being the geometric altitude at which this equation was applied.

This operation did not change the direction of that gradient, which was provided as a separate data.

Then, a second degree polynomial fit in two dimensions (five degrees of freedom) was used to model the atmosphere with pressure being a function of latitude, longitude, latitude squared and longitude squared. The pressure and pressure gradient at each balloon were used as limit conditions, resulting in the following system of equations. Solving these equations yielded to the desired model with pressure being a function of latitude and longitude.

$$\begin{cases} P_1 = aY_1^2 + bY_1 + cX_1^2 + dX_1 + e \\ P_2 = aY_2^2 + bY_2 + cX_2^2 + dX_2 + e \\ Grad_{P1} \times cos(Dir_1) = 2aY_1 + b \\ Grad_{P1} \times sin(Dir_1) = 2cX_1 + d \\ Grad_{P2} \times cos(Dir_2) = 2aY_2 + b \\ Grad_{P2} \times sin(Dir_2) = 2cX_2 + d \end{cases} \tag{D63}$$

with *X* being the distance between the reference point and the balloon on the latitude axis and *Y* being the distance between the reference point and the balloon on the longitude axis, both expressed in nautical miles. *P* was the pressure at the balloon, $Grad_P$ the pressure gradient at the balloon as calculated above, and Dir the axis (heading) along which that gradient was effective, expressed in degrees from true north. The subscript '1' designated the first balloon and the subscript '2' the second balloon.

Because the system had six equations for five variables only, the 'linsolve.m' MATLAB® tool was used to obtain the best solution to that system.

Pressure at any point could then be written as:

$$\boldsymbol{Pressure = aY^2 + bY + cX^2 + dX + e} \quad \text{(D64)}$$

This process was repeated for each altitude available in the balloon data file, thus creating a function describing the atmosphere pressure variation with horizontal position for each increment of geometric altitude.

This model was used as the truth source to analyze the cruise and LAD points.

APPENDIX E - BEDFORD WORKLOAD SCALE

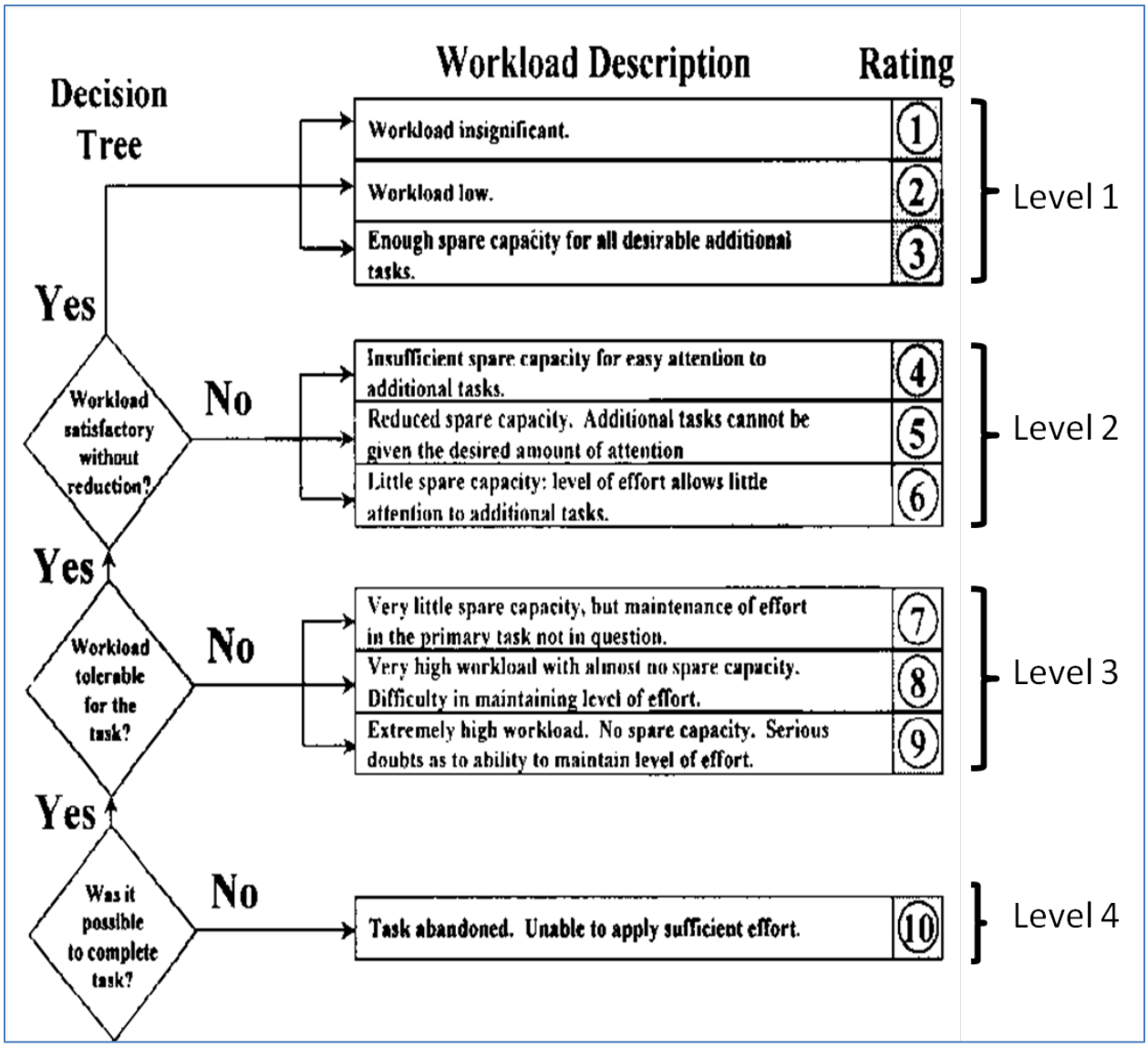

This page was intentionally left blank.

APPENDIX F - LIST OF ABBREVIATIONS, ACRONYMS, AND SYMBOLS

Abbreviation	Definition	Units
a	speed of sound	kt
AC	alternating current	---
ADS	Air Data System	---
AFB	Air Force Base	---
AFFTC	Air Force Flight Test Center	---
AFI	Air Force Instructioin	---
AGL	above ground level	---
AoA	angle-of-attack	deg
AOSS	angle-of-sideslip	deg
ARDS	Advanced Range Data System	---
b	bias	---
b_k	temperature calibration bias	n/d
b_η	temperature recovery correction bias	pct
CADC	Central Air Data Computer	---
DAS	Data Acquisition System	---
DC	direct current	---
Deg	degree	---
DGPS	Differential Global Positioning System	---
DoD	Department of Defense	---
DTIC	Defense Technical Information Center	---
FTE	Flight Test Engineer	---
FTT	flight test technique	---

Abbreviation	Definition	Units
G-Lite	GPS-Aided Inertial Navigation Reference-Lite	---
GPS	Global Positioning System	---
ICP	Instrumentation Control Panel	---
IGE	Instrumentation Ground Equipment	---
inHg	inches mercury	in
INS	inertial navigation system	---
INU	inertial navigation unit	---
IRIG	Inter-Range Instrumentation Group	---
KCAS	knots calibrated airspeed	---
K_r	recovery factor	n/d
KTAS	knots true airspeed	---
LAD	level acceleration and deceleration	---
LAU	Launcher Armament Unit	---
M	Mach	n/d
MB	megabyte	---
M_C	position corrected mach number	n/d
MSE	mean squared error	---
MSL	mean sea level	---
MUX	multiplex	---
N/A	not applicable/not available	---
NASA	National Aeronautics and Space Administration	---
nb	System 1 of the noseboom	---
nb2	System 2 of the noseboom	---
n/d	non-dimensional	---

Abbreviation	Definition	Units
NISPOM	National Industrial Security Program Operating Manual	---
nm	nautical mile	---
NTIS	National Technical Information System	---
PA	pressure altitude	---
PC	personal computer	---
PCM	pulse code modulation	---
PCMCIA	Personal Computer Memory Card International Association	---
pct	Percent	---
P/N	part number	---
PSA	Pneumatic Sensor Assembly	---
P_{si}	indicated static pressure	inHg
P_{sic}	instrument-corrected static pressure	inHg
P_{ti}	indicated total pressure	inHg
P_{tic}	instrument-corrected total pressure	inHg
q_{cic}	instrument-corrected differential pressure	inHg
RCP	rear cockpit	---
RTD-MP	Real-Time Display Main Processor	---
RVSM	Reduced Vertical Separation Minimum	---
s	standard deviation for a sample	---
S/N	serial number	---
$S_{y,x}$	standard error	---
T-2	temporary-2	---
T_a	ambient temperature	K
TAT	total air temperature	K

TFB	tower flyby	---
TIM	technical information memorandum	---
Abbreviation	Definition	Units
T_m	measured temperature	K
TMP	Test Management Project	---
TPS	Test Pilot School	---
T_r	recovery temperature	K
TSPI	time-space-position information	---
$T_{t,\ derived}$	derived total temperature	K
TTC	Teletronics Technology Corporation	---
USAF	United States Air Force	---
USB	universal serial bus	---
U.S.C.	United States Code	---
V_{eic}	instrument-corrected equivalent airspeed	knots
V_{ic}	instrument-corrected airspeed	kt
V_t	true airspeed	kt
YAPS	Yaw and Angle-of-Attack Pitot Static	---
Z	ZULU Time	---
$\frac{\Delta P_s}{P_{sic}}$	static source error correction	n/d
ΔP_{sic}	static pressure instrument error correction	inHg
ΔP_{tic}	total pressure instrument error correction	inHg
ΔP_T	total pressure error	inHg
η	temperature correction	pct

APPENDIX G – DISTRIBUTION LIST

Onsite Distribution	Number of Copies	
	Electronic	Paper
812 TSS/ENTL ATTN: Mr. Darrell Shiplett 307 E Popson Ave, Bldg 1400, Rm. 110 Edwards AFB CA 93524-6630	2	2
AFFTC/HO (History Office) ATTN: Ms. Jeannie Geiger 305 E Popson Ave Edwards AFB CA 93524-1115	1	1
USAF TPS/ED 220 S Wolfe Ave Edwards AFB CA 93524	1	1
USAF TPS/CS ATTN: Dottie Meyer 220 S Wolfe Ave Edwards AFB CA 93524	3	1
USAF TPS/ED ATTN: Russ Erb 220 S Wolfe Ave Edwards AFB CA 93524	1	1
773 TS/ENFA ATTN: Julie Clark 307 E Popson Ave Bldg 1400, Rm 102 Edwards AFB CA 93524	1	1
773 TS/ENFB ATTN: Reagan Woolf 307 E Popson Ave Bldg 1400, Rm 102 Edwards AFB CA 93524	2	2
445 FLTS/DOF ATTN: Mark Sherrier 245 S Flightline Rd Bldg 1199, Rm 114-6 Edwards AFB CA 93524	1	1

Offsite Distribution	Number of Copies	
	Electronic	Paper
Defense Technical Information Center ATTN: DTIC-O 8725 John J. Kingman Rd, Ste 0944 Ft Belvoir VA 22060-6218	1	1
DASD (DT&E) ATTN: Mr. Edward Greer 3040 Defense Pentagon Washington DC 20301-3040	1	0
AFIT Research Library 2950 Hobson Way Bldg 642 Wright-Patterson AFB OH 45433-7765	1	1
780 TS ATTN: Capt Ryan LeMaire & Capt Tomoyuki Ono 205 W D Ave, Bldg 350 Eglin AFB FL 32542	2	2
Total	17	14